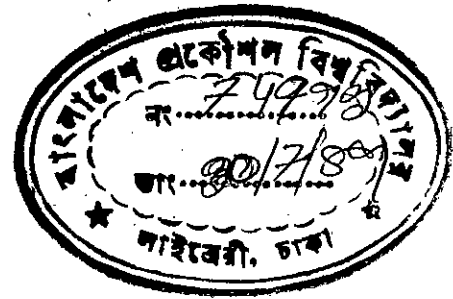


EFFECT OF SUPPORT MOVEMENT ON ELASTIC BEHAVIOUR
OF MASONRY ARCHES

A Thesis

By

MD. MAFIZ UDDIN



Submitted to the Department of Civil Engineering, Bangladesh
University of Engineering and Technology, Dhaka, in partial
fulfilment of the requirements for the Degree

of

MASTER OF SCIENCE IN CIVIL ENGINEERING



May, 1989

624,183

1989
MAF

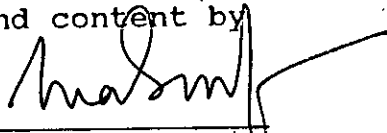
EFFECT OF SUPPORT MOVEMENT ON ELASTIC BEHAVIOUR
OF MASONRY ARCHES

A Thesis

By

MD. MAFIZ UDDIN

Approved as to style and content by



Chairman of the
Committee

DR. M. A. ROUF

Professor,

Dept. of Civil Engineering, BUET, Dhaka.

Member

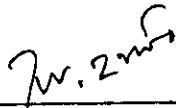


DR. MD. ALEE MURTUZA

Professor and Head,

Dept. of Civil Engineering, BUET, Dhaka.

Member

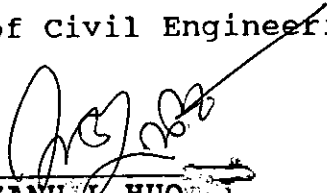


DR. ALAMGIR HABIB

Professor,

Dept. of Civil Engineering, BUET, Dhaka.

Member
(External)



DR. MIZANUL HUQUE

Managing Director,

Engineering Consulting Services (Pvt.) Ltd.

House no. 43, Road no. 9A, Dhanmondi R/A.

To my mother

ACKNOWLEDGEMENTS

The author wishes to express his indebtedness to Dr. M. A. Rouf under whose supervision the work was carried out. Without his constant guidance and invaluable suggestions at every stage, this work could not possibly have materialized.

Profound gratitude is expressed to Dr. Alamgir Habib, Professor, Department of Civil Engineering, BUET, and Dr. Alee Murtaza, Professor, Department of Civil Engineering, BUET, for their valuable comments, criticism and suggestions during this study which greatly improved its outcome.

Heartiest thanks are expressed to Mr. Nazmul Haque, senior programmer, Computer Centre, BUET and Mr. Zahidur Rahman, Lecturer, Department of Electrical Engineering, BIT, Chittagong, for their help in many different phases of developing the numerical model. Sincerest thanks are offered to other staff of the Computer Centre, BUET, for their full co-operation in using the Computer.

Grateful appreciation is also extended to Central Computer Cell, BWDB, for allowing to use their micro-computer for production run.

Finally, the author would like to express his gratitude and appreciation to many friends and colleagues who helped in carrying out this work.

ABSTRACT

The thesis deals with the analysis and design of fixed circular masonry arches with or without considering support displacement and the development of a numerical model for the above based on the elastic centre method. Mathematical formulation for elastic analysis of circular arches is presented due to different loadings and support yielding conditions. This was visualized as the basic step in developing a numerical model for elastic analysis of fixed circular arches.

The numerical model developed was utilised to analyse arches in two successive stages. In the first stage, the variation of internal forces in arches due to various loadings and support displacements varying with different arch parameters has been studied. The results presented in tabular and graphical form using non-dimensional values illustrate the most critical section and corresponding position of live load for different arches. In the second stage, the permissible live load capacity was computed for several arches with and without considering support displacement.

The live load capacity was calculated based on the allowable stresses of arch materials in compression, shear and tension. The live load was positioned at eleven different section of an arch to find out the combination of dead and live load giving excessive stresses.

The permissible live load capacity of an arch was observed to mainly depend on allowable stresses. It was further observed that most of the critical stress was tensile stress developed at

the support or at crown. However, for some arches with higher radial thicknes or higher fill depth shear stress at the support was found to be critical. The permissible live load capacity of arches was observed to increase linearly with the increase of allowable tensile stress and was observed to increase at a faster rate with the increase of radial thickness or depth of fill above the crown. The support displacements cause to distort the arches but the permissible live load capacity for some of the arches was found to be improved due to some support displacements.

CONTENTS

	<u>Page</u>
Acknowledgements	iv
Abstract	v
Contents	vi
CHAPTER - 1	INTRODUCTION
1.1	Introduction 1
1.2	Basic mechanism in masonry arches 3
1.3	Objective of the thesis 3
1.4	Scope of the thesis 4
CHAPTER - 2	REVIEW OF AVAILABLE DESIGN METHODS OF MASONRY ARCHES
2.1	Introduction 5
2.2	Graphical method of analysis 6
2.3	Pippard's elastic method 6
2.4	Plastic method of analysis 8
2.5	The WR method 9
CHAPTER - 3	ANALYTICAL SOLUTION BY ELASTIC CENTRE METHOD
3.1	Introduction 11
3.2	Assumptions 12
3.3	Basic Equations of Elastic Centre method 13

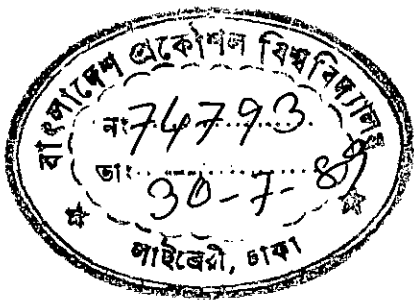
	<u>Page</u>
3.4 Expression for radius(R) and subtend angle(ϕ) at the centre in terms of rise-to-span ratio(r)	14
3.5 Expression for moment of inertia about X and Y axis and weighted area of analogous column section	15
3.6 Redundant Equations at the Elastic Centre due to different loading conditions	19
3.6.1 Equations for concentrated live load	19
3.6.2 Equations for uniformly distributed fill load above the crown	23
3.6.3 Equations for fill load below the crown	26
3.6.4 Equations for self weight of the arch-ring	32
3.6.5 Equations for partial uniformly distributed load	37
3.7 Redundant Equations for support yielding conditions	44

CHAPTER - 4

COMPUTER PROGRAMME BASED ON ELASTIC CENTRE METHOD

4.1 The programme	47
4.2 Computation of permissible live load capacity	50

	<u>Page</u>
4.3 Storage capacity and time	52
CHAPTER - 5	
INFLUENCE TABLES AND DIAGRAMS FOR ARCHES	
5.1 General	59
5.2 Introduction to Tables	62
5.3 Introduction to Graphical representation	63
5.4 General discussion on the results	64
CHAPTER - 6	
PERMISSIBLE LOAD CAPACITY OF ARCHES	
6.1 Introduction	95
6.2 Discussion	98
6.3 Conclusions	127
6.4 Scope for further research	128
REFERENCES	130
BIBLIOGRAPHY	132
APPENDIX - A	
COMPUTER PRINTED RESULTS	
A.1 Influence co-efficients due to moving unit load and co-efficient of different force components due to various loading and support displacements	
A.2 Detail analysis for particular live load and permissible live load capacity	
A.2.1 Analysis due to clockwise rotation	
A.2.2 Analysis due to counter clockwise rotation	
A.3 The permissible live load capacity for different arches	



CHAPTER - 1
INTRODUCTION

1.1 General

Brick arches were built in Egypt more than 5,000 years ago. They are one of the oldest and most attractive structural forms. Since arches are basically required to resist compressive forces, they are well suited to masonry construction. In recent years, there has been a growing interest in constructing the masonry arched bridges particularly over the canal in rural areas. Generally, the arch structures are more economical, durable and aesthetically pleasing. The size and shape of the arch structure depends primarily on the structural stability. Other consideration such as architectural demand or specific conditions of a site often influence the geometry. The shape of the arch largely affects the structural design and the cost of construction shuttering. Therefore, to find out the most economical shape design, structural engineers may have to try a few alternatives within the latitudes of their choice. Finally, the selection would then be based on the estimated total cost comprising the costs of bricks and shuttering for the different alternatives. However, as regards the preliminary choice of shape, an important observation is that different shapes prove to be economical in different spans and loading patterns. For span upto ten meters semi-circular masonry arches are economical for any type of loading. For span of ten to twenty meters with

uniformly loaded arches, most efficient shape is parabolic.

Although a brick arch is not a new structural concept, the various analytical and design approaches which have developed over the years tend to be rather baffling to engineers. Among the various methods, elastic analysis of arch structures has become popular. The elastic analysis involves much mathematical computations which may easily be solved by computers programme.

Chettoe and Henderson(2) made direct heavy loading tests on a large number of bridges. Although some permanent deformations were observed, the bridge behaved in a sufficiently elastic way to conclude that an elastic analysis would furnish a proper picture of the response of any particular arch bridge. The middle third rule is not adhered to, and Chettoe and Henderson proposed the 'safe' assumptions that mortars can not carry tensile stress, and that the structural contribution of any fill should be ignored.

The common terms used in arch design are depicted in figures 1.1 to 1.5 and may be useful to the engineer in discussions with architects and builders and in the production of working drawings. The economy of the circular arches results mainly from their efficient placement of the masonry units and easiest shuttering form.

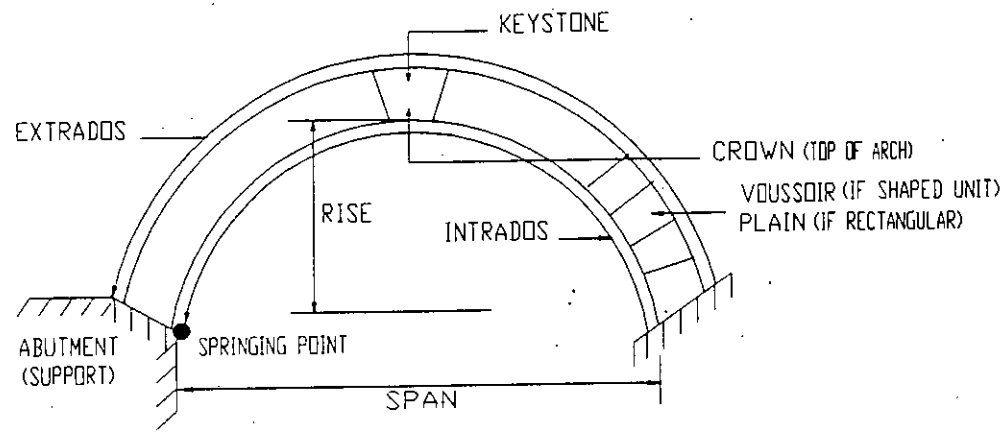


FIG. 1.1

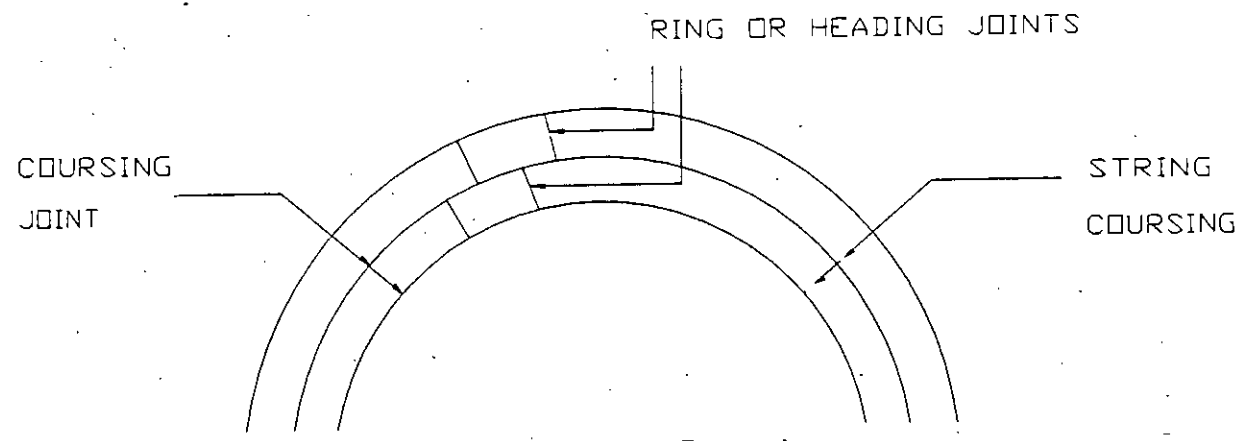


FIG. 1.2

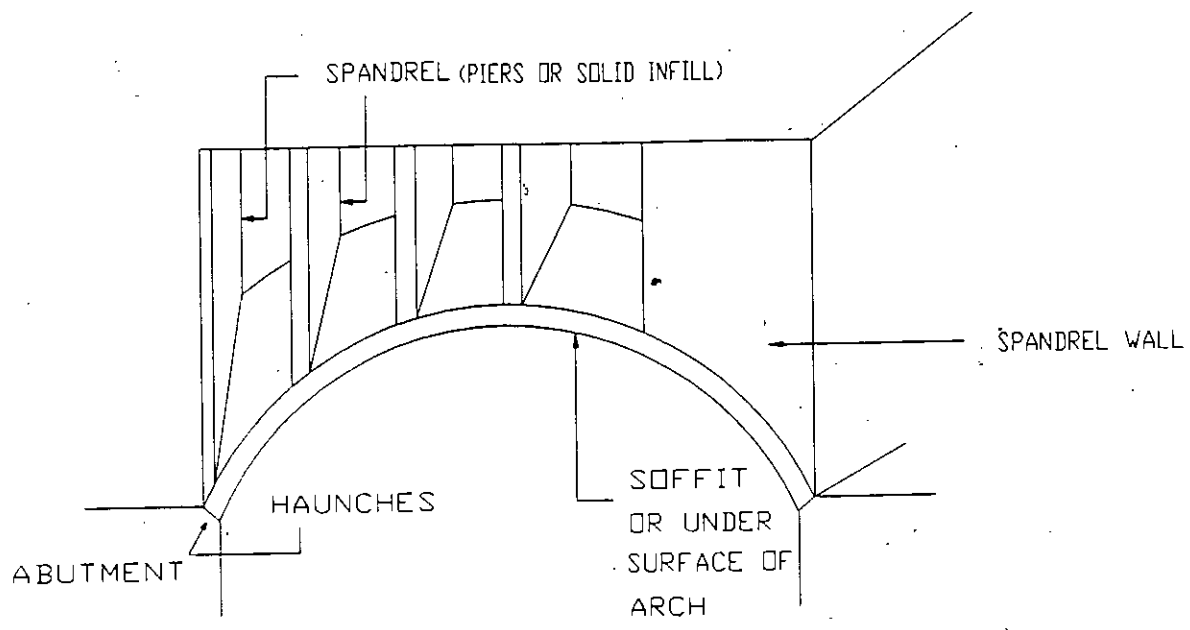


FIG. 1.3

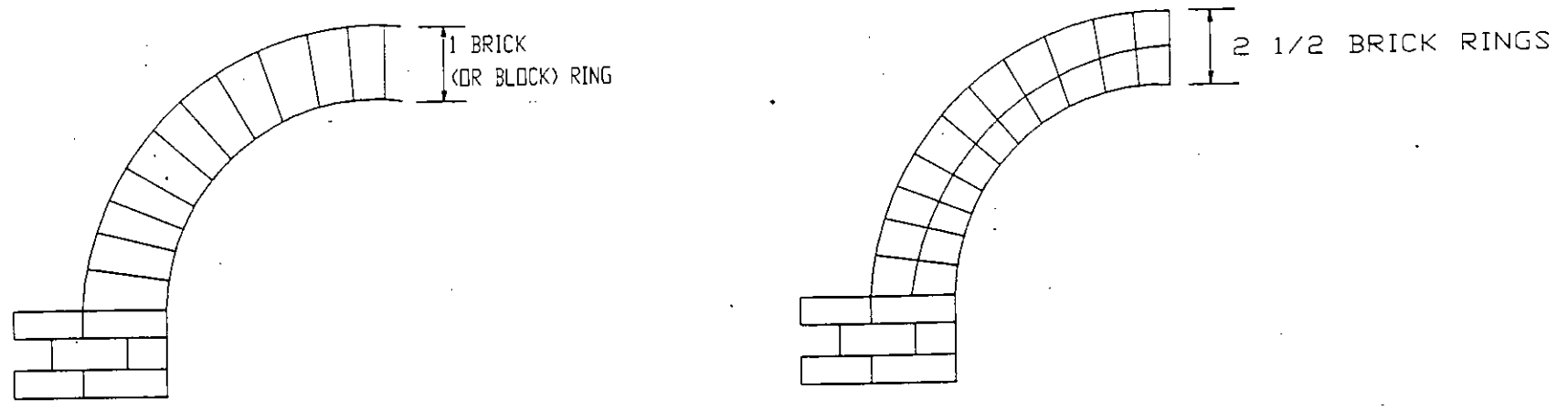


FIG. 1.4

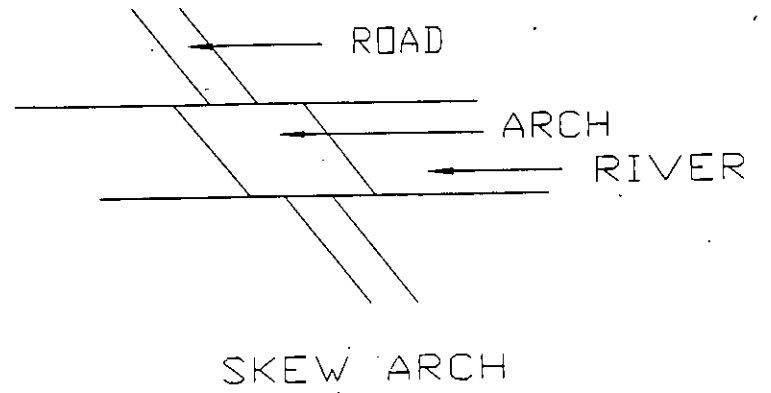
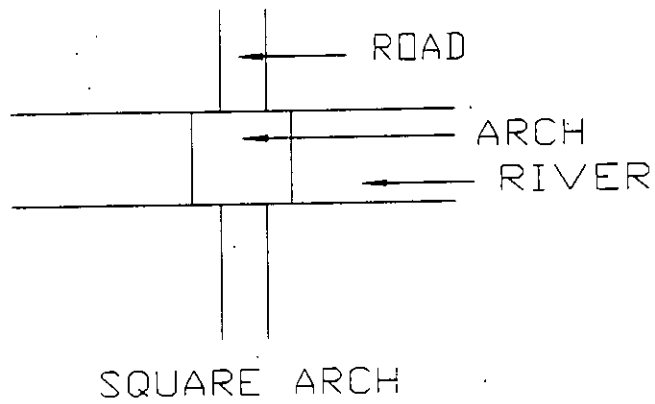
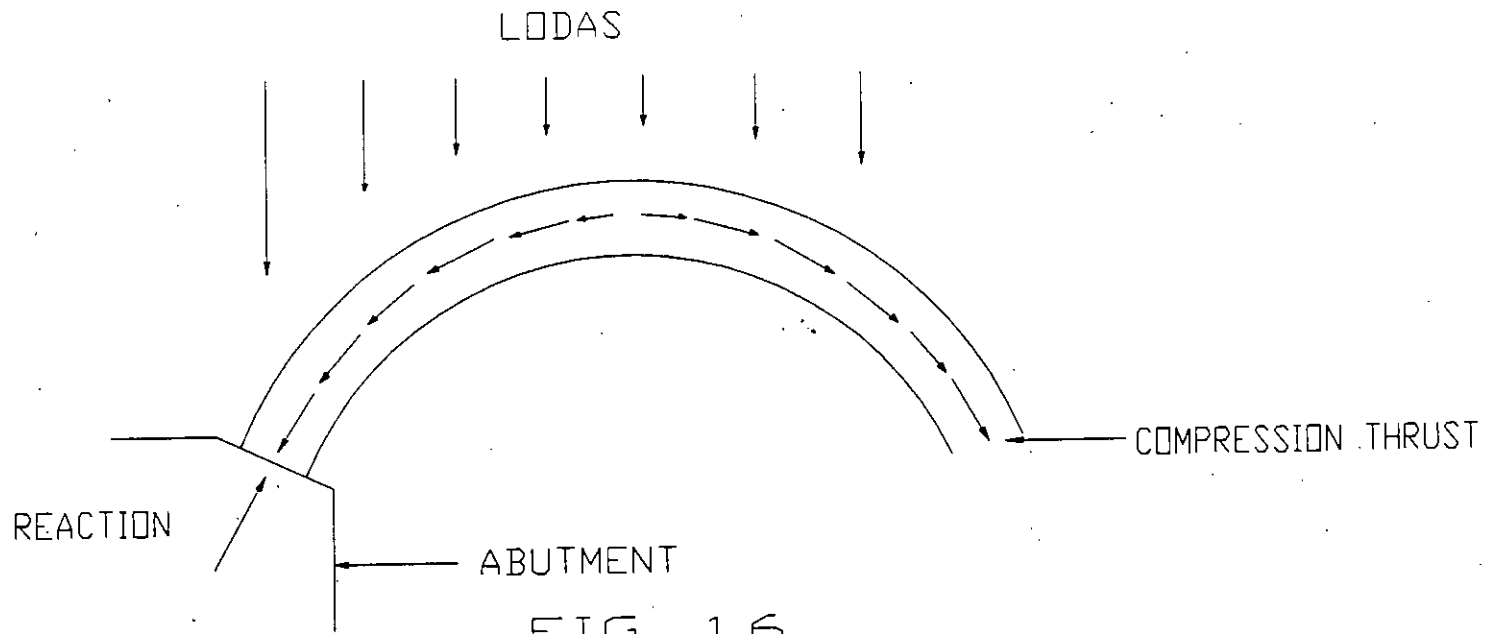
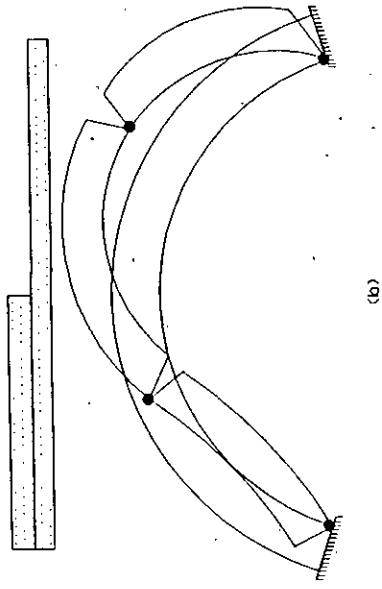
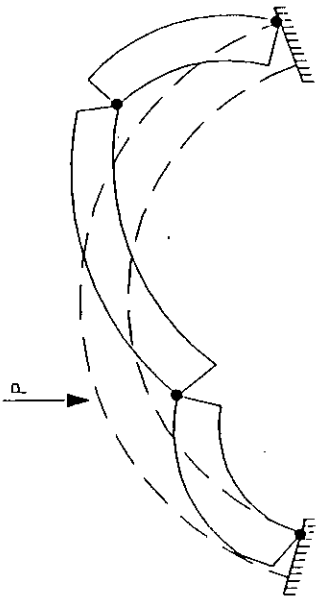


FIG. 1.5



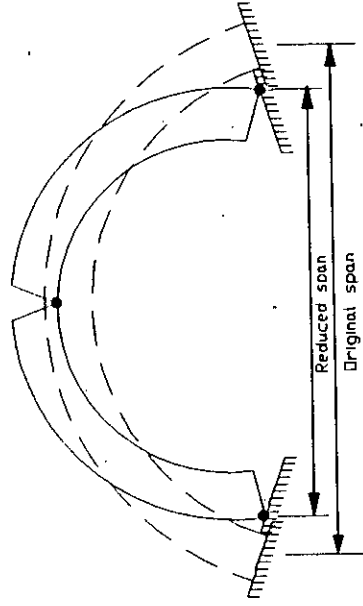


(a)

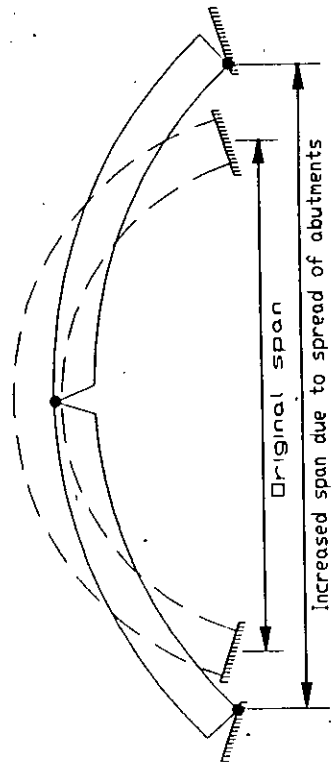


(b)

Fig. 1.7 Collapse mechanism under the action of point load and uniform superimposed loads



(a)



(b)

Fig. 1.8 collapse mechanism due to support displacements

1.2 Basic mechanism in masonry arches

Most masonry arches are considered to be fixed arches i.e. there are no hinges and they are not considered to be capable of resisting tensile stresses. The downward load on the arch creates lateral and compression thrusts in the arch span (Figure 1.6) which pushes the masonry units against each other and compresses them.

If the line of the thrust is on the centre of the arch, the arch ring is under uniform compressive stress. But actually, the line of the thrust does not always pass along the centre line of the arch, and the arch is not then in uniform compressive stress. Provided that the line of thrust does not pass outside the middle third zone, no tension stresses will develop. This, of course, is the well known middle third rule. In fact, the line of thrust can lie outside the middle third, tensile stresses can develop and cracks can occur. The line of thrust can move to the edge of the arch ring and a hinge will develop, but the arch will not necessarily collapse. Some common possible collapse mechanisms are illustrated in figures 1.7 to 1.8.

1.3 Objective of the thesis

At present several methods for analysis and design of arches exist e.g. the graphical method, the WR method, the elastic centre method etc. In this thesis, numerical models based on the elastic centre method have been developed to predict the load carrying capacity of arches. The models have also been utilised to study the effect of support movement on the load carrying capacity of arches.

Tables and curves are produced showing the load carrying capacity of arches with the variation of different arch parameters and support yielding. Finally the effect of support movements on arches and the consequent behaviour under loading are studied.

1.4 Scope of the thesis

Review of the different methods of analysis and design of masonry arches, outline of the graphical method, middle third rule, plastic method of analysis and the WR method are presented in chapter-2. Chapter 3 presents the detailed development of the elastic method to be applied to segmental circular arches. Necessary expressions are developed, starting from the basic equations of the method, in a form suitable for using in developing a numerical model.

The expressions developed in chapter 3 are then used to write a computer programme in FORTRAN-77. Outline of the programme is presented in chapter 4.

The results obtained by developed numerical model based on elastic centre method due to various loading and support yielding conditions are presented in tabular and graphical forms in chapter-5. The permissible loads capacity varying with different arch parameters and stress conditions are presented in graphical forms and discussed in chapter-6.

CHAPTER 2

REVIEW OF AVAILABLE DESIGN METHODS OF MASONRY ARCHES

2.1 Introduction

This chapter deals with available methods of analysis and design of masonry arches. It presents a brief discussion on the following four methods :

- (1) Graphical method of analysis.
- (2) Pippard's elastic method.
- (3) Plastic method of analysis.
- (4) The WR method.

Except the Elastic Centre or column analogy method, elaborate discussion on which is presented in chapter 3 as this work is based on it.

Since the beginning of the 19th century, these methods were developed with a view to solve the then controversial problems. It may be mentioned that these methods are completely different from each other, so that the results of these methods are not comparable to each other also.

An engineer can easily guess primarily the shapes, dimensions and above all the strength of arches using some of them. These are, however, still very popular among the practioners.

2.2 Graphical method of analysis

The graphical method of arch analysis is discussed in details with two case-study in Ref.(3), which were developed to avoid the mathematical complexity of analytical method of analysis. In this method of analysis, live load is considered to be distributed over the arch. The distributed live load, fill-load and self load of the arch ring are considered as a series of point loads by dividing the arch and the loads into a number of segments. By considering two hinges at the two springing points, thrust at the crown is calculated. Finally, thrust lines are drawn on the arch profiles. During design of arches by this method, stresses are checked at the critical location from the plotted force diagram. If the stresses are found to be greater than allowable stresses, then the thickness of the arch is increased. If the line of resultant thrust is considerably outside the middle third of the depth of the arch ring, it is likely that the shape of the arch will require adjustment.

Though the graphical method is employed for the design of brick arches for its simplicity, yet it is time consuming and it requires accurate draughtsmanship. Furthermore, when abnormal loads to be considered, the analysis can become very tedious because of the uncertainty about the worst possible position of the load(10).

2.3 Pippard's Elastic method

Elastic behaviour of arches were studied in details by Pippard(8). To calculate the three redundant forces in a fixed

ended arch, applying Castiglianos strain energy theorem. In this method, an expression was derived based on certain assumptions to compute the permissible loading capacity for parabolic arches. The arch was replaced by two pinned centre line arc of parabolic shape. Applying castiglianos strain energy theorem, expressions for the bending moment and abutment thrust due to dead load and concentrated load at the crown were developed. In developing above expressions it was assumed that the fill has no structural strength and that it imposes purely vertical loads on the arch and that the fill has the same density as the material of the arch ring. It was concluded that the compressive stress in the masonry may reach a maximum value before the thrust line departs from the middle half of the section and hence the middle third rule was based on a limiting compressive stress. Thus final expressions were developed giving the limiting value of concentrated live load. Based on this expression for concentrated live load, Pippard constructed some tables from which the value of safe axle load could be read for different values of span, ring depth and fill height at crown. The conclusion of his study was that an arch would be stable if the line of the thrust contains within the middle third of the section and an arch rib is weakest under the action of a point load at about quarter-span rather than at the crown.

The elastic analysis of an arch rib appears to be conservative but the use of permissible tensile stresses have an appreciable effect on the permissible loading capacity. Elastic methods tend to be lengthy and they rely heavily on a whole range

of conventional assumptions. The lack of knowledge of the extent and properties of the mortar beds between voussoirs, for example, make the more conservative results of an elastic analysis.

2.4 Plastic analysis

Heyman(6) developed a plastic method of analysis of arches concluding that the elastic approach is conservative. The concepts of the geometrical properties rather than the material properties of the arches at the equilibrium condition are generally applied in the plastic method. This method is the classic analytical method for predicting the collapse load of a masonry arch. As the analysis is not based on a limiting value of stresses, the strength of an arch is calculated considering the margin of safety against collapse caused by the formation of hinges between voussoirs.

The plastic method was developed specifically for investigation of Mediaval bridge(6). Detail derivation of expression to calculate the collapse load of an arch has been given in Ref.(6) Plastic method of analysis is suited to relatively small span narrow arches to determine the permissible axle load. When mechanism of collapse are investigated the fill is regarded as dead weight with no inherent strength.

The Plastic method is conservative in its assumption that a live load is transmitted without dispersion through the fill to the extrados of the arch. The error here may not be large, particularly for arches of the relatively small rise and small cover. This method does not predict the load deflection history of

an arch, although it can provide a check on any non-linear model developed because of its ability to determine the upper bound solution for the collapse load of a masonry arch.

2.5 The WR method

On the western region of British Railway, over a fairly short period of time in the late 1960s, three widely different structures presented the Bridge section with various problems of assessment(10). Those problems stimulated the quest for a simple method known as WR method of calculating the permissible loading for those bridges. The basic principle in this method is that the line of thrust is constructed by applying the concentrated loads. Loads are increased successively, until the point is reached at which the arch ring behaves plastically.

The thrust line bears a very definite relationship to the bending moment diagram due to the dead and live loads acting on a simply supported beam of the same span. This was proved by Fuller in 1875 and given formal expression by Professor Eddy in the theorem which bears his name:

'The line of thrust in an arch has the same shape as the bending moment diagram for those loads when placed on a simply supported beam of the same span. The free bending moment at any section is equal to the product of the horizontal thrust in the arch and the actual height of the line of thrust above base line at that point.'

If an arbitrary line of thrust is constructed which can be proved to obey Eddy's theorem, it follows that this must be a valid

line of thrust (although not necessary the real one) for a certain set of real loads. And if that thrust line must be confined to a certain thickness (e.g. middle third or middle half) of the arch ring, then the construction of such an arbitrary line of thrust, satisfying these conditions, would be a solution to the problem.

By using the simple WR method(10), the Engineer can easily predict the permissible loading capacity regarding the thickness of the arch ring at which line of thrust passes through the middle third or middle half zone.

The whole computation can be easily adapted for use on a microcomputer which can be programmed to produce a trace of the arch profile and thrust line.

The WR method has the advantage of dealing directly with the actual shape of the arch ring, the actual dead loads and any configuration of line load in any position. Also the sloping of road surface can be easily encountered by this approximate method.

CHAPTER 3

ANALYTICAL SOLUTION BY ELASTIC CENTRE METHOD

3.1 Introduction

The elastic theory gives the satisfactory solution of all arch problems and when the integrations involved are completed for infinitely small quantities the problem presents a complex and difficult solution. This mathematical complexity is directly related to the profile of the arch. Since the arch considered in this work is a symmetrical fixed circular arch hence the final expression of integration contains three common variables which are radius, span and subtend angle at the centre.

In this method of analysis one support is removed and as a result the system becomes cantilever and the free end is connected to the elastic centre by a bar of infinite stiffness. In order that the original stress distribution in the arch shall not alter, it is necessary to introduce three redundant forces at the elastic centre. For fill load below the crown, however, the arch is cut at the crown and the free ends are connected with the elastic centre

Radius and subtend angle are the main variables in all the final expressions and hence their expressions are presented separately in Art. 3.4, in term of rise-to-span ratio. The momen

of inertia about X, Y axis and weighted area of analogous column section, the common parameters of the basic equations of the elastic centre method, are derived in Art. 3.5. The elastic centre method is particularly convenient in computing influence lines, as well as for estimating effects of rib shortening, temperature change and support displacement.

3.2 Assumptions:

In this method of analysis the following assumptions are made:

- (i) The span of the arch remains unchanged
- (ii) There is no relative settlement of the abutments, that is the abutments are unyielding and
- (iii) The slope of the tangents to the arch axis at the springing remains unchanged, that is there are no rotations of abutments.

3.3 Basic Equations of Elastic Centre method

Details derivation of the basic equations are available in Ref. 7 and any other standard text book on structural analysis. The method develops the following three equations (Fig.3.1) for symmetrical fixed circular arches.

$$H_o = - \frac{\int_A^B M_p y \frac{ds}{EI}}{I_x} \quad 3.3.1$$

$$V_o = \frac{\int_A^B M_p x \frac{ds}{EI}}{I_y} \quad 3.3.2$$

$$M_o = \frac{\int_A^B M_p \frac{ds}{EI}}{S_b} \quad 3.3.3$$

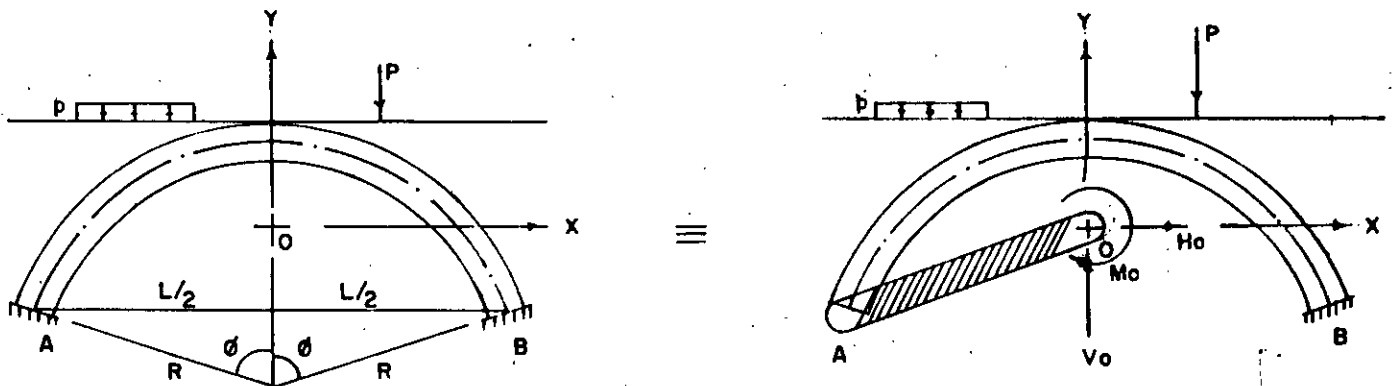


Fig. 3.1

Where, H_o , V_o & M_o = Horizontal, vertical & moment redundant forces respectively at the elastic centre.

M_p = Bending moment due to applied loading.

I_x & I_y = Moment of inertia about the X and Y axis respectively

S_b = Weighted area of the analogous column section

EI = Elastic rigidity of the section.

ds = Elementary length.

3.4 Expression for Radius(R) and subtend angle(ϕ) at the centre in terms of rise-to-span ratio(r)

Considering a fixed circular arch with radius R and rise h , (Fig.3.2), Rise-to-span ratio, $r=h/L$ and hence $h=rL$,

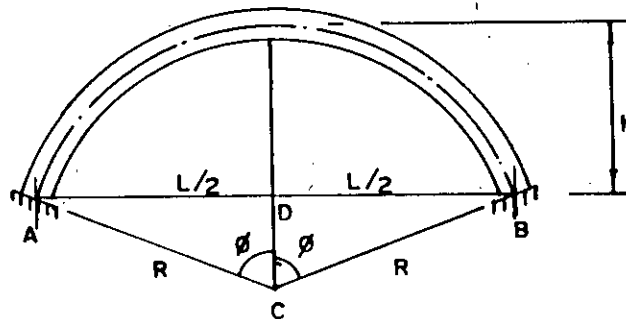


Fig.3.2

From the right angled triangle ACD (Fig.3.2), we get :

$$(R-h)^2 + (L/2)^2 = R^2$$

$$\text{or, } R = \frac{h}{2} + \frac{L^2}{8h}$$

$$\text{or, } R = \frac{rL}{2} + \frac{L^2}{8rL}$$

$$\text{or, } R = \left(\frac{r}{2} + \frac{1}{8r}\right)L$$

$$R = \alpha L$$

3.4.1

$$\text{Where, } \alpha = \frac{r}{2} + \frac{1}{8r}$$

and if the angle subtend at the centre by the arch axis is considered to be 2ϕ , then ϕ is given by (Fig. 3.2)

$$\text{or, } \tan\phi = \frac{\frac{L}{2}}{R-h}$$

$$\text{or, } \tan\phi = \frac{1}{2} \frac{8r}{1-4r^2}$$

$$\text{or, } \phi = \tan^{-1} \left(\frac{4r}{1-4r^2} \right)$$

3.4.2

3.5 Expression for moment of inertia about X, Y axis and weighted area of analogous column section

The elastic centre of symmetrical circular arch, (Fig.3.3),
 $R\sin\phi$

is located at a distance $\frac{R\sin\phi}{\phi}$ from the centre of the arch axis

(Ref.11). Taking the origin at the elastic centre, the equation of the arch axis can be written as :

$$x^2 + \left(y + \frac{R\sin\phi}{\phi} \right)^2 = R^2$$

Where, R = radius of arch-axis

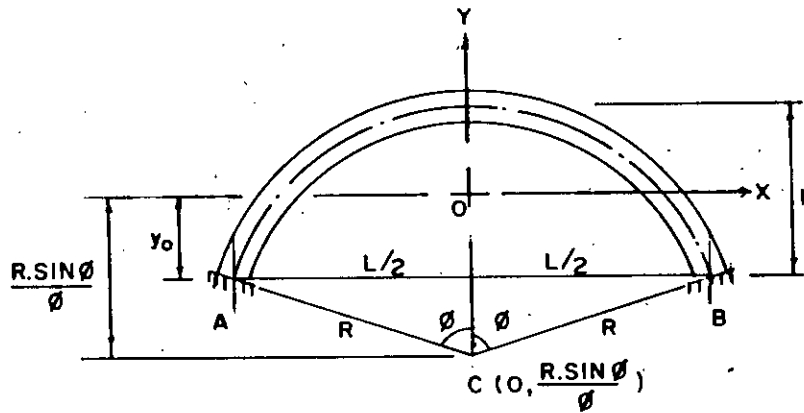


Fig. 3.3

Simplifying the above equation, we get :

$$y = \sqrt{(R^2 - x^2)} - \frac{R \sin \phi}{\phi} \quad 3.5.1$$

differentiating with respect to x, we get :

$$\frac{dy}{dx} = - \frac{x}{\sqrt{(R^2 - x^2)}} \quad 3.5.2$$

Considering an elementary length ds as shown in Fig.(3.4)

$$(ds)^2 = (dx)^2 + (dy)^2$$

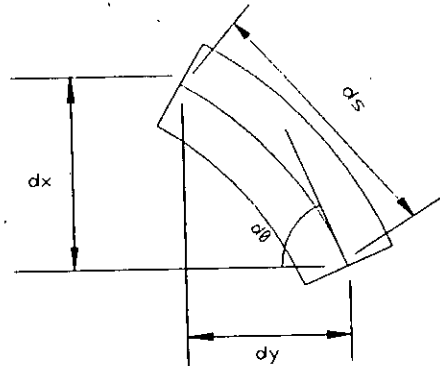


Fig. 3.4

Where, dx and dy are the projected length on x and y axis of the above element ds, we can write the above expression as :

$$(ds)^2 = (dx)^2 \left[1 + \left(\frac{dy}{dx} \right)^2 \right]$$

Utilising the equation (3.5.2), it can be written as :

$$ds = \frac{R}{\sqrt{(R^2 - x^2)}} dx \quad 3.5.3$$

The weighted area of analogous column section of an arch is given as :

$$S_b = \int_A^B \frac{ds}{EI}$$

Substituting the expression of the equation (3.5.3), we get :

$$S_b = \int_{-\frac{L}{2}}^{+\frac{L}{2}} \frac{R}{\sqrt{(R^2 - x^2)}} \frac{dx}{EI}$$

Integrating and putting the limits, we get :

$$S_b = \frac{2R}{EI} \sin^{-1} \frac{L}{2R}$$

Substituting, $R = \alpha L$ from equation (3.4.1), we get :

$$S_b = \left[2 \sin^{-1} \frac{1}{2\alpha} \right] \left[\frac{\alpha L}{EI} \right]$$

Hence the weighted area of analogous column section of an arch can be expressed as :

$$S_b = K_1 \left[\frac{\alpha L}{EI} \right] \quad 3.5.4$$

$$\text{where, } K_1 = 2 \sin^{-1} \frac{1}{2\alpha}$$

Moment of inertia about X axis is given as :

$$I_x = \int_A^B y^2 \frac{ds}{EI}$$

Substituting the expression of y from equation (3.5.1) and ds from the equation (3.5.3), we get :

$$I_x = \frac{R}{EI} \int_{-\frac{L}{2}}^{+\frac{L}{2}} \left[\sqrt{(R^2 - x^2)} - \frac{R \sin \phi}{\phi} \right]^2 \frac{1}{\sqrt{(R^2 - x^2)}} dx$$

Integrating and putting the limits, we get :

$$I_x = \frac{R}{EI} \left[\frac{L \sqrt{(R^2 - \frac{L^2}{4})}}{2} + R^2 \sin^{-1} \frac{L}{2R} - 2RL \frac{\sin \phi}{\phi} + 2R^2 \frac{\sin^2 \phi}{\phi^2} \cdot \sin^{-1} \frac{L}{2R} \right]$$

Substituting $R = \alpha L$ from equation (3.4.1), we get :

$$I_x = \left[\frac{\sqrt{(\alpha^2 - \frac{1}{4})}}{2} + \alpha^2 \sin^{-1} \frac{1}{2\alpha} - 2\alpha \frac{\sin \phi}{\phi} + 2\alpha^2 \frac{\sin^2 \phi}{\phi^2} \cdot \sin^{-1} \frac{1}{2\alpha} \right] \left[\frac{\alpha L^3}{EI} \right]$$

Hence the moment of inertia about x axis can be expressed as :

$$I_x = [K_2] \left[\frac{\alpha L^3}{EI} \right] \quad 3.5.5$$

$$\text{Where, } K_2 = \left[\frac{\sqrt{(\alpha^2 - \frac{1}{4})}}{2} + \alpha^2 \sin^{-1} \frac{1}{2\alpha} - 2\alpha \frac{\sin \phi}{\phi} + 2\alpha^2 \frac{\sin^2 \phi}{\phi^2} \cdot \sin^{-1} \frac{1}{2\alpha} \right]$$

Moment of inertia about Y axis is given as :

$$I_Y = \int_A^B x^2 \frac{ds}{EI}$$

Similarly as before, substituting the expression ds from equation (3.5.3).

$$I_Y = \frac{R}{EI} \int_{-\frac{L}{2}}^{+\frac{L}{2}} \frac{x^2}{\sqrt{(R^2 - x^2)}} dx$$

Integrating and putting the limits, we get :

$$I_Y = \frac{R}{EI} \left[R^2 \sin^{-1} \frac{L}{2R} - \frac{L}{2} \sqrt{R^2 - \frac{L^2}{4}} \right]$$

Substituting $R = \alpha L$ from equation (3.4.1), we get :

$$I_Y = \left[\alpha^2 \sin^{-1} \frac{1}{2\alpha} - \frac{1}{2} \sqrt{\alpha^2 - \frac{1}{4}} \right] \left[\frac{\alpha L^3}{EI} \right]$$

Hence the moment of inertia about Y axis can be expressed as :

$$I_Y = [K_3] \left[\frac{\alpha L^3}{EI} \right] \quad 3.5.6$$

$$\text{Where, } K_3 = \left[\alpha^2 \sin^{-1} \frac{1}{2\alpha} - \frac{1}{2} \sqrt{\alpha^2 - \frac{1}{4}} \right]$$

3.6 Redundant Equations at the Elastic centre due to different loading conditions

3.6.1 Equations for Concentrated live load

Considering a symmetrical fixed circular arch under the action of a concentrated live load q , as shown in Fig.3.5, the expression for the horizontal thrust at the elastic centre is given by equation (3.3.1) as :

$$H_o = - \int_A^B \frac{M_p y}{I_x} \frac{ds}{EI}$$

Where, $M_p = q(x-a)$

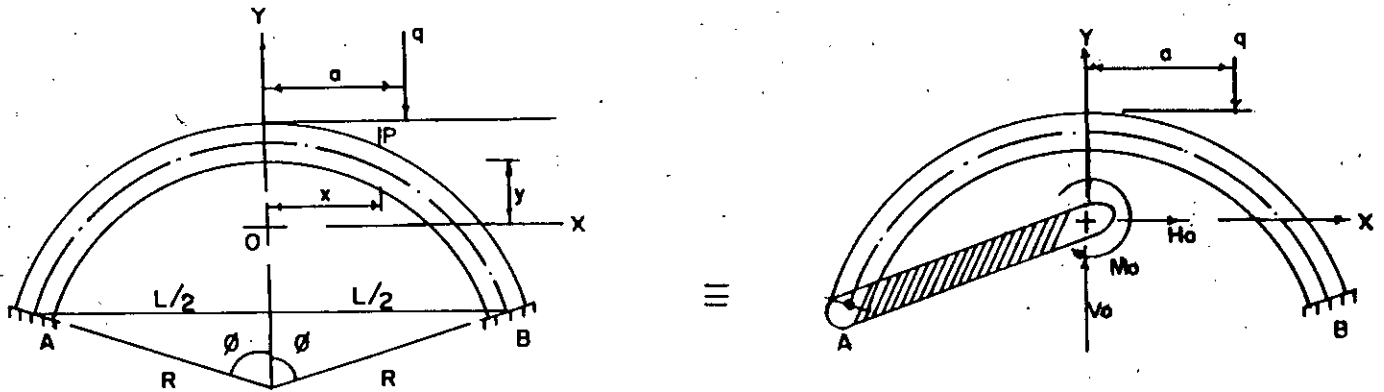


Fig.3.5

Substituting the expression of M_p , y from equation (3.5.1) and ds from equation (3.5.3) and simplifying, we can write :

$$\int_A^B M_p y \frac{ds}{EI} = \frac{R}{EI} \int_a^{L/2} 2q(x-a) \left[\sqrt{(R^2 - x^2)} - \frac{R \sin \phi}{\phi} \right] \frac{1}{\sqrt{(R^2 - x^2)}} dx$$

$$\int_A^B M_p y \frac{ds}{EI} = \left[\sqrt{(R^2 - \frac{L^2}{4})} - \sqrt{(R^2 - a^2)} \right] \frac{R \sin \phi}{\phi} + \left(\sin^{-1} \frac{L}{2R} - \sin^{-1} \frac{a}{R} \right) \frac{a R \sin \phi}{\phi} + \frac{L^2}{8} - \frac{aL}{2} + \frac{a^2}{2} \left[\frac{qR}{EI} \right]$$

Substituting $a = \beta L$ and $R = \alpha L$, Where, β is the distance factor,

we get :

$$\int_A^B M_p y \frac{ds}{EI} = \left[\frac{\alpha \sin \phi}{\phi} \left(\sqrt{(\alpha^2 - \beta_1^2)} - \sqrt{(\alpha^2 - \frac{1}{4})} \right) + \right.$$

$$\alpha\beta_1 \frac{\sin\phi}{\phi} \left(\sin^{-1} \frac{\beta_1}{\alpha} - \sin^{-1} \frac{1}{2\alpha} \right) - \frac{1}{8} + \frac{\beta_1}{2} - \frac{\beta_1^2}{2} \left] \left[\frac{\alpha q L^2}{EI} \right]$$

$$= [Z_1] \left[\frac{\alpha q L^2}{EI} \right]$$

Where,

$$Z_1 = \alpha \frac{\sin\phi}{\phi} \left(\sqrt{\alpha^2 - \beta_1^2} - \sqrt{\alpha^2 - \frac{1}{4}} \right) + \alpha\beta_1 \frac{\sin\phi}{\phi} \left(\sin^{-1} \frac{\beta_1}{\alpha} - \sin^{-1} \frac{1}{2\alpha} \right) - \frac{1}{8} + \frac{\beta_1}{2} - \frac{\beta_1^2}{2}$$

Now, the required horizontal thrust at the elastic centre can be written as :

$$H_0 = \left[\frac{Z_1}{K_2} \right] [q] \quad 3.6.1$$

The vertical redundant force (V_0) is given in equation (3.3.2), as

$$V_0 = - \frac{\int_A^B M_p \times \frac{ds}{EI}}{I_y}$$

Similarly as before, substituting the expression of M_p and simplifying the numerator, we can write :

$$\int_A^B M_p \times \frac{ds}{EI} = \frac{R}{EI} \int_a^{+\frac{L}{2}} q(x-a) \times \frac{1}{\sqrt{(R^2-x^2)}} dx$$

or,

$$\int_A^B M_p \times \frac{ds}{EI} = \left[\frac{Rq}{EI} \right] \left[\sqrt{\left(R^2 - \frac{L^2}{4}\right)} \left(a - \frac{L}{4}\right) - \frac{a}{2} \sqrt{(R^2 - a^2)} + \frac{R^2}{2} \left(\sin^{-1} \frac{L}{2R} - \sin^{-1} \frac{a}{R} \right) \right]$$

Putting the value of $a = \beta L$ and $R = \alpha L$, we get :

$$\int_A^B M_p \times \frac{dx}{EI} = \left[\sqrt{\left(\alpha^2 - \frac{1}{4}\right) \left(\beta_1 - \frac{1}{4}\right)} - \frac{\beta_1}{2} \sqrt{\left(\alpha^2 - \beta_1^2\right)} + \frac{\alpha^2}{2} \left(\sin^{-1} \frac{1}{2\alpha} - \sin^{-1} \frac{\beta_1}{\alpha} \right) \right] \left[\frac{\alpha q L^2}{EI} \right]$$

$$= [Z_2] \left[\frac{\alpha q L^2}{EI} \right]$$

Where, $Z_2 = \sqrt{\left(\alpha^2 - \frac{1}{4}\right) \left(\beta_1 - \frac{1}{4}\right)} - \frac{\beta_1}{2} \sqrt{\left(\alpha^2 - \beta_1^2\right)} + \frac{\alpha^2}{2} \left(\sin^{-1} \frac{1}{2\alpha} - \sin^{-1} \frac{\beta_1}{\alpha} \right)$

The required vertical redundant force at the elastic centre is given as :

$$V_o = \left[\frac{Z_2}{K_3} \right] [q] \quad 3.6.2$$

The redundant force of bending moment (M_o) at the elastic centre is given in equation (3.2.3), as :

$$M_o = \frac{\int_A^B M_p \frac{ds}{EI}}{S_b}$$

Substituting the expression of M_p and ds in the numerator of the above expression and simplifying, we can write :

$$\int_A^B M_p \frac{ds}{EI} = \frac{Rq}{EI} \int_a^{+\frac{L}{2}} (x-a) \frac{1}{\sqrt{(R^2 - a^2)}} dx$$

$$= \left[\sqrt{(R^2 - a^2)} - \sqrt{\left(R^2 - \frac{L^2}{4}\right)} - a \sin^{-1} \frac{L}{2R} + a \sin^{-1} \frac{a}{R} \right] \left[\frac{Rq}{EI} \right]$$

Putting $a = \alpha L$ and $R = \beta L$, we get :

$$\int_A^B M_p \frac{ds}{EI} = \left[\sqrt{\left(\alpha^2 - \beta_1^2\right)} - \sqrt{\left(\alpha^2 - \frac{1}{4}\right)} - \beta \sin^{-1} \frac{1}{2\alpha} + \sin^{-1} \frac{\beta_1}{\alpha} \right] \left[\frac{\alpha q L^2}{EI} \right]$$

$$= [Z_3][qL]$$

Where, $Z_3 = \sqrt{(\alpha^2 - \beta_1^2)} - \sqrt{(\alpha^2 - \frac{1}{4})} - \beta \sin^{-1} \frac{1}{2\alpha} + \sin^{-1} \frac{\beta_1}{\alpha}$

The required redundant force of bending moment at the elastic centre is given as :

$$M_o = \left[\frac{Z_3}{K_1} \right] [qL] \quad 3.6.3$$

3.6.2 Equations for uniformly distributed fill-load above the crown

Considering a fixed circular arch under the action of uniformly distributed fill-load above the crown of intensity q_1 , as shown in Fig.(3.6), the expression of the horizontal redundant thrust(H_o) at the elastic centre is given as :

$$H_o = - \int_A^B \frac{M_p y \frac{ds}{EI}}{Ix}$$

$$\text{Where, } M_p = \frac{1}{2} q_1 \left(\frac{L}{2} + x \right)^2$$

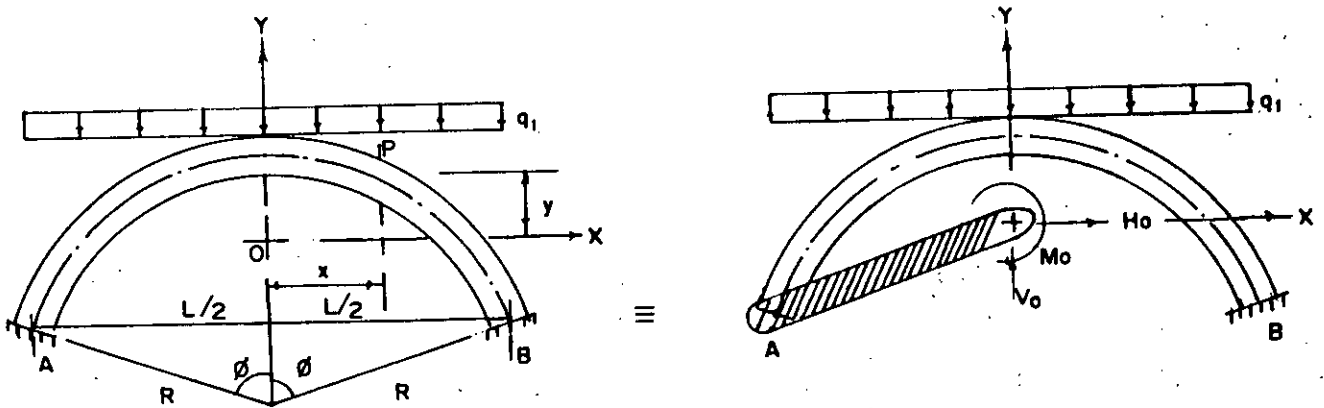


Fig.3.6

Substituting the expression M_p, y from equation (3.5.1) and ds from equation (3.5.3) in the numerator of the above equation and simplifying, we can write :

$$\int_A^B M_p y \frac{ds}{EI} = \frac{R}{EI} \int_{-\frac{L}{2}}^{+\frac{L}{2}} q_1 \left(\frac{L}{2} + x\right)^2 \left[\sqrt{(R^2 - x^2)} - \frac{R \sin \phi}{\phi} \right] \frac{1}{\sqrt{(R^2 - x^2)}} dx$$

or,
$$\int_A^B M_p y \frac{ds}{EI} = \left[\left(\frac{RL^2}{2} \sin^{-1} \frac{L}{2R} + R^3 \sin^{-1} \frac{L}{2R} - \frac{RL}{2} \sqrt{\left(R^2 - \frac{L^2}{4} \right)} \right) \cdot \frac{\sin \phi}{2\phi} - \frac{L^3}{6} \right] \left[\frac{Rq_1}{EI} \right]$$

putting the value of $R = \alpha L$, we get :

$$\int_A^B M_p y \frac{ds}{EI} = \left[\left(\frac{\alpha}{2} \sin^{-1} \frac{1}{2\alpha} + \alpha^3 \sin^{-1} \frac{1}{2\alpha} - \frac{\alpha}{2} \sqrt{\left(\alpha^2 - \frac{1}{4} \right)} \right) \frac{\sin \phi}{2\phi} - \frac{1}{6} \right] \left[\frac{\alpha q_1 L^4}{EI} \right]$$

$$= [B_1] \left[\frac{\alpha q_1 L^4}{EI} \right]$$

$$\text{Where, } B_1 = \left[\frac{\alpha}{2} \sin^{-1} \frac{1}{2\alpha} + \alpha^3 \sin^{-1} \frac{1}{2\alpha} - \frac{\alpha}{2} \sqrt{\left(\alpha^2 - \frac{1}{4} \right)} \right] \frac{\sin \phi}{2\phi} - \frac{1}{6}$$

Now, the required horizontal redundant thrust (H_o) at the elastic centre can be written as :

$$H_o = \left[\frac{B_1}{K_2} \right] [q_1 L] \quad 3.6.4$$

The vertical redundant force (V_o) is given in equation (3.3.2), as :

$$V_o = \frac{\int_A^B M_p x \frac{ds}{EI}}{I_y}$$

Similarly as before, substituting the expression of M_p and ds from equation (3.5.3) in the numerator of the above expression and simplifying, we can write :

$$\int_A^B M_p \times \frac{ds}{EI} = \frac{Rq_1}{EI} \int_{-\frac{L}{2}}^{+\frac{L}{2}} \frac{1}{2} \left(\frac{L}{2} + x\right)^2 x \frac{1}{\sqrt{(R^2 - x^2)}} dx$$

or, $\int_A^B M_p \times \frac{ds}{EI} = \left[R^2 L \sin^{-1} \frac{L}{2R} - \frac{L^2}{2} \sqrt{\left(R^2 - \frac{L^2}{4}\right)} \right] \left[\frac{q_1 R}{2EI} \right]$

Putting the value of $R = \alpha L$, we get :

$$\int_A^B M_p \times \frac{ds}{EI} = \frac{1}{2} \left[\alpha^2 \sin^{-1} \frac{1}{2\alpha} - \frac{1}{2} \sqrt{\left(\alpha^2 - \frac{1}{4}\right)} \right] \left[\frac{\alpha q_1 L^4}{EI} \right]$$

or, $\int_A^B M_p \times \frac{ds}{EI} = [B_2] \left[\frac{\alpha q_1 L^4}{EI} \right]$

Where, $B_2 = \frac{1}{2} \left[\alpha^2 \sin^{-1} \frac{1}{2\alpha} - \frac{1}{2} \sqrt{\left(\alpha^2 - \frac{1}{4}\right)} \right]$

Now the required expression of the vertical redundant force (V_o) at the elastic centre due to fill load below the crown is given as :

$$V_o = 0.50 [q_1 L] \quad 3.6.5$$

The redundant force of bending moment (M_o) is given in equation (3.3.3), as :

$$M_o = \frac{\int_A^B M_p \frac{ds}{EI}}{S_b}$$

Substituting the expression of M_p and ds from equation (3.5.3) in the numerator of the above expression and simplifying, we can write :

$$\int_A^B M_p \frac{ds}{EI} = \frac{R}{EI} \int_{-\frac{L}{2}}^{+\frac{L}{2}} \frac{1}{2} \left(\frac{L}{2} + x\right)^2 q_1 \frac{1}{\sqrt{(R^2 - x^2)}} dx$$

$$\text{or, } \int_A^B M_p \frac{ds}{EI} = \left[\frac{L^2}{2} \sin^{-1} \frac{1}{2R} - \frac{L}{2} \sqrt{(R^2 - \frac{L^2}{4})} + R^2 \sin^{-1} \frac{1}{2R} \right] \left[\frac{q_1 L^3}{2EI} \right]$$

Putting the value of $R = \alpha L$, we get :

$$\int_A^B M_p \frac{ds}{EI} = \left[\frac{1}{4} \sin^{-1} \frac{1}{2\alpha} - \frac{1}{4} \sqrt{(\alpha^2 - \frac{1}{4})} + \frac{\alpha^2}{2} \sin^{-1} \frac{1}{2\alpha} \right] \left[\frac{\alpha q_1 L^3}{EI} \right]$$

$$= [B_3] \left[\frac{\alpha q_1 L^3}{EI} \right]$$

$$\text{Where, } B_3 = \left[\frac{1}{4} \sin^{-1} \frac{1}{2\alpha} - \frac{1}{4} \sqrt{(\alpha^2 - \frac{1}{4})} + \frac{\alpha^2}{2} \sin^{-1} \frac{1}{2\alpha} \right]$$

Now, the required redundant force of bending moment (M_o) at the elastic centre is given as :

$$M_o = \left[\frac{B_3}{K_1} \right] [q_1 L^3] \quad 3.6.6$$

3.6.3 Equations for fill-load below the crown

To simplifying the mathematical complexity for this loading condition, arch has been cut at the crown and free ends joined with the elastic centre by an infinitely rigid arm as shown in the following Fig.3.7. Many text books on structural analysis are

suggested this technique for analyzing the arch due the fill load below the crown. Detail derivation for the redundant forces at the elastic centre are available in Ref.(1), in which final expressions for the redundant forces are given as :

$$H_o = - \frac{\int_C^A (M_A + M_B) y \frac{ds}{EI}}{I} \quad 3.6.7$$

$$V = - \frac{\int_C^A (M_A - M_B) x \frac{ds}{EI}}{I} \quad 3.6.8$$

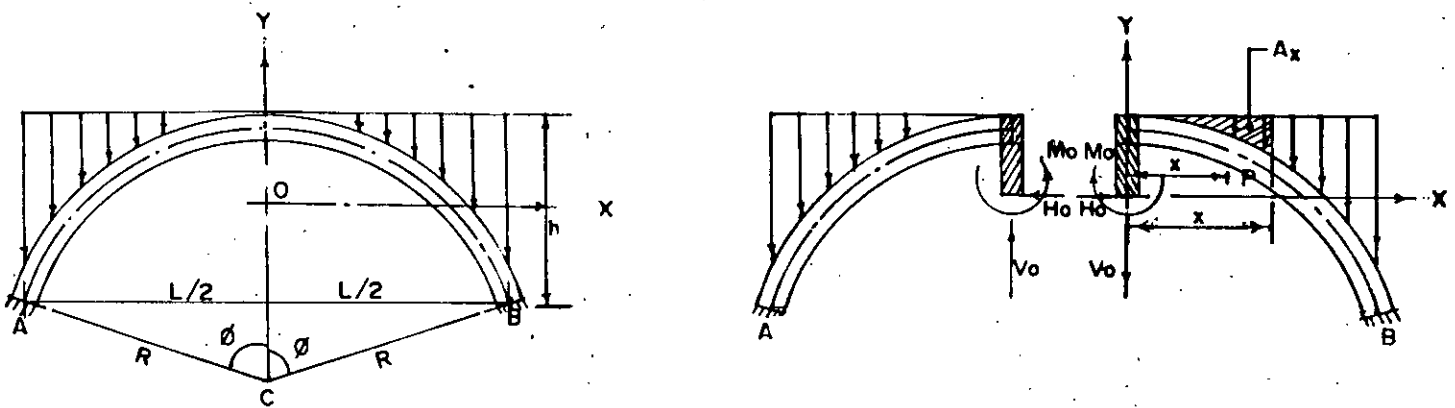


Fig.3.7

$$M_o = \frac{\int_C^A (M_A - M_B) \frac{ds}{EI}}{S_b} \quad 3.6.9$$

Where, M_A and M_B are the bending moments at the left and right support respectively due to applied loading on the left and right parts, considering both parts of the arch as in cantilevers.

From Fig. (3.7), bending moment at any section P on the arch due to fill-load below the crown is given as :

$$M_B = A_x (x - \bar{x}) \Gamma_1$$

Where, A_x is the cross-sectional area of the fill load from free end to the section at P, \bar{x} is the centroidal distance of the above cross-sectional area from section P and Γ_1 is the unit weight of the fill materials.

$$\text{Here, } A_x = \left[Rx - \frac{R^2}{2} \sin^{-1} \frac{x}{R} - \frac{x}{2} \sqrt{(R^2 - x^2)} \right]$$

By using the formula of centroidal distance of any cross-sectional area, we can write :

$$\bar{x} = \frac{\left[\frac{Rx^2}{2} + \frac{1}{3} (R^2 - x^2)^{3/2} - \frac{1}{3} R^3 \right]}{\left[Rx - \frac{R^2}{2} \sin^{-1} \frac{x}{R} - \frac{x}{2} \sqrt{(R^2 - x^2)} \right]}$$

Now, substituting the expression of A_x , \bar{x} into the above expression of M_B for right portion and simplifying, we get :

$$M_B = \frac{Rx^2}{2} - \frac{R^2}{2} x \sin^{-1} \frac{x}{R} - \frac{x^2}{2} \sqrt{R^2 - x^2} - \frac{1}{3} (R^2 - x^2)^{3/2} + \frac{1}{3} R^3$$

Similarly, cantilever moment (M_A) at the left support due to

fill load over the left portion is given as :

$$M_A = \frac{Rx^2}{2} - \frac{R^2}{2} x \sin^{-1} \frac{x}{R} - \frac{x^2}{2} \sqrt{(R^2 - x^2)} - \frac{1}{3} (R^2 - x^2)^{3/2} + \frac{1}{3} R^3$$

The expression of horizontal redundant thrust (Ho) at the elastic centre is given by equation (3.6.7), as :

$$H_o = - \frac{\int_C^A (M_A + M_B) y \frac{ds}{EI}}{I_x}$$

Substituting the expression of M_A , M_B , y from equation (3.5.1)

and ds from equation (3.5.3) in the numerator of the above expression and simplifying, we can write :

$$\int_C^A (M_A + M_B) y \frac{ds}{EI} = \frac{R \Gamma_1}{EI} \int_0^{L/2} [Rx^2 - R^2 x \sin^{-1} \frac{x}{R} - x^2 \sqrt{(R^2 - x^2)} - \frac{2}{3} (R^2 - x^2)^{3/2} + \frac{2}{3} R^3] [\sqrt{(R^2 - x^2)} - \frac{R \sin \phi}{\phi}] \frac{1}{\sqrt{(R^2 - x^2)}} dx$$

$$\text{or, } \int_C^A (M_A + M_B) y \frac{ds}{EI} = \left[\left\{ \frac{RL^3}{24} - \frac{R^2 L^2}{8} \sin^{-1} \frac{L}{2R} - \frac{5}{16} R^2 L^2 \left(R - \frac{2}{4} L \right) + \frac{L}{24} \left(R^2 - \frac{L^2}{4} \right)^{3/2} \frac{R^4}{8} \sin^{-1} \frac{L}{2R} + \frac{R^3 L}{3} \right\} + \left\{ \frac{RL^3}{72} + \frac{R^2 L}{4} \sqrt{(R^2 - \frac{L^2}{4})} - \frac{7}{6} R^4 \sin^{-1} \frac{L}{2R} + \frac{5}{6} R^3 L - R^3 \sqrt{(R^2 - \frac{L^2}{4})} \sin^{-1} \frac{L}{2R} \right\} \frac{\sin \phi}{\phi} \right] \left[\frac{R \Gamma_1}{EI} \right]$$

Putting the value of $R = \alpha L$, we get :

$$\int_C^A (M_A + M_B) y \frac{ds}{EI} = \left[\left\{ \frac{\alpha}{24} - \frac{\alpha^2}{8} \sin^{-1} \frac{1}{2\alpha} - \frac{5}{16} \alpha^2 \sqrt{(\alpha^2 - \frac{1}{4})} + \right. \right.$$

$$+ \frac{1}{24} \left(\alpha^2 - \frac{1}{4} \right)^{3/2} - \frac{\alpha^4}{8} \sin^{-1} \frac{1}{2\alpha} + \frac{\alpha^3}{3} \} + \left(\frac{\alpha}{72} + \frac{\alpha^2}{4} \sqrt{\alpha^2 - \frac{1}{4}} \right) -$$

$$\frac{7}{6} \alpha^4 \sin^{-1} \frac{1}{2\alpha} + \frac{5}{6} \alpha^3 - \alpha^3 \sqrt{\alpha^2 - \frac{1}{4}} \sin^{-1} \frac{1}{2\alpha} \left. \frac{\sin \theta}{\theta} \right\}$$

$$\left[\frac{\Gamma_1 \alpha L^5}{EI} \right]$$

$$= \left[F_1 + F_2 \frac{\sin \theta}{\theta} \right] \left[\frac{\Gamma_1 \alpha L^5}{EI} \right]$$

where, $F_1 = \left(\frac{\alpha}{24} - \frac{\alpha^2}{8} \sin^{-1} \frac{1}{2\alpha} - \frac{5}{16} \alpha^2 \sqrt{\alpha^2 - \frac{1}{4}} + \frac{1}{24} \left(\alpha^2 - \frac{1}{4} \right)^{3/2} - \frac{\alpha^4}{8} \sin^{-1} \frac{1}{2\alpha} + \frac{\alpha^3}{3} \right)$

and $F_2 = \left(\frac{\alpha}{72} + \frac{\alpha^2}{4} \sqrt{\alpha^2 - \frac{1}{4}} - \frac{7}{6} \alpha^4 \sin^{-1} \frac{1}{2\alpha} + \frac{5}{6} \alpha^3 - \alpha^3 \sqrt{\alpha^2 - \frac{1}{4}} \sin^{-1} \frac{1}{2\alpha} \right)$

Now, the required horizontal redundant thrust at the elastic centre is given as :

$$H_0 = - \left[\frac{F_1 + F_2 \frac{\sin \alpha}{\alpha}}{K_1} \right] [\Gamma_1 L^2] \quad 3.6.10$$

The vertical redundant force (V_0) at the elastic centre in Fig.(3.7) for this loading condition will be zero, which can be shown easily from equation (3.6.8).

$$V_0 = 0.0$$

$$3.6.11$$

The bending moment redundant force (M_0) is given in equation (3.6.9).

$$M_0 = \frac{\int_C^A (M_A + M_B) \frac{ds}{EI}}{S_b}$$

Substituting the expression of M_A , M_B and ds from equation (3.5.3) and simplifying the numerator, we can write :

$$\int_C^A (M_A + M_B) \frac{ds}{EI} = \left[\frac{\Gamma_1 R}{EI} \right] \left[-\frac{RL}{4} \sqrt{\left(R^2 - \frac{L^2}{4}\right)} + \frac{7}{6} R^3 \sin^{-1} \frac{L}{2R} - \frac{5}{6} R^2 L + R^2 \sqrt{\left(R^2 - \frac{L^2}{4}\right)} \sin^{-1} \frac{L}{2R} - \frac{L^3}{72} \right]$$

$$\text{or, } \int_C^A (M_A + M_B) \frac{ds}{EI} = \left[\frac{\Gamma_1 R}{EI} \right] \left[\left(-\frac{RL}{4} \sqrt{\left(R^2 - \frac{L^2}{4}\right)} - \frac{5}{6} R^2 L - \frac{L^3}{72} \right) + \left(\frac{7}{6} R^3 + R^2 \sqrt{\left(R^2 - \frac{L^2}{4}\right)} \right) \sin^{-1} \frac{L}{2R} \right]$$

Substituting the value of $R = \alpha L$, we get :

$$\int_C^A (M_A + M_B) \frac{ds}{EI} = \left[\frac{\Gamma_1 \alpha L^4}{EI} \right] \left[\left(-\frac{\alpha}{4} \sqrt{\left(\alpha^2 - \frac{1}{4}\right)} - \frac{5}{6} \alpha^2 - \frac{1}{72} \right) + \left(\frac{7}{6} \alpha^3 + \alpha^2 \sqrt{\left(\alpha^2 - \frac{1}{4}\right)} \right) \sin^{-1} \frac{1}{2\alpha} \right]$$

$$\text{or, } \int_C^A (M_A + M_B) \frac{ds}{EI} = [F_1 + F_2] \left[\frac{\Gamma_1 \alpha L^4}{EI} \right]$$

$$\text{where, } F_1 = -\frac{\alpha}{4} \left(\alpha^2 - \frac{1}{4}\right) - \frac{5}{6} \alpha^2 - \frac{1}{72}$$

$$\text{and } F_2 = \left(\frac{7}{6} \alpha^3 + \alpha^2 \sqrt{\left(\alpha^2 - \frac{1}{4}\right)}\right) \sin^{-1} \frac{1}{2\alpha}$$

Hence the required redundant force of bending moment at the Elastic centre is given as :

$$M_o = \left[\frac{F_1 + F_2}{K_1} \right] [\Gamma_1 L^3] \quad 3.6.12$$

3.6.4 Equations for self weight of the arch-ring

Considering a fixed circular arch AB of uniform radial thickness (t) under the action of self load only as shown in Fig. (3.8). Taking an elementary area (dA), where, $dA = t ds$

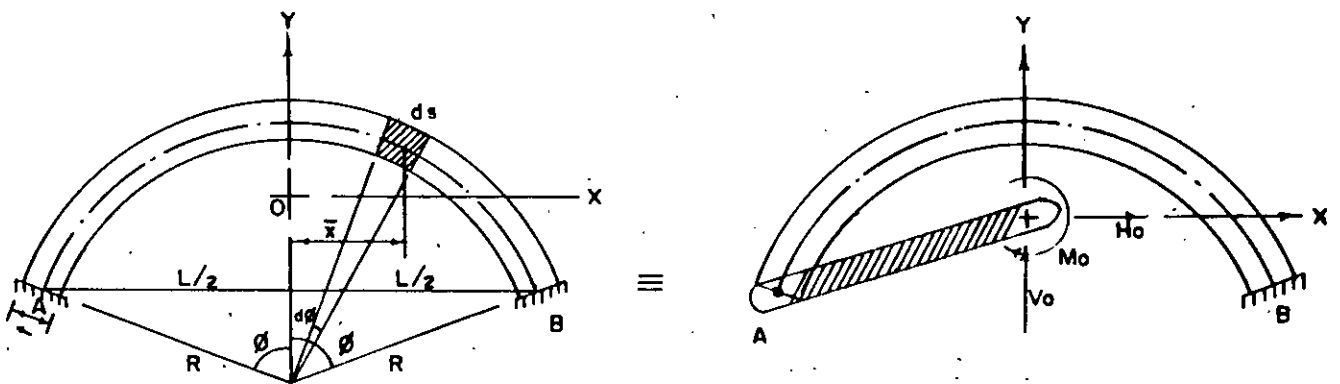


Fig. 3.8

Now, substituting the value of ds from equation (3.5.1) in the above expression.

$$dA = \frac{Rt}{\sqrt{(R^2 - x^2)}} dx$$

$$\text{or, } Ax = \int_{-L/2}^{L/2} \left[\frac{Rt}{\sqrt{(R^2 - x^2)}} \right] dx$$

Integrating and substituting the limits, we get the expression of

cross-sectional area from the left support to the corresponding section P

$$Ax = \left[\sin^{-1} \frac{x}{R} + \sin^{-1} \frac{L}{2R} \right] [Rt]$$

The equation of centroidal distance from Y axis is given as :

$$\bar{x} = \frac{\int x \, dA}{A}$$

Again, simplifying the term \bar{x} after substituting the expression of dA , as :

$$\bar{x} = \frac{\sqrt{\left(R^2 - \frac{L^2}{4}\right)} - \sqrt{R^2 - x^2}}{\sin^{-1} \frac{x}{R} + \sin^{-1} \frac{L}{2R}}$$

Bending moment at any section P (Fig. 3.8) due to self-load of the arch ring is given as :

$$M_p = [Ax.1] [x - \bar{x}] [\Gamma_2]$$

Substituting the expression of Ax and \bar{x} into the above bending moment expression and simplifying, we can write :

$$M_p = \left[x \sin^{-1} \frac{x}{R} + x \sin^{-1} \frac{L}{2R} - \sqrt{R^2 - \frac{L^2}{4}} + \sqrt{R^2 - x^2} \right] [Rt]$$

The redundant horizontal force (H_0) at the elastic centre is given by equation (3.3.1) as :

$$H_o = - \frac{\int_B^A M_p y \frac{ds}{EI}}{I_x}$$

Substituting the expression M_p , y from equation (3.5.1) and ds from equation (3.5.3) and simplifying the numerator of the above expression, we can write :

$$\int_B^A M_p y \frac{ds}{EI} = \int_{-L/2}^{+L/2} [Rt] \left[x \sin^{-1} \frac{x}{2R} + x \sin^{-1} \frac{L}{2R} - \sqrt{R^2 - \frac{L^2}{4}} + \sqrt{R^2 - x^2} \right] \left[\sqrt{R^2 - x^2} - \frac{R \sin \phi}{\phi} \right] \frac{R}{\sqrt{R^2 - x^2}} \frac{dx}{EI}$$

$$\text{or, } \int_B^A M_p y \frac{ds}{EI} = \left[\frac{L^2}{4} \sin^{-1} \frac{L}{2R} + \frac{L}{4} \sqrt{R^2 - \frac{L^2}{4}} - \frac{R^2}{2} \sin^{-1} \frac{L}{2R} - \frac{L}{2} \sqrt{R^2 - \frac{L^2}{4}} + R^2 \sin^{-1} \frac{L}{2R} - 2RL \frac{\sin \phi}{\phi} + 4R \sqrt{R^2 - \frac{L^2}{4}} \sin^{-1} \frac{L}{2R} \right] \left[\frac{\Gamma_2 R^2 t}{EI} \right]$$

Putting the value of $R = \alpha L$, we get :

$$\int_{+L/2}^{-L/2} M_p y \frac{ds}{EI} = \left[\frac{1}{4} \sin^{-1} \frac{1}{2\alpha} + \frac{1}{4} \sqrt{\alpha^2 - \frac{1}{4}} - \frac{\alpha^2}{2} \sin^{-1} \frac{1}{2\alpha} - \frac{1}{2} \sqrt{\alpha^2 - \frac{1}{4}} + \alpha^2 \sin^{-1} \frac{1}{2\alpha} - 2\alpha \frac{\sin \phi}{\phi} + 4\alpha \sqrt{\alpha^2 - \frac{1}{4}} \sin^{-1} \frac{1}{2\alpha} \frac{\sin \phi}{\phi} \right] \left[\frac{\Gamma_2 \alpha^2 t L^4}{EI} \right]$$

$$\int_B^A M_p y \frac{ds}{EI} = [D_1] \left[\frac{\Gamma_2 \alpha^2 t L^4}{EI} \right]$$

Where, $D_1 = \left[\frac{1}{4} \sin^{-1} \frac{1}{2\alpha} + \frac{1}{4} \sqrt{\alpha^2 - \frac{1}{4}} - \frac{\alpha^2}{2} \sin^{-1} \frac{1}{2\alpha} - \frac{1}{2} \sqrt{\alpha^2 - \frac{1}{4}} + \alpha^2 \sin^{-1} \frac{1}{2\alpha} - 2\alpha \frac{\sin \phi}{\phi} + 4\alpha \sqrt{\alpha^2 - \frac{1}{4}} \sin^{-1} \frac{1}{2\alpha} \frac{\sin \phi}{\phi} \right]$

Now the required expression of horizontal redundant force at the elastic centre is given as :

$$H_0 = \left[\frac{\alpha D_1}{K_2} \right] [\Gamma_2 tL] \quad 3.6.13$$

The vertical redundant force (V_0) at the elastic centre is given from equation (3.3.2), as :

$$V_0 = \frac{\int_A^B M_p \times \frac{ds}{EI}}{I_y}$$

Similarly as before, substituting the expression of M_p , ds from equation (3.5.3) and simplifying the numerator, we can write :

$$\int_A^B M_p \times \frac{ds}{EI} = \int_{-L/2}^{+L/2} [\Gamma_2 tR] \left[x \sin^{-1} \frac{x}{R} + x \sin^{-1} \frac{L}{2R} - \sqrt{R^2 - \frac{L^2}{4}} + \sqrt{R^2 - x^2} \right] x \frac{R}{\sqrt{R^2 - x^2}} \frac{dx}{EI}$$

$$\int_A^B M_p \times \frac{ds}{EI} = \left[-\frac{L}{2} \sqrt{R^2 - \frac{L^2}{4}} \sin^{-1} \frac{L}{2R} + R^2 \left(\sin^{-1} \frac{L}{2R} \right)^2 \right] \left[\frac{\Gamma_2 tR^2}{EI} \right]$$

Putting the value of $R = \alpha L$, we get :

$$\int_A^B M_p \times \frac{ds}{EI} = \left[-\frac{1}{2} \sqrt{\alpha^2 - \frac{1}{4}} \sin^{-1} \frac{1}{2\alpha} + \alpha^2 \left(\sin^{-1} \frac{1}{2\alpha} \right)^2 \right] \left[\frac{\Gamma_2 \alpha^2 tL^4}{EI} \right]$$

$$\int_A^B M_p \times \frac{ds}{EI} = [D_2] \left[\frac{\Gamma_2 \alpha^2 t L^4}{EI} \right]$$

$$\text{Where, } D_2 = \left[-\frac{1}{2} \sqrt{\alpha^2 - \frac{1}{4}} \sin^{-1} \frac{1}{2\alpha} + \alpha^2 \left(\sin^{-1} \frac{1}{2\alpha} \right)^2 \right]$$

The required expression of vertical redundant force (V_0) at the elastic centre is given as :

$$V_0 = \left[\frac{D_2}{K_3} \right] [\Gamma_2 \alpha t L] \quad 3.6.14$$

The redundant force of bending moment (M_0) at the elastic centre is given from equation (3.3.3), as :

$$M_0 = \frac{\int_A^B M_p \frac{ds}{EI}}{S_b}$$

Substituting the expression of M_p and ds from equation (3.5.3) and simplifying the numerator of the above expression, we can write :

$$\int_A^B M_p \frac{ds}{EI} = \int_{-L/2}^{+L/2} \left[\Gamma_2 R t \right] \left[x \sin^{-1} \frac{x}{R} + x \sin^{-1} \frac{L}{2R} - \sqrt{\left(R^2 - \frac{L}{4} \right)^2 + \left(R^2 - x^2 \right)} \right] \frac{R}{\sqrt{\left(R^2 - x^2 \right)}} \frac{dx}{EI}$$

$$\int_A^B M_p \frac{ds}{EI} = \left[2L - 4\sqrt{\left(R^2 - \frac{L}{4} \right)} \sin^{-1} \frac{L}{2R} \right] \left[\frac{\Gamma_2 t R^2}{EI} \right]$$

Putting the value of $R = \alpha L$, we get :

$$\int_A^B M_p \frac{ds}{EI} = \left[2 - 4\sqrt{\alpha^2 - \frac{1}{4}} \sin^{-1} \frac{1}{2\alpha} \right] \left[\frac{\Gamma_2 \alpha^2 t L^3}{EI} \right]$$

$$\text{or, } \int_A^B M_p \frac{ds}{EI} = [D_3] \left[\frac{\Gamma_2 \alpha^2 t L^3}{EI} \right]$$

$$\text{Where, } D_3 = \left[2 - 4 \sqrt{\alpha^2 - \frac{1}{4}} \sin^{-1} \frac{1}{2\alpha} \right]$$

Finally, the required expression of redundant force of bending moment is given as :

$$M_o = \left[\frac{D_3}{K_1} \right] [\Gamma_2 \alpha t L^2] \quad 3.6.15$$

3.6.5 Equations for partial uniformly distributed load

Considering a symmetrical fixed circular arch under the action of partial uniformly distributed load of intensity $\frac{q}{2}$ as shown in Fig. 3.9.

Let $x = c_1 L$ and $x = c_2 L$

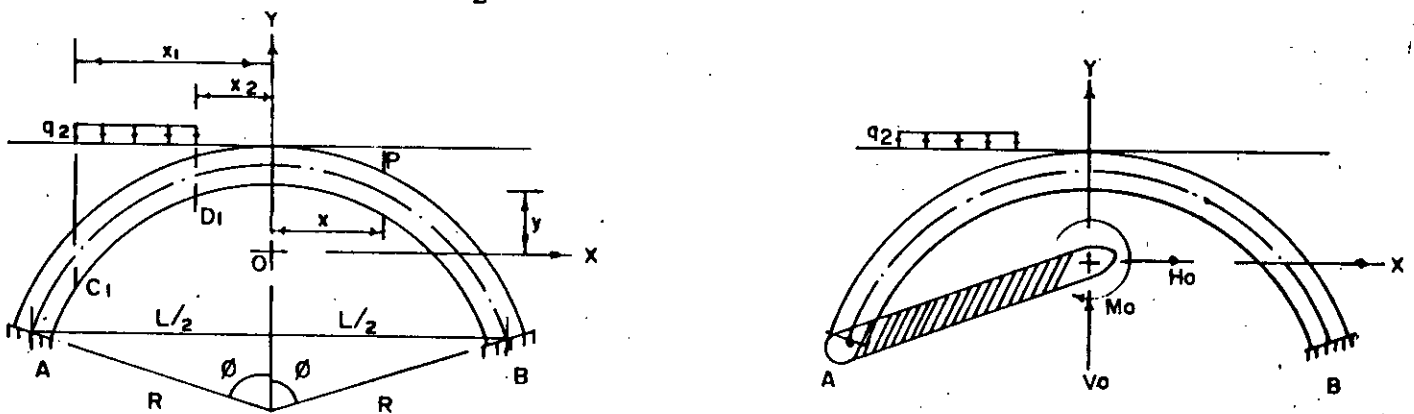


Fig. 3.9

Now, the bending moment at any section P due to applied loading over the portion (B - D) of the arch is given as :

$$M_p = q_2(x_2 - x_1) \left(x - \frac{x_1 + x_2}{2} \right)$$

$$\text{or, } M_p = (c_2 - c_1) Lxq_2 - \frac{1}{2} (c_2^2 - c_1^2) L^2q_2$$

$$\text{or, } M_p = A_0Lxq_2 - B_0L^2q_2$$

$$\text{Where, } A_0 = c_2 - c_1 \quad \text{and} \quad B_0 = \frac{1}{2} (c_2^2 - c_1^2)$$

Similarly, bending moment at any section P due to applied loading over the portion (C-D) of the arch is given as :

$$M_p = q_2(x - x_1) (x - x_1) / 2$$

$$\text{or, } M_p = \frac{1}{2} (x - x_1)^2 q_2$$

The horizontal redundant force at the elastic centre is given from equation (3.3.1), as :

$$H_0 = - \frac{\int_A^B M_p y \frac{ds}{EI}}{Ix}$$

Substituting, the expression of bending moment M_p , y from equation (3.5.1), ds from equation (3.5.3) and simplifying the numerator of the above expression, we can write :

$$\begin{aligned} \int_A^B M_p y \frac{ds}{EI} &= \int_{x_2}^{+L/2} (A_0Lxq_2 - B_0L^2q_2) \left[\sqrt{(R^2 - x^2)} - \frac{R \sin\phi}{\phi} \right] \frac{R}{\sqrt{(R^2 - x^2)}} \frac{dx}{EI} \\ &+ \int_{x_1}^{x_2} \frac{1}{2} (x - x_1)^2 q_2 \left[\sqrt{(R^2 - x^2)} - \frac{R \sin\phi}{\phi} \right] \frac{R}{\sqrt{(R^2 - x^2)}} \frac{dx}{EI} \\ &= \left[\frac{Rq_2}{EI} \right] \int_{x_2}^{+L/2} (A_0Lx - B_0L^2) \left(1 - \frac{R \sin\phi}{\phi} \frac{1}{\sqrt{(R^2 - x^2)}} \right) dx + \end{aligned}$$

$$\left[\frac{Rq_2}{EI} \right] \int_{x_1}^{x_2} (x^2 - 2x_1x + x_1^2) \left(1 - \frac{R \sin \phi}{\phi} \frac{1}{\sqrt{(R^2 - x^2)}} \right) dx$$

$$\begin{aligned} \text{or, } \int_A^B M_p y \frac{ds}{EI} &= \left[\frac{Rq_2}{EI} \right] \left[\frac{AoL}{2} \left(\frac{L^2}{4} - x_2^2 \right) + AoLR \frac{\sin \phi}{\phi} \left(\sqrt{(R^2 - \frac{L^2}{4})} - \right. \right. \\ &\left. \left. \sqrt{(R^2 - x_2^2)} \right) - BoL^2 \left(\frac{L}{2} - x_2 \right) + BoL^2 R \frac{\sin \phi}{\phi} \left(\sin^{-1} \frac{L}{2R} - \sin^{-1} \frac{x_2}{R} \right) \right] \\ &+ \left[\frac{Rq_2}{2EI} \right] \left[\frac{1}{3} (x_2^3 - x_1^3) - \frac{R \sin \phi}{\phi} \left(-\frac{x_2^2}{2} \sqrt{(R^2 - x_2^2)} + \frac{R^2}{2} \sin^{-1} \frac{x_2}{R} + \right. \right. \\ &\left. \left. \frac{x_1^2}{2} \sqrt{(R^2 - x_1^2)} - \frac{R^2}{2} \sin^{-1} \frac{x_1}{R} \right) - x_1(x_2^2 - x_1^2) - 2x_1R \frac{\sin \phi}{\phi} \right. \\ &\left. \left(\sqrt{(R^2 - x_2^2)} - \sqrt{(R^2 - x_1^2)} \right) + x_1^2 (x_2 - x_1) - x_1^2 R \frac{\sin \phi}{\phi} \left(\sin^{-1} \frac{x_2}{R} - \right. \right. \\ &\left. \left. \sin^{-1} \frac{x_1}{R} \right) \right] \end{aligned}$$

Putting the value of $x_1 = c_1L$, $x_2 = c_2L$ and $R = \alpha L$

$$\begin{aligned} \int_A^B M_p y \frac{ds}{EI} &= \left[\frac{\alpha q_2 L^4}{EI} \right] \left[Ao \left(\left[\sqrt{\left(\alpha^2 - \frac{1}{4} \right)} - \sqrt{\left(\alpha^2 - c_2^2 \right)} \right] \frac{\alpha \sin \phi}{\phi} + \frac{1}{8} - \right. \right. \\ &\left. \left. \frac{c_2^2}{2} \right) + Bo \left(\left(\sin^{-1} \frac{1}{2\alpha} - \sin^{-1} \frac{c_2}{\alpha} \right) \frac{\alpha \sin \phi}{\phi} + c_2 - \frac{1}{2} \right) + \frac{1}{6} (c_2^3 - c_1^3) \right. \\ &\left. + \left(\left(\sin^{-1} \frac{c_1}{\alpha} - \sin^{-1} \frac{c_2}{\alpha} \right) \left(\frac{c_1}{2} + \frac{\alpha^2}{4} \right) + \left(\sqrt{\left(\alpha^2 - c_1^2 \right)} - \sqrt{\left(\alpha^2 - c_2^2 \right)} \right) c_1 + \right. \right. \\ &\left. \left. \frac{1}{4} (c_2 \sqrt{\left(\alpha^2 - c_2^2 \right)} - c_1 \sqrt{\left(\alpha^2 - c_1^2 \right)}) \right] \frac{\alpha \sin \phi}{\phi} \right] \end{aligned}$$

$$\text{or, } \int_A^B M_p y \frac{ds}{EI} = [E_1' + E_1''] \left[\frac{\alpha q_2 L^4}{EI} \right]$$

$$\text{Where, } E_1' = Ao \left[\left(\sqrt{\left(\alpha^2 - \frac{1}{4} \right)} - \sqrt{\left(\alpha^2 - c_2^2 \right)} \right) \frac{\alpha \sin \phi}{\phi} + \frac{1}{8} - \frac{c_2^2}{2} \right] +$$

$$B_0 \left[\left(\sin^{-1} \frac{1}{2\alpha} - \sin^{-1} \frac{c_2}{\alpha} \right) \frac{\alpha \sin \phi}{\phi} + c_2 - \frac{1}{2} \right] + \frac{1}{6} (c_2 - c_1)^3$$

and $E_1'' = \left[\left(\sin^{-1} \frac{c_1}{\alpha} - \sin^{-1} \frac{c_2}{\alpha} \right) \left(\frac{c_1^2}{2} + \frac{\alpha^2}{4} \right) + \left(\sqrt{\alpha^2 - c_1^2} - \sqrt{\alpha^2 - c_2^2} \right) c_1 + \frac{1}{4} \left(c_2 \sqrt{\alpha^2 - c_2^2} - c_1 \sqrt{\alpha^2 - c_1^2} \right) \right] \frac{\alpha \sin \phi}{\phi}$

The required horizontal redundant force (H_0) at the elastic centre is given as :

$$H_0 = - \frac{E_1 + E_1''}{K_2} [q_2 L] \quad 3.6.16$$

The vertical redundant force (V_0) at the elastic centre is given from equation (3.3.2), as :

$$V_0 = \frac{\int_A^B M_p \times \frac{ds}{EI}}{I_y}$$

Similarly, as before substituting M_p , ds from equation (3.5.3) and simplifying the numerator of the above expression, we can write :

$$\int_A^B M_p \times \frac{ds}{EI} = \int_{x_2}^{+L/2} (A_0 L x q_2 - B_0 L^2 q_2) \times \frac{R}{\sqrt{(R^2 - x^2)}} \frac{dx}{EI} + \int_{x_1}^{x_2} \frac{1}{2} (x - x_1)^2 q_2 x \times \frac{R}{\sqrt{(R^2 - x^2)}} \frac{dx}{EI}$$

$$\text{or, } \int_A^B M_p \times \frac{ds}{EI} = \left[\frac{R q_2}{EI} \right] \left[A_0 L \left(-\frac{L}{4} \sqrt{R^2 - \frac{L^2}{4}} \right) + \frac{R^2}{2} \sin^{-1} \frac{L}{2R} + \right]$$

$$\begin{aligned}
& \frac{x_2}{2} \sqrt{(R^2 - x_2^2)} - \frac{R^2}{2} \sin^{-1} \frac{x_2}{R} + BoL^2 \left(\sqrt{(R^2 - \frac{L^2}{4})} - \sqrt{(R^2 - x_2^2)} \right) \\
& + \left[\frac{Rq_2}{2EI} \right] \left[- \frac{x_2^2}{2} \sqrt{(R^2 - x_2^2)} - \frac{1}{6} (R^2 - x_2^2)^{\frac{3}{2}} - \frac{R^2}{2} \sqrt{(R^2 - x_2^2)} + \right. \\
& \left. \frac{x_1^2}{2} \sqrt{(R^2 - x_1^2)} + \frac{1}{6} (R^2 - x_1^2)^{\frac{3}{2}} + \frac{R^2}{2} \sqrt{(R^2 - x_2^2)} - 2x \left(- \frac{x_2^2}{2} \sqrt{(R^2 - x_2^2)} + \right. \right. \\
& \left. \left. \frac{R^2}{2} \sin^{-1} \frac{x_2}{R} + \frac{x_1^2}{2} \sqrt{(R^2 - x_1^2)} - \frac{R^2}{2} \sin^{-1} \frac{x_1}{R} \right) - x_1^2 \left(\sqrt{(R^2 - x_2^2)} - \right. \right. \\
& \left. \left. \sqrt{(R^2 - x_1^2)} \right) \right]
\end{aligned}$$

Putting $x = c_1L$, $x = c_2L$ and $R = \alpha L$, we get :

$$\begin{aligned}
\int_A^B M_p x \frac{ds}{EI} &= \left[\frac{\alpha q_2 L^4}{EI} \right] \left[Ao \left(- \frac{1}{4} \sqrt{(\alpha^2 - \frac{1}{4})} + \frac{c_2^2}{2} \sqrt{(\alpha^2 - c_2^2)} + \right. \right. \\
& \left. \frac{\alpha^2}{2} \left(\sin^{-1} \frac{1}{2\alpha} - \sin^{-1} \frac{c_2}{\alpha} \right) \right) + Bo \left(\sqrt{(\alpha^2 - \frac{1}{4})} - \sqrt{(\alpha^2 - c_2^2)} \right) + \\
& \left. \sqrt{(\alpha^2 - c_2^2)} \left(- \frac{c_2^2}{6} - \frac{1}{3} \alpha^2 + \frac{c_1}{2} (c_2 - c_1) \right) + \sqrt{(\alpha^2 - c_1^2)} \left(\frac{c_1^2}{6} - \frac{\alpha^2}{3} \right) + \right. \\
& \left. + \frac{c_1 \alpha^2}{2} \left(\sin^{-1} \frac{c_1}{\alpha} - \sin^{-1} \frac{c_2}{\alpha} \right) \right]
\end{aligned}$$

$$\text{or, } \int_A^B M_p x \frac{ds}{EI} = [E_2' + E_2''] \left[\frac{\alpha q_2 L^4}{EI} \right]$$

$$\begin{aligned}
\text{Where, } E_2' &= Ao \left(- \frac{1}{4} \sqrt{(\alpha^2 - \frac{1}{4})} + \frac{c_2^2}{2} \sqrt{(\alpha^2 - c_2^2)} + \frac{\alpha^2}{2} \left(\sin^{-1} \frac{1}{2\alpha} - \right. \right. \\
& \left. \left. \sin^{-1} \frac{c_2}{\alpha} \right) \right) + Bo \left(\sqrt{(\alpha^2 - c_2^2)} - \sqrt{(\alpha^2 - c_2^2)} \right)
\end{aligned}$$

$$\text{and } E'' = \sqrt{(\alpha - c)^2} \left(-\frac{c^2}{2} - \frac{1}{6} \alpha^2 + \frac{c}{2} (\alpha - c) \right) + \sqrt{(\alpha - c)^2} \left(-\frac{1}{6} + \frac{\alpha}{3} \right) +$$

$$\frac{c^2}{2} \left(\sin^{-1} \frac{1}{\alpha} - \sin^{-1} \frac{c}{\alpha} \right)$$

The required expression of vertical redundant force (V_0) at the elastic centre is given as :

$$V_0 = \left[\frac{E_2 + E_2''}{K_3} \right] [q_2 L] \quad 3.6.17$$

The redundant force of bending moment (M_0) at the elastic centre is given from equation (3.3.3), as :

$$M_0 = \frac{\int_A^B M_p \frac{ds}{EI}}{S_b}$$

Substituting the expression of M_p , ds from equation (3.5.3) and simplifying the numerator of the above expression, as :

$$\int_A^B M_p \frac{ds}{EI} = \int_{x_2}^{+L/2} (A_0 L x q_2 - B_0 L^2 q_2) \frac{R}{\sqrt{(R^2 - x^2)}} \frac{dx}{EI} + \int_{x_1}^{x_2} \left(\frac{1}{2} x - x_1 \right) q_2$$

$$\frac{R}{\sqrt{(R^2 - x^2)}} \frac{dx}{EI}$$

$$\text{or, } \int_A^B M_p \frac{ds}{EI} = \left[\frac{Rq_2}{EI} \right] \left[-AoL \left(\sqrt{(R^2 - \frac{L^2}{4})} - \sqrt{(R^2 - x^2)} \right) - BoL \left(\sin^{-1} \frac{x_2}{R} - \sin^{-1} \frac{x_1}{R} \right) \right] + \left[\frac{Rq_2}{2EI} \right] \left[-\frac{x_2}{2} \sqrt{(R^2 - x_2^2)} + \frac{R^2}{2} \sin^{-1} \frac{x_2}{R} + \frac{x_1}{2} \sqrt{(R^2 - x_1^2)} - \frac{R^2}{2} \sin^{-1} \frac{x_1}{R} \right] + 2x_1 \left(\sqrt{(R^2 - x_2^2)} - \sqrt{(R^2 - x_1^2)} \right) + x_1 \left(\sin^{-1} \frac{x_2}{R} - \sin^{-1} \frac{x_1}{R} \right)$$

Putting the value of $x = c_1L$, $x = c_2L$ and $R = \alpha L$, we get :

$$\int_A^B M_p \frac{ds}{EI} = \left[\frac{\alpha q L^3}{EI} \right] \left[Ao \left(\sqrt{(\alpha^2 - c_2^2)} - \sqrt{(\alpha^2 - \frac{1}{4})} \right) + Bo \left(\sin^{-1} \frac{c_2}{\alpha} - \sin^{-1} \frac{c_1}{\alpha} \right) + \sqrt{(\alpha^2 - c_2^2)} \left(c_1 - \frac{c_2}{4} \right) - \frac{3}{4} c_1 \sqrt{(\alpha^2 - c_1^2)} + \left(\frac{\alpha^2}{4} + \frac{c_1^2}{2} \right) \left(\sin^{-1} \frac{c_2}{\alpha} - \sin^{-1} \frac{c_1}{\alpha} \right) \right]$$

$$\int_A^B M_p \frac{ds}{EI} = [E_3 + E_3''] \left[\frac{\alpha q_2 L^3}{EI} \right]$$

$$\text{Where, } E_3 = Ao \left(\sqrt{(\alpha^2 - c_2^2)} - \sqrt{(\alpha^2 - \frac{1}{4})} \right) + Bo \left(\sin^{-1} \frac{c_2}{\alpha} - \sin^{-1} \frac{c_1}{\alpha} \right)$$

$$\text{and } E_3'' = \sqrt{(\alpha^2 - c_2^2)} \left(c_1 - \frac{c_2}{4} \right) - \frac{3}{4} c_1 \sqrt{(\alpha^2 - c_1^2)} + \left(\frac{\alpha^2}{4} + \frac{c_1^2}{2} \right) \left(\sin^{-1} \frac{c_2}{\alpha} - \sin^{-1} \frac{c_1}{\alpha} \right)$$

$$- \sin^{-1} \left(\frac{c}{\alpha} \right)$$

The required expression of bending moment redundant force at the elastic centre is given as :

$$M_o = \left[\frac{E_3 + E_3''}{K_1} \right] [q_2 L^2] \quad 3.6.18$$

3.7 Redundant Equations for support yielding conditions

Expression for the redundant horizontal force(H_o), vertical force(V_o) and bending moment (M_o) at the elastic centre for a symmetrical fixed circular arch due to clock-wise rotation (α_o), out-ward horizontal displacement (ΔH_o) and down-ward vertical displacement (ΔV_o) at the left springing are taken from Ref.(9), which are given below :

The horizontal redundant force (H_o) :

$$H_o = - \frac{\Delta H_o + y_A \alpha_o}{I_x} \quad 3.7.1$$

where, ΔH_o = Out-ward horizontal displacement at the left support.

α_o = Clock-wise rotation at the left support

y_A = Vertical distance of the left support from the elastic centre.

Substituting the expression of I_x from equation (3.5.5), y from equation (3.5.1) and simplifying, we get :

$$H_o = \left[\frac{1}{K_2} \right] \left[\frac{EI}{L^3} \right] [\Delta H_o] - \left[\frac{c_o}{K_2} \right] \left[\frac{EI}{L^2} \right] [\alpha_o] \quad 3.7.2$$

$$\text{Where, } c_o = - \left[\frac{\sin \phi}{\phi} - \cos \phi \right]$$

The vertical redundant force (V_o) at the elastic centre :

$$V_o = - \frac{\Delta V_o + x_A \alpha_o}{I_y} \quad 3.7.3$$

Where, ΔV_o = Downward vertical displacement at the left support.

x_A = Horizontal distance of the left support from the elastic centre.

Substituting the expression of I_y from equation (3.5.6), $x = L$ in the above expression and simplifying, we get :

$$V_o = - \left[\frac{1}{K_3} \right] \left[\frac{EI}{L^3} \right] [\Delta V_o] - \left[\frac{0.5}{K_3} \right] \left[\frac{EI}{L^2} \right] [\alpha_o] \quad 3.7.4$$

The redundant force of bending moment (M_o) at the elastic centre :

$$M_o = \frac{\alpha_o}{S_b} \quad 3.7.5$$

Substituting the expression of S_b from equation (3.5.4) and simplifying, we can write :

$$M_o = \left[\frac{1}{K_1} \right] \left[\frac{EI}{L} \right] [\alpha_o] \quad 3.7.6$$

CHAPTER 4

COMPUTER PROGRAM BASED ON ELASTIC CENTRE METHOD

4.1 The programme

General equations for different force components due to different loading and support yielding conditions are presented in chapter-3 in a form which is suitable for developing a computer programme.

This programme has been developed in FORTRAN-77 to analyze and to find load carrying capacity of symmetrical fixed-circular arches. The programme contains a total of eighteen subroutine subprogrammes in addition to the main programme. A Flow chart explaining the sequence of different operations done in the programme is presented in Fig. 4.2.

The programme can be used to obtain six different forms of output on circular masonry arches. These forms of output can also be grouped in any desired combination by adjusting the values of some input identifiers as mentioned in Appendix-A and B. The six forms of output are as follows :

(i) Influence tables for bending moments, vertical shear forces, horizontal thrusts and variation of these force components due to fill load and self load of the arch-ring for arches of different rise-to-span ratio.

(ii) Influence tables for bending moments, radial shear forces, axial thrusts and variation of these force components due to fill load and self load of the arch-ring for arches of different rise-to-span ratio.

(iii) Variation of bending moments, vertical shear forces and horizontal thrusts due to various types of partial uniform distributed loads for arches of different rise-to-span ratio.

(iv) Variation of bending moments, vertical shear forces, horizontal thrusts, radial shear forces and axial thrusts due to different support displacements for arches of different rise-to-span ratio.

(v) Detail computation of bending moments, vertical shear forces, horizontal thrusts, radial shear forces, axial thrusts and different stresses due to concentrated live loads or any types partial uniform distributed loads for any particular arch.

(vi) Computation of permissible loads and identification of critical sections for any particular arch.

The results obtained as the above first four forms are presented in detail in Appendix A.1. The detail analysis, the fifth form of output, for an arch under concentrated live load of 500 lbs due to particular clockwise and counter clockwise rotation at the left support are presented in Appendix A.2.1 and A.2.2 respectively. The sixth form of results obtained for different arches are presented and discussed in chapter-6. The permissible

loads capacity for arches having span 10', 20' and 30' with rise-to-span ratio varying from 0.10 to 0.30 at an increment of 0.10, radial thickness 5" to 15" at an increment of 5" and depth of fill above the crown varying from 1.00' to 2.00' at an increment of 0.50' are tabulated in Appendix A.3.

The programme uses two set of input data. The first set of input data contains only the alphanumeric characters, which are different table heading used for printing the tables. A subprogramme named VREAD has been used to read in all the alphanumeric characters from these input data cards. The second set of input data contains all the arch parameters and value of some identifiers which control the execution of the programme. A subroutine named INPUT reads in and stores these values.

The programme has been developed based on the units of F.P.S. system. It is mentioned worthy that the first four types of output do not depend on the units since they all show the influence coefficients and the coefficients of different force components. Any arch to be analyzed should be referred to the system of cartesian axes ("X" and "Y") and origin should be located at the elastic centre of the arch. The programme divides the arch into ten segments of equal horizontal projection.

The programme prints out influence coefficients which are then printed in condensed form using microcomputer and HEWLETT-PACKARD LaserJet series II printer.

The required storage capacity and time needed to execute the different conditions are discussed in article 4.3.

4.2 Computation of permissible live load capacity

Different force components such as bending moments, radial shear forces and axial thrusts at the different radial plane due to the dead weight of the arch ring and fill load above the arch can be computed separately by using the equations in articles 3.6.2, 3.6.3 and 3.6.4. The resultant bending moment, radial shear force and axial thrust at any section due to the total dead load are calculated by adding together the values obtained for different types of dead weights.

A moving concentrated load is considered to be the live load applied over arch. The live load is positioned at eleven different sections. The concentrated live load is considered to be dispersed through the arch fill at an angle of 45 degree. Thus the live load is considered to be uniformly distributed over a horizontal circular plane while the intensity of the load is given by

(Fig. 6.1) $p_i = \frac{P}{\pi d_i^2}$, Where P is the concentrated live load at

position i, d_i is the depth of fill upto the extrados of the arch and as well as the radius of the circular plane.

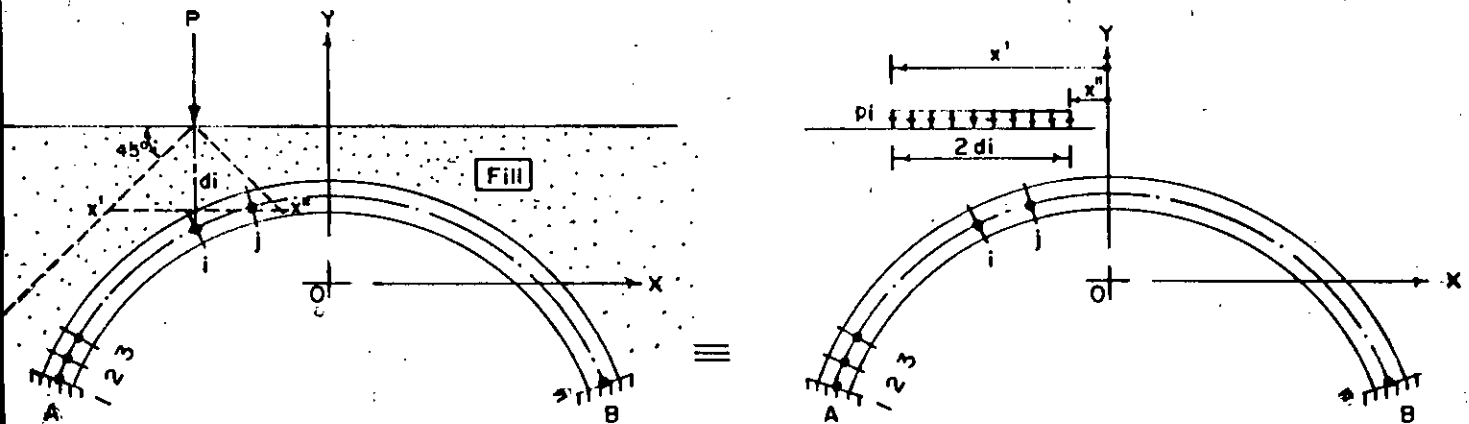


Fig. 4.1 dispersion of concentrated live load

Thus the concentrated live load at any position is replaced by a partial uniformly distributed load over arch, for which bending moment, radial shear force and axial thrust at all the eleven sections are computed by using expressions in Art.(3.6.5). Similarly, the above force components due to the live load placed at other sections are easily computed. Thus eleven different set of force components are obtained for different position of live loads.

Redundant equations at the elastic centre of an arch for three different support displacements are developed and presented in Art. (3.7). For any particular support displacement different set of force components are computed at different sections of the arch.

Force components at different sections thus computed are then added together into all possible combinations of three different

loads such as dead load, live load at eleven different positions and any one of three different support displacements. Bending and shearing stresses are then computed at different sections for all these combined forces and compared to the range of the allowable stresses of masonry. The process is repeated several time and every time the value of live load is either increased or decreased depending on the stress conditions in the previous cycle. Thus the live load which just satisfied all the allowable stress conditions is found out and the permissible load capacity for a particular arch is obtained. This capacity can be calculated with or without considering any one of three support displacements. The programme prints "IMPOSSIBLE" when arch fail under dead load only.

4.3 Storage capacity and time

The programme was developed using VM environment of the IBM 4331 computer of BUET computer centre. At the end of the thesis work, the programme was successfully compiled and run its different operations by microsoft FORTRAN 4.1 optimizing compiler using micro-computer ALR 386/220 model in central computer cell of BWDB. Initially the programme was tested and run with single precision. To overcome the round off error the programme was subsequently written in double precision and the production run were made using this version. As a terminal user 2048 k storage area was allotted

to the author and no extra storage was necessary during execution of the programme.

The execution time for getting any one of the first five forms of output, mentioned earlier, was almost the same. It is observed that the execution time for an arch with nine rise-to-span ratios was 10 seconds from micro-computer ALR 386/220 model. The execution time for computation of permissible load capacity mainly depends on the allowable stresses in tension. It was 10 seconds from the above micro-computer for an arch when allowable limit of tensile stresses lies within 5.0 psi to 0.0 psi, While the same was 15 seconds if the allowable tensile stresses lies within 0.50 psi to 0.0 psi. It happens so because the number of iterations increases when the allowable tensile stresses varies within a short range.

The time requirement by the ALR 386/220 model micro-computer to compile this programme was 3 minutes including eighteen subroutine subprogramme along with the main programme. The compilation time was saved during production run by using the compiled version of the programme.

Flow Diagram

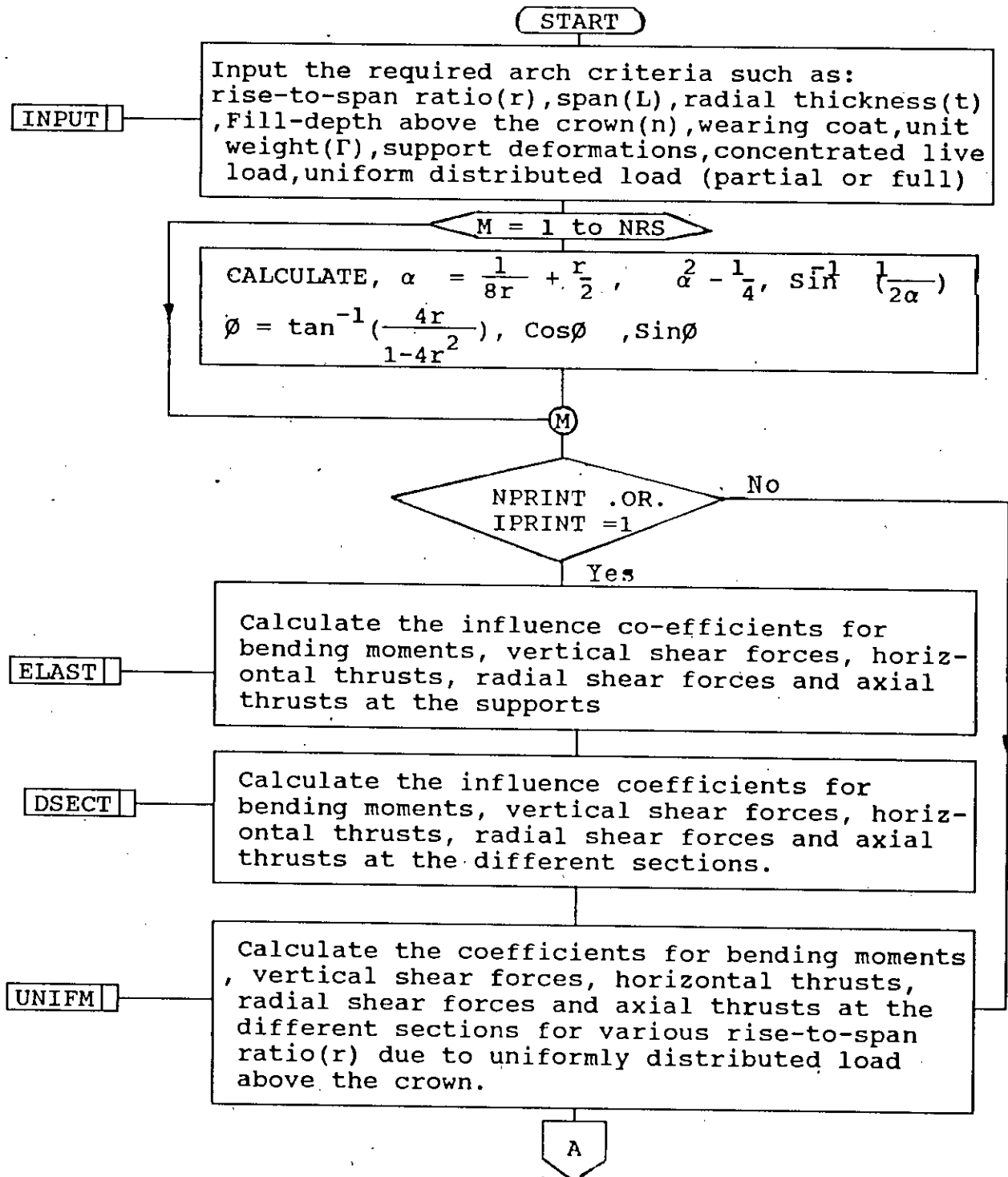
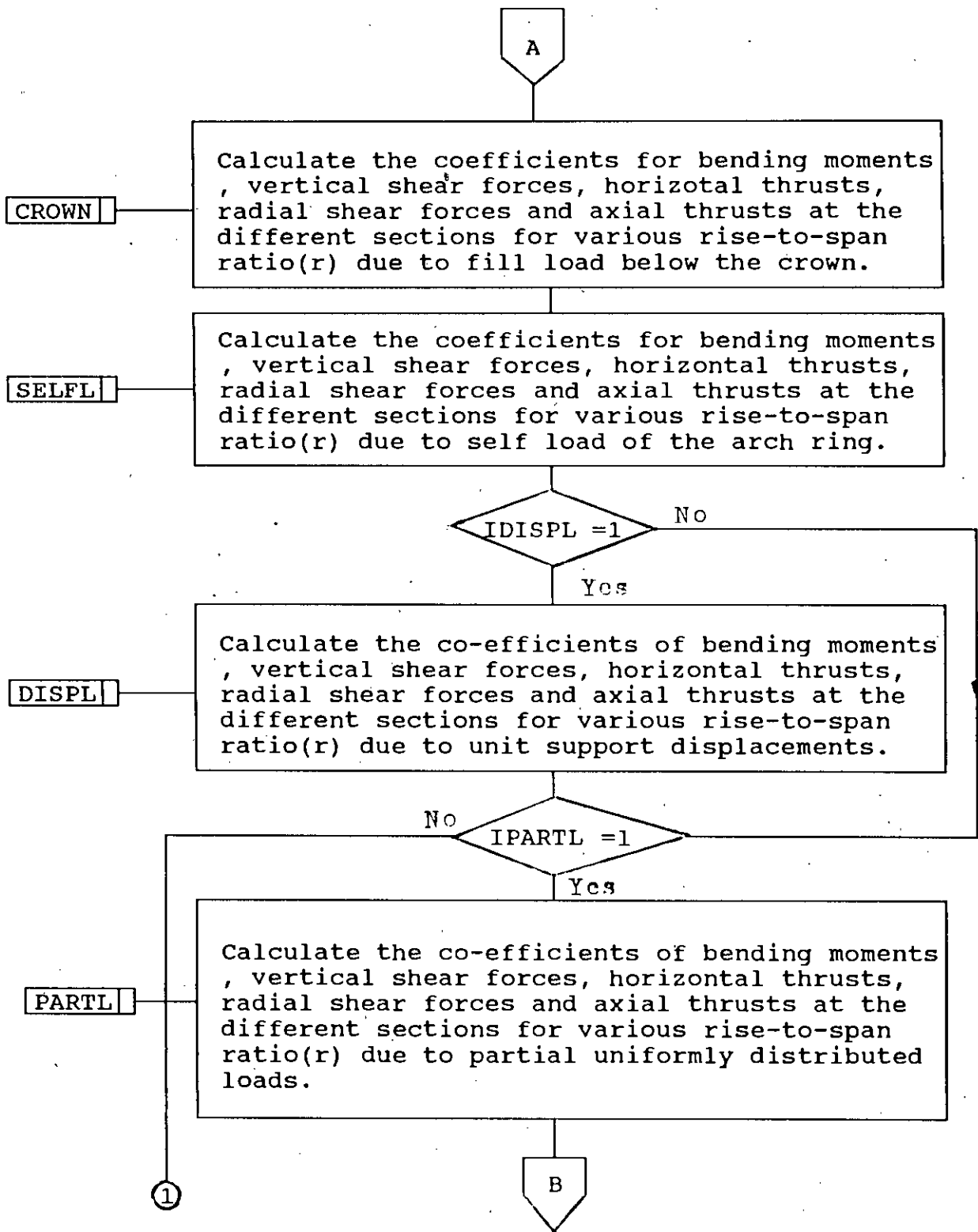
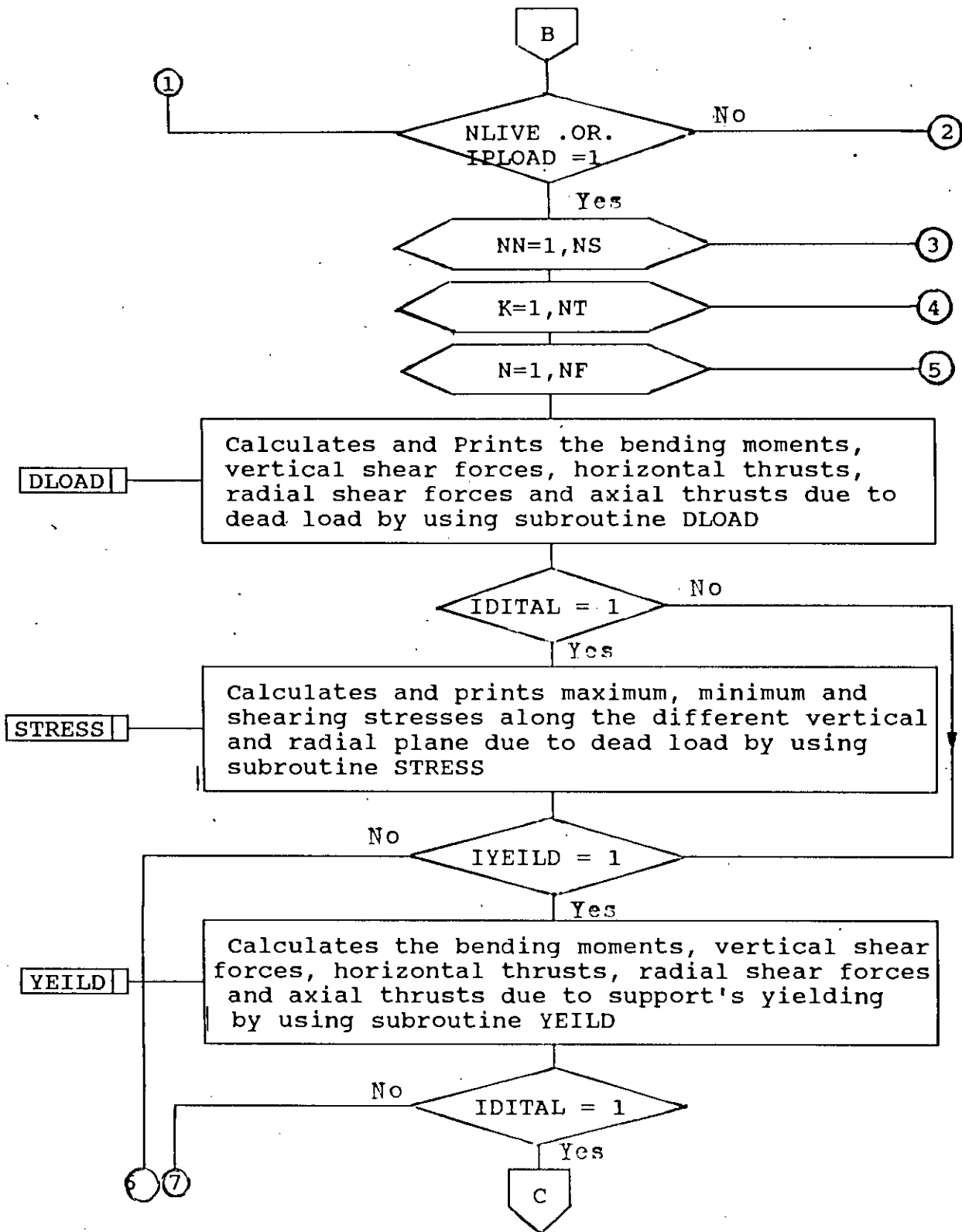


Fig. 4.2





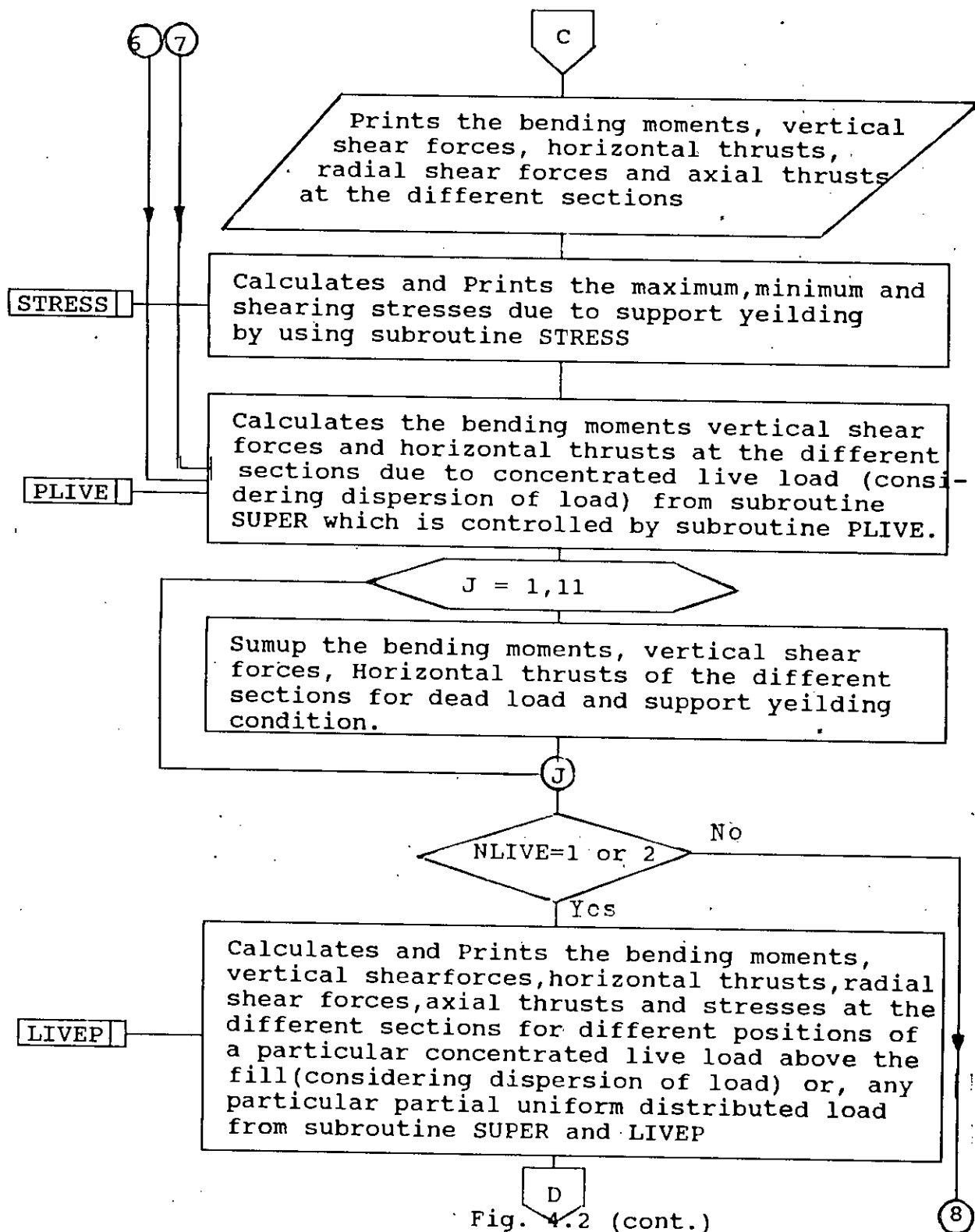


Fig. 4.2 (cont.)

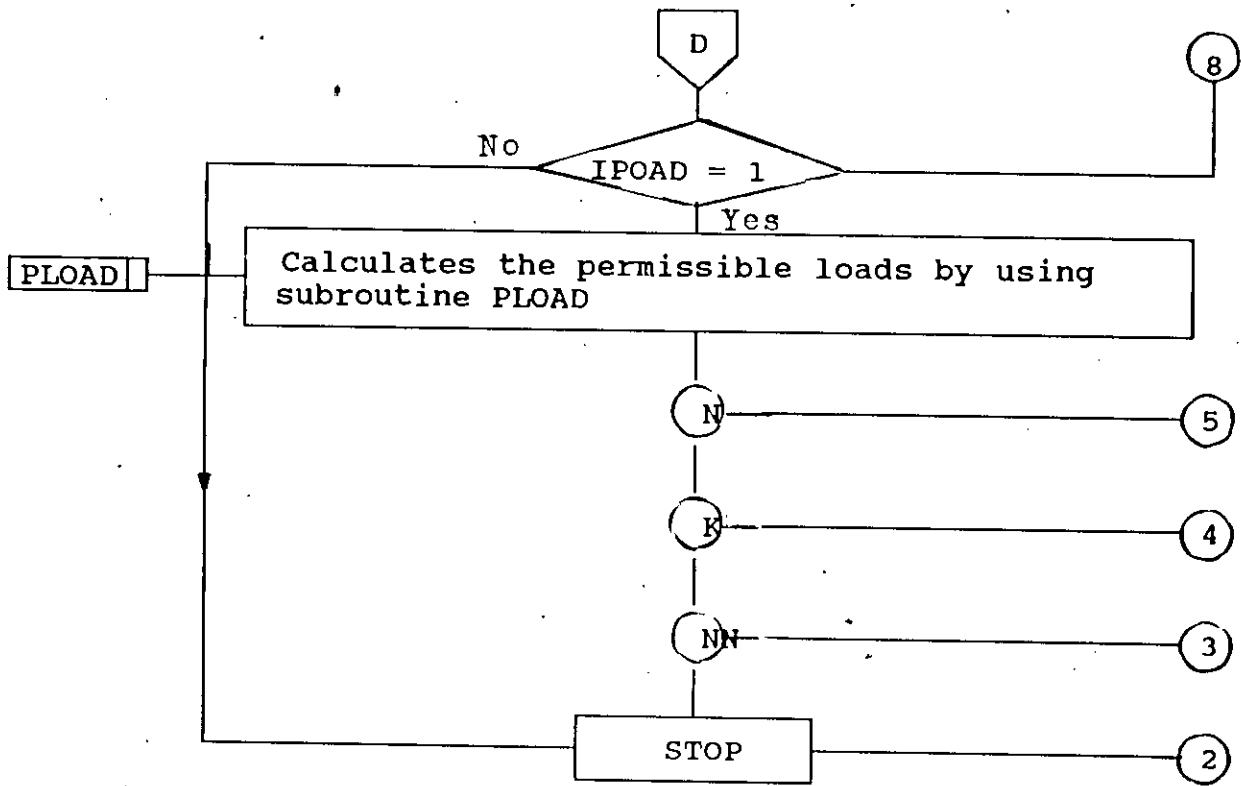


Fig. 4.2 (cont.)

CHAPTER-5

Influence tables and diagrams for arches

5.1 General

This chapter presents the influence coefficients due to a unit moving load and co-efficients of different force components due to various loading and support yielding conditions in graphical forms for the fixed circular arches. The influence co-efficients and different force components at the different sections were obtained using the numerical model developed and presented in chapter-4. The influence co-efficients and co-efficients of different force components are obtained from using main frame IBM 4331 computer of BUET computer centre. The output files then transferred to microcomputer and are printed in condensed form.

The graphical representation of the printed results shows the variation of the different force components with different arch parameters. All computation has been done for rise-to-span ratios(r) 0.05 to 0.45 at an increment of 0.05 due to various loading and support yielding conditions. The two sets of generalized equations have been derived for fill load (chapter-3) above and below the crown. The results obtained for these two types of fill loads are presented separately. A rapid change of negative

bending moments at crown section are observed at rise-to-span ratio 0.05 due to fill load below the crown and hence these are plotted for rise-to-span ratio 0.06 and 0.07.

The bending moments, vertical shear forces and horizontal thrusts have also been computed due to six different types of partial uniformly distributed loads for rise-to-span ratios (r) 0.05 to 0.45 at an increment of 0.05. They are : (i) loads over full span (ii) loads over left half span (iii) loads over left quarter span (iv) loads over second quarter span (v) loads over left three-fourth and (vi) loads over middle half span of the arch. Finally, the results obtained for bending moments, vertical shear forces, horizontal thrusts, radial shear forces and axial thrusts due to unit clockwise rotation, unit downward vertical displacement and unit outward horizontal displacement at the left support of an arch for the above rise-to-span ratios are presented. From these graphical representation, the worst type of loading for a particular rise-to-span ratio can be easily obtained.

It is intended that figures contained in this chapter, considerably shorten and simplifies the work in selecting an economical arch dimension and thus considerable saving in time is gained. Detail descriptions of tabular and graphical represented of the result has made in next two article. Some important observations have been made in article (5.4).

The sign conventions used in analysis for support displacements, support reactions and force components at the different sections are illustrated in Fig. 5.2.1.

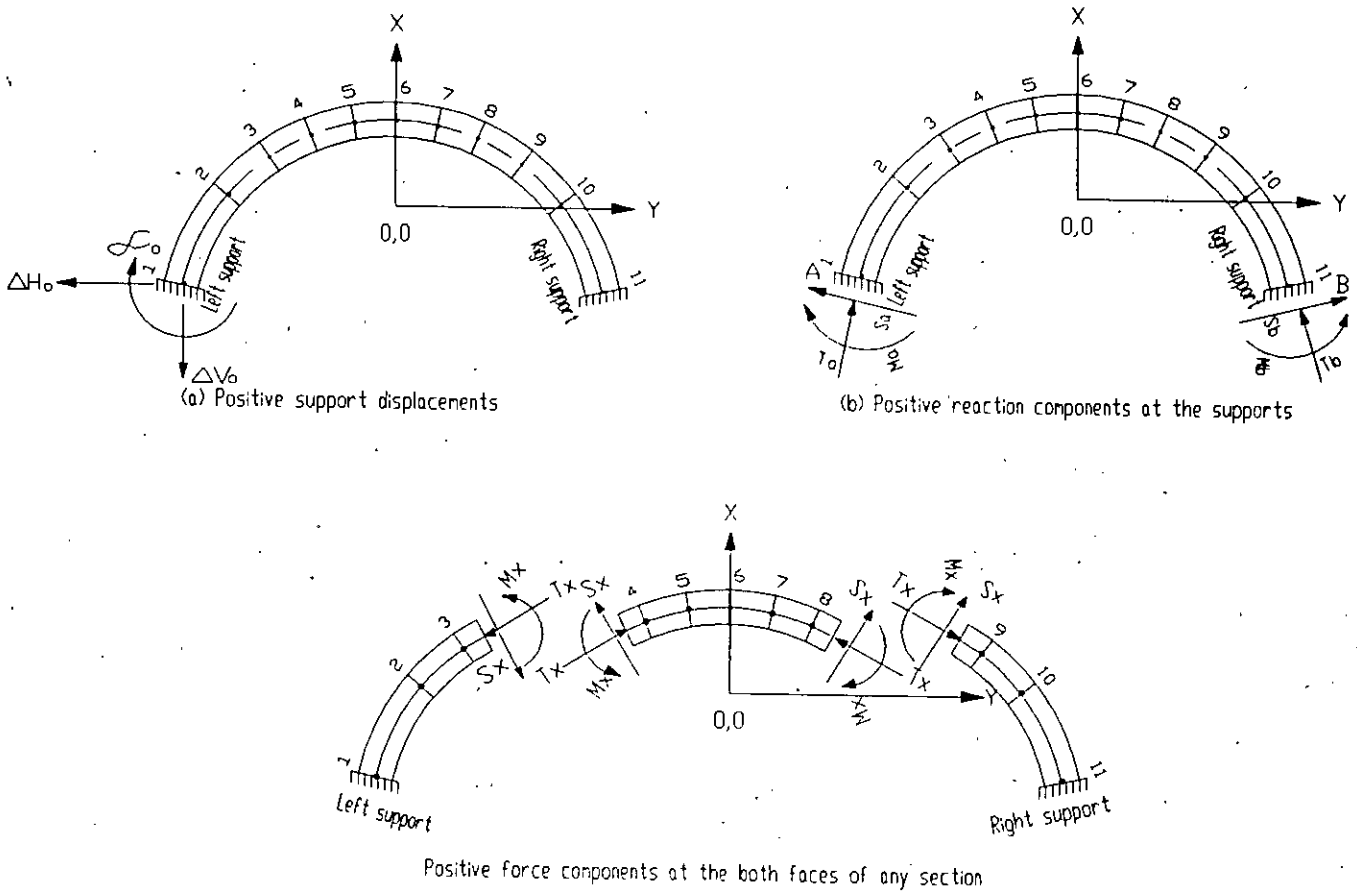


Fig. 5.2.1 Sign convention

5.2 Introduction to Tables

The influence tables for different force components are obtained based on elastic centre method. The co-efficients of different force components due to different loading and support yielding conditions are also obtained in tabulation forms. These computer printed tables presented in Appendix A.1 are arranged in following order :

(a) The influence tables for different force components at the left support and at the right face of eleven sections of an arch due to a moving unit load are presented in Table A.1 to A.50.

(b) Tables showing the values of different force components at different sections of an arch due to self load of the arch of unit radial thickness, fill load above and below the crown are given in Table A.51 to A.65.

(c) The co-efficient of different force components at the different sections due to six different forms of partial uniformly distributed load of unit intensity in Table A.66 to A.92.

(d) The co-efficient of different force components at the different sections due to different unit support displacements are also recorded in Table A.93 to A.105.

The tables in above cover the range of rise-to-span ratio of 0.05 to 0.45 at an increment of 0.05. The first row and second column of these tables indicate different section number and rise-to-span ratio.

74793

5.3 Introduction to Graphical representations

Computer printed results obtained in tabular form are also presented graphically in this chapter and in following order :

(a) Influence lines for bending moments, vertical shearforces and horizontal thrusts at the different sections for different rise-to-span ratios as in Fig. 5.1 to 5.12, 5.14.

(b) The variation of maximum positive bending moments at different sections due to unit load with different rise-to-span ratio as narrated in Fig.5.13.

(c) The variation of bending moments, vertical shear forces and horizontal thrusts with different rise-to-span ratios due to fill and self load of the arch ring as portrayed in Fig. 5.15 to 5.20.

Fig 5.21 to 5.22
(d) Variation of bending moments, vertical shear forces due to six different types of partial uniform distributed loads for rise-to-span ratio 0.05 to 0.45 at an increment of 0.05 as said in Fig. 5.21 to 5.22.

(e) The variation of horizontal thrusts due to above different partial uniform distributed loads with different rise-to-span ratio as given in Fig. 5.23.

(f) Fig. 5.24 to 5.30 indicates the effect of different support movements on bending moments, vertical shear forces and horizontal thrusts in arches of different rise-to-span ratios.

From these graphical display, the most worst possible cases under different loading and support yielding conditions can easily be predicted. Though the results for nine different rise-to-span ratios are available, some of the curves are not shown in the graph for clarity. The results for intermediate value of rise-to-span ratio may be interpolated, if necessary.

5.4 General discussion on the results

In this article some important observation have been discussed from the presented tabular and graphical forms of results. It can be observed from Fig. 5.1 to 5.3 that the variation of the influence co-efficients for bending moments and horizontal thrusts with rise-to-span ratio is significant while that for vertical reactions is negligible. The maximum negative and positive bending moment at the left support of an arch occurs due to the position of unit load at arround $.1L$ and $.38L$ away from the left and right support respectively(Fig. 5.1). The maximum negative bending moment decreases gardually with the increase of rise-to-span ratio while the corresponding position of the live load shifts towards the left support. The variation of the maximum positive bending moment with the rise-to-span ratio is relatively smaller and the corresponding location of the live load is almost fixed at around $0.38L$ away from the right support. It is further observed

that the bending moment at the left support becomes zero when the live load is at $0.1L$ away from the left for arch with rise-to-span ratio of 0.05 . The live load position causing zero bending moment shifts towards the left support with the increase of rise-to-span ratio.

The position of live load at the crown section (Fig. 5.3) gives the maximum horizontal thrust in fixed arches and it decreases with the increase of rise-to-span ratio. Again, the variation of the maximum thrust is observed to be rapid for lower rise-to-span ratios while it is gradual for higher rise-to-span ratio.

A parabolic variation of vertical shear force at the left support and at different sections is observed for different arches as illustrated in Fig. 5.2 and 5.14. The figures also indicate a negligible variation of vertical shear force with rise-to-span ratio.

The maximum axial thrust (Table A.4) at the left support occurs for rise-to-span ratio upto 0.20 while the load is at crown section and it decreases very rapidly with the increase of rise-to-span ratio. The maximum axial thrust at the left support of an arch for rise-to-span ratio 0.25 occurs due to the position of live load at $.4L$ away from the left support. For rise-to-span ratio greater than 0.25 , the live load position at the left springing point causes the maximum axial thrust at the left support and it

increases gradually with the increase of rise-to-span ratio. It may be concluded from the above influence table that the arch of rise-to-span ratio 0.30 gives a comparatively smaller axial thrust at the supports. The maximum axial thrust at any section (Table A.9, A.14 and A.19) for flatter arches occurs at the support while the live load position is at crown section. But the position of live load causing maximum axial thrust gradually shifts towards the corresponding section (Table A.24, A.29, A.34, A.39, A.44 and A.49) at higher rise-to-span ratio.

It may be mentioned from table A.5 that the maximum radial shear force of an arch occurs at the left support while the live load is at the corresponding left support for lower rise-to-span ratio. This maximum shear force influence decreases gradually with the gradual movement of live load from left support to right support. The live load position at $0.80L$ away from the left support causes maximum negative shear force at the left support for rise-to-span ratio upto 0.40.

Fig. 5.4 to 5.12 indicate that the maximum positive bending moment due to concentrated live load at a section of an arch occurs while the live load is at the corresponding section. The positive bending moment at any section increases gradually with the increase of rise-to-span ratio as shown in Fig. 5.13. In the figure it is also observed that the positive bending moment occurs at section four (nearer to the quarter span section) for arches of rise-to-

span ratio upto 0.38 which shifts towards the crown for arches with higher rise-to-span ratio. Fig. 5.15 and 5.18 display the similar types of variation of bending moment due to the uniformly distributed fill load above the crown and self load of the arch. The maximum positive bending moment occurs at supports and at crown and maximum negative bending moment occurs at section around $0.15L$ away from the left and right support of the arch. Both the maximum positive and negative bending moment increase with the increase of rise-to-span ratio. It is observed that the positive bending moment at the supports increases at a faster rate than that at other sections. It is further observed that the location of maximum negative moment gradually shifts towards the supports with the increase of rise-to-span ratio. The point of contraflexures are observed to occur at sections around $0.30L$ away from the supports which gradually shifts towards the supports with the increase of rise-to-span ratio. The maximum negative bending moment (Fig. 5.16) due to fill load below the crown occurs at the supports and it increases at a faster rate with the increase of rise-to-span ratio. The negative bending moment also occurs at the crown section for arches with rise-to-span ratio greater than 0.08. The positive bending moment has been observed at the crown section for flatter arches. The arch of rise-to-span ratio 0.05 gives a very high positive bending moment at the crown section. On the other hand, the arch of rise-to-span ratio greater than 0.10 gives the maximum

positive bending moment at section around $0.35L$ away from support which gradually reduces with the decrease of rise-to-span ratio.

A very high horizontal thrust (Fig. 5.20) develops due to uniformly distributed fill load above the crown and self load of the arch for flatter arches but decreases sharply with the increase of rise-to-span ratio. From the above figure, it is also observed that the maximum thrust due to fill load below the crown occurs for rise-to-span ratio 0.15. The horizontal thrust decreases gradually for arches with rise-to-span ratio greater than 0.15 and abruptly for arches with rise-to-span ratio lower than 0.15.

Fill load below the crown increases gradually towards the support with the increase of rise-to-span ratio of arches, consequently vertical shear force in Fig. 5.17 increases towards the supports with the increase of corresponding rise-to-span ratio. The vertical shear force in Fig. 5.19 due to self load of the arch ring shows almost linear variation for flatter arches which gradually increases, showing a parabolic variation over the span, with the increase of rise-to-span ratio.

The maximum axial thrust (Table A.54 and A.64) due to uniformly distributed load above the crown or self load of the arch occurs at supports and it decreases gradually towards the crown. It is also observed from the above tables that the axial thrust decreases with the increase of rise-to-span ratio. The maximum axial thrust (Table A.59) due to fill load below the crown occurs

at the supports and it gradually increases with the increase of rise-to-span ratio.

Values of different force components due to six different type of partial uniformly distributed loads at eleven sections of arches with different rise-to-span ratio are presented in Table A.66 to A.92. These values are plotted in Fig. 5.21 to 5.23 but only for the arch with rise-to-span ratio 0.25. Figure 5.21 illustrates the typical bending moment over an arch due to six different types of partial uniformly distributed loads. From the Fig. 5.21 and Tables A.66, A.69, A.72, A.75, A.78, A.78, A.81, A.84, A.87 and A.90, it can be observed that the greatest positive bending moment in an arch due to the above six partial uniformly distributed loads always occurs at the right support. But it is caused due to the uniform load spread over left half span for arches with rise-to-span ratio upto 0.20 and due to the load spread over left three-fourth span for arches with rise-to-span ratio more than 0.20. It can further be observed that the greatest negative bending moment occurs at the left support for arches with rise-to-span ratio upto 0.30. But for arches with rise-to-span ratio upto 0.20 it is caused due to the distributed load spread over left half span and for arches having rise-to-span ratio within 0.20 to 0.30 it is caused by the load spread over left quarter span. For arches with rise-to-span ratio more than 0.30 the negative bending moment at the second location becomes greatest and it is caused due to the

uniform load spread over left three-fourth span.

Fig. 5.23 illustrates the variation of horizontal thrust in arches with the rise-to-span ratio for six cases of partial uniformly distributed loads. In an arch the load distributed over the full span develops higher horizontal thrusts while distributed load over the left quarter span gives the smallest horizontal thrust. It may be concluded from the above figure that the horizontal thrust mainly depends on the location and total amount of load over the span.

Fig. 5.22 reveals that the maximum vertical shear force in arches occurs at the supports due to the distributed load over the full span, as expected.

It is observed from Fig. 5.24 that the maximum negative moment of an arch due to clockwise rotation of the left support occurs at section around $0.6L$ away from left support of the arch and it increases gradually with the decrease of rise-to-span ratio. Due the induced rotation at the left support, the maximum positive bending moment develops at the left support which is almost three times higher than the positive moment developed at the right support. Both the positive and negative bending moment gradually increase with the decrease of rise-to-span ratio. It is further observed that the above support deformation develops the constant negative bending moment in arches at a section $0.38L$ and $0.18L$ away from left and right support of the arch respectively. The point of

contrafluxares are observed to occur at the both side, which gradually shifts towards the supports with the increase of rise-to-span ratio.

Fig. 5.27 shows a symmetrical linear variation of bending moment for arches due to vertical support displacements. Both the positive and negative bending moment occurs at the springing and it gradually decreases with the increase of rise-to-span ratio. The symmetrical bending moments(Fig. 5.29) are also observed in arches due to horizontal support displacement. The maximum negative and positive bending moment occurs at springing and crown section respectively and are observed to increase with the decrease of rise-to-span ratio but with a higher rate for flatter arches. It is also observed that the points of contrafluxare occur at around $0.2L$ away from supports and gradually shift towards the crown with the decrease of rise-to-span ratio. From Fig. 5.27 and 5.29, it may be concluded that the horizontal support displacement is much more critical than vertical support displacement.

Fig. 5.25 and 5.28 show that the vertical shear force in an arch due to end rotation or vertical support displacement gradually decreases with the increase of rise-to-span ratio. The variation can be observed to be non-linear for flatter arches and almost linear and at comparatively higher rate for arches with higher rise-to-span ratio. It is illustrated in Fig. 5.26 and 5.30 that the arch of lower rise-to-span ratio gives a very high horizontal

thrust due to end rotation or horizontal support displacement but decreases sharply with the increase of rise-to-span ratio and the rate of variation becomes flatter for arches with higher rise-to-span ratio.

It is illustrated from table A.96 that a very high axial thrust develops due to clockwise rotation at the left support for flatter arches and it decreases rapidly with the increase of rise-to-span ratio. But a gradual variation of axial thrusts is observed at higher rise-to-span ratio. It is also observed that a negative axial thrust at the left springing occurs for rise-to-span ratio 0.40 and 0.45. The outward horizontal support displacement causes a constant axial thrust over the span (Table A.104) and it decreases very rapidly with the increase of rise-to-span ratio. From the above tables, it may be concluded that the outward horizontal support displacement is much more critical than the vertical support displacement.

The clockwise rotation of the left support (Table A.97) develops maximum positive radial shear force at $0.6L$ away from the left support. It is also observed from above table that the maximum negative radial shear force occurs at the left support and it decreases gradually with the increase of rise-to-span ratio. The high radial shear force at the supports for flatter arches under horizontal support displacements decreases sharply with the increase of rise-to-span ratio.

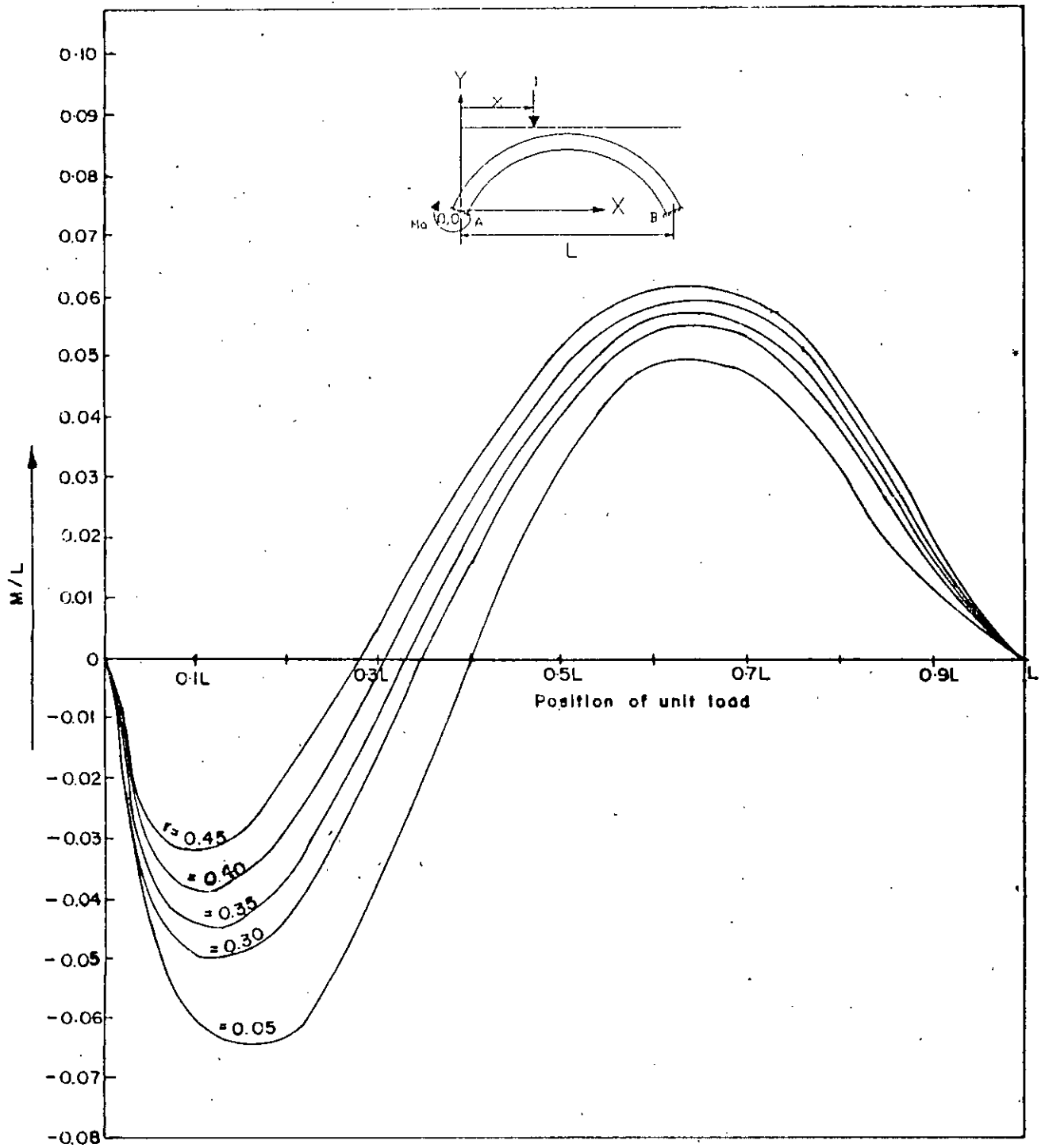


Fig. 5-1 Influence line diagrams for Bending moment at left springing for different rise to span ratio (r).

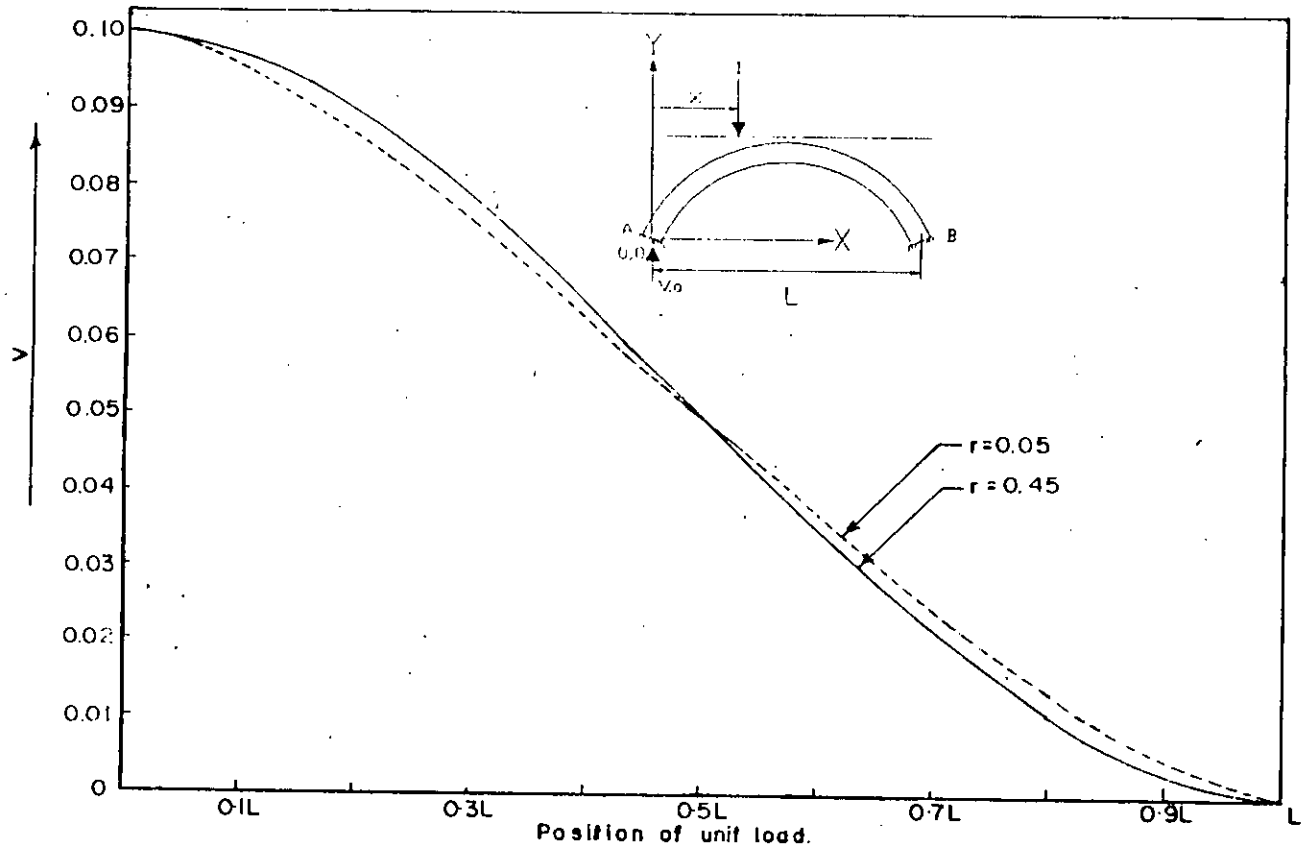


Fig. 5-2 Influence line diagrams for vertical reaction at left spring for different rise-to-span ratio(r).

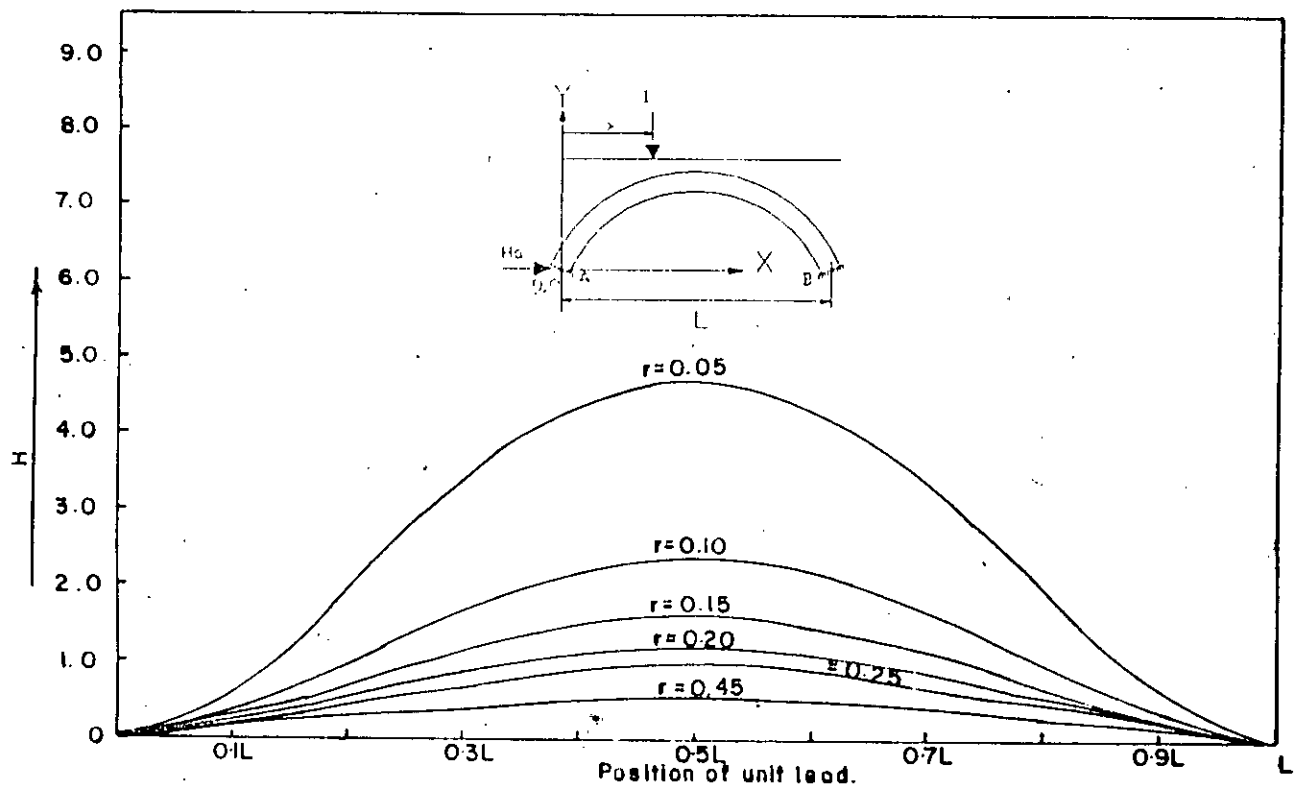


Fig. 5-3 Influence line diagrams for Horizontal thrust at left spring for different rise-to-span ratio (r).

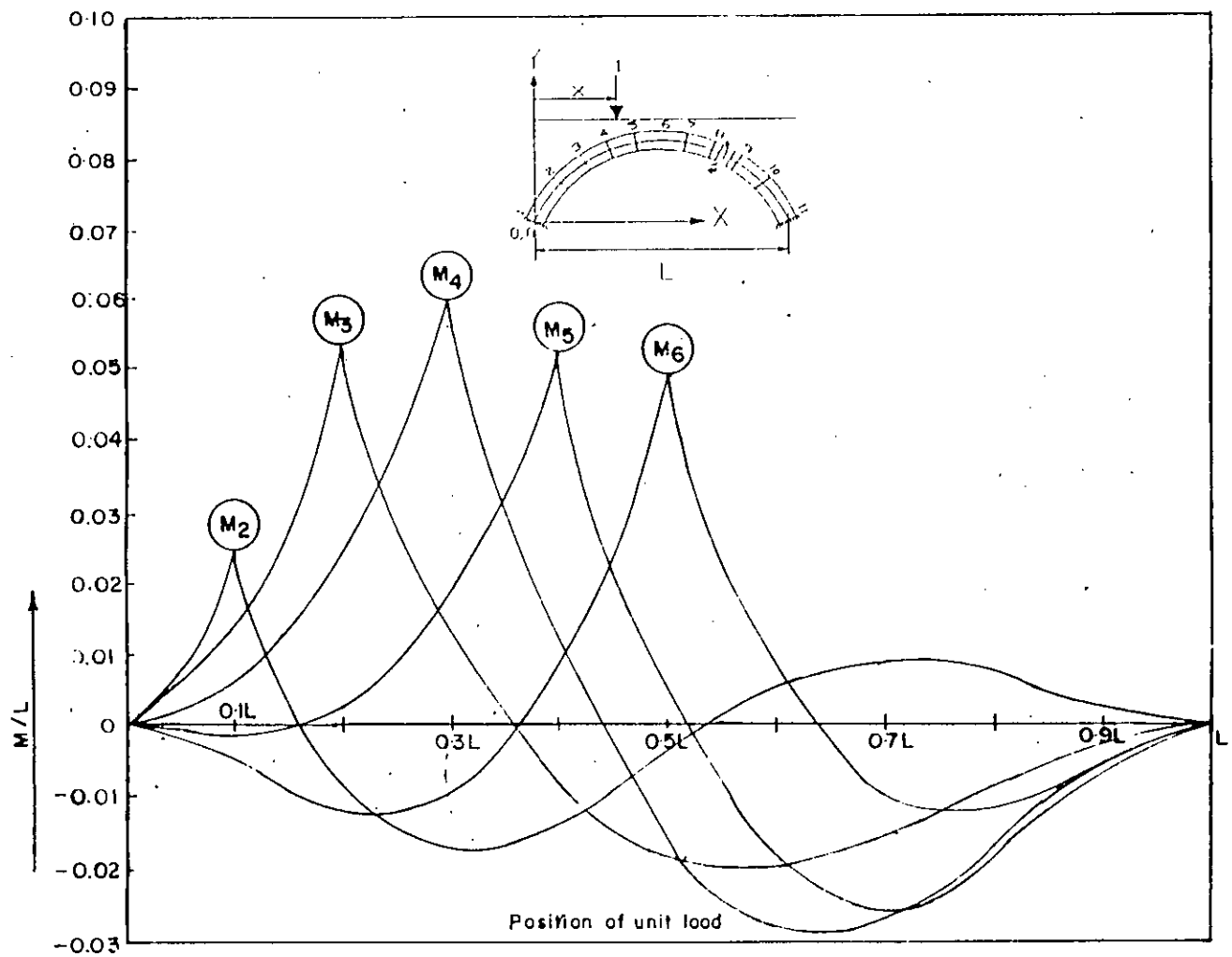


Fig. 5.4 Influence line diagrams for bending moment at different section for rise-to-span ratio (r) = 0.05

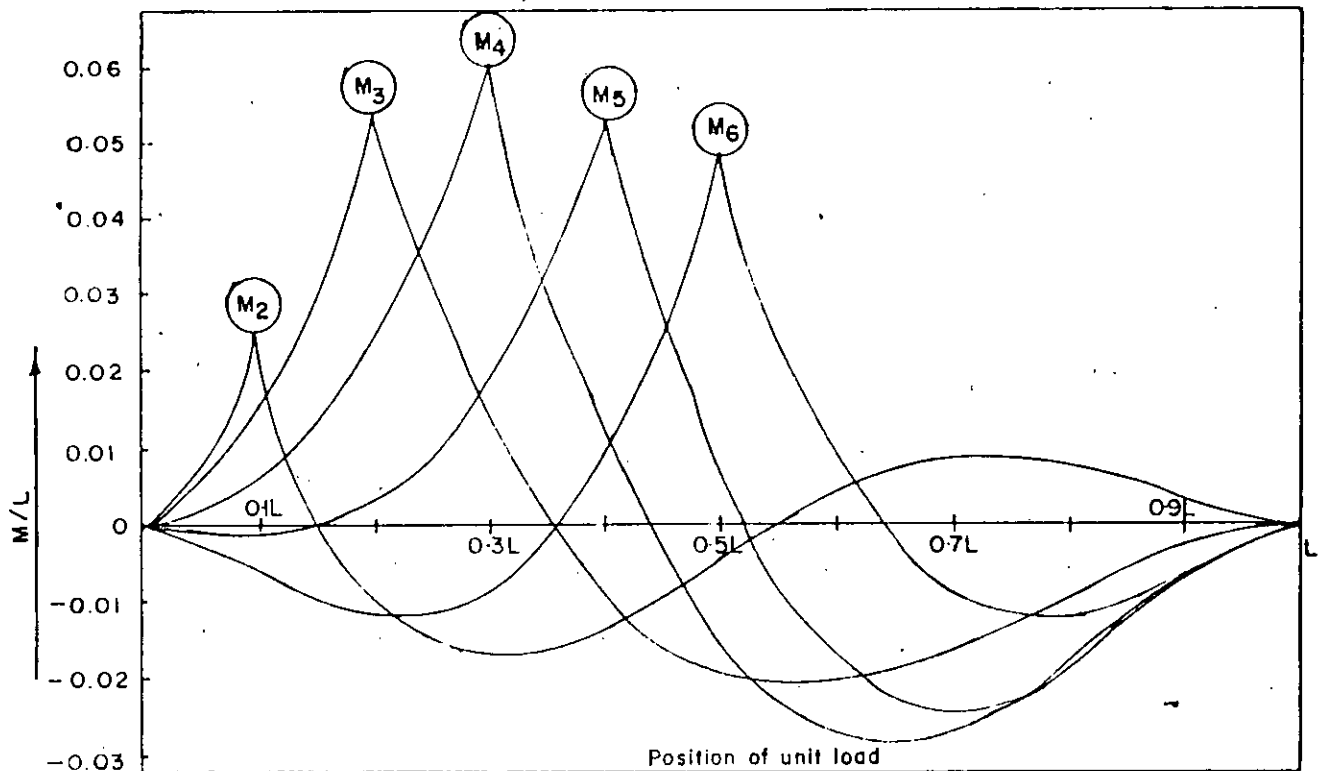


Fig. 5.5 Influence line diagrams for bending moment at different section for rise-to-span ratio (r) = 0.10.

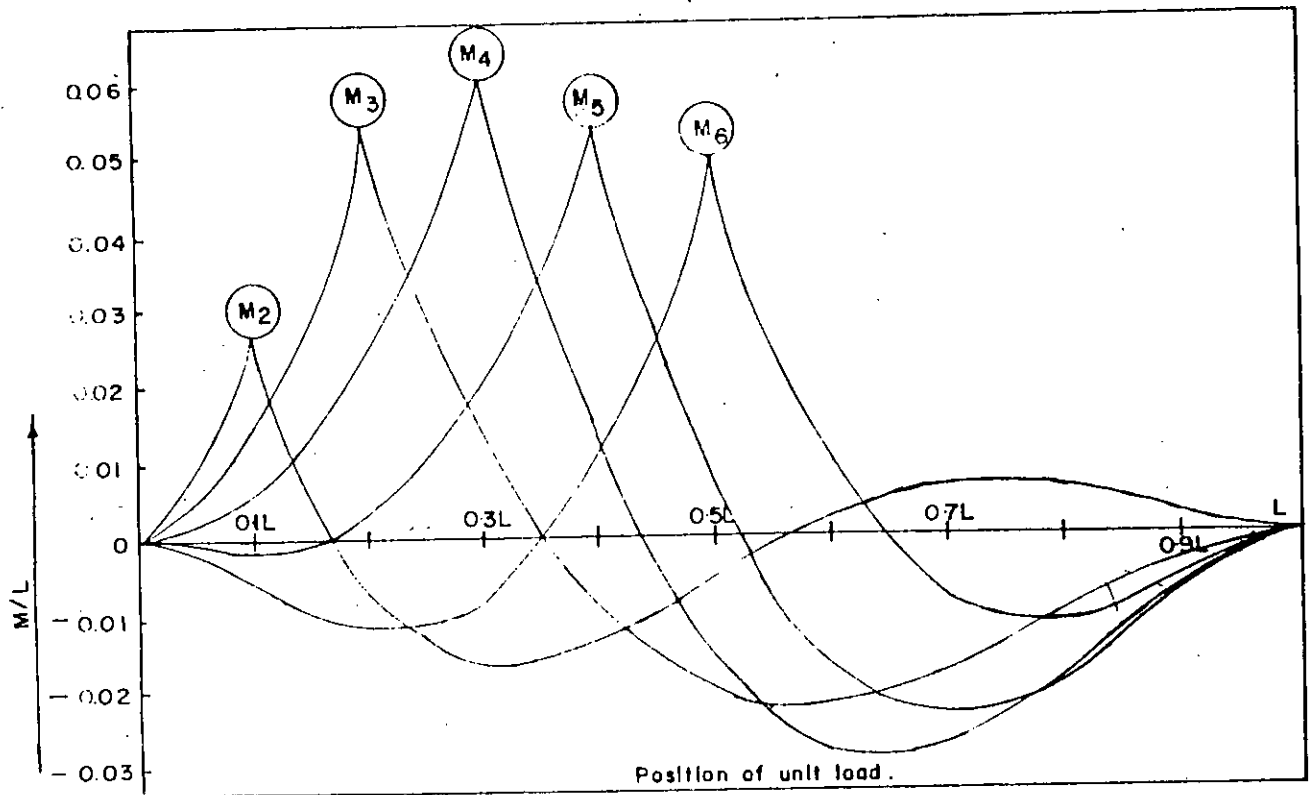


Fig. 5-6 Influence line diagrams for bending moment at different section for rise-to-span ratio (r) = 0.15

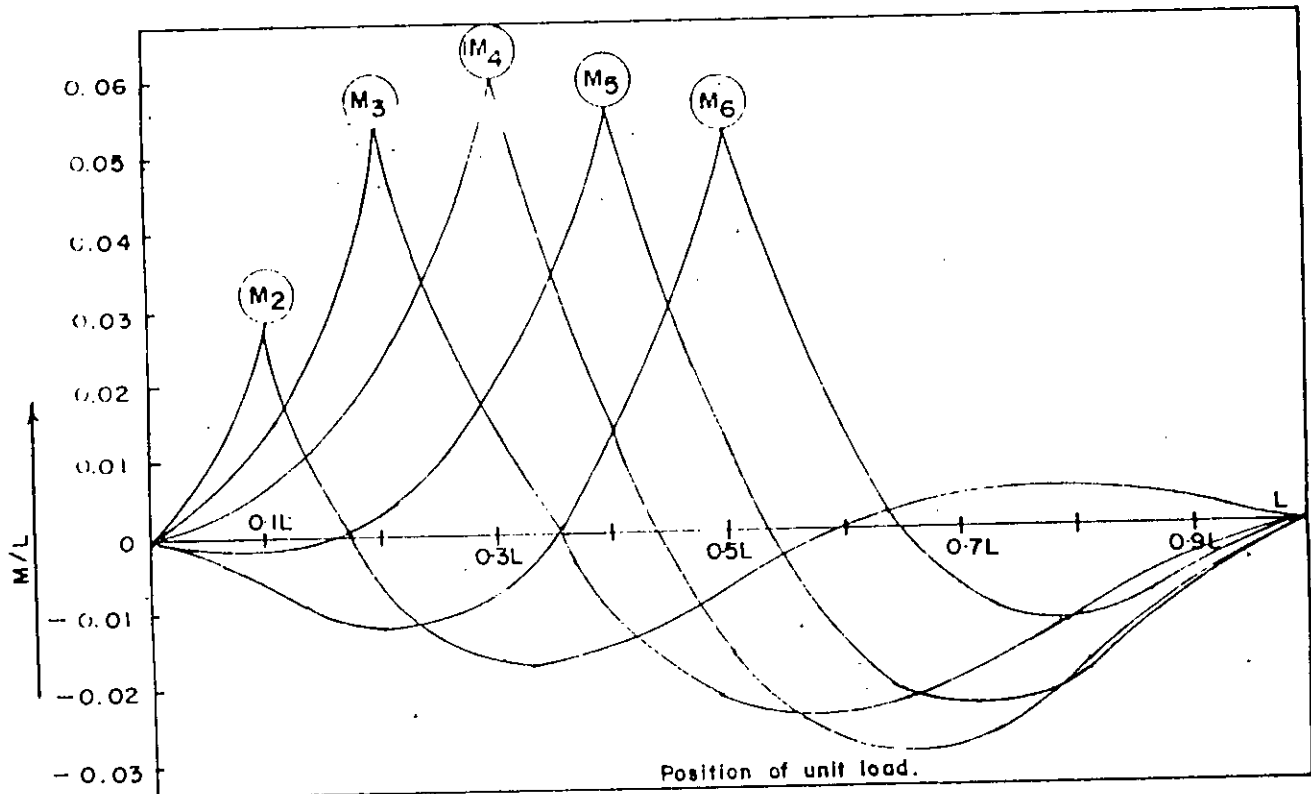


Fig. 5-7 Influence line diagrams for bending moment at different section for rise-to-span ratio (r) = 0.20.

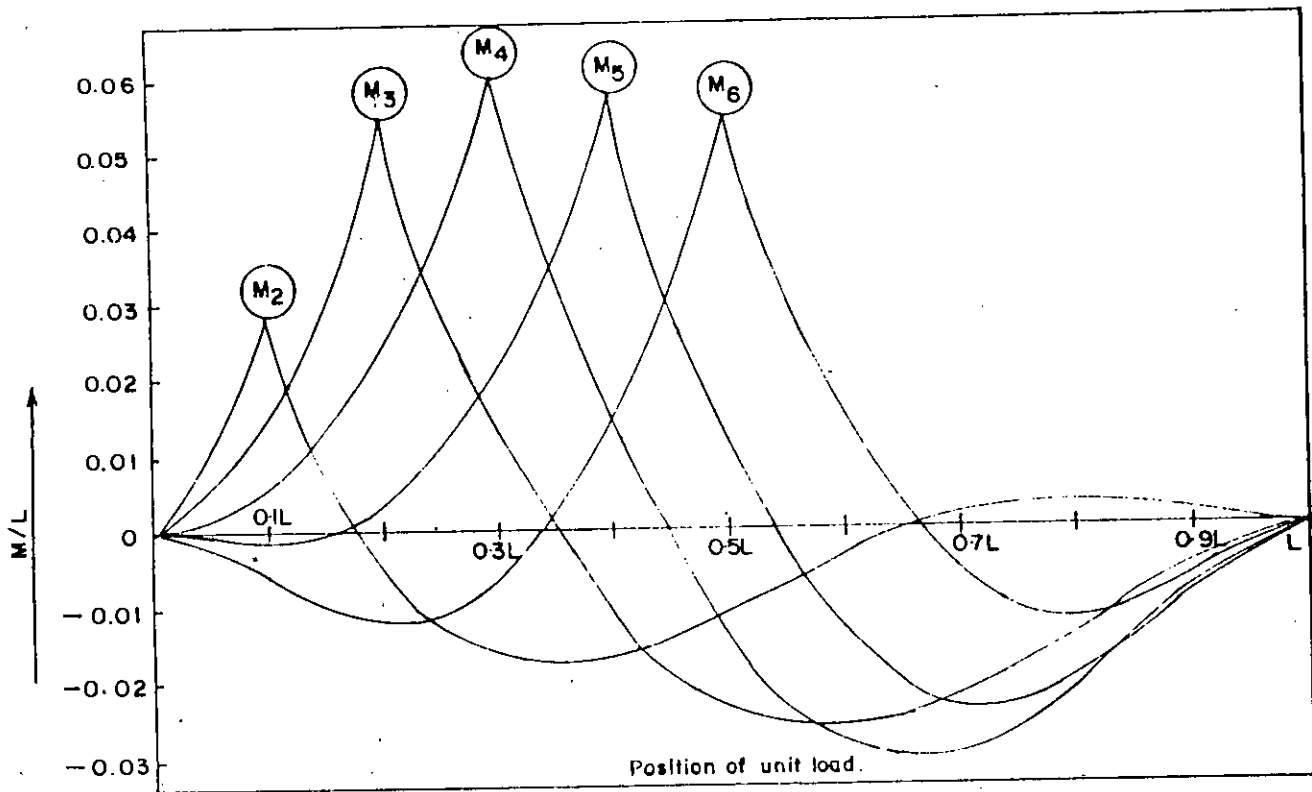


Fig. 5-8 Influence line diagrams for bending moment at different section for rise-to-span ratio (r) = 0.25.

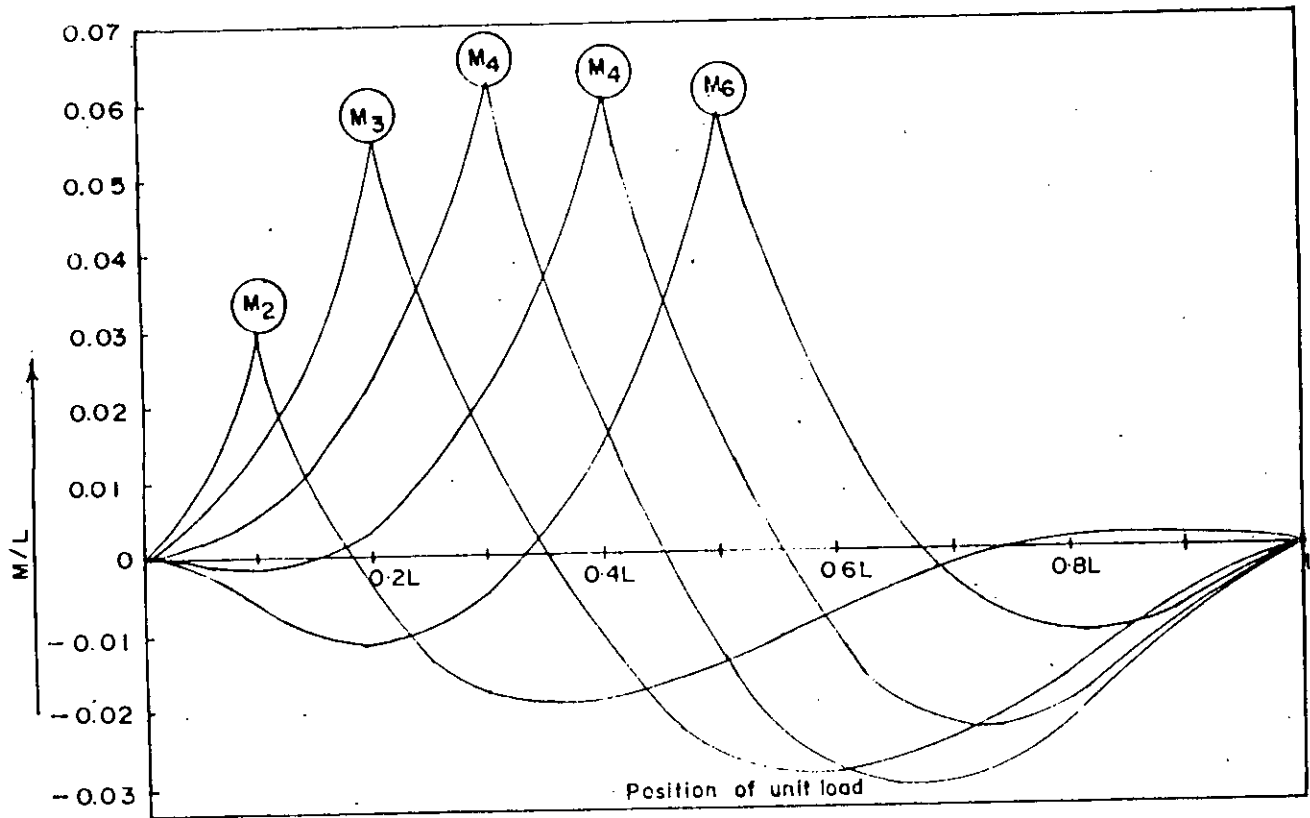


Fig. 5-9 Influence line diagrams for bending moment at different section for rise-to-span ratio (r) = 0.30.

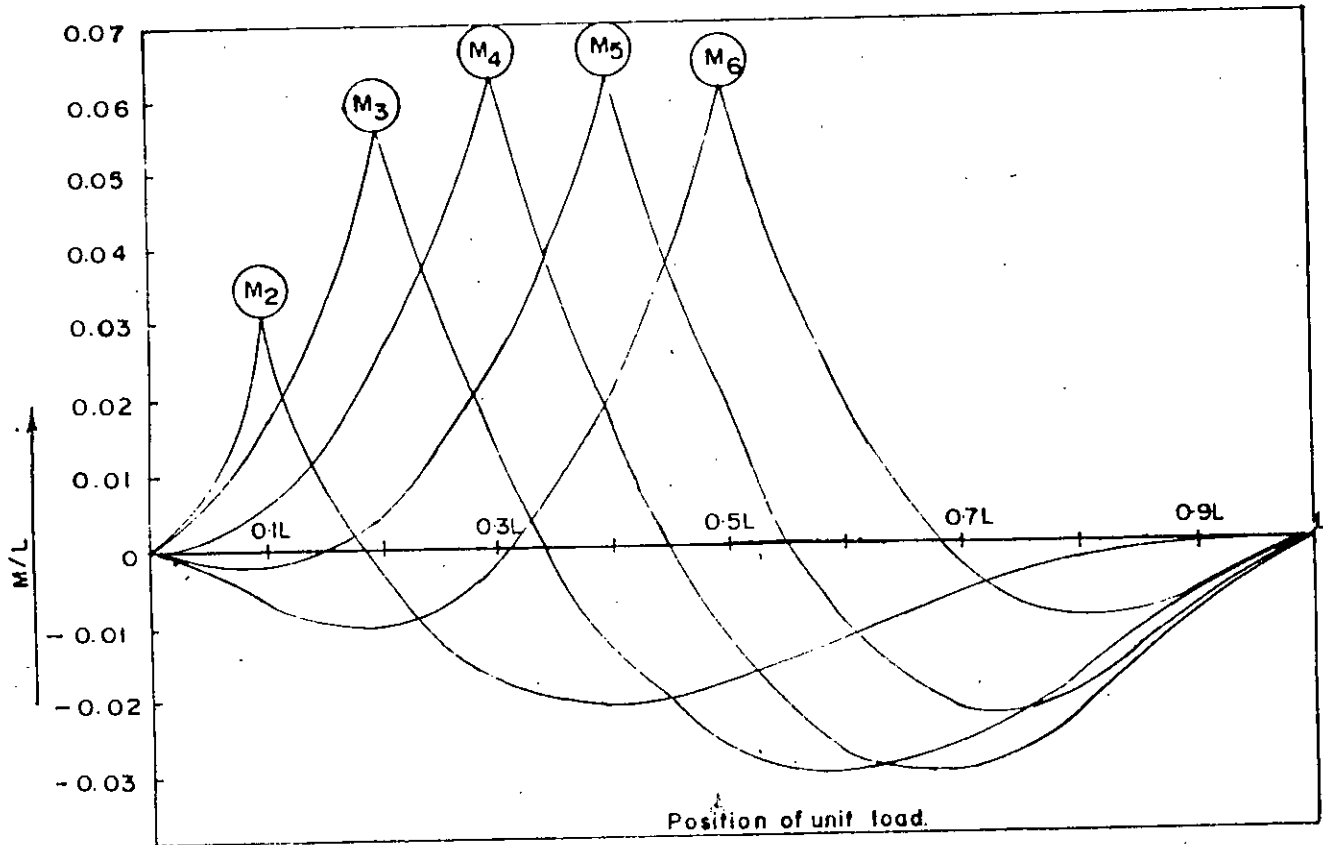


Fig. 5-10 Influence line diagrams for bending moment at different section for rise-to-span ratio (r) = 0.35.

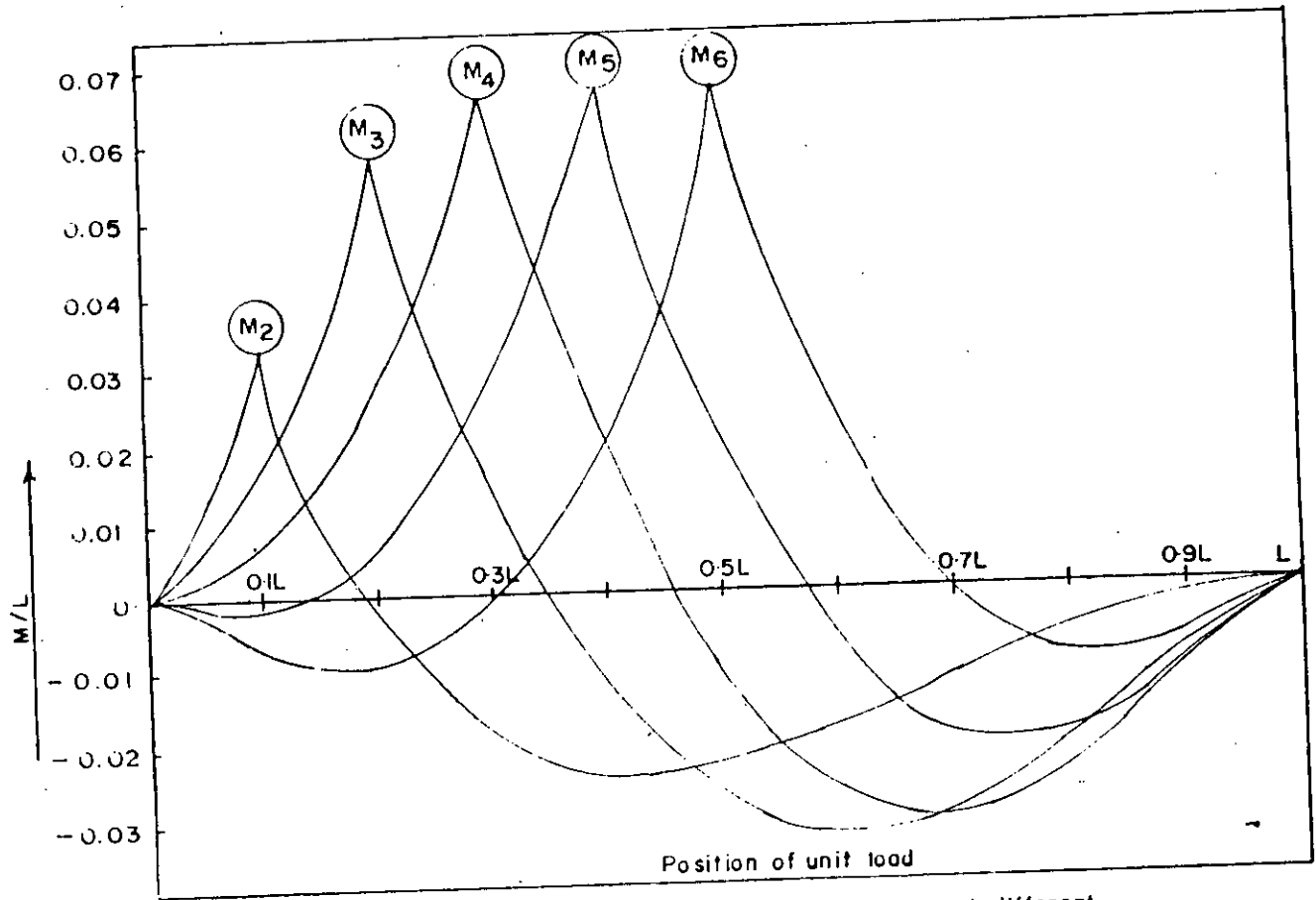


Fig. 5-11 Influence line diagrams for bending moment at different section for rise-to-span ratio (r) = 0.40

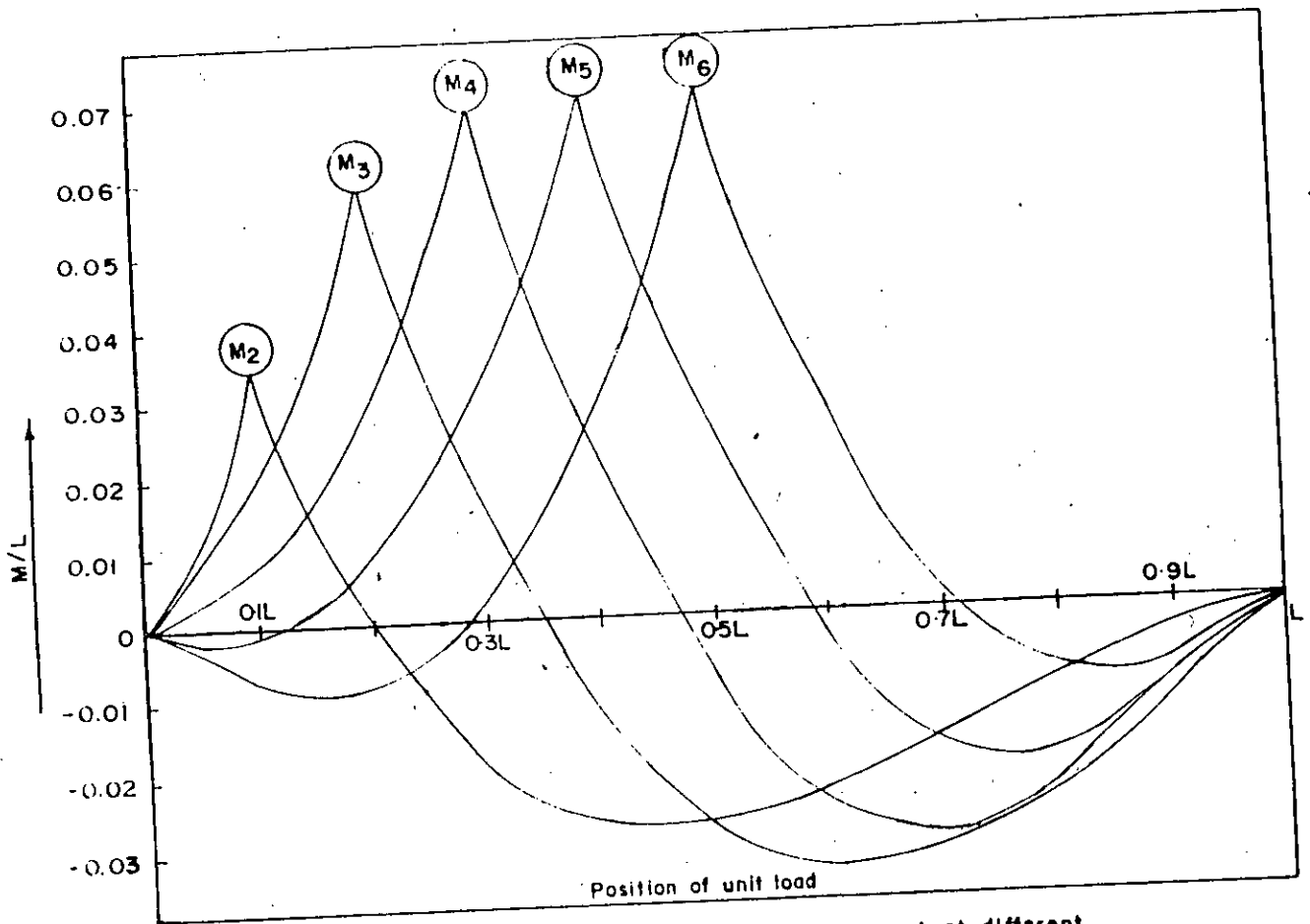


Fig. 5-12 Influence line diagrams for bending moment at different section for rise-to-span ratio (r) = 0.45

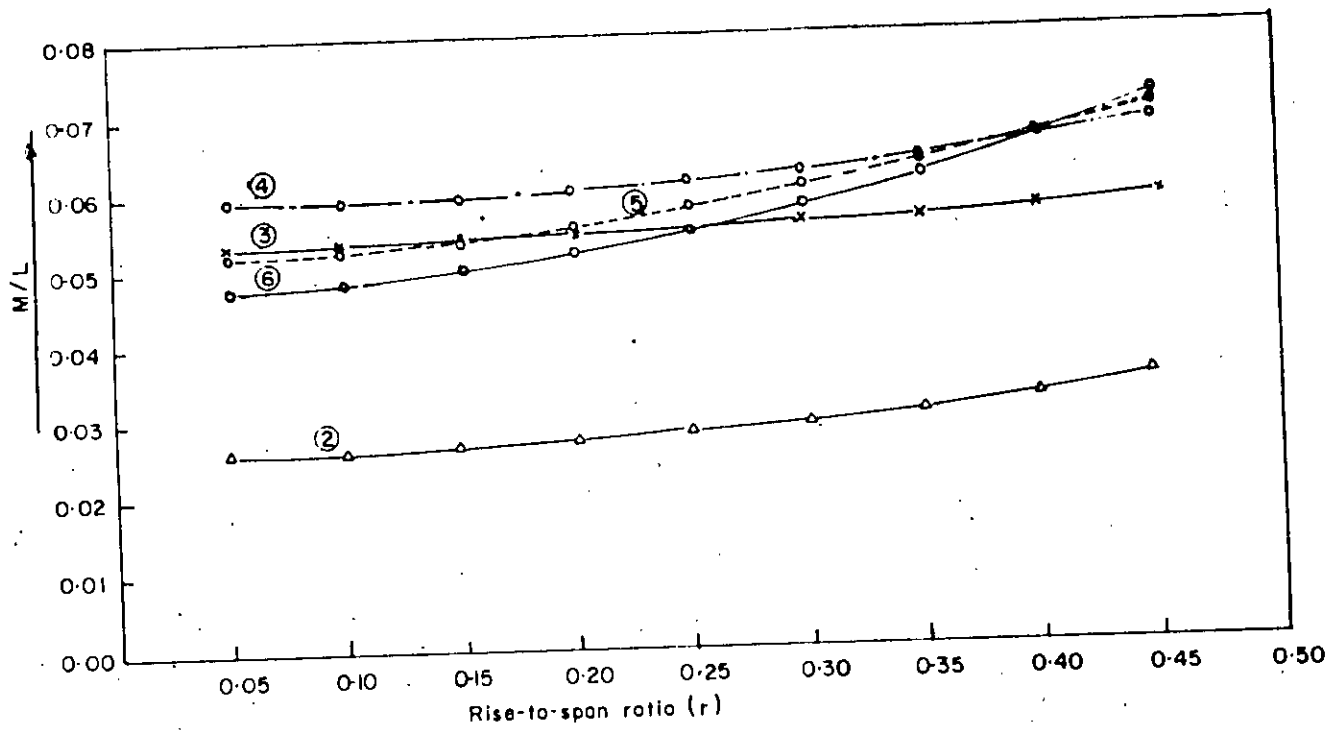


Fig. - 5-13 Variation of maximum +ve bending moments at different sections with different rise-to-span ratios.

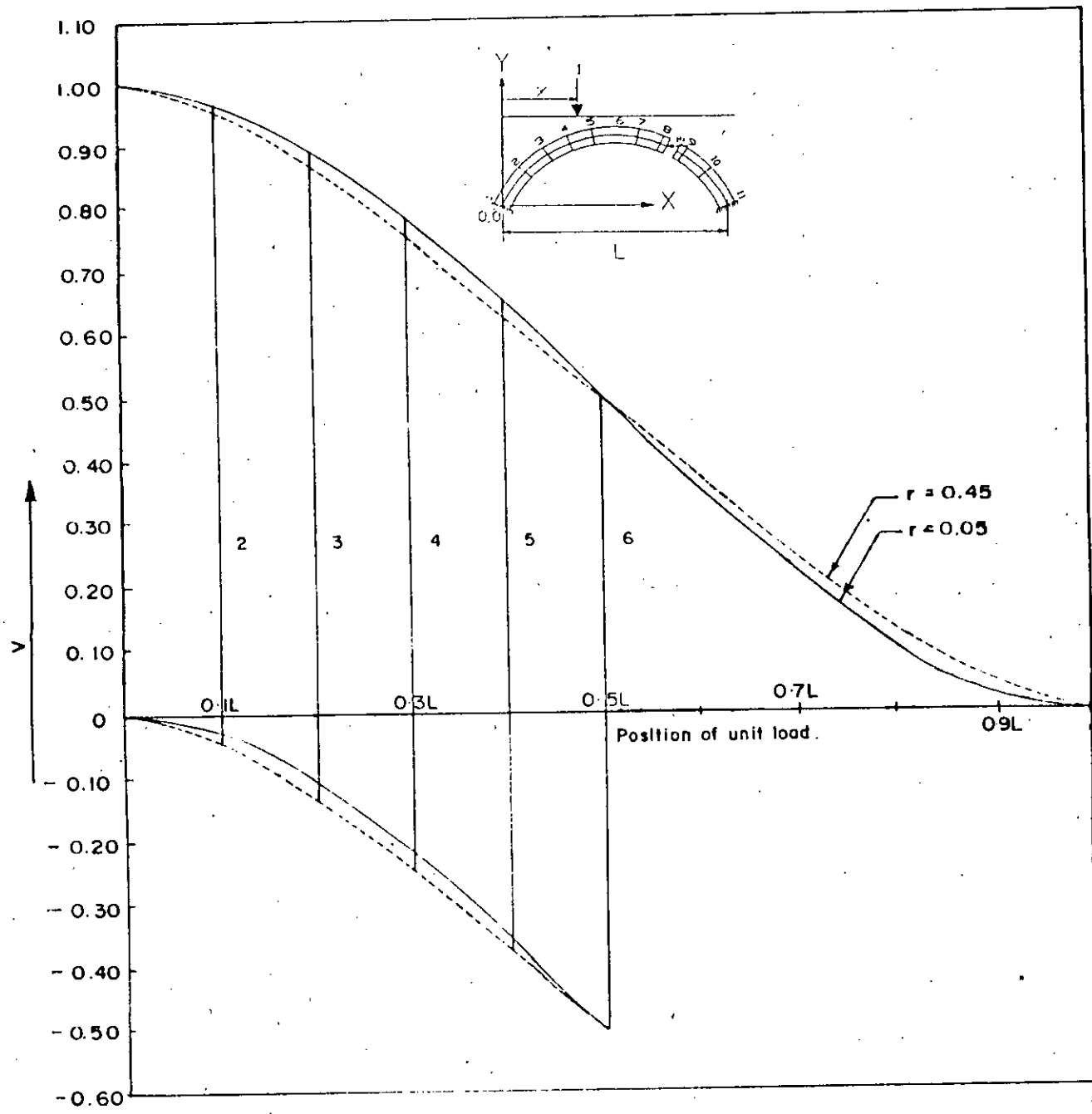


Fig. 5-14 Influence line diagrams for vertical shear force at different sections for different rise-to-span ratio (r).

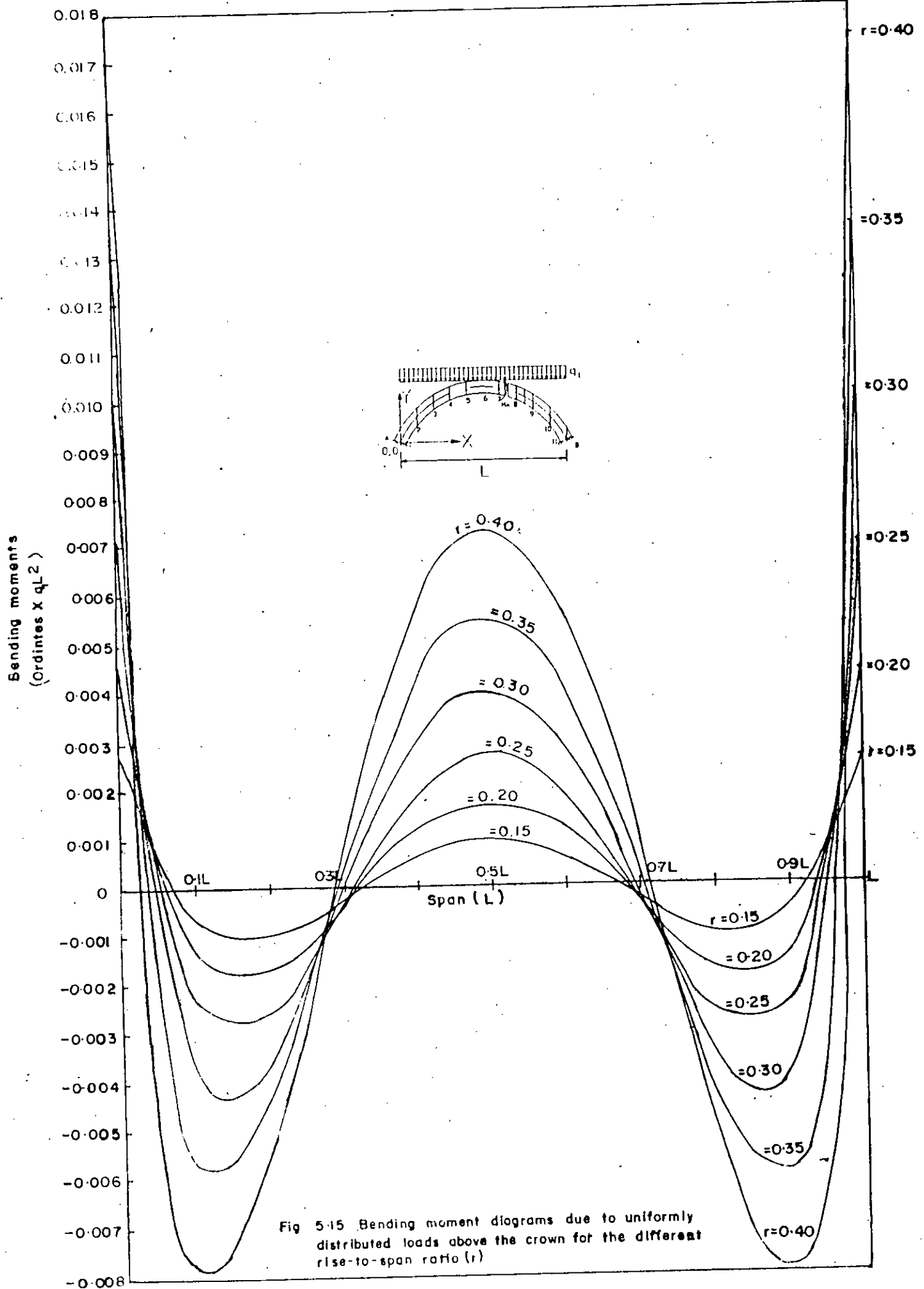


Fig 5.15 Bending moment diagrams due to uniformly distributed loads above the crown for the different rise-to-span ratio (r)

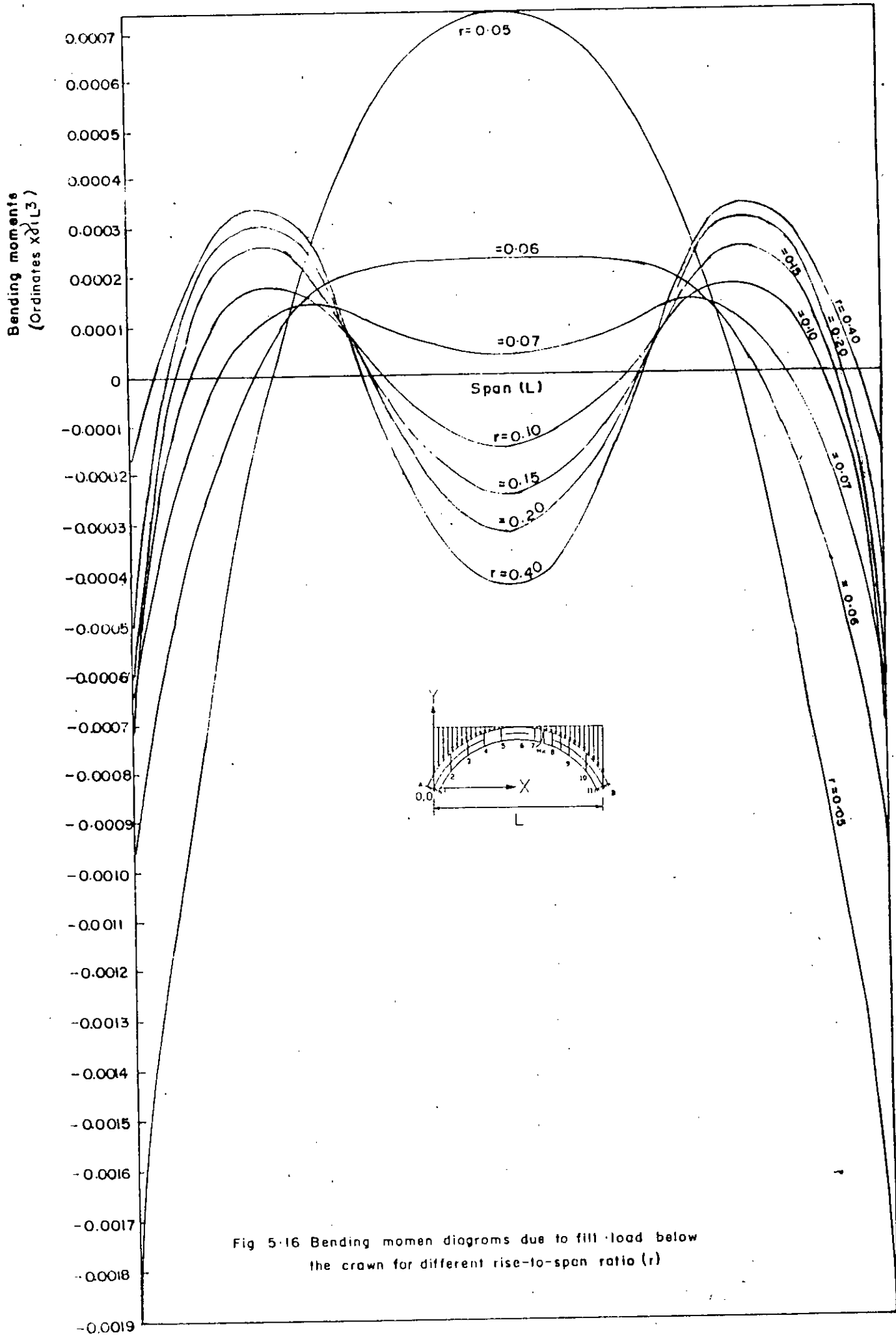


Fig 5-16 Bending momen diagrams due to fill load below the crown for different rise-to-span ratio (r)

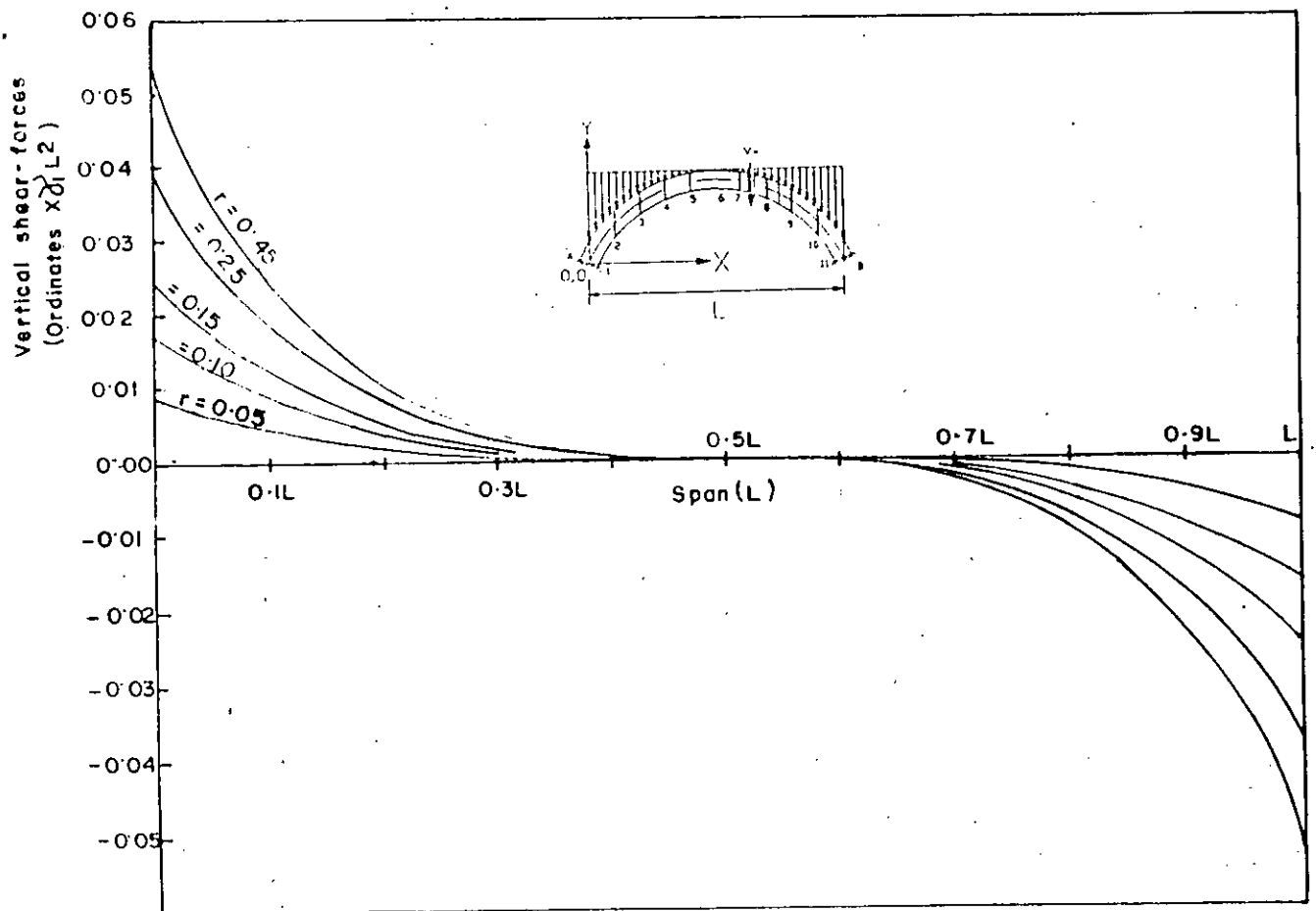


Fig. 5.17 Vertical shear-force diagrams due to fill-load below the crown for different rise-to-span ratio(r).

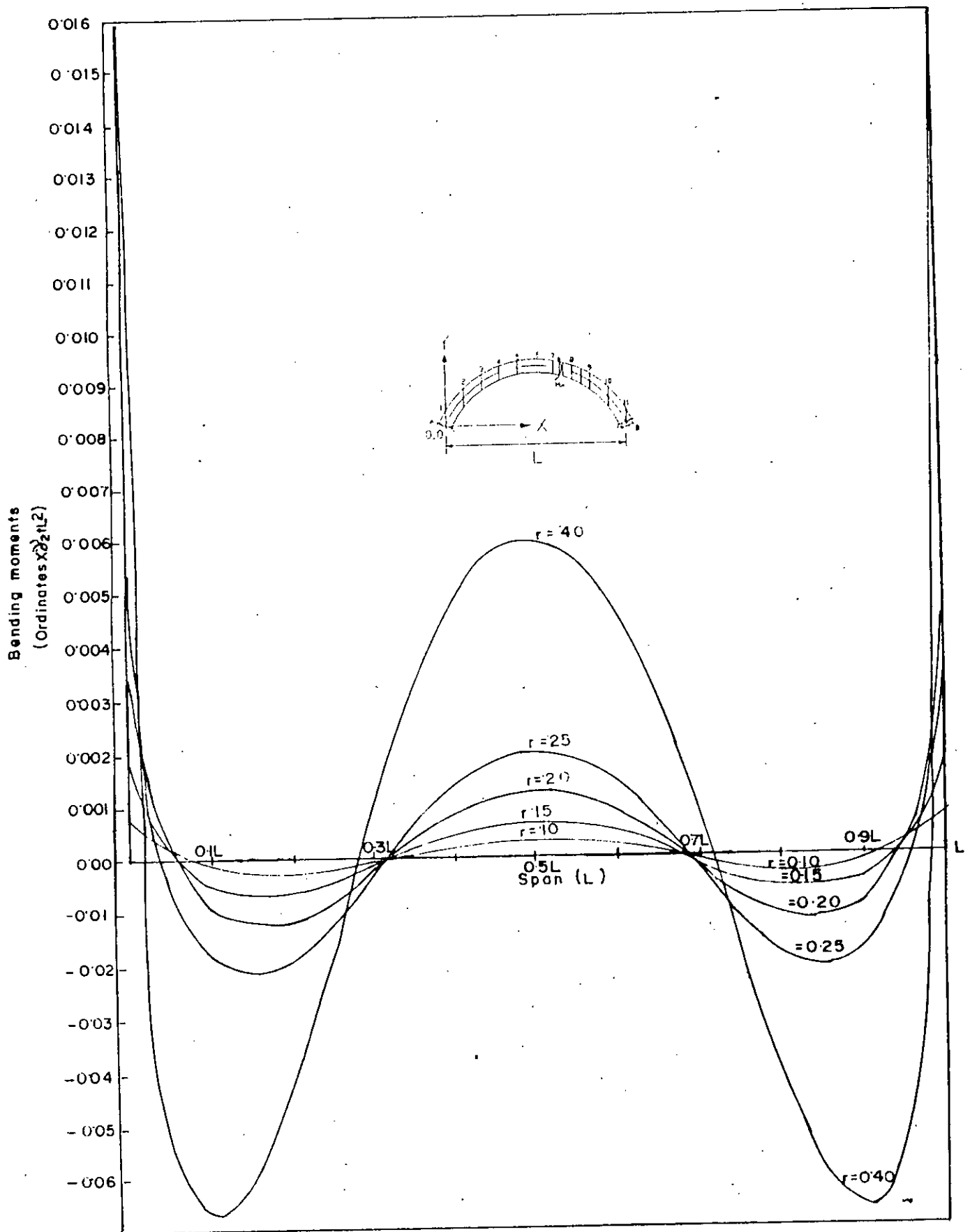


Fig. 5-18 Bending moment diagrams due to self load of the arch-ring for different rise-to-span ratio (r).

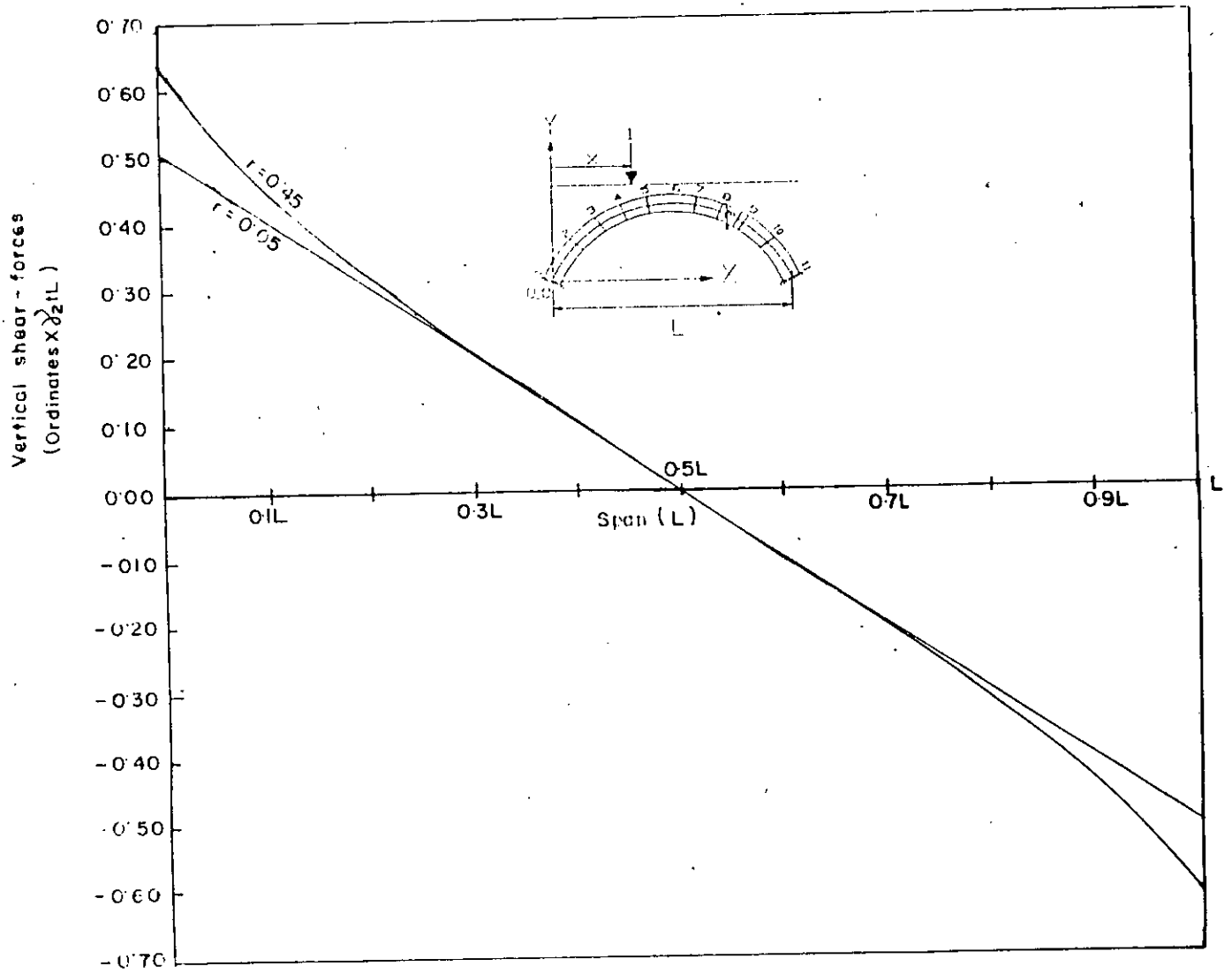


Fig. 5-19 Vertical shear-force diagrams due to self load of the arch-ring for different rise-to-span ratio (r)

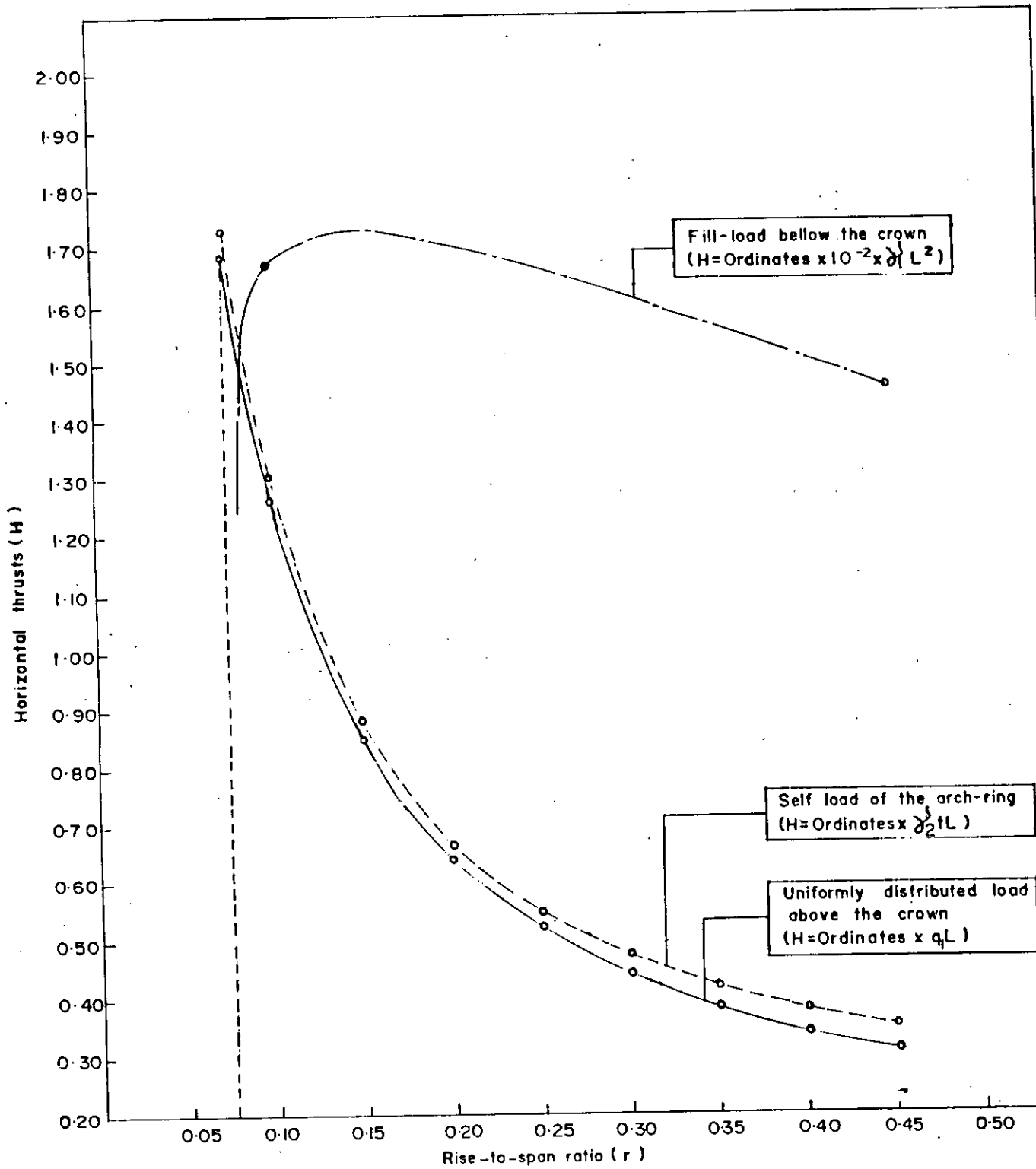


Fig.-5-20 Variation of Horizontal thrusts with different rise-to-span ratios due to fill and self loads.

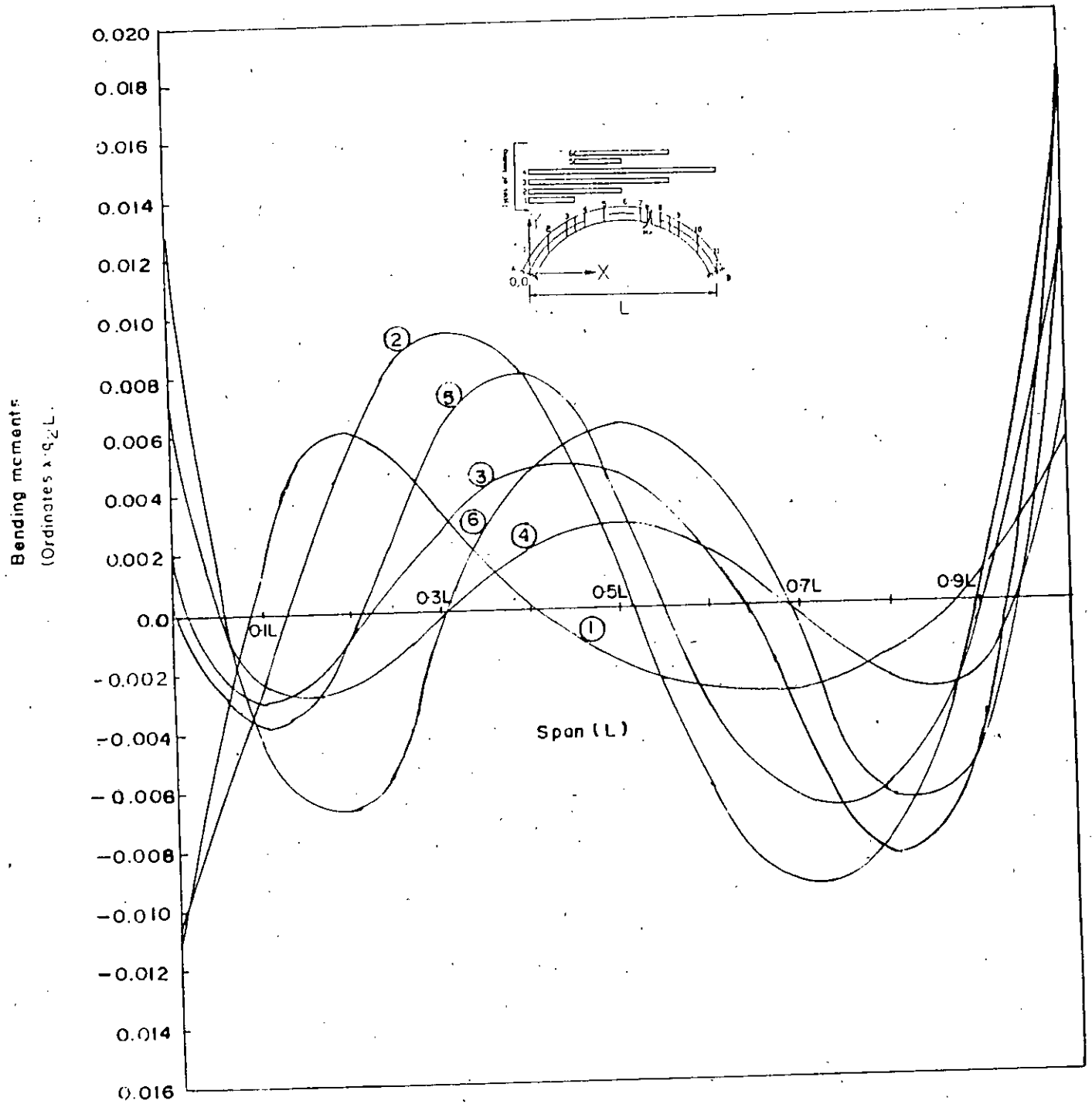


Fig-5.21 Bending moment diagrams due to different types of uniform Partially distributed loads for rise to Span ratio (r) = 0.25.

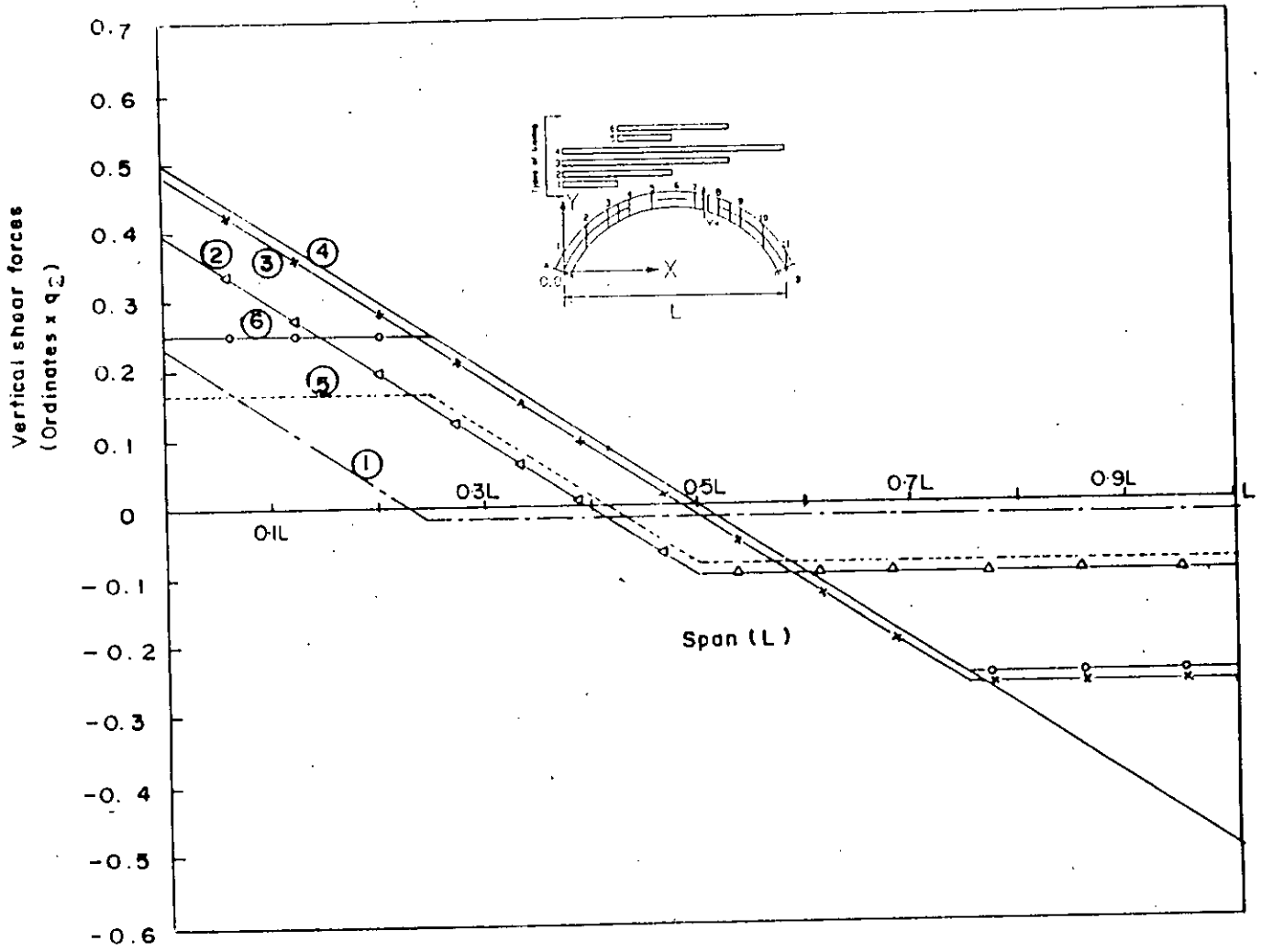


Fig-5:22 Vertical shear force diagrams due to different types of uniform partially distributed loads.

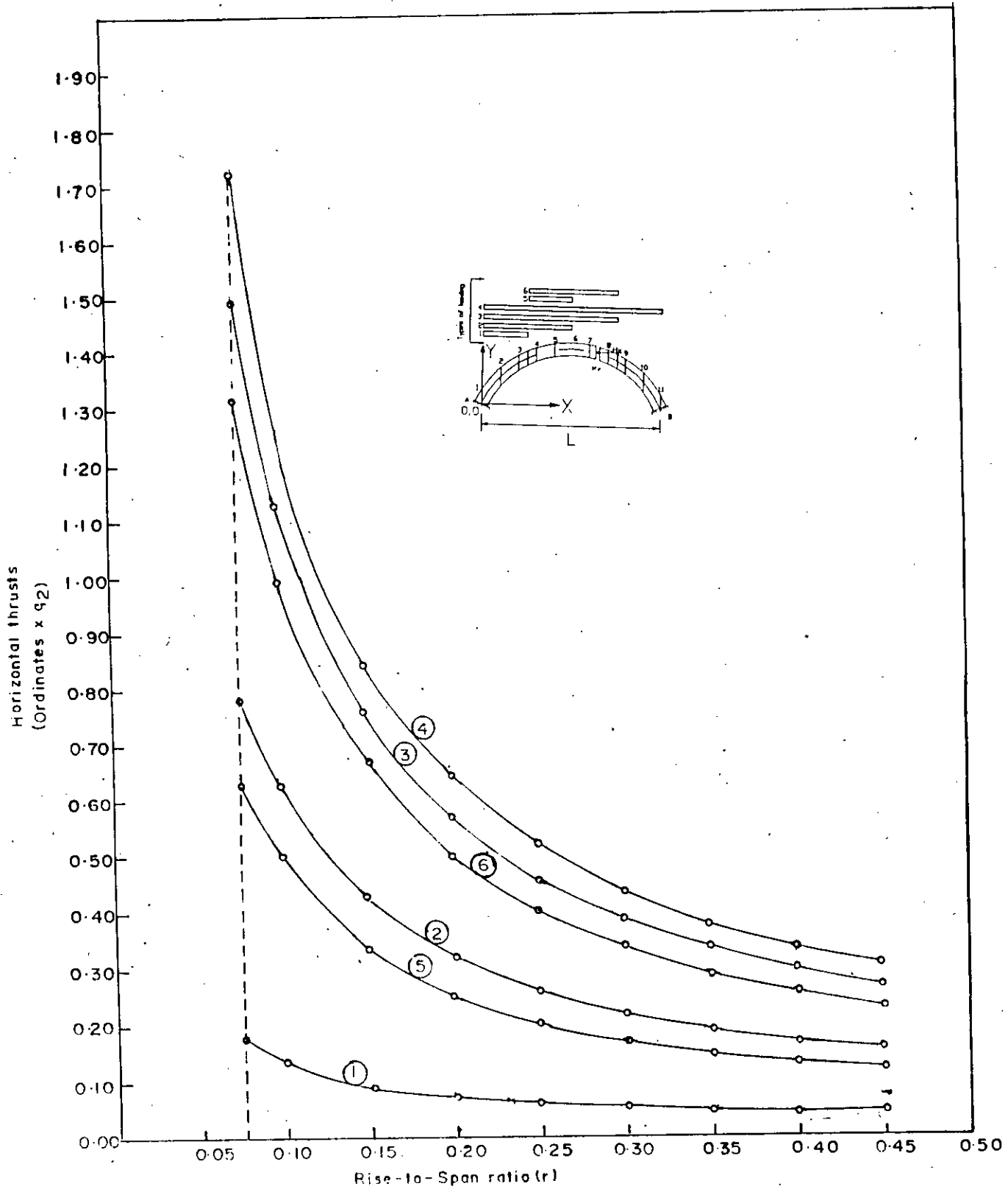


Fig. 5-23 Variation of Horizontal thrusts with different rise-to-span ratio due to different types of uniform partially distributed loads.

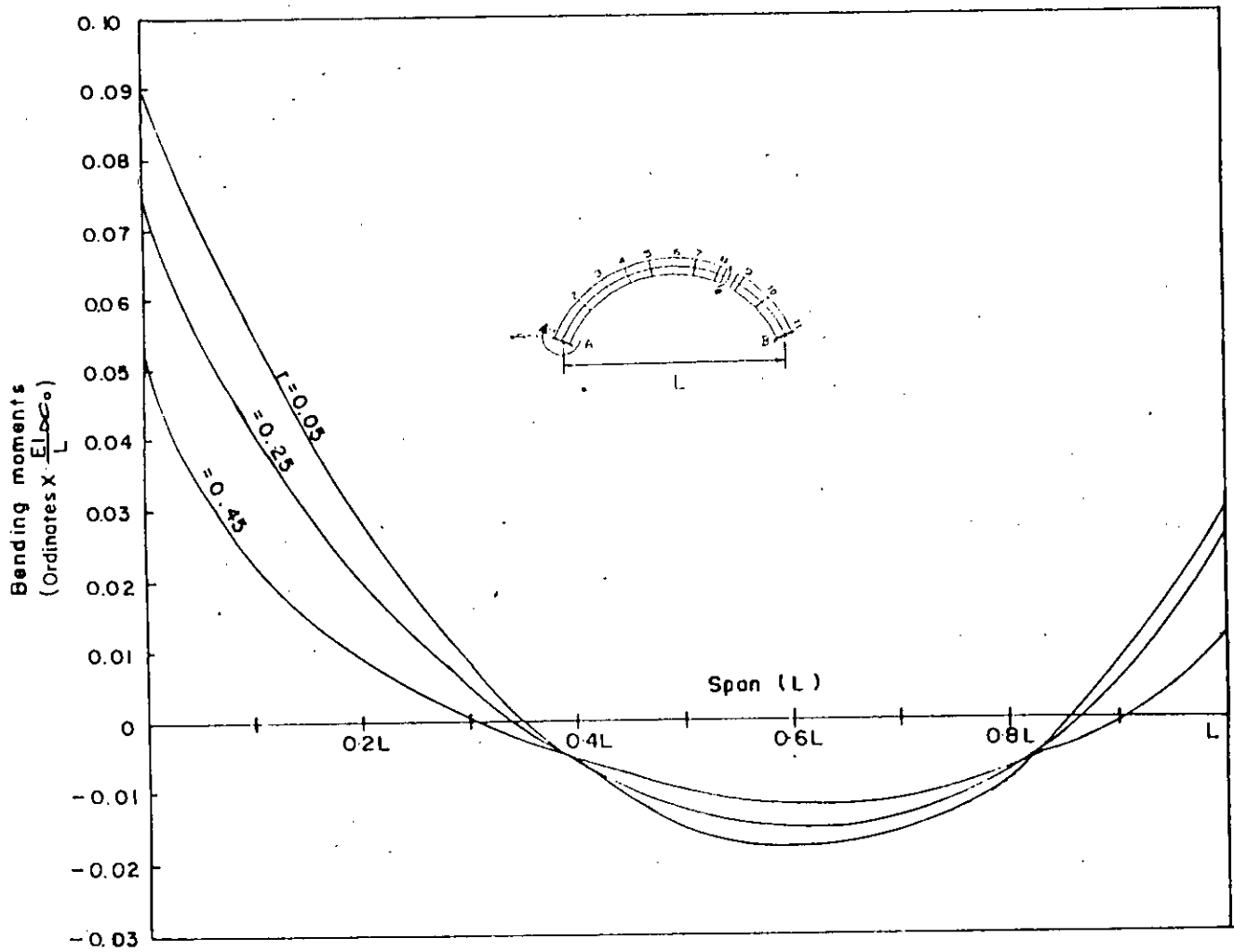


Fig-5-24. Bending moment diagrams due to unit rotation (clock-wise) at left support for different rise-to-span ratio (r).

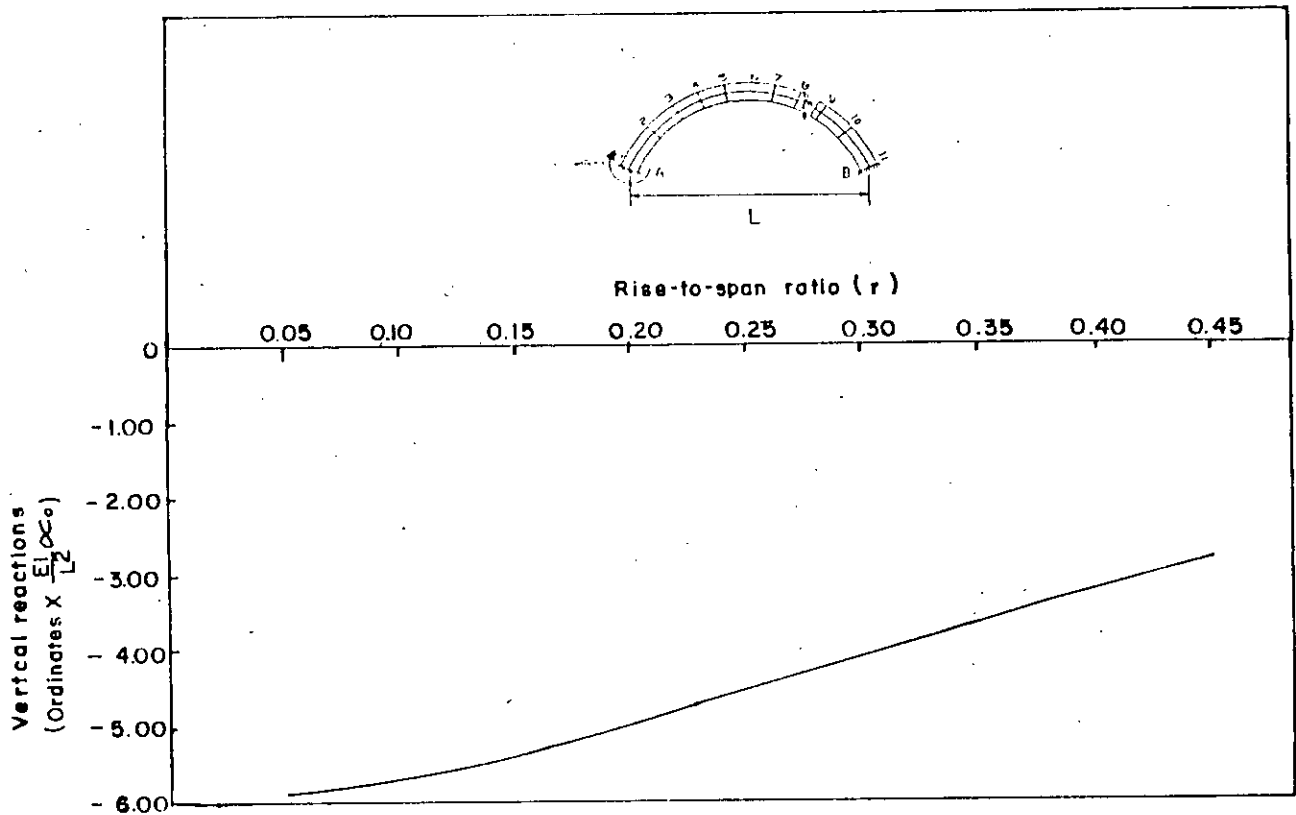


Fig-5-25 Variation of vertical reactions due to unit clock-wise rotation at left support with different rise-to-span ratio (r)

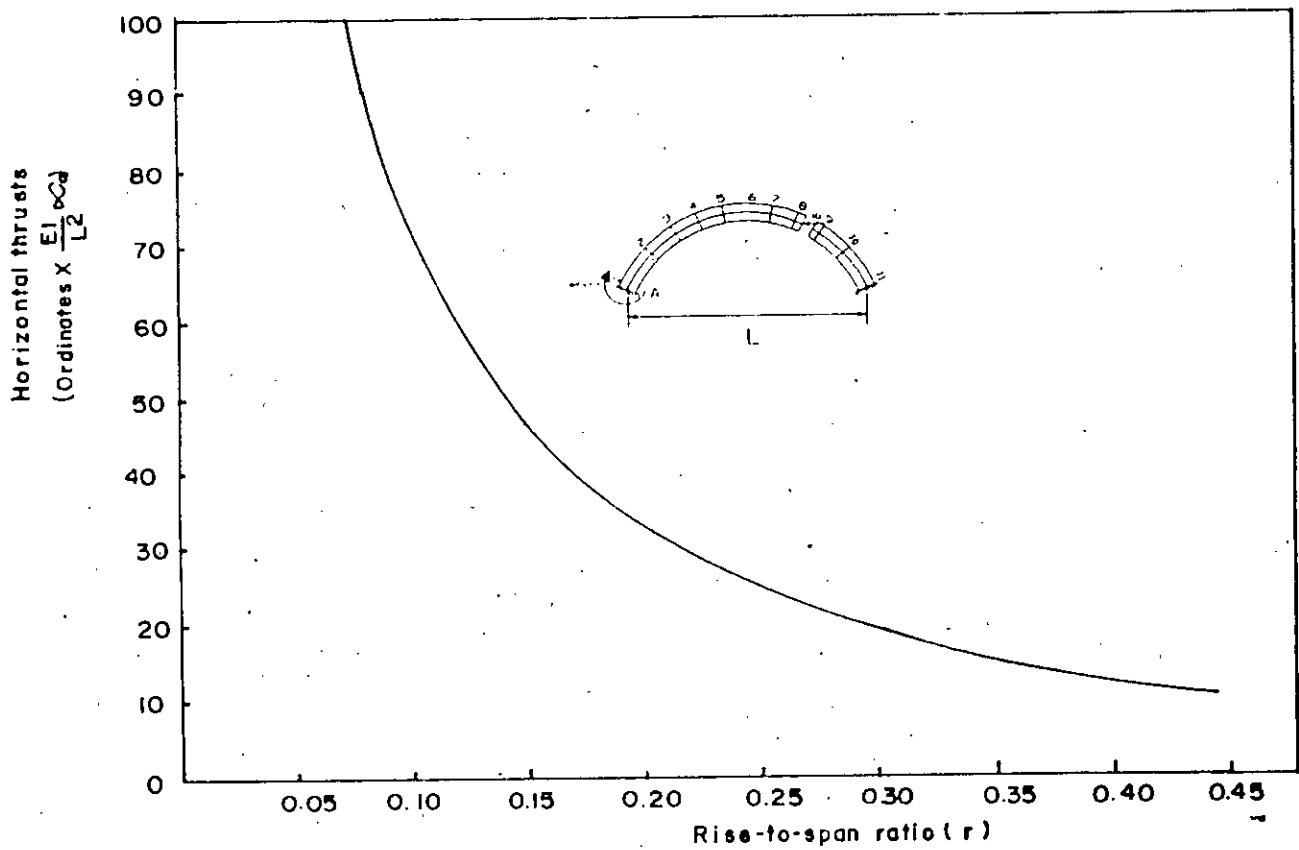


Fig-5-26 Variation of horizontal thrusts due to unit clock-wise rotation at left support with different rise-to-span ratio.

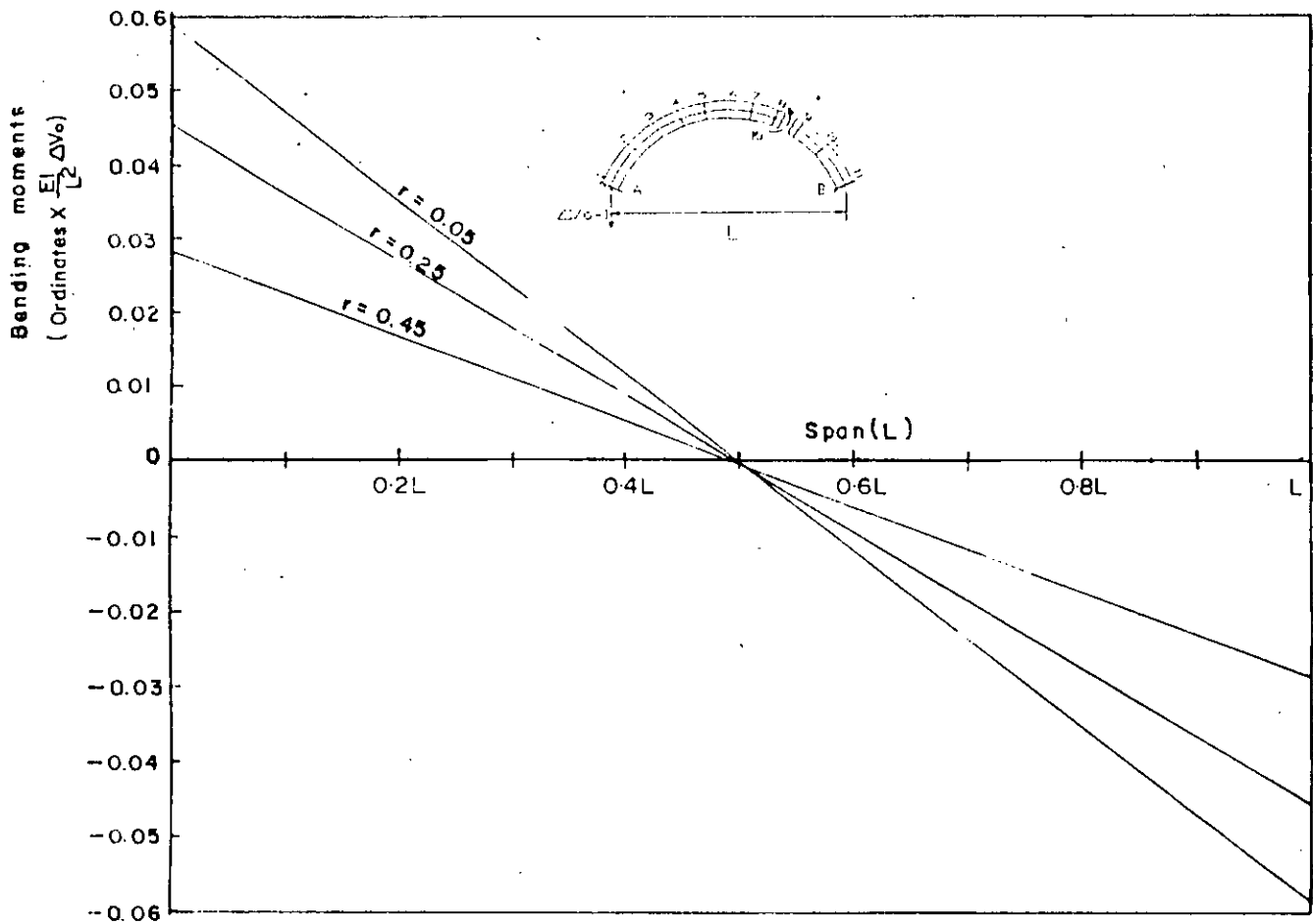


Fig-5-27 Bending moment diagrams due to unit down-ward vertical displacement at left support, for different rise-to-span ratio (r).

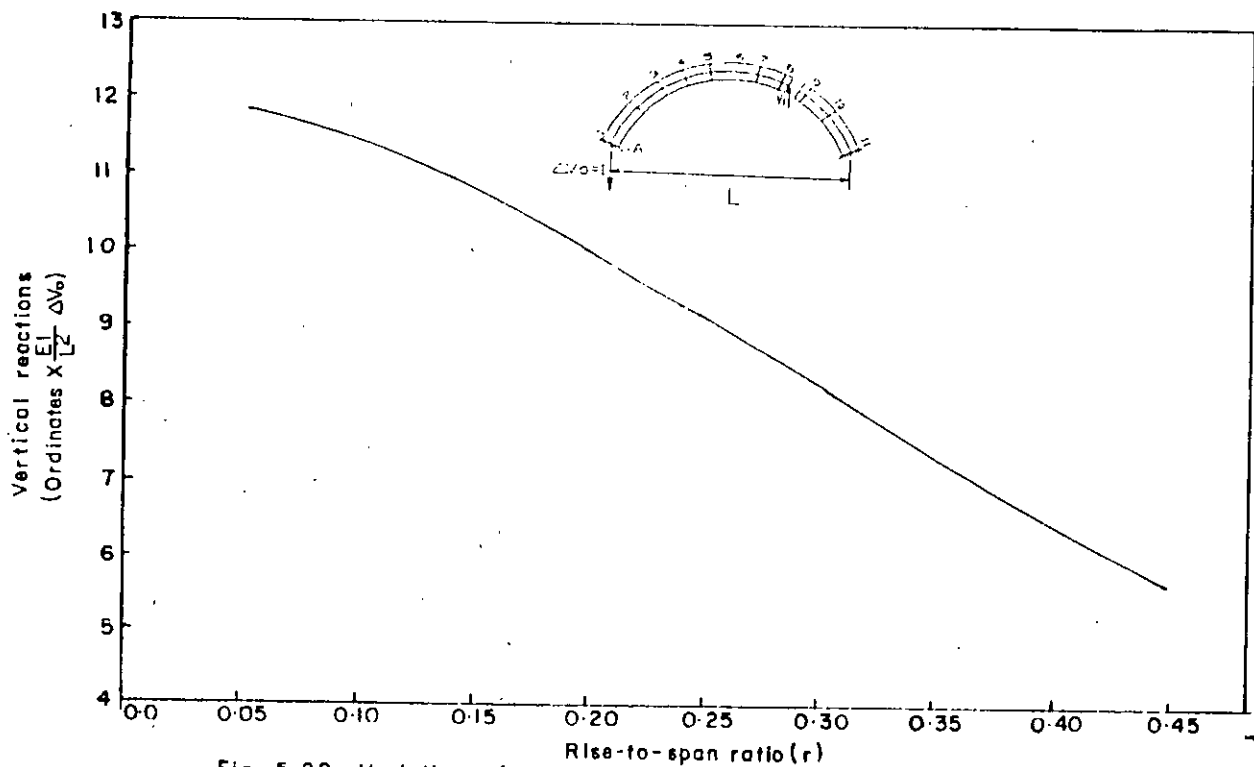


Fig-5-28 Variation of vertical reactions due to unit down-ward vertical displacement at left support with different rise-to-span ratio.

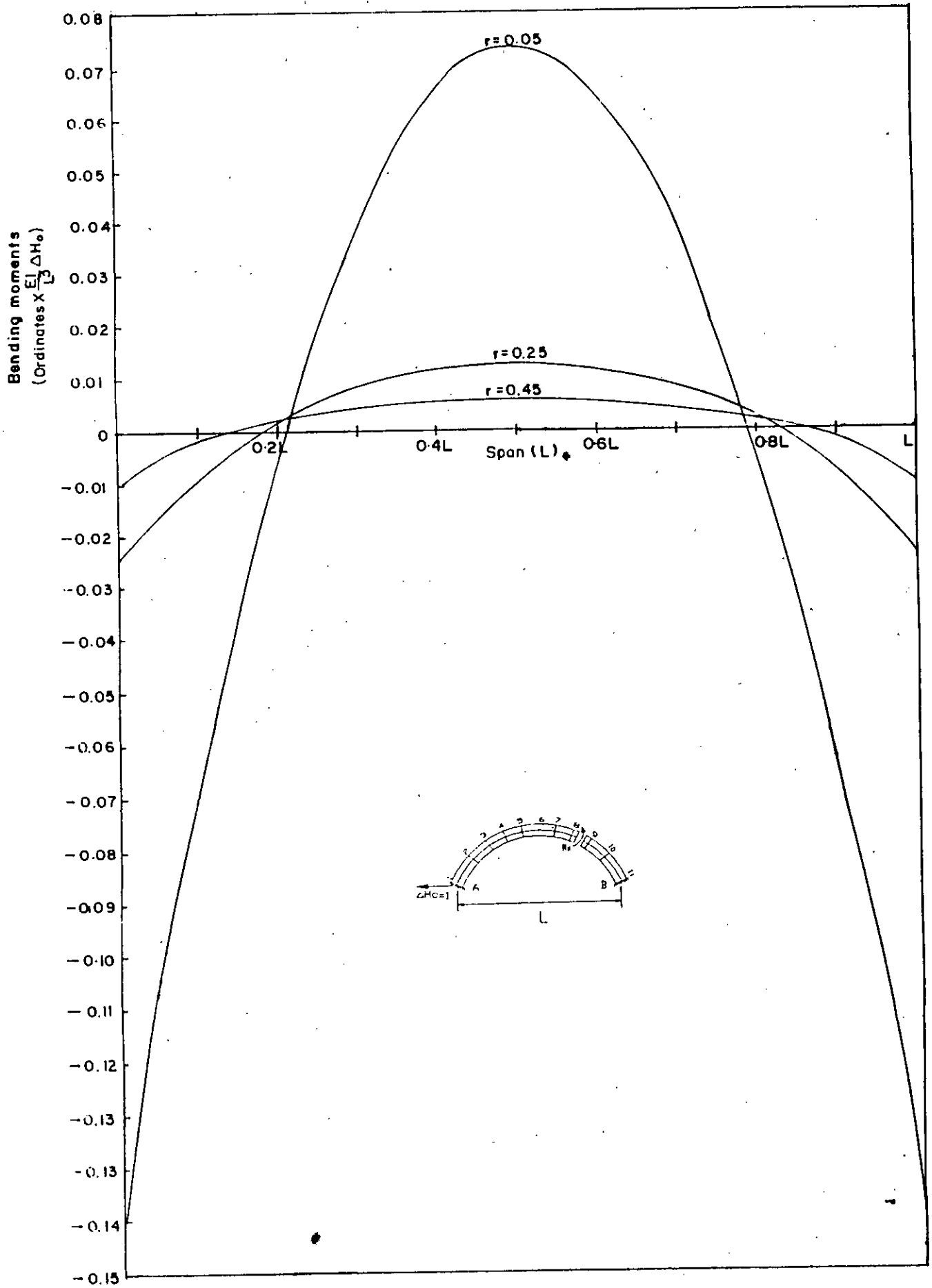


Fig. 5-29 Bending moment diagrams due to unit horizontal displacement (out-ward) at left support with different rise-to-span ratio(r).

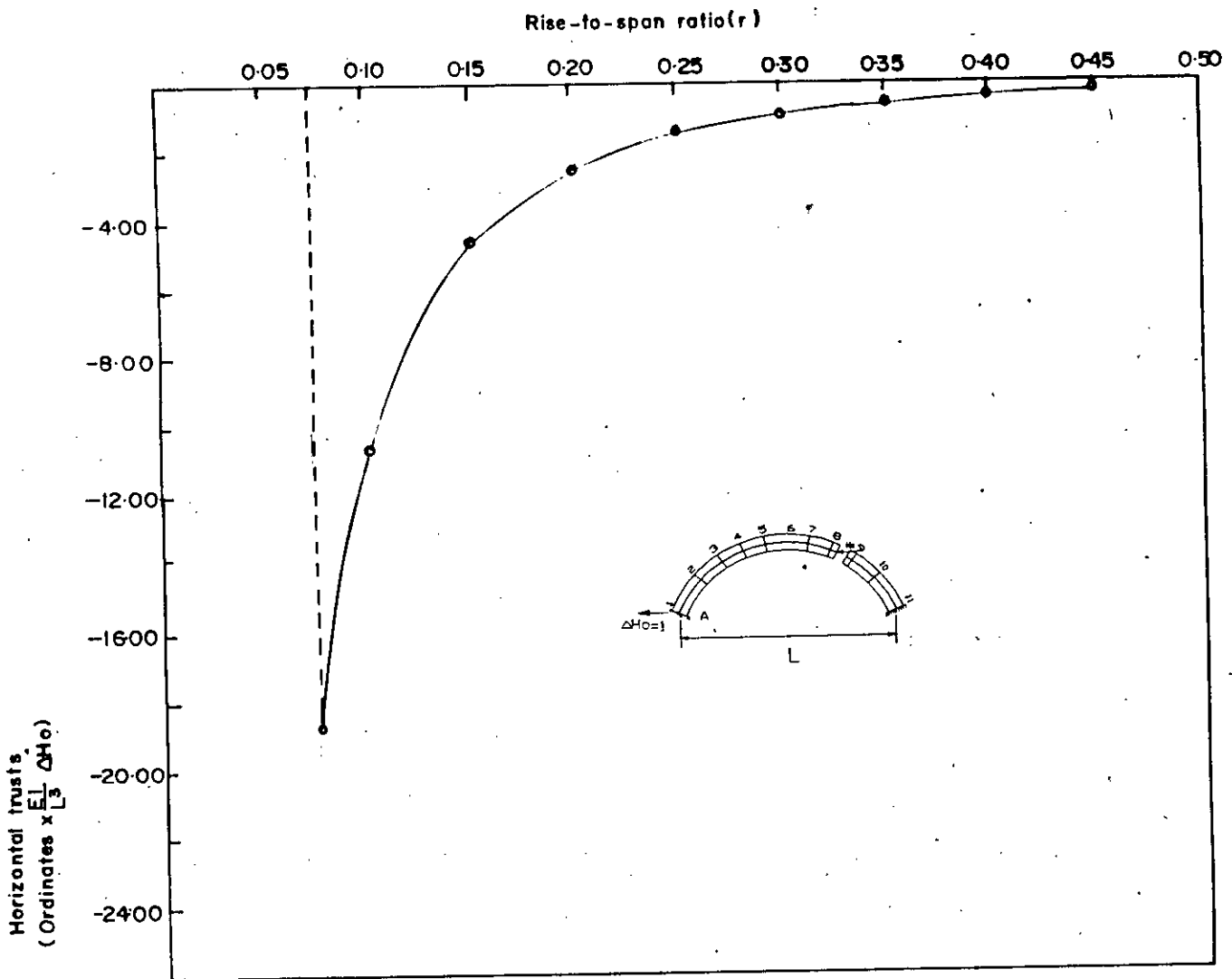


Fig- 5-30 Variation of Horizontal thrusts with different rise-to-span ratios due to unit Horizontal displacement (out-ward) at left support.

CHAPTER - 6

Permissible load capacity of arches

6.1 Introduction

The permissible load capacities obtained using the numerical model developed on the elastic centre method are discussed in this chapter. The results were obtained considering different arch parameters e.g., span(L), rise-to-span ratio(r), radial thickness(t), depth of fill above the crown and support displacements.

The permissible load capacity has been computed considering allowable stresses in compression, tension and shear. For the purpose of computation, an arch have been divided into ten segments of equal horizontal projection. The material properties and the allowable stresses are presented in Table 6.1. The procedure followed in determining the permissible load capacity is described in Art. 4.2. At any stage of loading the maximum compressive stress, tensile stress and shear stress being developed in the arch due to the dead weight and applied live load are computed and compared with the allowable stresses. The model also identifies the corresponding sections where above stresses are developed.

The programme has been utilised to compute the permissible load capacity without considering support yielding for arches having different spans and with following variations :

- (a) radial thickness of 5" to 50" with an increment of 5".
- (b) depth of fill above the crown of 0.5' to 5.0' with an increment of 0.50' and
- (c) rise-to-span ratio of 0.05 to 0.45 with an increment of 0.05.

The results obtained for the above mentioned data have been plotted in various combinations in Fig. 6.3 to 6.10, to show the variation of permissible load capacities with different arch parameters. They are also useful in predicting the load carrying capacity of a particular arch having similar parameters.

The results obtained considering support displacements for arches of different spans having rise-to-span ratio 0.25, depth of fill above the crown 1.00' and 1.50' and radial thickness of 10", 15" are illustrated in Fig. 6.10 to 6.18. The clockwise rotation, downward vertical and outward horizontal displacements are applied at the left support of the arch separately and then the load capacity of the arch is computed using the numerical model developed. They are useful in assessing the effect of support displacements on load carrying capacity of an arch. Moreover, the permissible load capacity for the arches of span 10' and 15' considering different support displacements have been compared in various combinations with those obtained without considering support displacement.

TABLE 6.1

Material properties	
Density of fill over the arch	110 psf
Density of masonry units	110 psf
Density of wearing coat material	110 psf
Elasticity of arch ring material	432000000 psf
Limiting allowable stresses	
Maximum compressive stresses	1000 - 1125 psi
Maximum tensile stress	0.0 psi
Shear stresses	50 - 55 psi

6.2 Discussion

The results presented in Fig. 6.1 to 6.28 indicate the variation of permissible live loads capacity with different arch parameters.

Among the three basic modes of limiting stresses, as discussed earlier, it has been observed that for maximum number of arches tensile stress at the supports was critical. The permissible live load position of an arch mainly depends on rise-to-span ratio and depth of fill above the crown. Critical tensile stress is reached when the live load is located near the support for arches with lower rise-to-span ratio, which shifts towards the crown for arches with higher rise-to-span ratio or under higher depth of fill. The arches having longer span, higher rise-to-span ratio and under higher depth of fill develop tensile stress at the crown when the live load is situated at the crown.

It can also be observed that some arches of higher radial thickness or higher depth of fill develop excessive shear stress at the supports due to the position of the live load near the crown or quarter section. For an example, the arch of effective span 5', rise-to-span ratio 0.25, radial thickness 10" and depth of fill of the crown 3' suffers excessive shear stress due to position of the live load at section 3 which is $0.20L$ away from the left support.

A significant effect of permissible live load capacity has been observed by changing the allowable stress in tension as indicated in Fig. 6.1 and 6.2. The permissible live load capacity increases linearly with the increase of allowable tensile stress. The rate of increase of load capacity for shorter span arches is faster than that of longer span. It is to be noted that, at higher allowable tensile stress, there is a possibility of reduction in load capacity of an arch due to the limiting compressive shear stresses rather than due to the tensile stresses. This is indicated by the arch of 5' span, with a live load capacity of 1449 Ibs when the allowable tensile stress is zero while the live load capacity increases to 26000 Ibs by increasing the allowable tensile stress to 100 psi. The same arch shows a load capacity of 24000 Ibs while the allowable tensile stress is further increased to 125 psi, but in this case shear stress becomes critical instead of tensile stress.

The permissible live load capacity increases very rapidly with the increase of radial thickness as illustrated in (Fig. 6.3) as expected. The increment of radial thickness increases the cross-sectional area and moment of inertia of the section and thus the bending stress is reduced and consequently the live load capacity of the arch is increased. The load capacity also increases with increasing depth of fill above the crown (Fig. 6.5). The live load intensity on the arch after dispersion through the fill decreases

with the increasing depth of fill. Thus for a particular live load the actual load on one feet strip of the arch, considered in the analysis, is relatively small when it is under higher depth of fill and hence arches under higher depth of fill supports higher amount of live load. It is further observed that the rate of increase of permissible live load capacity for shorter span is very much significant than those of longer span with the increase of both the radial thickness and the depth of fill. It is to be noted from Fig 6.3 and 6.5 that the permissible live load capacity of arches varies within a small range both for the lower radial thickness and lower depth of fill. The permissible live load capacity of arches decreases (Fig. 6.4 and 6.6) with the increase of the effective span. But at certain instances, as indicated in the figures, the load capacity is observed to be increased gradually. This is because at the vulnerable position of the live load the arch of longer span has a higher depth of fill. Thus the live load disperses comparatively on larger area for arches of longer spans and consequently the arches take a little higher amount of live load.

It is observed from Fig. 6.7 to 6.8 that the permissible live load capacity of arches of shorter span increases very rapidly with the decrease of rise-to-span ratio while it decreases for longer span. The permissible load capacity of arches varies within a small range for rise-to-span ratio 0.20 to 0.30. It is also observed from

Fig. 6.7 that an arch of effective span 20' having radial thickness 10" and depth of fill 1.00' gives a comparatively higher permissible load capacity at rise-to-span ratio 0.25 and 0.30 than the load capacity for arches of effective spans 7.50', 10' and 15'. The high permissible load capacity (Fig. 6.9) of arches of shorter span at lower rise-to-span ratio decreases sharply with the increase of effective span upto 10'. Further increase of effective span causing gradual decrease of the permissible load capacity upto failure of the arch. It is also observed that the permissible load capacity for arches of comparatively higher span with higher rise-to-span ratio increases gradually.

From the study of support deformation, it may be observed that the effect of support deformation is very much significant for shorter span than those of longer span and it is more critical for horizontal support displacement than the vertical displacements.

It is observed from Fig. 6.10, 6.11 and 6.12 that the load carrying capacity of the arches of shorter span decreases very sharply with increasing rotation in the clockwise direction at the left support but it increases gradually upto some extent in case of arches of comparatively higher effective span. The permissible load capacity due to counter clockwise rotation varies at almost reverse rate than that of clockwise rotations. From the figures it is further observed that under the same amount of rotation at the support the load carrying capacity of arches increases with the

increase of fill depth above the crown and also with the increase of rib thickness.

A spurious result has been observed due to vertical support displacements. A minute downward settlement at the left support of arches of shorter span tends to increase the load carrying capacity rapidly and then it decreases with the same rate for further increase of the displacement. For relatively longer span the load capacity is observed to be reduced gradually at a very small rate. For upward vertical displacement the load carrying capacity is observed to be reduced sharply for shorter span and for higher span it can be observed to be unaffected at least upto a displacement of $(1/104)$ inch. From the figures it can further be observed that under the same amount of vertical support displacement the load capacity of arches increases with the increase of the fill depth and also with the increase of rib thickness.

The load capacity of arches is found to be reduced drastically, as illustrated in Fig. 6.16, 6.17 and 6.18, under the action of horizontal support displacement. Under the action of outward displacement the load carrying capacity of arches reduces sharply, while the load capacity is observed to increase to some extent before being reduced under the action of inward support displacement. The increased depth of fill, however, is observed to flatten the load capacity curves(Fig. 6.16 and 6.17), and thus it decreases the rate of reduction of load capacity for arches. The

similar behaviour is not observed for arches with increased rib thickness though the arches are found to carry more loads.

The permissible live load capacity of the arch, illustrated in Fig. 6.19, shows a little variation due to a small clockwise rotation of 0.000001 radian at the left support. But it does carry no live load when the rotation is increased to 0.00001 radian. Fig. 6.20 displays a little variation with increasing depth of fill of the permissible live load capacity of the arch due to similar clockwise rotation. The permissible live load capacity (Fig. 6.21) of an arch of effective span 10', radial thickness 10" and depth of fill 1.00' increases at lower rise-to-span ratio and decreases at higher rise-to-span ratio under clockwise rotation of 0.00001 radian.

Fig. 6.22 illustrates that the arch of effective span 10' allows a very little amount of downward vertical support displacements at lower radial thickness while the arch of span 15' (Fig. 6.23) allows a small displacement with increasing variation in live load capacity with increasing radial thickness. It may be further observed from Fig. 6.22 and 6.23 that the effect of vertical support displacement on the permissible load capacity is considerably higher for shorter span arches mentioned earlier. The permissible live load capacity (Fig. 6.24) of the 15' span is observed to be reduced increasingly, arch under any particular downward vertical support displacement, with the increase of depth

of fill. Again, the live load capacity of the arch (Fig. 6.25) at lower rise-to-span ratio is found to be increased with the increase of downward vertical support displacement while it decreases at higher rise-to-span ratio.

It was observed that the arch of effective span upto 10', rise-to-span ratio 0.25 and depth of fill 1.00' does carry no live load under any amount of outward horizontal support displacement. The effect on permissible live load capacity of the arch of span 15' due to outward horizontal displacement is presented in Fig. 6.26 to 6.28. The live load capacity of the arch is reduced to zero due to a small outward horizontal support displacement of 1/1000" for any radial thickness greater than 15". It may be mentioned that a small horizontal vertical support displacement causes a very high tensile and shear stresses at higher radial thickness. The permissible live load capacity of the arch in Fig. 6.27 under higher depth of fill increases with the increase of outward horizontal support displacement while it decreases at lower depth of fill. It is also observed that the permissible load capacity varies within a small range at lower depth of fill. Erratic behaviour of permissible live load capacity is observed for the arch in Fig. 6.28, when it is plotted with increases rise-to-span ratio. It is, however, observed that the live load capacity of an arch is greatly reduced if it suffers any form of support displacements.

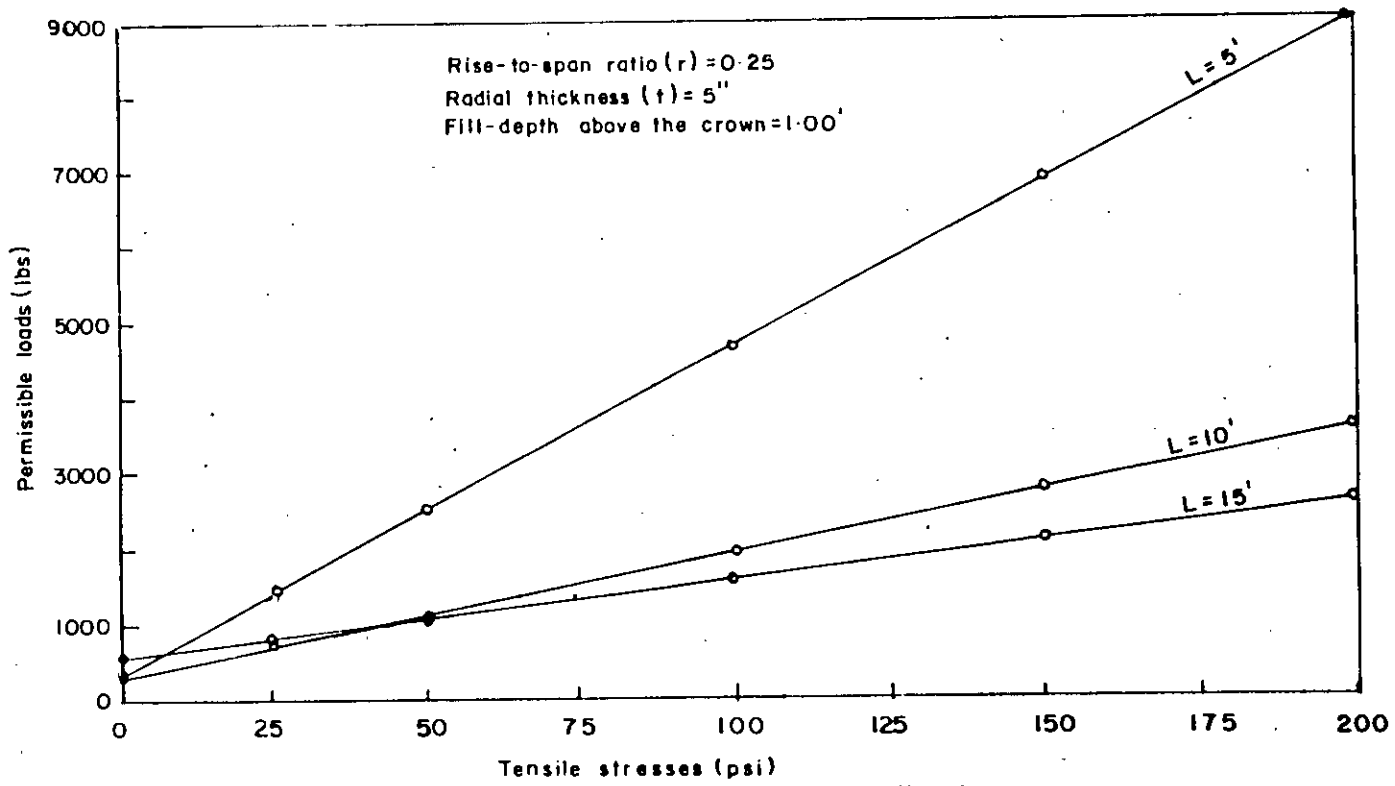


Fig-6-1 Variation of permissible load with various tensile stresses.

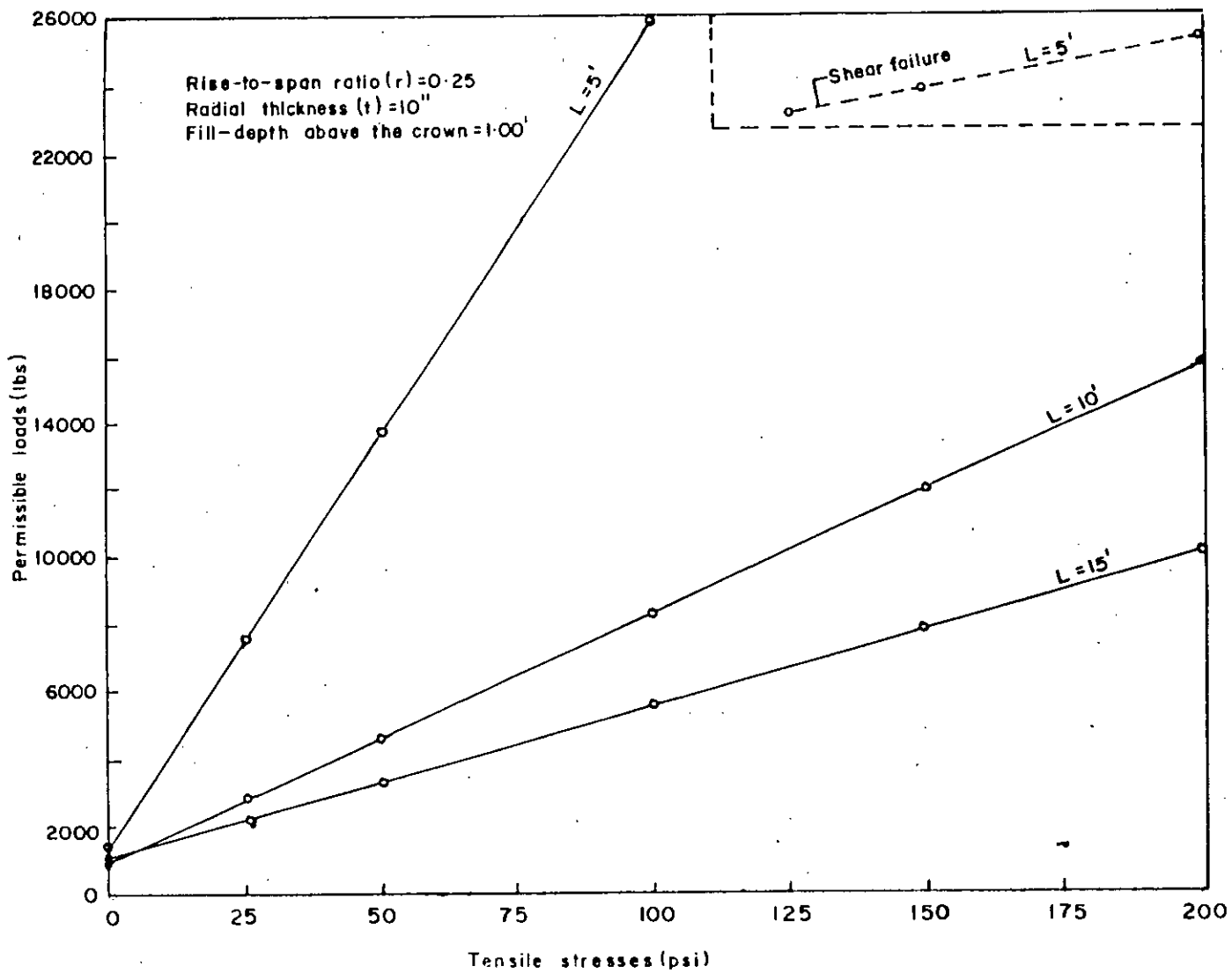


Fig-6-2 Variation of permissible loads with various tensile stresses.

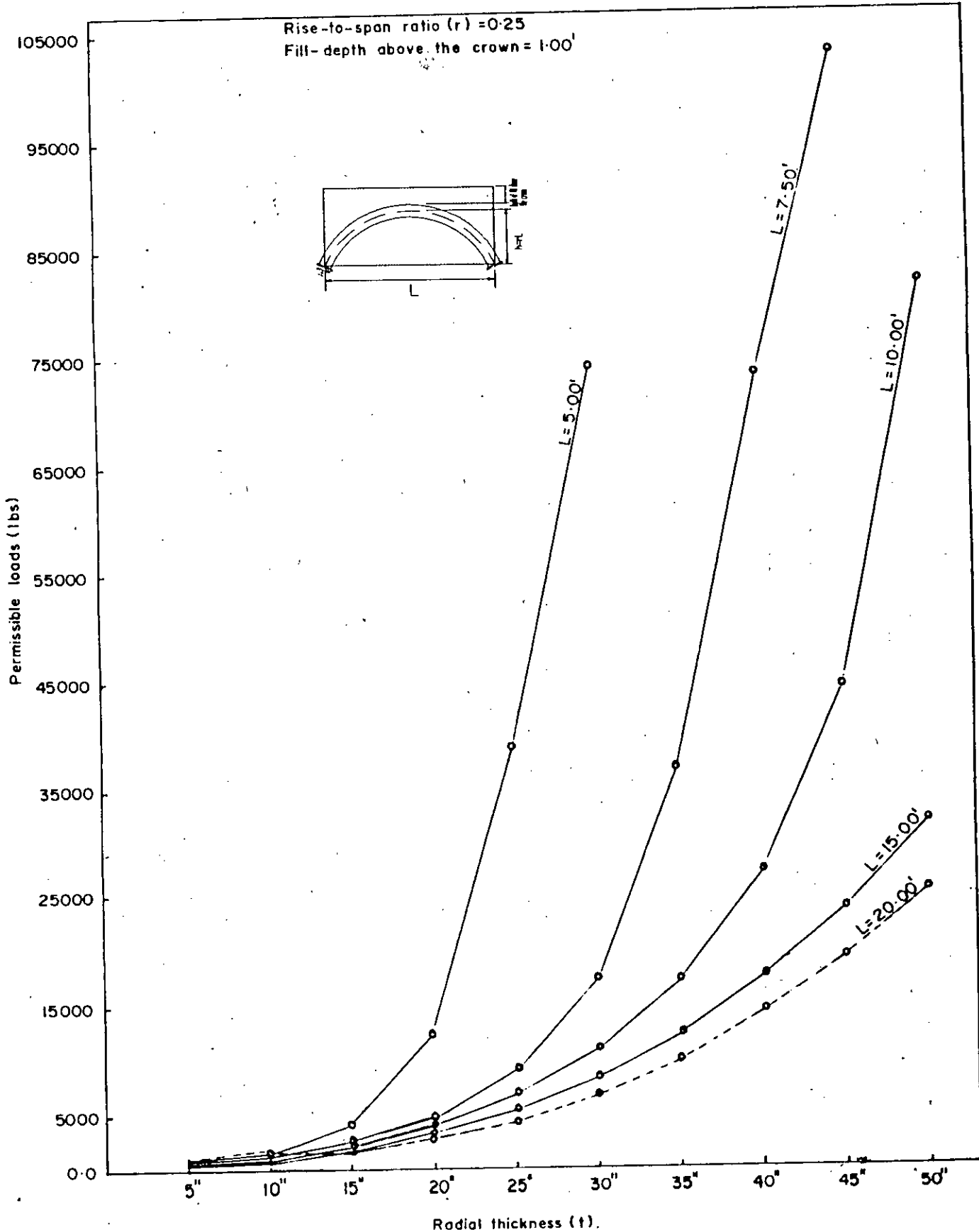


Fig. 6-3 Variation of permissible loads with different radial thickness

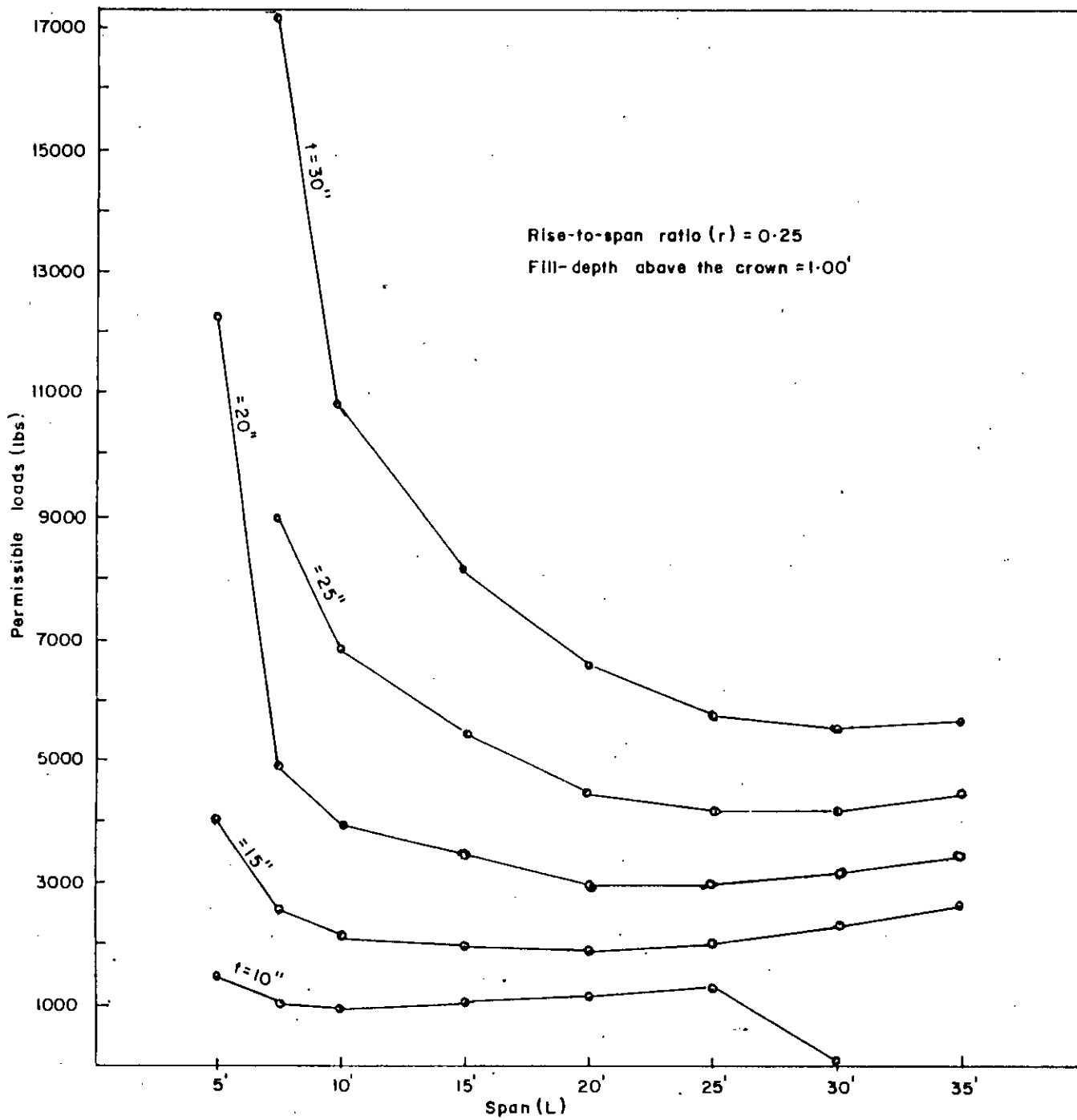


Fig. - 6.4 Variation of permissible loads with different spans.

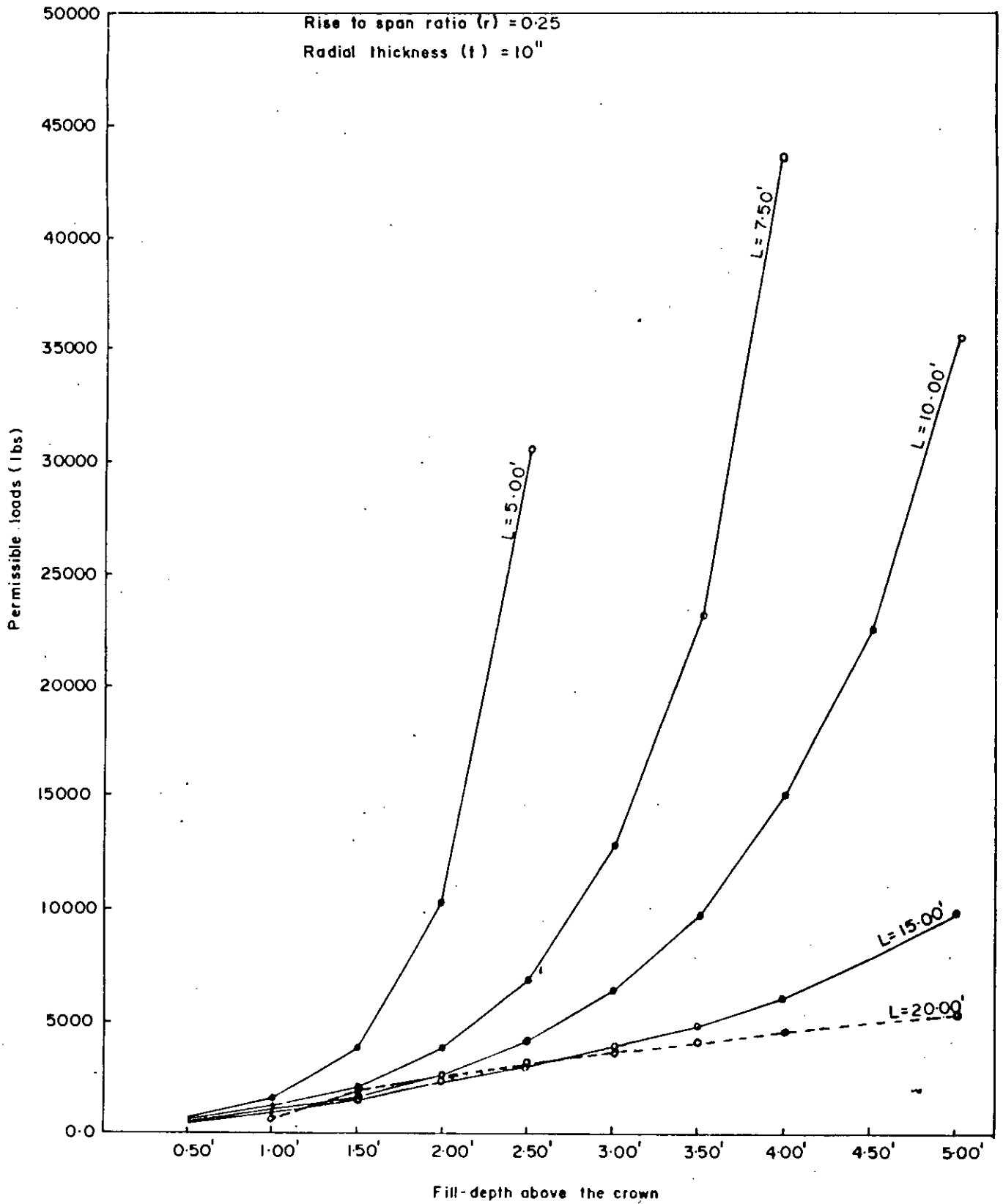


Fig. 6.5 Variation of permissible loads with different Fill-depth above the crown.

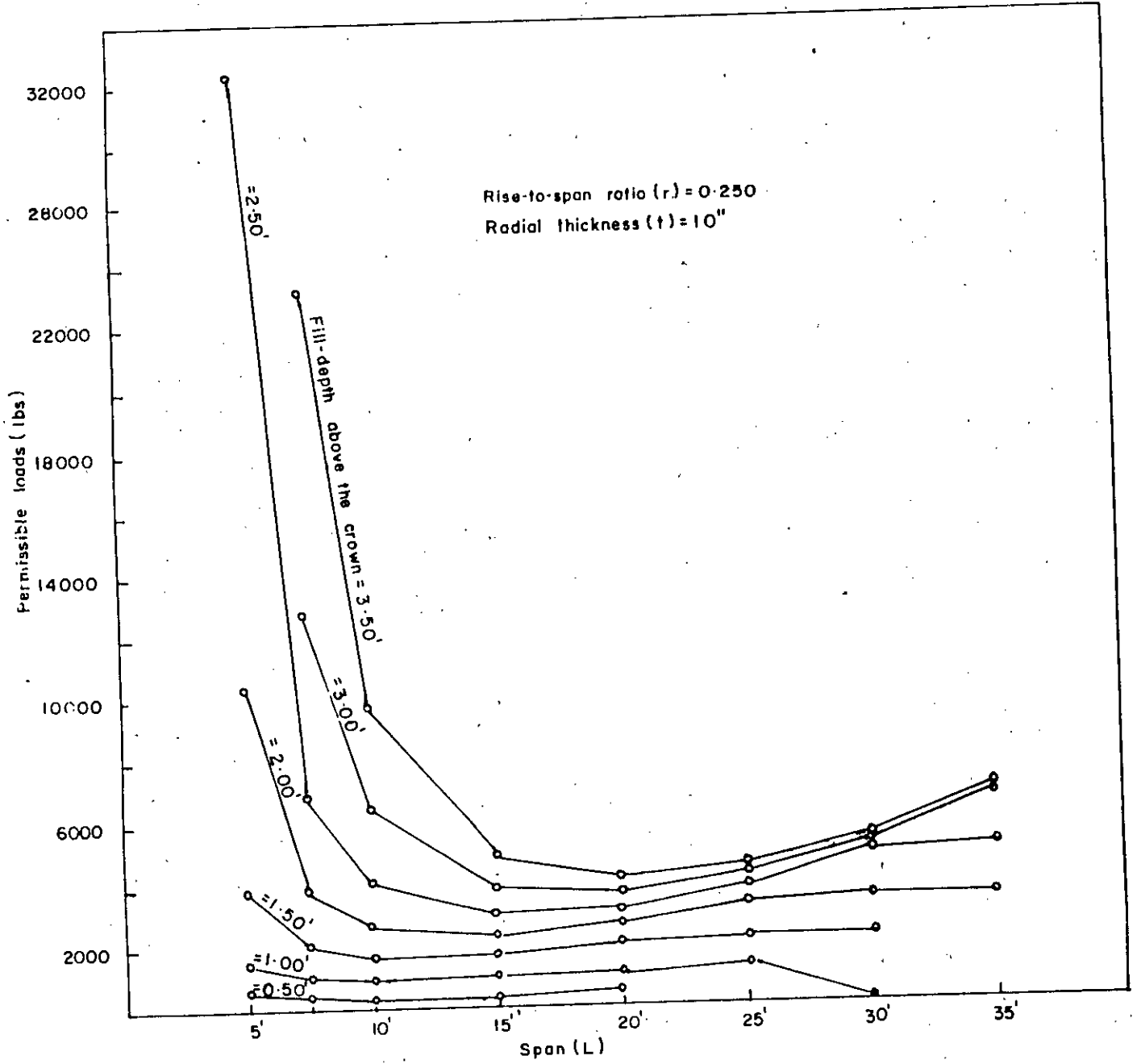


Fig. - 6.6 Variation of permissible loads with different spans.

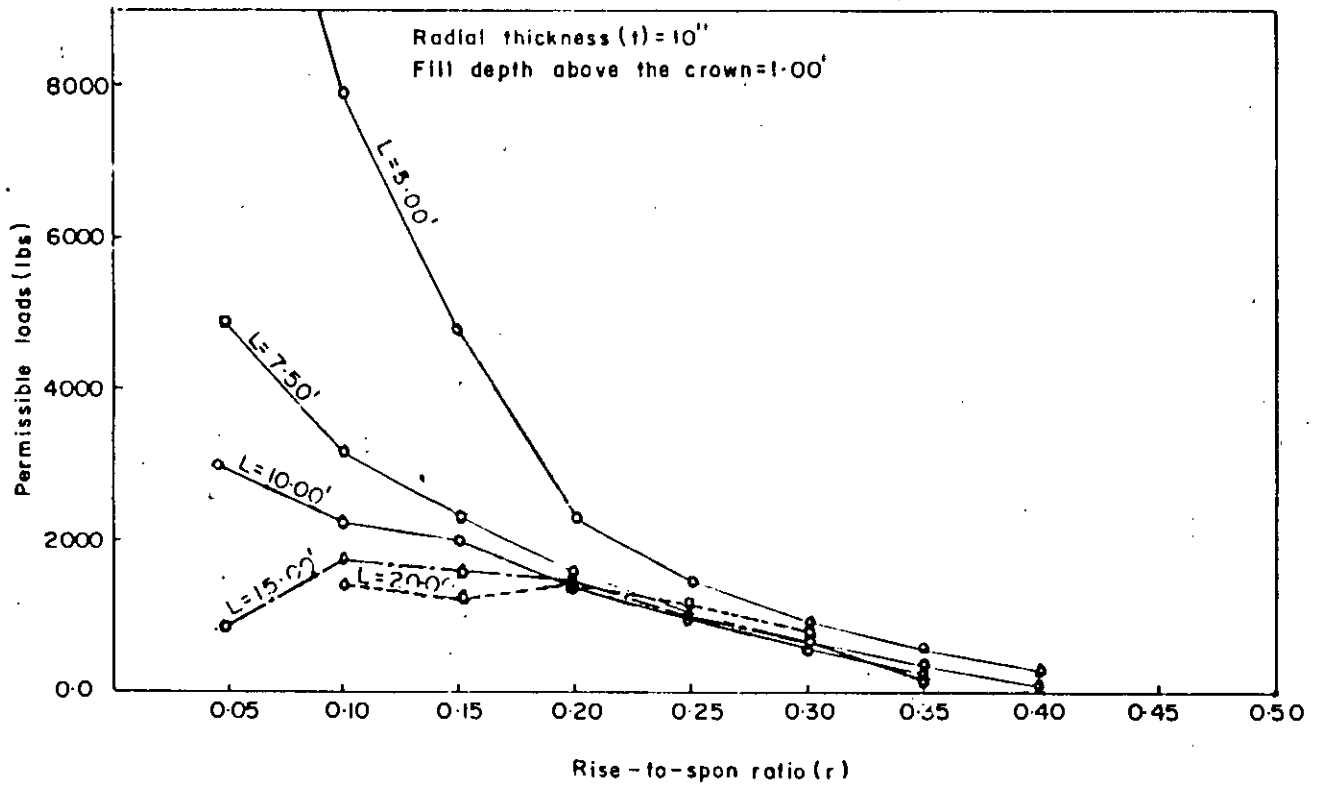


Fig- 6-7 Variation of permissible loads with different rise-to-span ratio

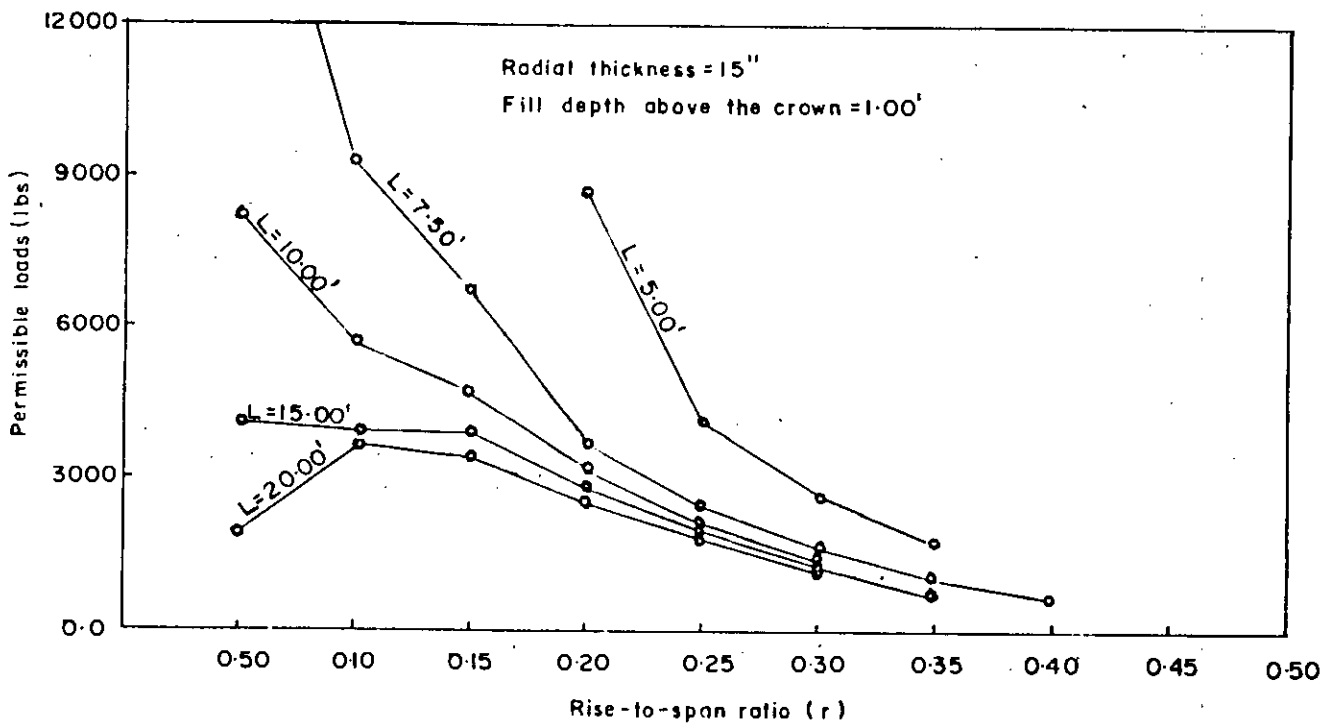


Fig. 6-8 Variation of permissible loads with different rise-to-span ratio

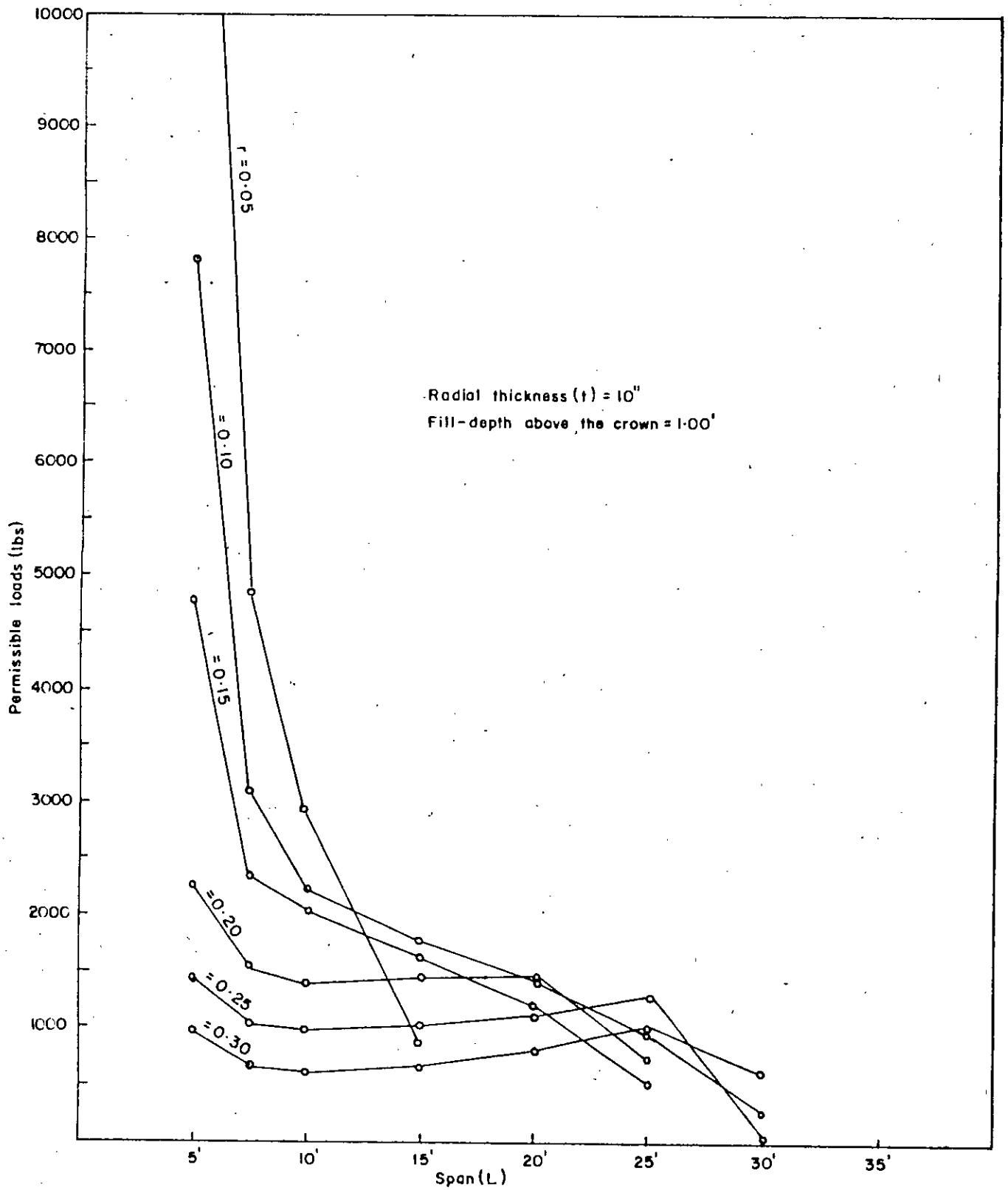


Fig.-6.9 Variation of permissible loads with different spans.

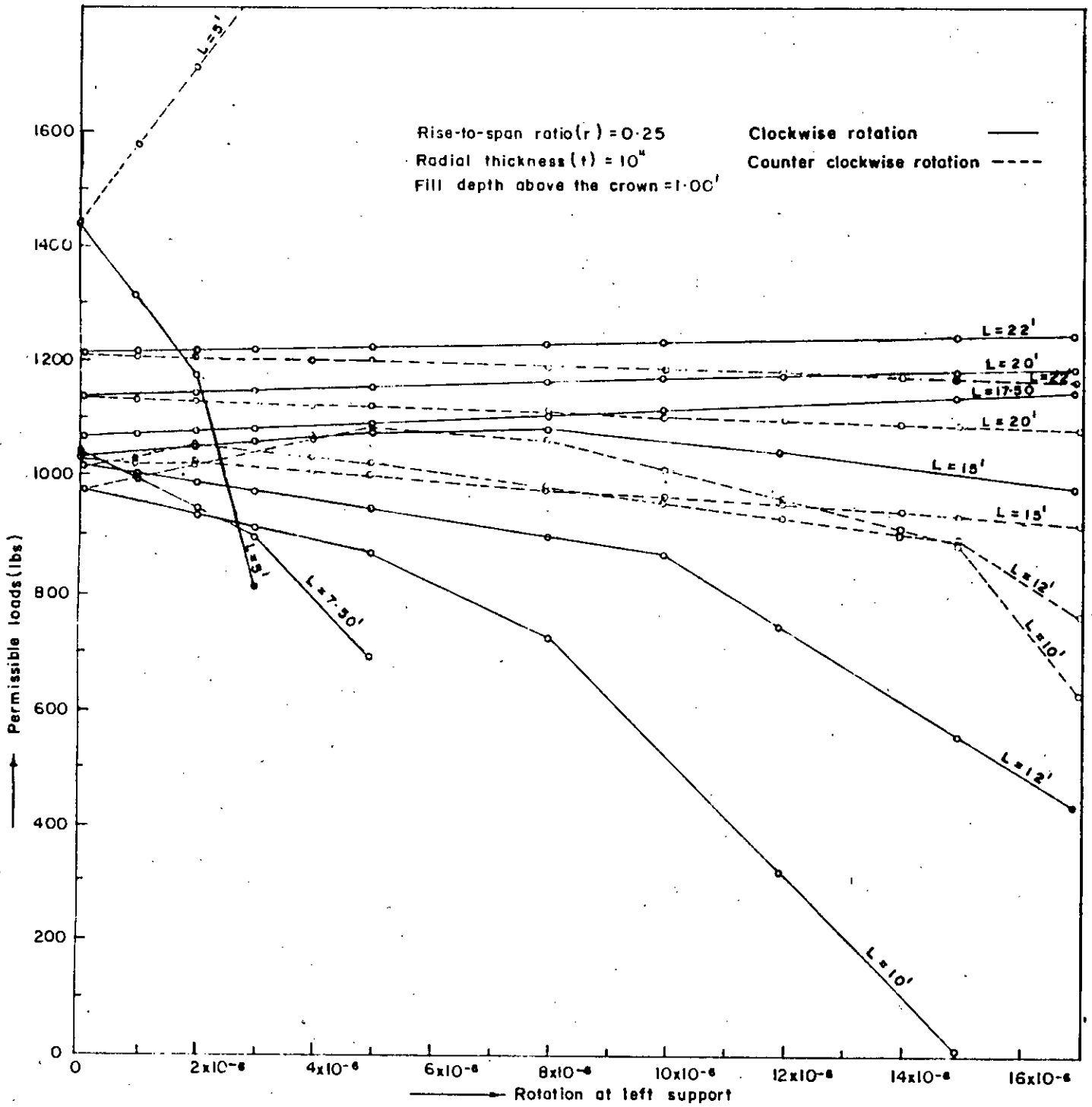


Fig-6-10 Variation of permissible loads with different clockwise rotation at the left support

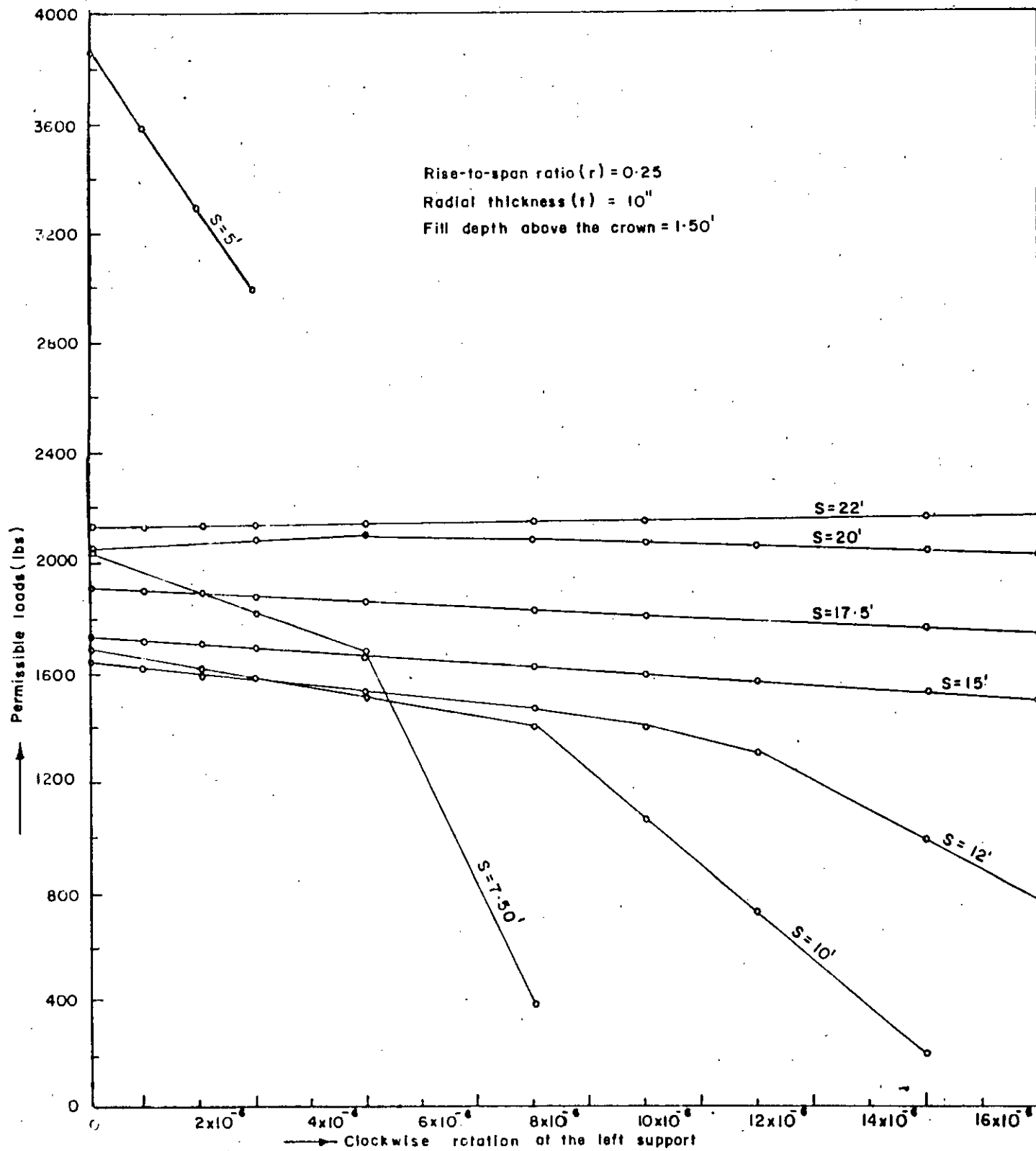


Fig-6-11 Variation of permissible loads with different clockwise rotation at the left support.

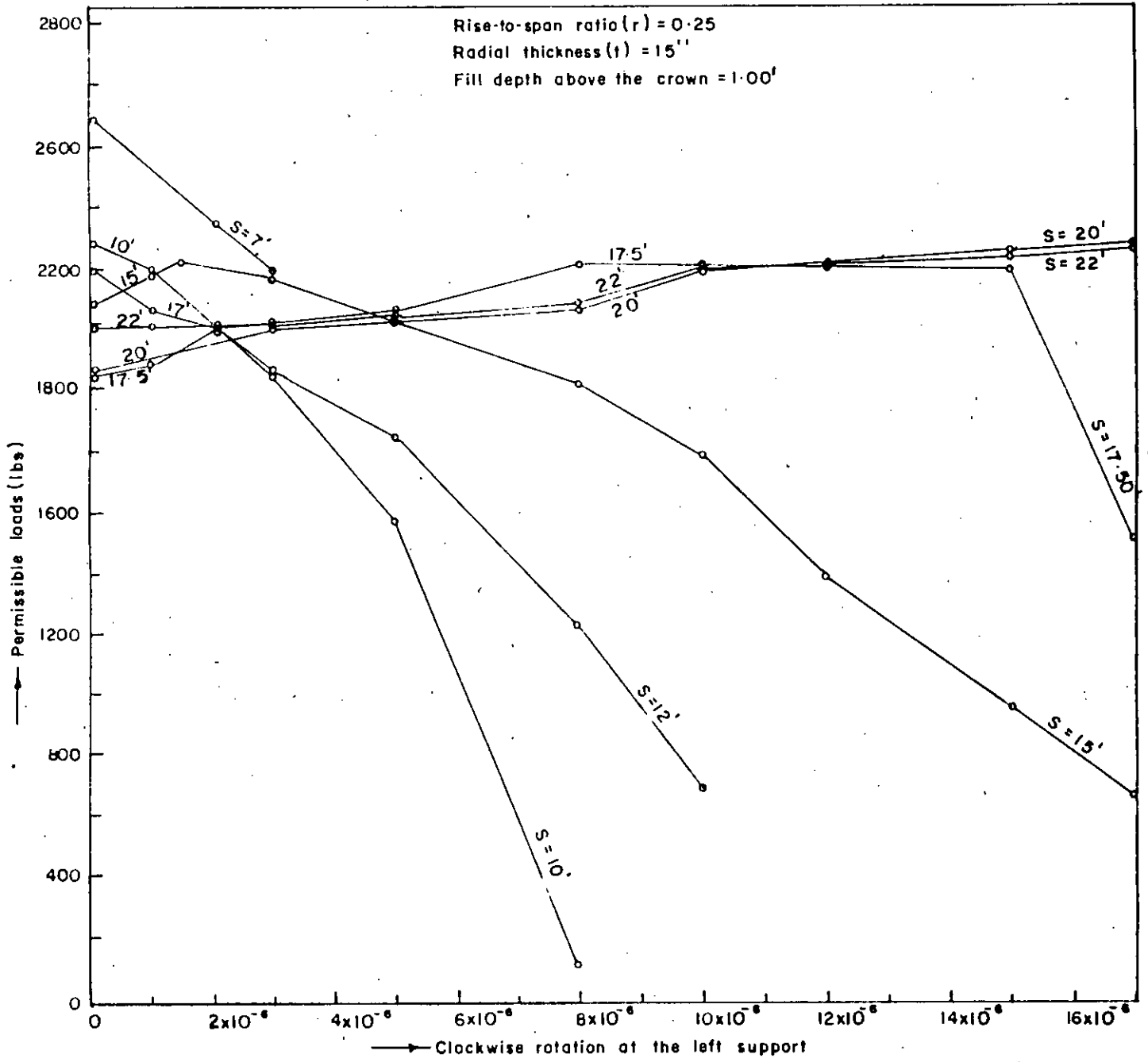


Fig-6-12 Variation of permissible loads with different clockwise rotation at the left support.

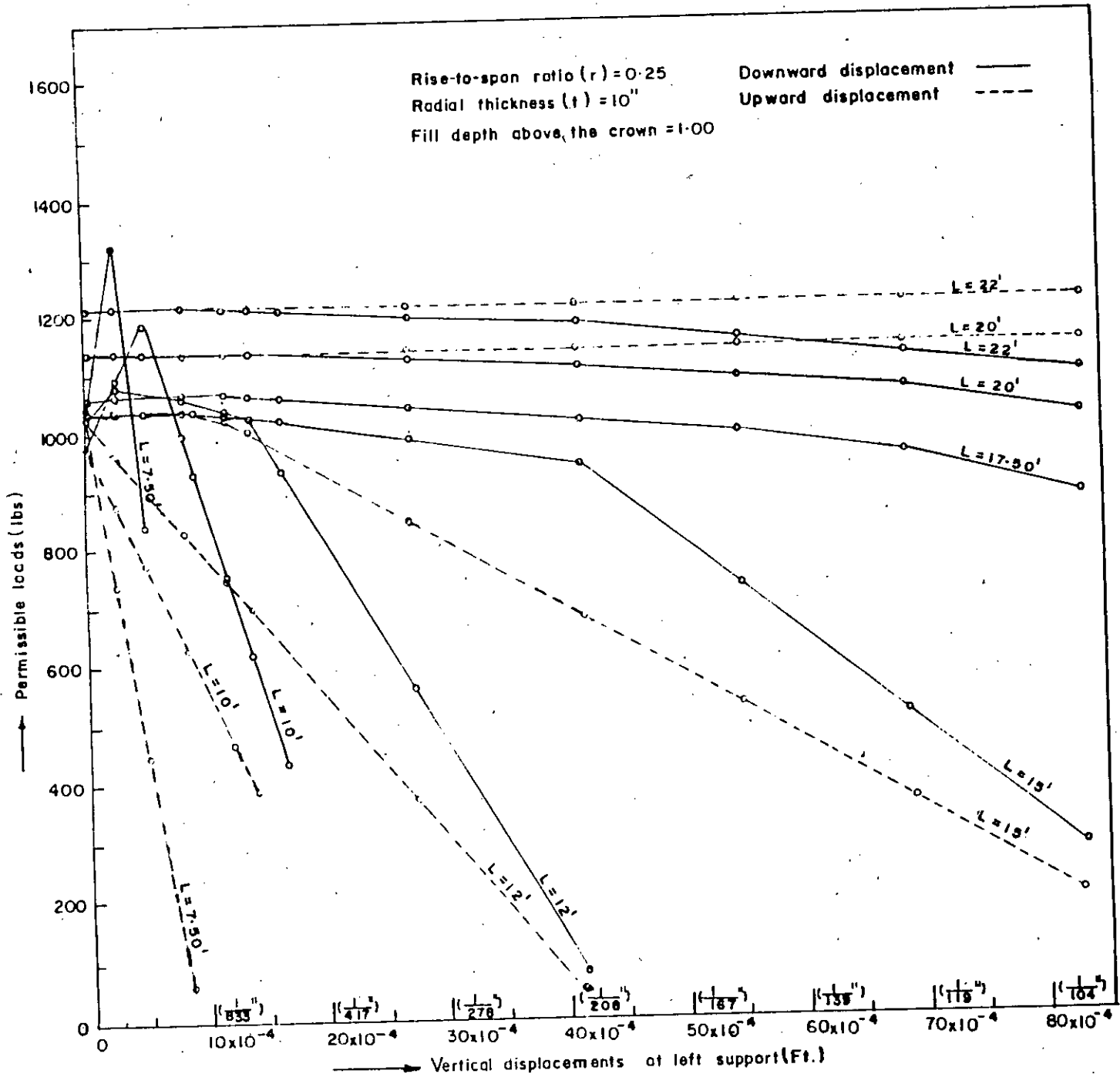


Fig-6-13 Variation of permissible loads with different downward vertical displacements at the left support

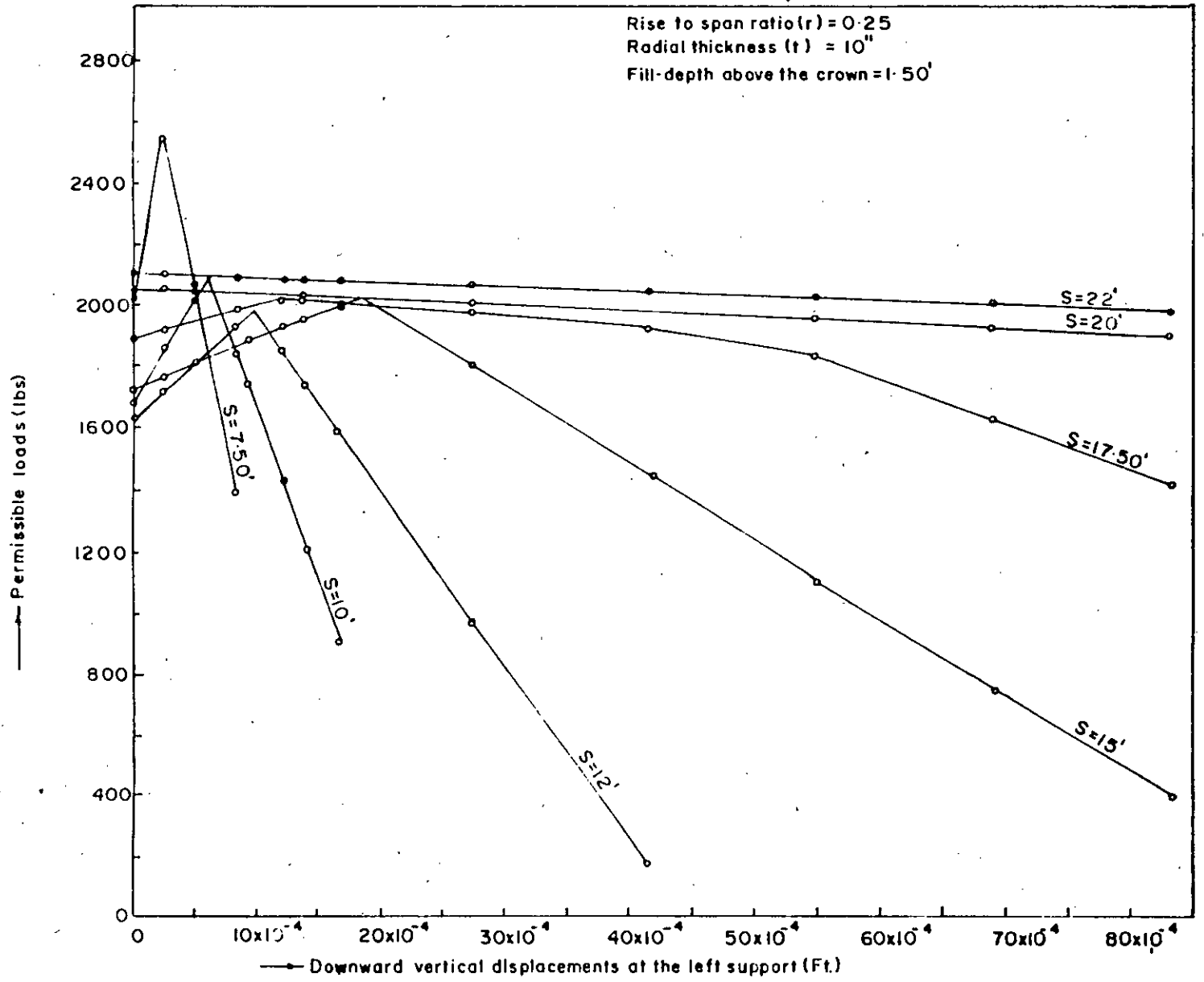


Fig-6-14 Variation of permissible loads with different downward vertical displacements at the left support.

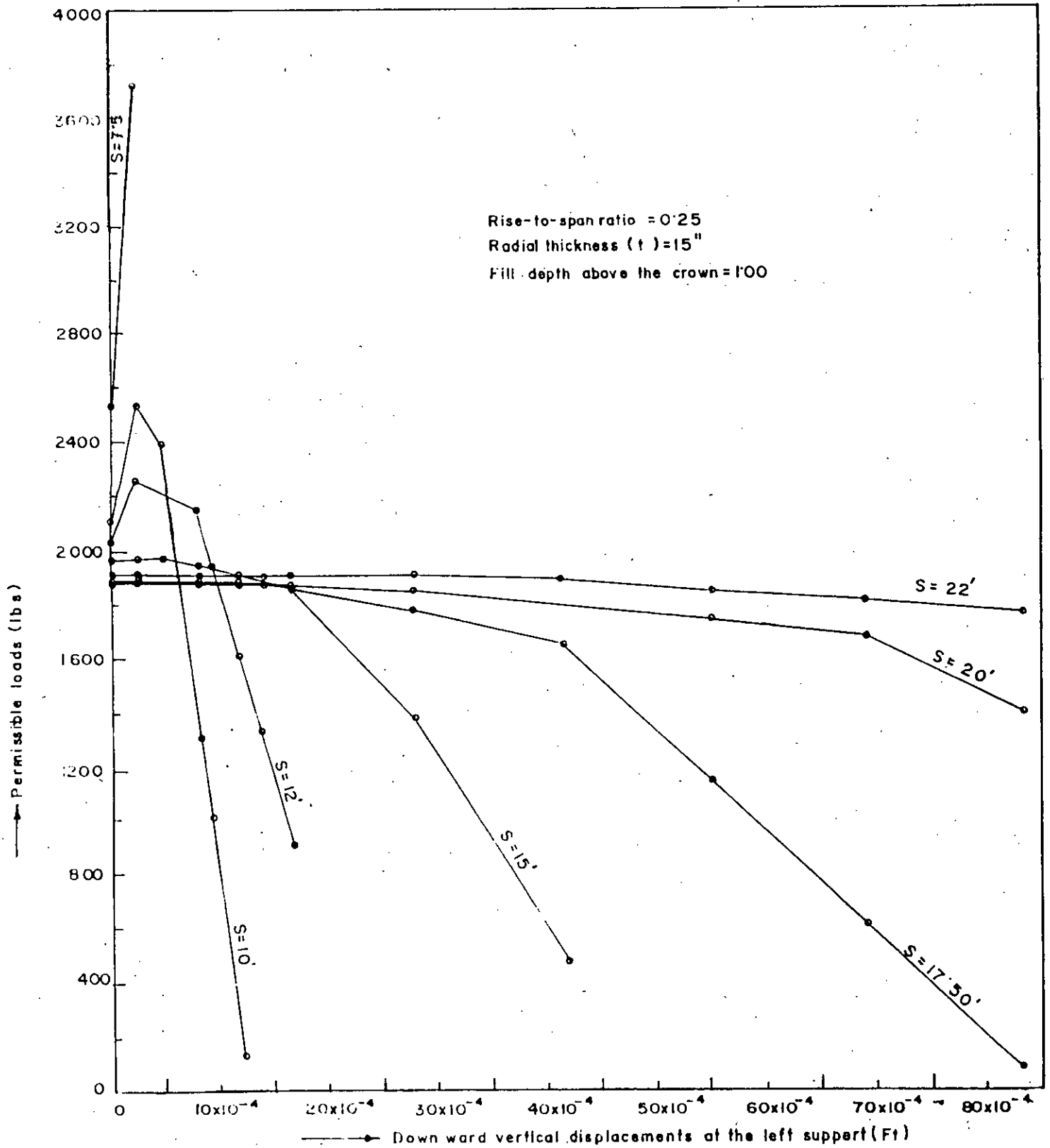


Fig-6-15 Variation of permissible load with different downward vertical displacement of the left support

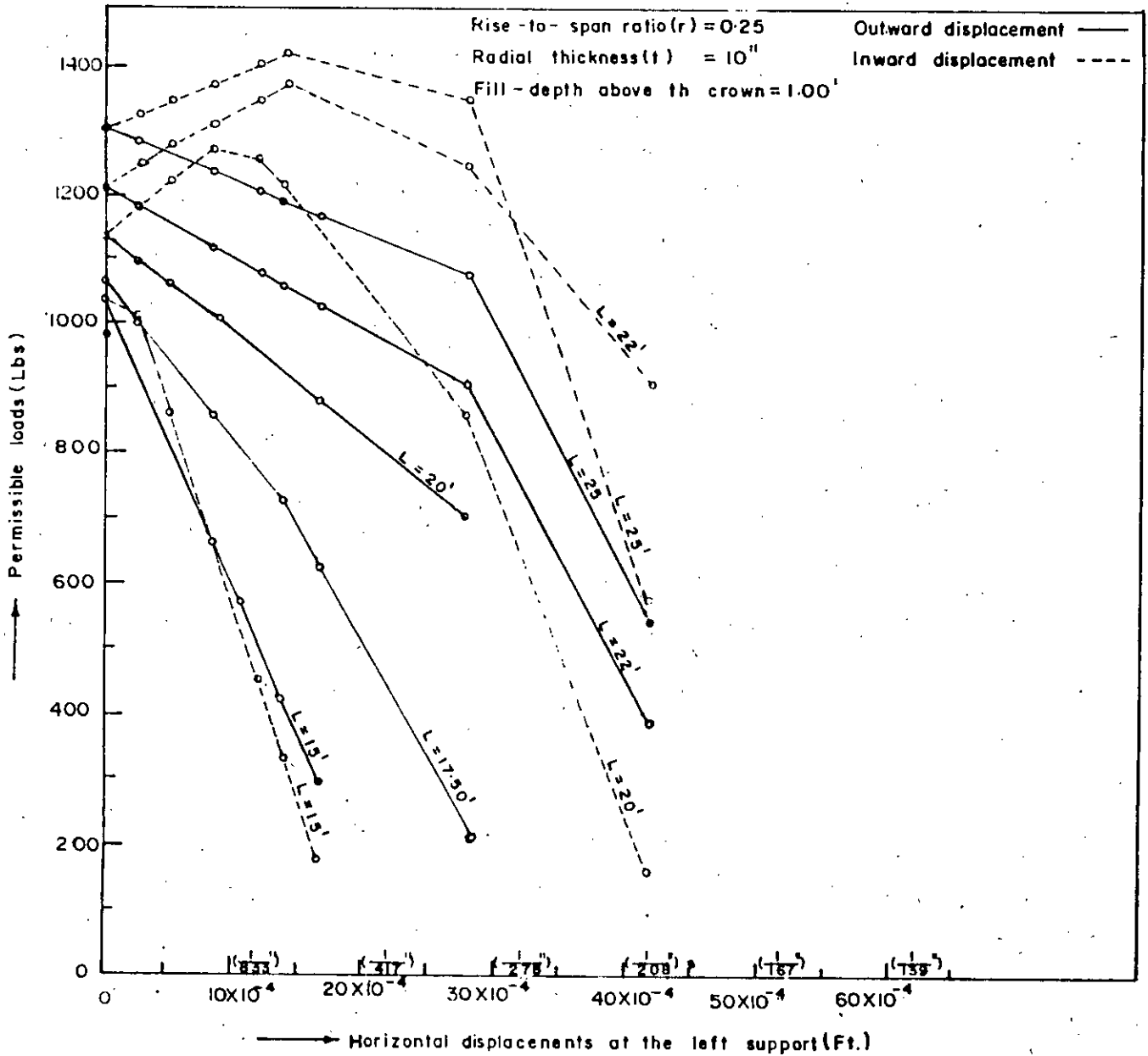


Fig-6-16 Variation of permissible loads with different outward horizontal displacements at the left support.

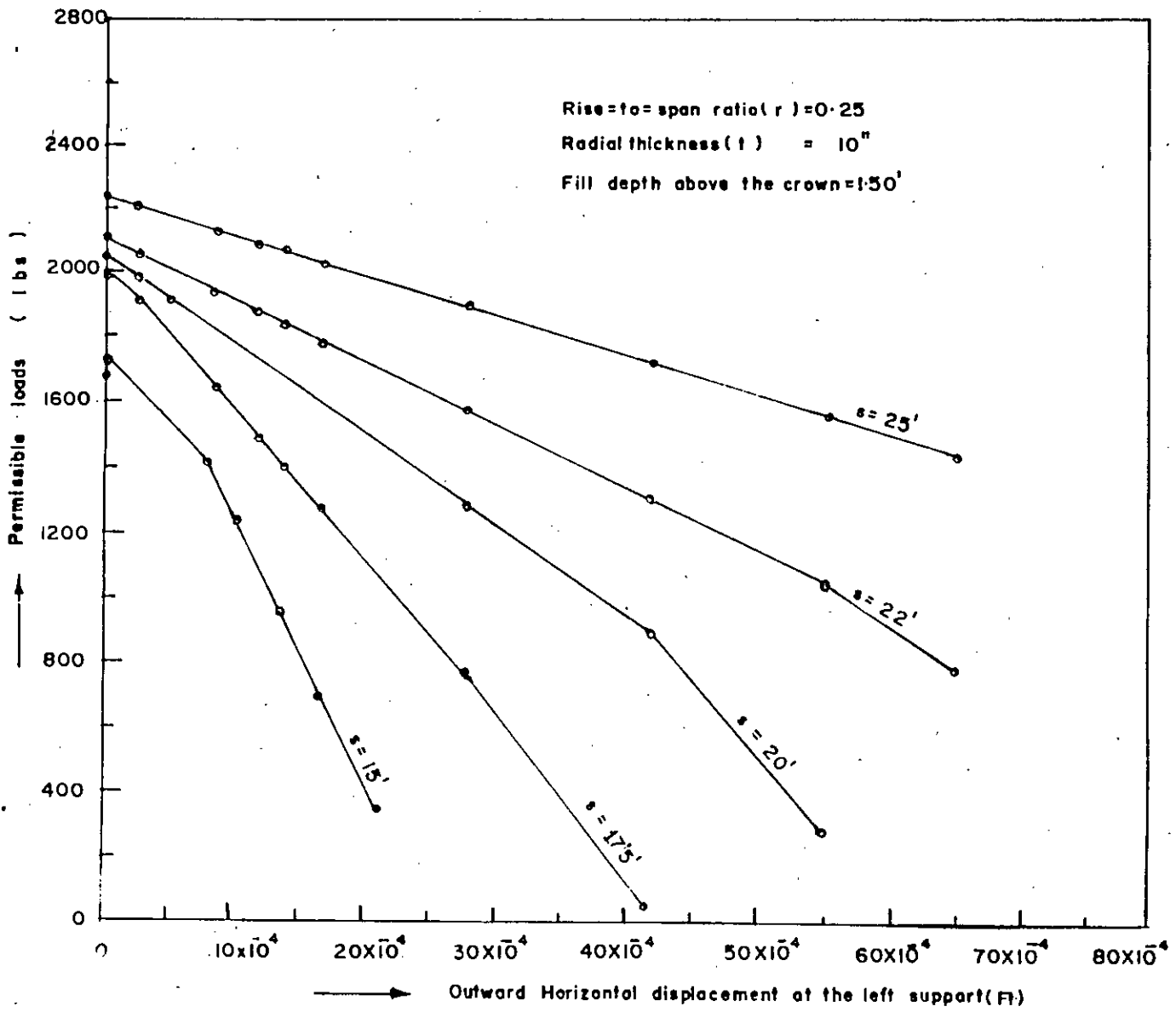


Fig-6-17 variation of permissible loads with different outward horizontal displacement at the left support

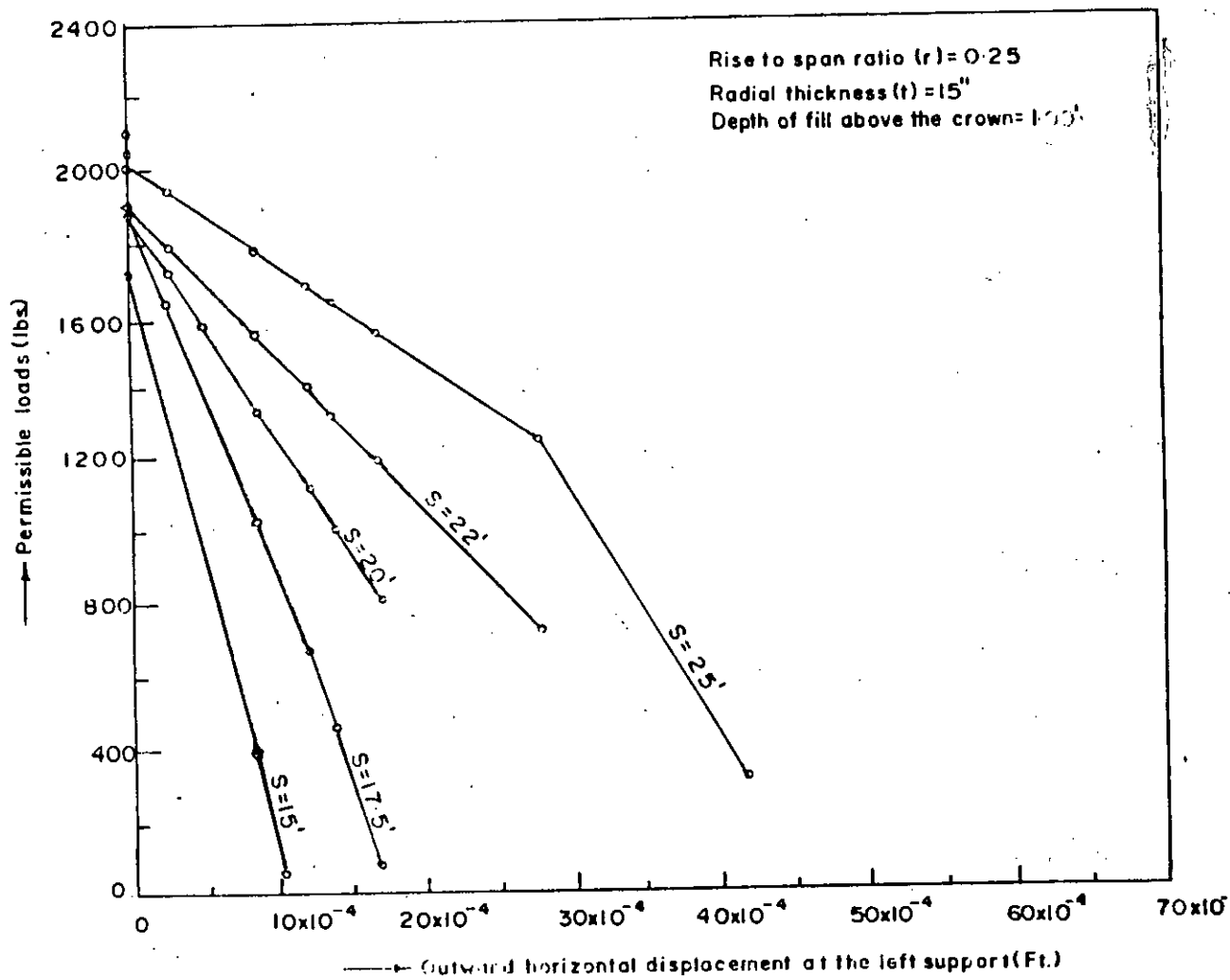


Fig-6-18 Variation of permissible loads with different outward horizontal displacement at the left support

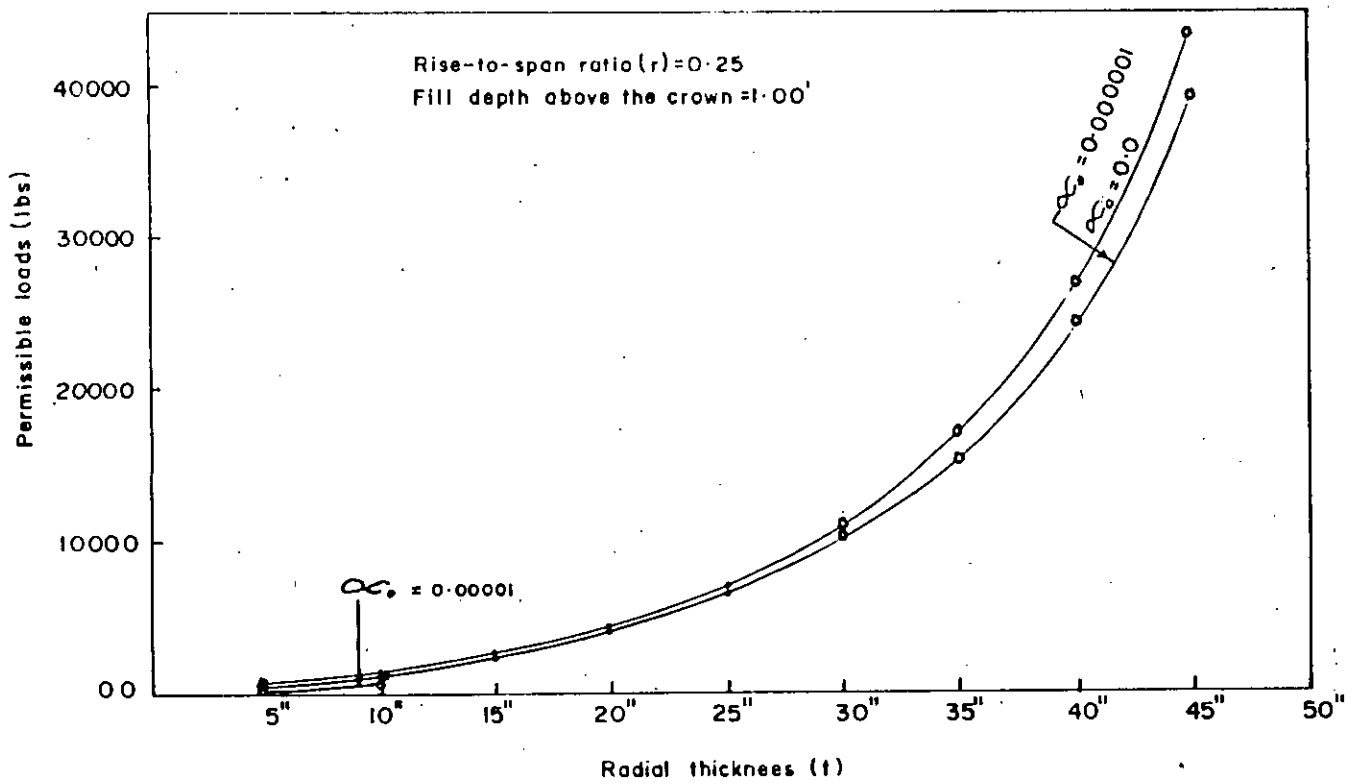


Fig. 6-19 Variation of permissible loads with different radial thickness (t) due to various rotation in radian (Clock-wise) at left support for span (L) = 10'

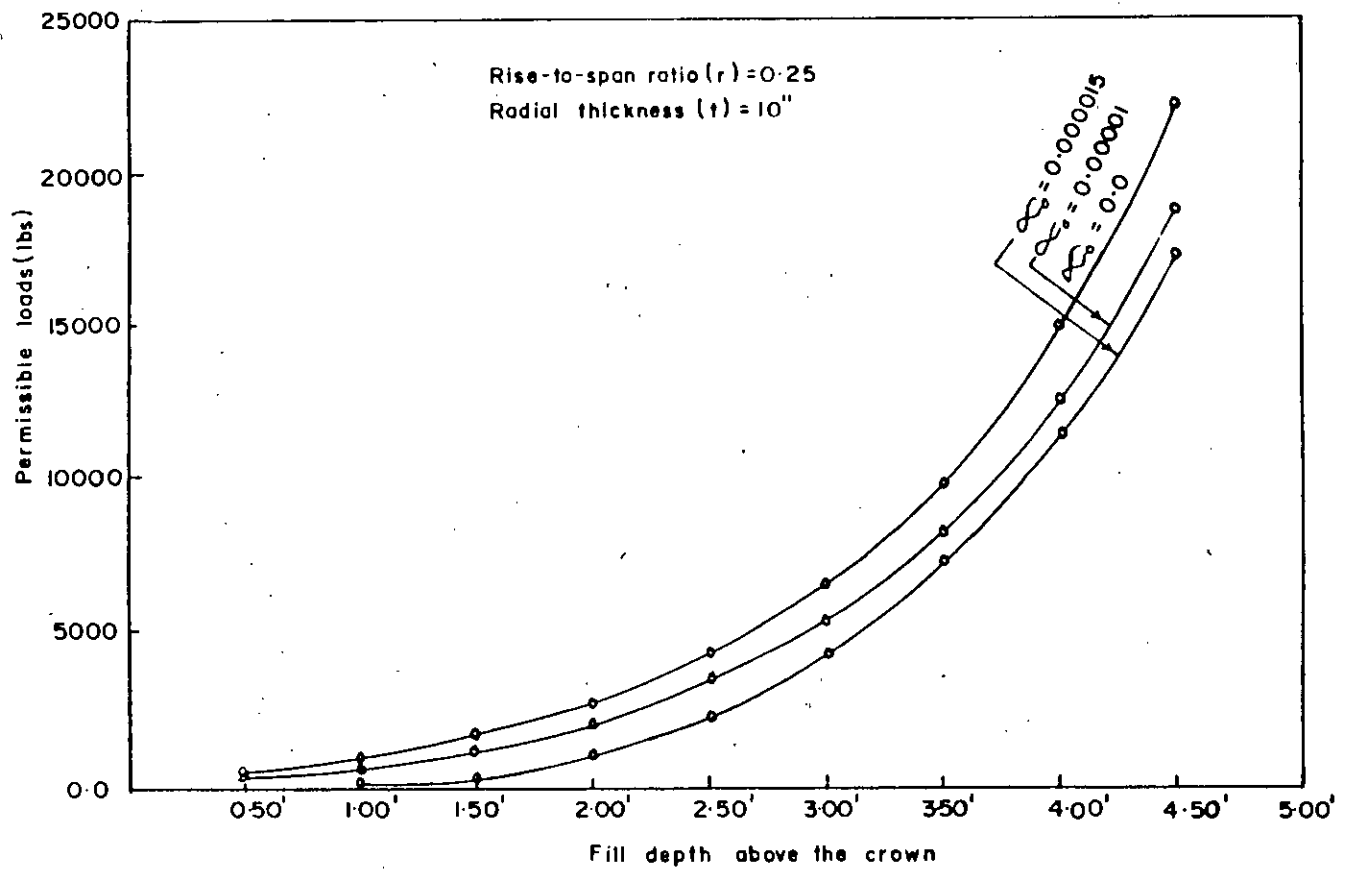


Fig. 6-20 Variation of permissible loads with different Fill depth above the crown due to various rotations in radian (Clock-wise) at left support for span (L) = 10'

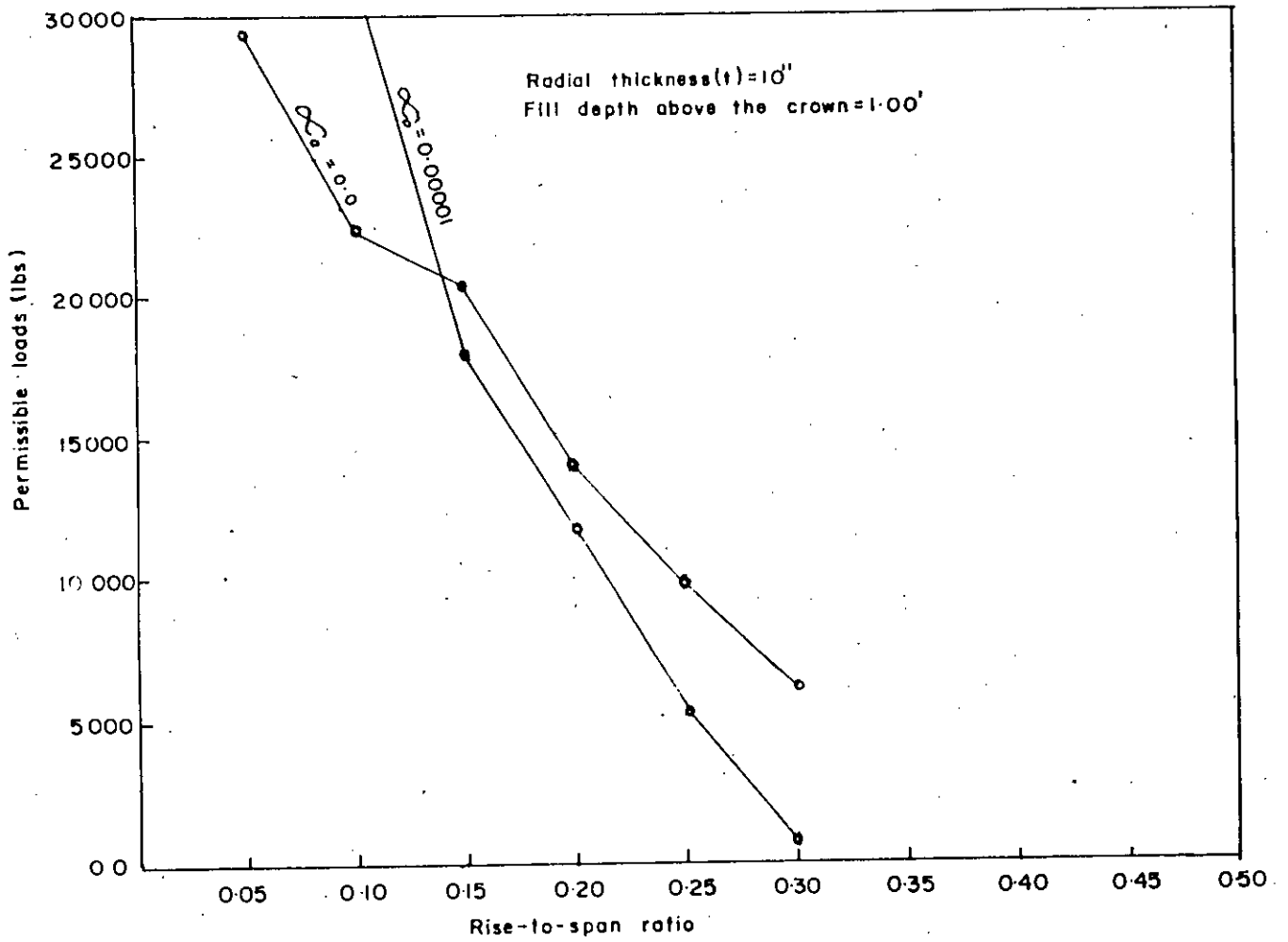


Fig. - 6.21 Variation of permissible loads with various rise to span ratio (r) due to different rotations in radian (Clock wise) of left support for span (L) = 10'

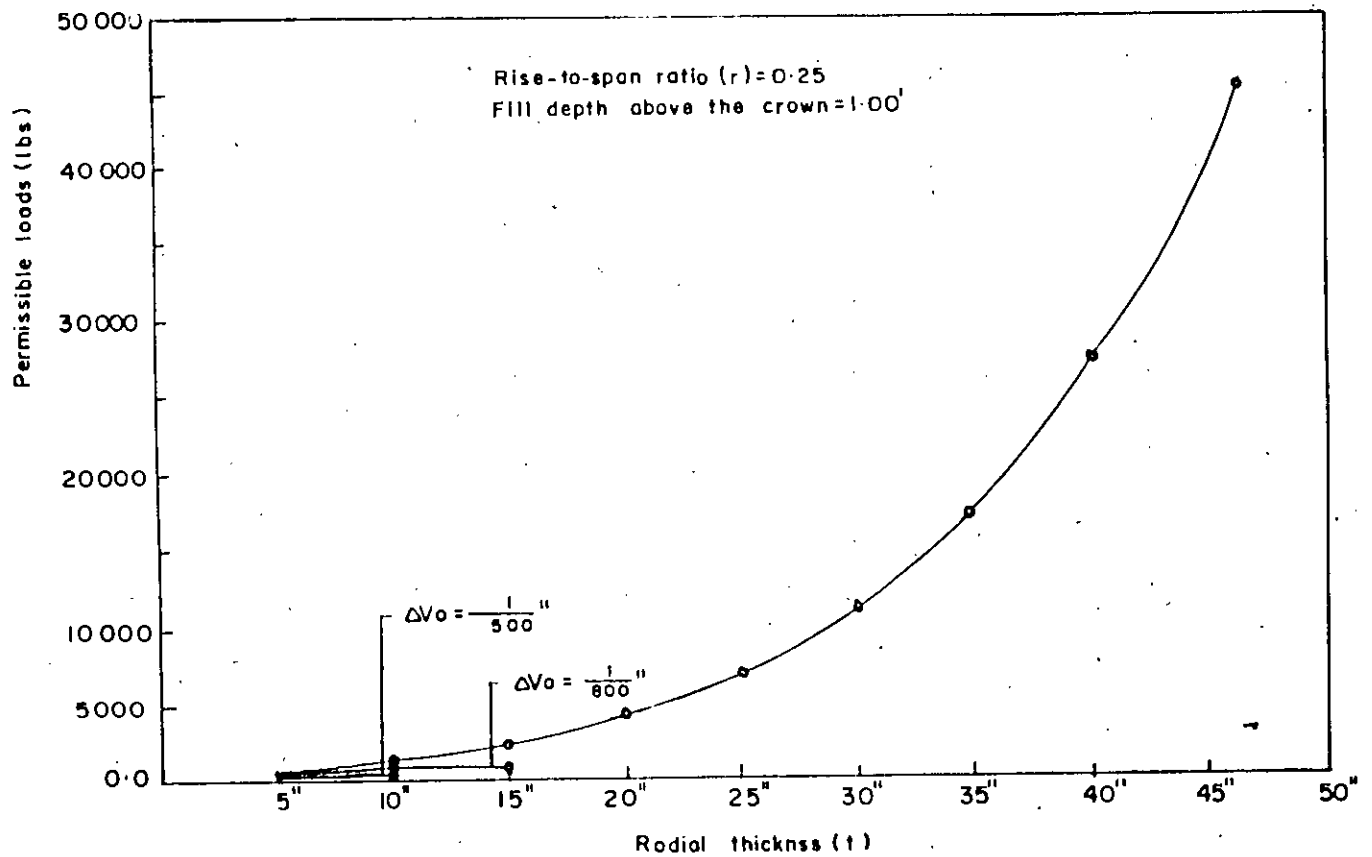


Fig. - 6.22 Variation of permissible loads with different radial thickness (t) due to various vertical displacements (Down-ward) of left support for span (L) = 10'

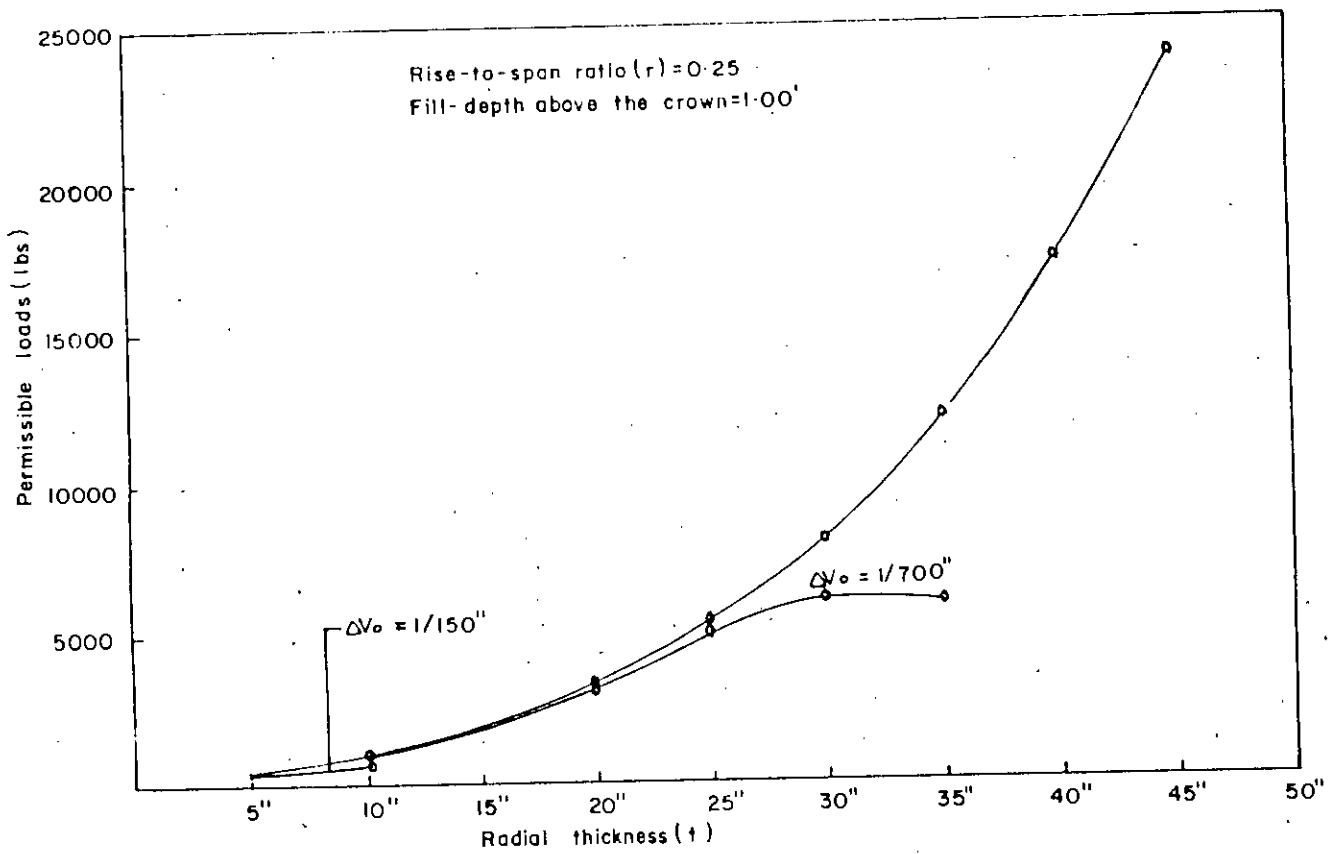


Fig:- 6-23 Variation of permissible loads with different Radial thickness (t) due to various vertical displacements (down-ward) at the left support for span (L) = 15'

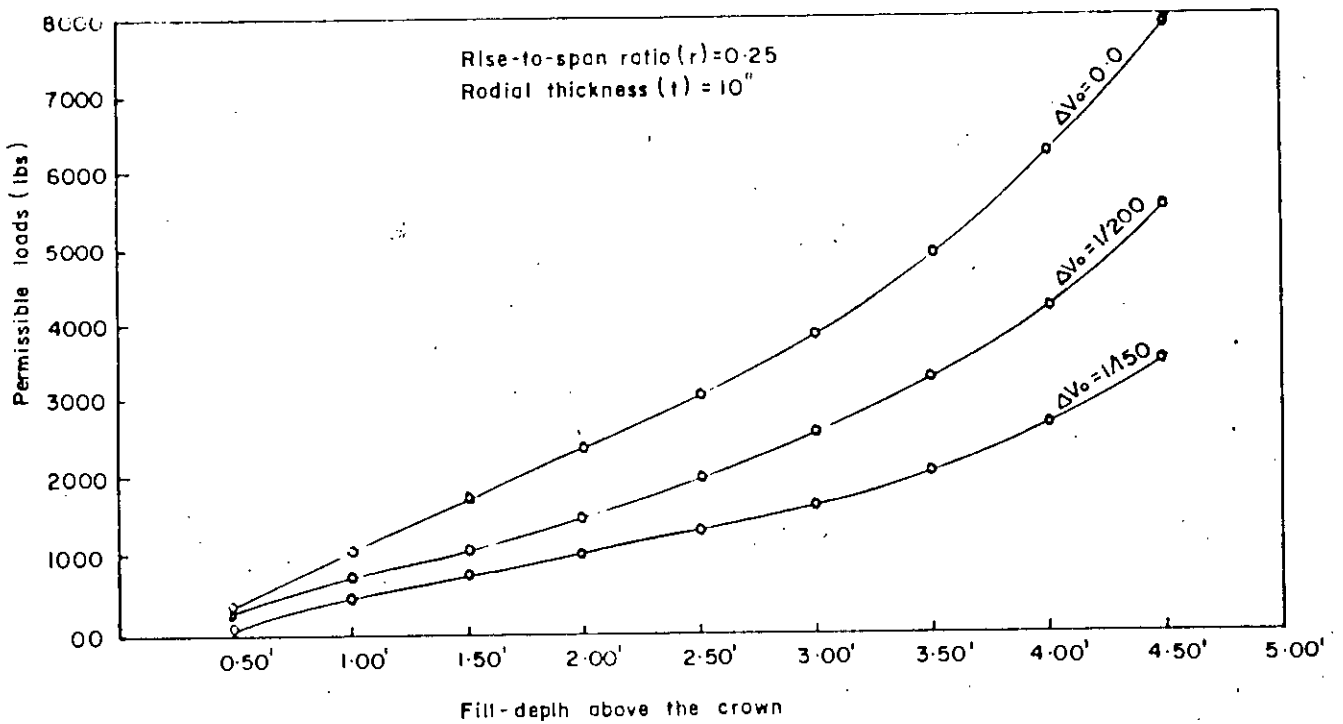


Fig:- 6-24 Variation of permissible loads with different Fill depth above the crown due to various vertical displacements (down-ward) at the left support for span (L) = 15'

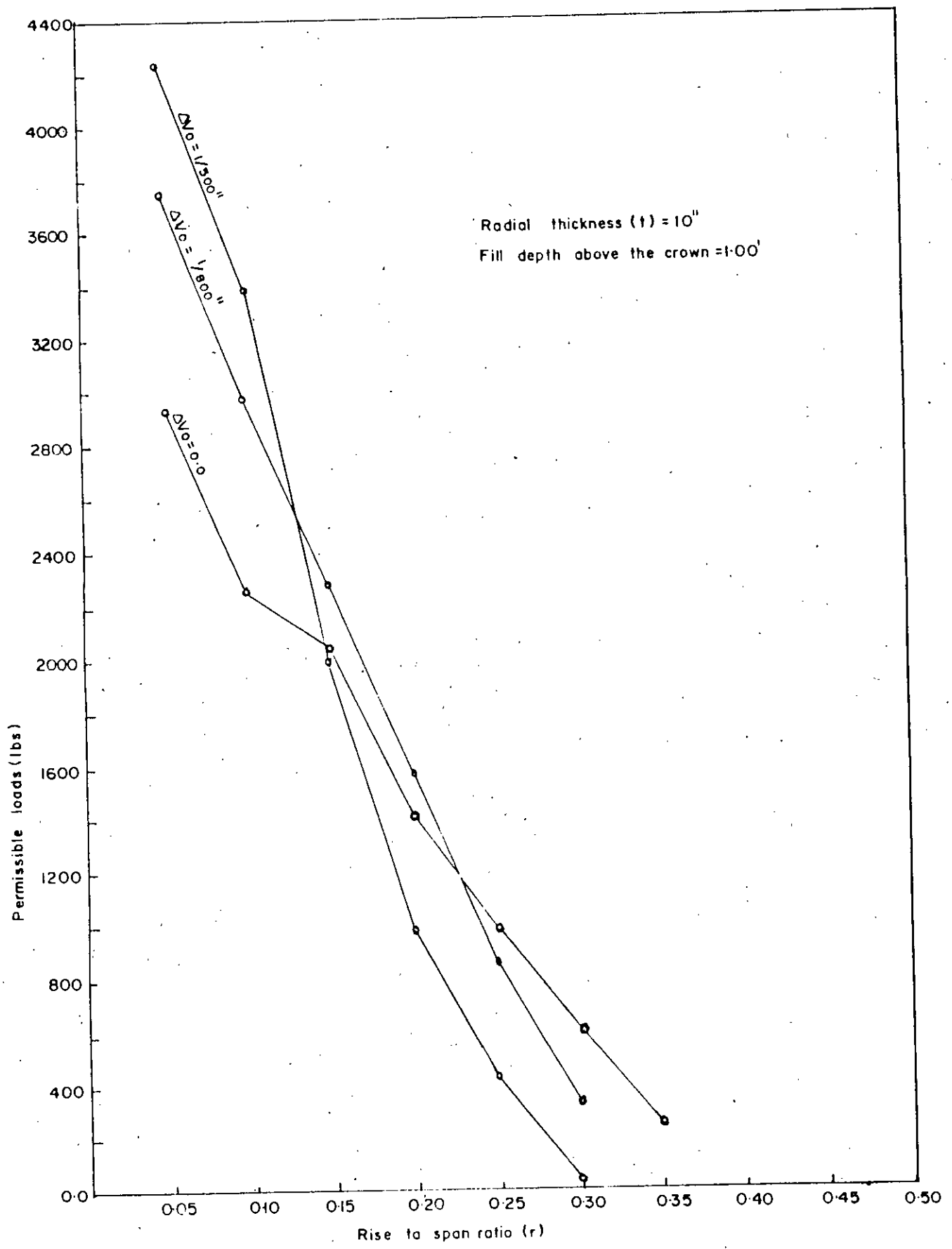


Fig.- 6.25 Variation of permissible loads with different rise-to-span ratio (r) due to various vertical displacements (Down ward) of left support for span (L) = 10'

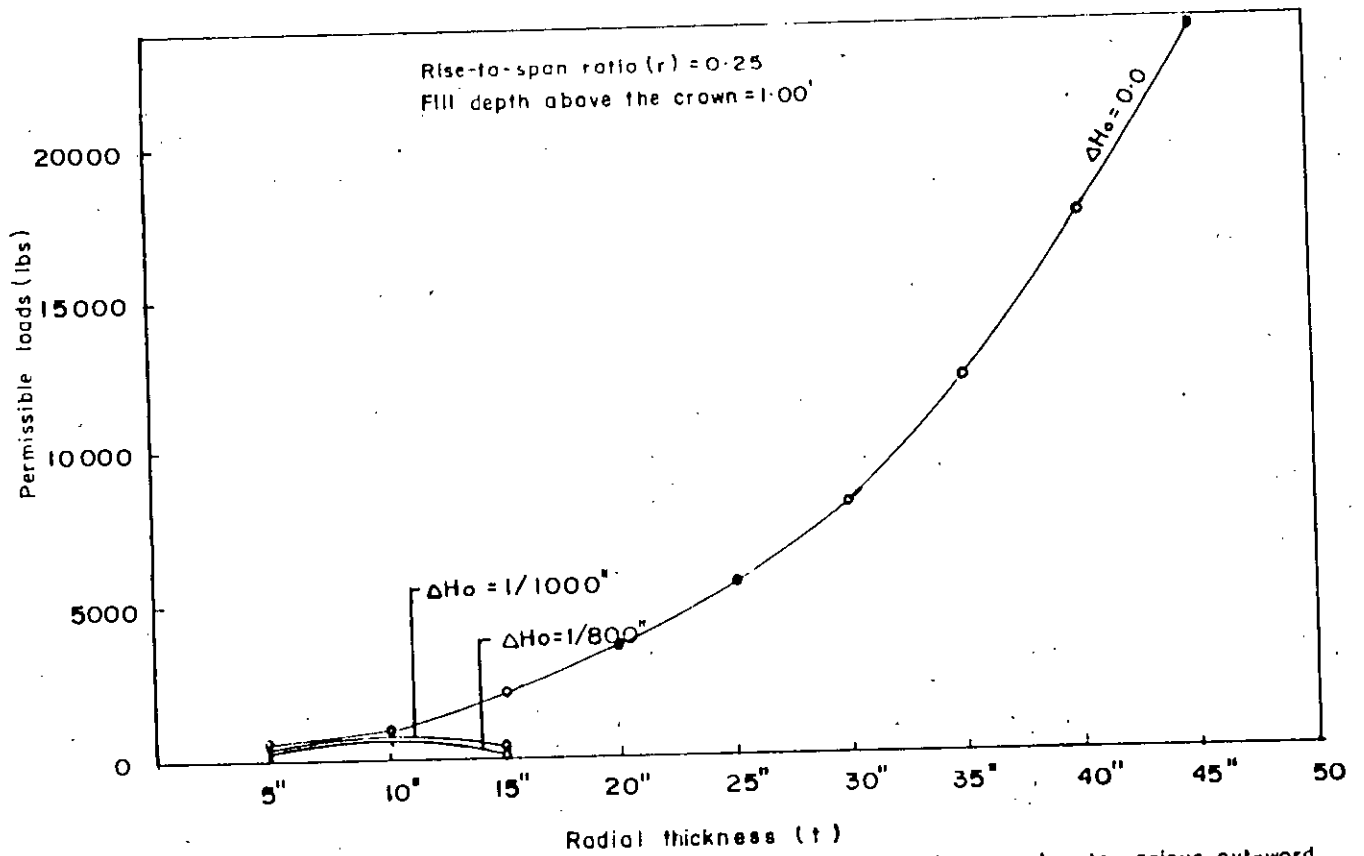


Fig. 6-26 Variation of permissible loads with different radial thickness due to various out-ward horizontal displacements of left support for span (L) = 15'

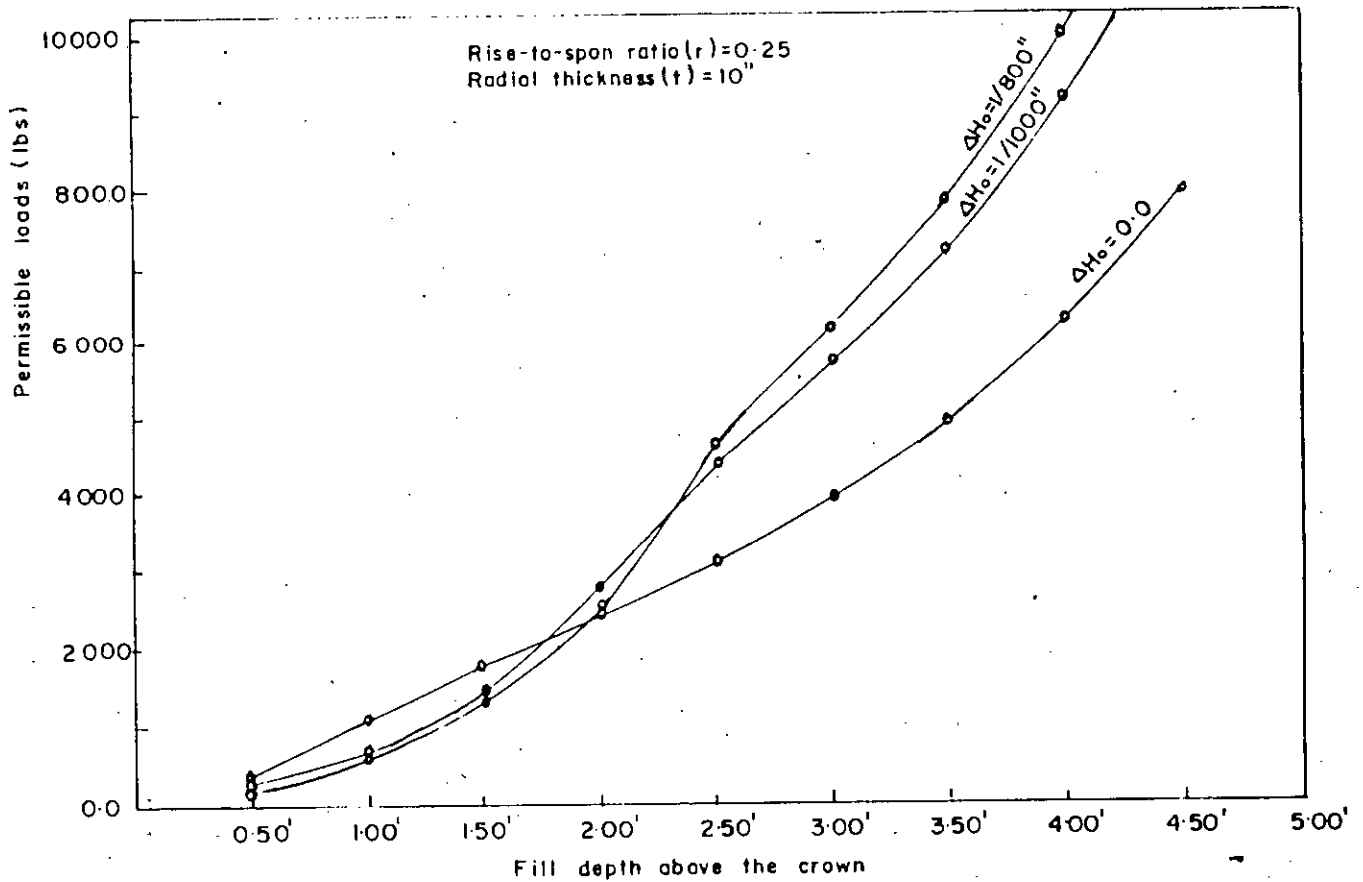


Fig. - 6-27 Variation of permissible loads with different Fill depth above the crown due to various horizontal displacements (Out-ward) of left support for span (L) = 15'

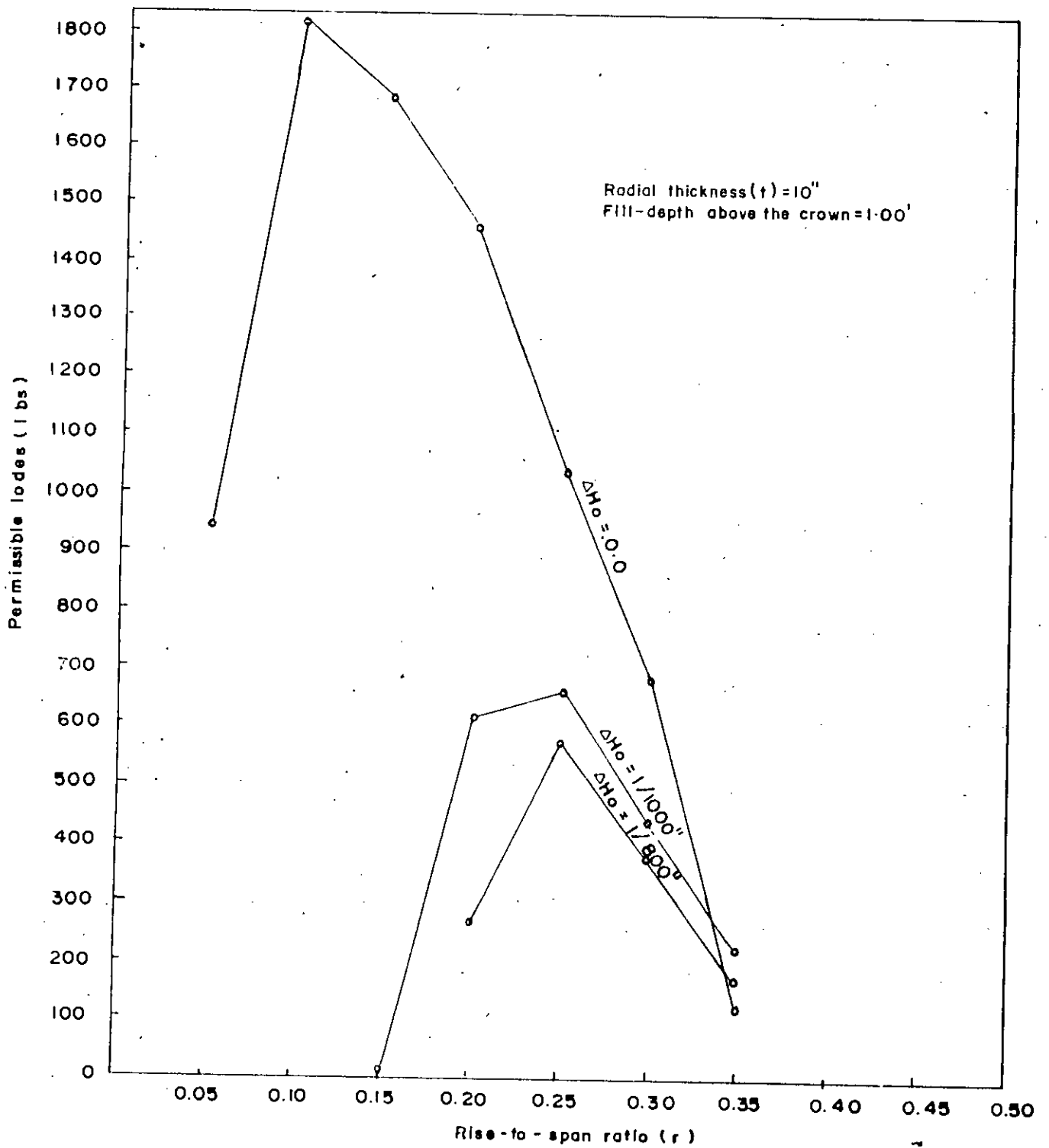


Fig.-6-28 Variation of permissible loads with different rise-to-span ratio (r) due to various horizontal displacements (out-ward) of left support for span (L) = 15'

6.3 Conclusions

The conclusions stemming from the results of elastic analysis are as follows :

- (1) Rise-to-span ratio is the main parameter in designing the circular masonry arches which has a dramatic effect on the permissible live load capacity and abutment thrusts. The arch designer can easily fix up the most effective rise-to-span ratio from the influence diagrams and graphical display of the variation of loading capacity with rise-to-span ratio presented in the thesis.
- (2) The elastic analysis of an arch though conservative, the use of permissible tensile stresses has an appreciable effect on the permissible live load capacity.
- (3) The load carrying capacity of an arch is very much dependent on the position of live load, the most vulnerable position is either the crown or the quarter sections. Considering stresses the most critical section of masonry arches lie at the springing and at the crown.
- (4) The load carrying capacity of arches considering tensile, compressive or shear stress mainly depends on the allowable limits

of these stresses and the study reveals that for most of the arches tension is the critical stress.

(5) A significant effect of support displacement on the permissible live load capacity was observed. It is further observed that the direction of support displacements has also a very much significant effect on load carrying capacity of arches.

6.4 Scope for further study

(1) The permissible load capacity has been computed in the thesis by dividing an arch into ten segments of equal horizontal projection but it can be divided into more segments than ten to get more precise result.

(2) The fill is considered to be of uniform density and to exercise a purely vertical load upon the arch-ring. It may however be possible to consider non-homogeneous fill, the load of which is acting vertically or in any direction on the arch.

(3) Effect of any thermal expansion, temperature change and shrinkage may be considered in further study.

(4) The computer programme developed analyzes the fixed circular arches of uniform radial thickness only. It is possible to improve the model to include arches of variable radial thickness by slight modification of the programme.

(5) The basic equations and assumptions used to derive the generalized equations due to various loading and support yielding conditions for circular arches may also be utilised for any other shape of arch. The numerical model thus developed may be improved for analyzing arches of any arbitrary shape.

(6) The numerical model developed computes the permissible live load capacity based on the limiting allowable stresses and support deformations. The model may be further extended to include the buckling behaviour of the masonry arches.

REFERENCES

- (1) ASWANI, M.G., VAZIRANI, V.N. & RATWANI, M.M.
"Design of concrete Bridges".
- (2) CHETTOE, C.S. & HENDERSON, W.
"Masonry arch bridges", a study. Proc. Instn. Civ. Engrs., 1957, 7, August, P 723-762.
- (3) CURTIN, W.G., SHAW, G., BECK, J.K. & BRAY, W.A.
"Structural Masonry Designer's Manual", P 427-445.
- (4) ERIKSEN, B.
"Influence lines for thrust and bending moments in the fixed arch", A.M.I Struct. E., London, concrete publication limited.
- (5) HEYMAN, J.
"The estimation of the strength of masonry arches", Proc. Instn. Civ. Engrs., 1980, 69, P-921.
- (6) HEYMAN, J.
"The safety of masonry arches", Proc. Intn. J. Mech. Sci., 1969, 11, P-363.
- (7) NICHOLAS WILLEMS & LUCAS WILLIAM, M. JR.
"Structural analysis for Engineers", International student edition, P 169-205.

(8) PIPPARD, A. J. S.

"The approximate estimation of safe loads on masonry bridges", Civil Engineer in war, vol. 1, P-365, Inst. of Civil Engineers, London, 1948.

(9) WANG CHU-KIA

"Statically Indeterminate Structures", International student edition, P 345-383.

(10) WALKLATE, R.P. & MANN., J.W.

"A method for determining the permissible loading of brick and masonry arches", Proc. Instn. Civ. Engrs., part-2, 1983, 75, Dec., P 585-597.

BIBLIOGRAPHY

- (1) FULLAR, G.
"Curve of equilibriums for a rigid arch under vertical forces", Min. Proc. Instn. Civ. Engineers, 1875, 40, P 143-149.
- (2) FAIRHURST, W.A.
"Arch design simplified".
- (3) GAYLORD, E.H.JR. & GAYLORD, C.N.
"Structural Engineering Hand Books" second edition, P 17-1 to 17-53.
- (4) KOOHARIAN, A.
"Limit analysis of voussoir (segmental) and concrete arches", Proc. Am. Concr. Inst., 1953, 49, P-317.
- (5) REYNOLDS, C.E.
"Basic Reinforced Concrete Design", vol. II, Concrete publication limited.
- (6) ROUF, M.A. AND SAWKO, F.
"Shear Stress Distribution in Masonry Elements", Proc. ICE, TN 425, March 1985, PP 181-191.
- (7) ROUF, M. A.
"The Fundamental Properties of Brickwork with particular Emphasis to Brickwork Arches", Ph. D. Thesis, University of Liverpool, Sept. 1984.

- (10) SAWKO, F. AND ROUF, M. A.
"A Proposed Numerical Model for Structural Masonry",
International, No. 5, July 1985.
- (11) TERRINGTON, J. S.
"Design of arch ribs for reinforced concrete roofs".
- (12) TOWLER, K. D. S.
"The Non-linear Finite Element Analysis of Bridgemill
Masonry Arch Bridge", Taylor woodrow construction ltd.,
Middlesex, UB1 2QX.
- (13) VAZIRANI, V.N. & RATWANI, M.M.
"Analysis of Structures ", Vol. II, Khanna Publishers,
P 510 - 543.

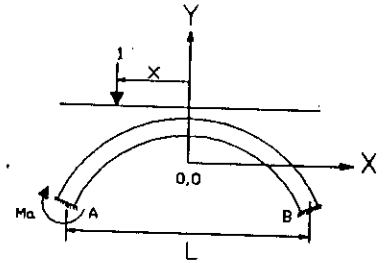
APPENDIX - A

COMPUTER PRINTED RESULTS

A.1 Influence co-efficient due to moving unit load and
co-efficient of different force components due to
various loading and support displacements

BENDING MOMENTS AT LEFT SPRINGING
=INFLUENCE VALUE*(L)

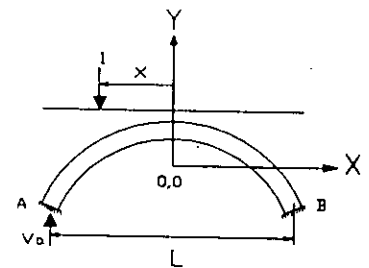
TABLE A.1



		POSITION OF UNIT LOAD FROM THE CROWN											
X/L		-0.50	-0.40	-0.30	-0.20	-0.10	0.00	0.10	0.20	0.30	0.40	0.50	
RISE- -TO- SPAN RATIO	0.050	0.0000	-0.0605	-0.0634	-0.0361	0.0005	0.0315	0.0482	0.0474	0.0322	0.0114	0.0000	
	0.100	0.0000	-0.0597	-0.0617	-0.0343	0.0018	0.0323	0.0487	0.0480	0.0328	0.0117	0.0000	
	0.150	0.0000	-0.0582	-0.0589	-0.0313	0.0040	0.0336	0.0496	0.0489	0.0338	0.0123	0.0000	
	0.200	0.0000	-0.0562	-0.0549	-0.0273	0.0070	0.0355	0.0508	0.0501	0.0351	0.0131	0.0000	
	0.250	0.0000	-0.0533	-0.0497	-0.0222	0.0107	0.0377	0.0523	0.0516	0.0367	0.0142	0.0000	
	0.300	0.0000	-0.0496	-0.0435	-0.0162	0.0151	0.0405	0.0541	0.0532	0.0386	0.0156	0.0000	
	0.350	0.0000	-0.0449	-0.0363	-0.0095	0.0200	0.0436	0.0562	0.0551	0.0408	0.0173	0.0000	
	0.400	0.0000	-0.0390	-0.0282	-0.0022	0.0255	0.0472	0.0585	0.0572	0.0430	0.0193	0.0000	
	0.450	0.0000	-0.0320	-0.0193	0.0057	0.0313	0.0511	0.0611	0.0594	0.0454	0.0216	0.0000	

VERTICAL REACTIONS AT LEFT SPRINGING

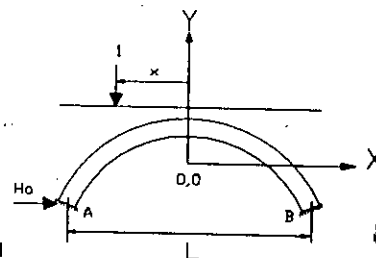
TABLE A.2



		POSITION OF UNIT LOAD FROM THE CROWN											
X/L		-0.50	-0.40	-0.30	-0.20	-0.10	0.00	0.10	0.20	0.30	0.40	0.50	
RISE- -TO- SPAN RATIO	0.050	1.0000	0.9718	0.8956	0.7836	0.6477	0.5000	0.3523	0.2164	0.1044	0.0282	0.0000	
	0.100	1.0000	0.9714	0.8945	0.7823	0.6469	0.5000	0.3531	0.2177	0.1055	0.0286	0.0000	
	0.150	1.0000	0.9705	0.8926	0.7802	0.6456	0.5000	0.3544	0.2198	0.1074	0.0295	0.0000	
	0.200	1.0000	0.9693	0.8900	0.7774	0.6438	0.5000	0.3562	0.2226	0.1100	0.0307	0.0000	
	0.250	1.0000	0.9675	0.8865	0.7738	0.6416	0.5000	0.3584	0.2262	0.1135	0.0325	0.0000	
	0.300	1.0000	0.9652	0.8822	0.7695	0.6390	0.5000	0.3610	0.2305	0.1178	0.0348	0.0000	
	0.350	1.0000	0.9622	0.8771	0.7647	0.6361	0.5000	0.3639	0.2353	0.1229	0.0378	0.0000	
	0.400	1.0000	0.9583	0.8712	0.7593	0.6330	0.5000	0.3670	0.2407	0.1288	0.0417	0.0000	
	0.450	1.0000	0.9536	0.8647	0.7536	0.6298	0.5000	0.3702	0.2464	0.1353	0.0464	0.0000	

HORIZONTAL REACTIONS AT LEFT SPRINGING

TABLE A.3

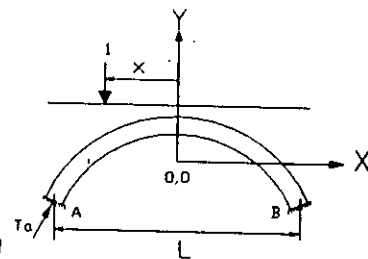


POSITION OF UNIT LOAD FROM THE CROWN

	X/L	-0.50	-0.40	-0.30	-0.20	-0.10	0.00	0.10	0.20	0.30	0.40	0.50
RISE-	0.050	0.0000	0.6120	1.9277	3.3129	4.3208	4.6862	4.3208	3.3129	1.9277	0.6120	0.0000
	0.100	0.0000	0.3128	0.9754	1.6643	2.1616	2.3411	2.1616	1.6643	0.9754	0.3128	0.0000
-TO-	0.150	0.0000	0.2164	0.6628	1.1179	1.4422	1.5586	1.4422	1.1179	0.6628	0.2164	0.0000
	0.200	0.0000	0.1707	0.5099	0.8466	1.0827	1.1669	1.0827	0.8466	0.5099	0.1707	0.0000
SPAN	0.250	0.0000	0.1457	0.4207	0.6850	0.8671	0.9314	0.8671	0.6850	0.4207	0.1457	0.0000
	0.300	0.0000	0.1311	0.3628	0.5778	0.7233	0.7743	0.7233	0.5778	0.3628	0.1311	0.0000
RATIO	0.350	0.0000	0.1226	0.3226	0.5015	0.6205	0.6618	0.6205	0.5015	0.3226	0.1226	0.0000
	0.400	0.0000	0.1179	0.2931	0.4443	0.5432	0.5774	0.5432	0.4443	0.2931	0.1179	0.0000
	0.450	0.0000	0.1157	0.2705	0.3997	0.4831	0.5117	0.4831	0.3997	0.2705	0.1157	0.0000

THRUSTS AT THE LEFT SPRINGING

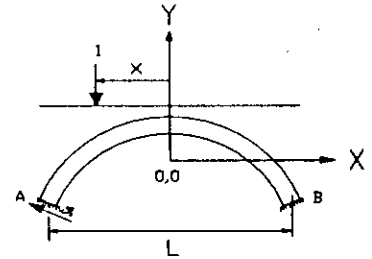
TABLE A.4



POSITION OF UNIT LOAD FROM THE CROWN

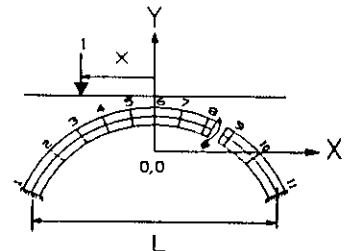
	X/L	-0.50	-0.40	-0.30	-0.20	-0.10	0.00	0.10	0.20	0.30	0.40	0.50
RISE-	0.050	0.1980	0.7582	2.0205	3.3645	4.3431	4.6862	4.3314	3.3196	1.9265	0.6087	0.0000
	0.100	0.3846	0.5966	1.1555	1.7649	2.2050	2.3411	2.1824	1.6780	0.9734	0.3065	0.0000
-TO-	0.150	0.5505	0.6216	0.9204	1.2622	1.5045	1.5586	1.4725	1.1388	0.6611	0.2072	0.0000
	0.200	0.6897	0.6772	0.8325	1.0282	1.1612	1.1669	1.1215	0.8752	0.5098	0.1593	0.0000
SPAN	0.250	0.8000	0.7312	0.7945	0.8965	0.9586	0.9314	0.9133	0.7213	0.4235	0.1327	0.0000
	0.300	0.8824	0.7742	0.7749	0.8122	0.8247	0.7743	0.7756	0.6220	0.3702	0.1174	0.0000
RATIO	0.350	0.9396	0.8041	0.7609	0.7521	0.7289	0.6618	0.6778	0.5532	0.3358	0.1093	0.0000
	0.400	0.9756	0.8217	0.7477	0.7054	0.6563	0.5774	0.6044	0.5030	0.3130	0.1062	0.0000
	0.450	0.9945	0.8288	0.7330	0.6665	0.5987	0.5117	0.5471	0.4647	0.2978	0.1070	0.0000

TABLE A.5
SHEAR FORCES ALONG THE RADIAL SECTION AT THE LEFT SPRINGING



		POSITION OF UNIT LOAD FROM THE CROWN										
X/L		-0.50	-0.40	-0.30	-0.20	-0.10	0.00	0.10	0.20	0.30	0.40	0.50
RISE- TO- SPAN RATIO	0.050	0.9802	0.8626	0.6602	0.5187	0.4761	0.5000	0.1809	-0.0467	-0.1254	-0.0692	0.0000
	0.100	0.9231	0.8280	0.6453	0.5170	0.4787	0.5000	0.1858	-0.0410	-0.1224	-0.0690	0.0000
	0.150	0.8349	0.7761	0.6236	0.5149	0.4829	0.5000	0.1935	-0.0318	-0.1176	-0.0688	0.0000
	0.200	0.7241	0.7142	0.5992	0.5137	0.4883	0.5000	0.2035	-0.0195	-0.1108	-0.0686	0.0000
	0.250	0.6000	0.6502	0.5758	0.5139	0.4946	0.5000	0.2151	-0.0048	-0.1023	-0.0683	0.0000
	0.300	0.4706	0.5912	0.5563	0.5160	0.5013	0.5000	0.2277	0.0117	-0.0921	-0.0679	0.0000
	0.350	0.3423	0.5424	0.5425	0.5201	0.5082	0.5000	0.2408	0.0296	-0.0804	-0.0672	0.0000
	0.400	0.2195	0.5071	0.5348	0.5257	0.5149	0.5000	0.2539	0.0482	-0.0672	-0.0660	0.0000
	0.450	0.1050	0.4857	0.5325	0.5324	0.5211	0.5000	0.2667	0.0670	-0.0528	-0.0640	0.0000

TABLE A.6
BENDING MOMENTS AT DIFFERENT SECTIONS (RISE-TO-SPAN RATIO 0.050)
=INFLUENCE VALUE*(L)



		POSITION OF UNIT LOAD FROM THE CROWN										
X/L		-0.50	-0.40	-0.30	-0.20	-0.10	0.00	0.10	0.20	0.30	0.40	0.50
DIFFER- ENT SECTIONS	1	0.0000	-0.0605	-0.0634	-0.0361	0.0005	0.0315	0.0482	0.0474	0.0322	0.0114	0.0000
	2	0.0000	0.0256	-0.0088	-0.0178	-0.0130	-0.0034	0.0051	0.0091	0.0077	0.0031	0.0000
	3	0.0000	0.0142	0.0538	0.0142	-0.0088	-0.0190	-0.0201	-0.0157	-0.0088	-0.0027	0.0000
	4	0.0000	0.0053	0.0242	0.0596	0.0130	-0.0156	-0.0279	-0.0270	-0.0176	-0.0059	0.0000
	5	0.0000	-0.0011	0.0023	0.0182	0.0521	0.0065	-0.0184	-0.0251	-0.0186	-0.0068	0.0000
	6	0.0000	-0.0052	-0.0120	-0.0100	0.0083	0.0472	0.0083	-0.0100	-0.0120	-0.0052	0.0000
	7	0.0000	-0.0068	-0.0186	-0.0251	-0.0184	0.0065	0.0521	0.0182	0.0023	-0.0011	0.0000
	8	0.0000	-0.0059	-0.0176	-0.0270	-0.0279	-0.0156	0.0130	0.0596	0.0242	0.0053	0.0000
	9	0.0000	-0.0027	-0.0088	-0.0157	-0.0201	-0.0190	-0.0088	0.0142	0.0538	0.0142	0.0000
	10	0.0000	0.0031	0.0077	0.0091	0.0051	-0.0034	-0.0130	-0.0178	-0.0088	0.0256	0.0000
	11	0.0000	0.0114	0.0322	0.0474	0.0482	0.0315	0.0005	-0.0361	-0.0634	-0.0605	0.0000

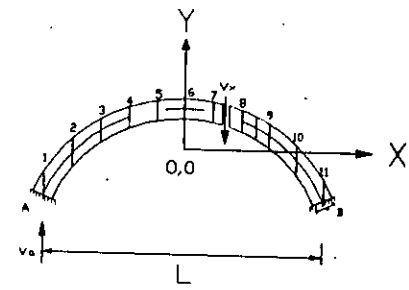


TABLE A.7

VERTICAL SHEAR FORCES AT DIFFERENT SECTIONS (RISE-TO-SPAN RATIO 0.050)

		POSITION OF UNIT LOAD FROM THE CROWN										
X/L		-0.50	-0.40	-0.30	-0.20	-0.10	0.00	0.10	0.20	0.30	0.40	0.50
DIFFER- ENT SECTIONS	1	0.0000	0.9718	0.8956	0.7836	0.6477	0.5000	0.3523	0.2164	0.1044	0.0282	0.0000
	2	0.0000	-0.0282	0.8956	0.7836	0.6477	0.5000	0.3523	0.2164	0.1044	0.0282	0.0000
	3	0.0000	-0.0282	-0.1044	0.7836	0.6477	0.5000	0.3523	0.2164	0.1044	0.0282	0.0000
	4	0.0000	-0.0282	-0.1044	-0.2164	0.6477	0.5000	0.3523	0.2164	0.1044	0.0282	0.0000
	5	0.0000	-0.0282	-0.1044	-0.2164	-0.3523	0.5000	0.3523	0.2164	0.1044	0.0282	0.0000
	6	0.0000	-0.0282	-0.1044	-0.2164	-0.3523	0.5000	0.3523	0.2164	0.1044	0.0282	0.0000
	7	0.0000	-0.0282	-0.1044	-0.2164	-0.3523	-0.5000	0.3523	0.2164	0.1044	0.0282	0.0000
	8	0.0000	-0.0282	-0.1044	-0.2164	-0.3523	-0.5000	-0.6477	0.2164	0.1044	0.0282	0.0000
	9	0.0000	-0.0282	-0.1044	-0.2164	-0.3523	-0.5000	-0.6477	-0.7836	0.1044	0.0282	0.0000
	10	0.0000	-0.0282	-0.1044	-0.2164	-0.3523	-0.5000	-0.6477	-0.7836	-0.8956	0.0282	0.0000
	11	0.0000	-0.0282	-0.1044	-0.2164	-0.3523	-0.5000	-0.6477	-0.7836	-0.8956	-0.9718	0.0000

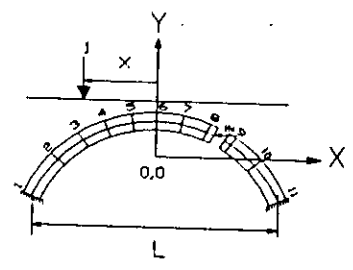


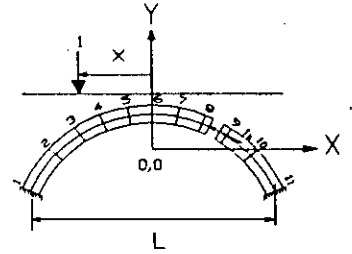
TABLE A.8

HORIZONTAL THRUSTS AT DIFFERENT SECTIONS (RISE-TO-SPAN RATIO 0.050)

		POSITION OF UNIT LOAD FROM THE CROWN										
X/L		-0.50	-0.40	-0.30	-0.20	-0.10	0.00	0.10	0.20	0.30	0.40	0.50
DIFFER- ENT SECTIONS	1	0.0000	0.6120	1.9277	3.3129	4.3208	4.6862	4.3208	3.3129	1.9277	0.6120	0.0000
	2	0.0000	0.6120	1.9277	3.3129	4.3208	4.6862	4.3208	3.3129	1.9277	0.6120	0.0000
	3	0.0000	0.6120	1.9277	3.3129	4.3208	4.6862	4.3208	3.3129	1.9277	0.6120	0.0000
	4	0.0000	0.6120	1.9277	3.3129	4.3208	4.6862	4.3208	3.3129	1.9277	0.6120	0.0000
	5	0.0000	0.6120	1.9277	3.3129	4.3208	4.6862	4.3208	3.3129	1.9277	0.6120	0.0000
	6	0.0000	0.6120	1.9277	3.3129	4.3208	4.6862	4.3208	3.3129	1.9277	0.6120	0.0000
	7	0.0000	0.6120	1.9277	3.3129	4.3208	4.6862	4.3208	3.3129	1.9277	0.6120	0.0000
	8	0.0000	0.6120	1.9277	3.3129	4.3208	4.6862	4.3208	3.3129	1.9277	0.6120	0.0000
	9	0.0000	0.6120	1.9277	3.3129	4.3208	4.6862	4.3208	3.3129	1.9277	0.6120	0.0000
	10	0.0000	0.6120	1.9277	3.3129	4.3208	4.6862	4.3208	3.3129	1.9277	0.6120	0.0000
	11	0.0000	0.6120	1.9277	3.3129	4.3208	4.6862	4.3208	3.3129	1.9277	0.6120	0.0000

TABLE A.9

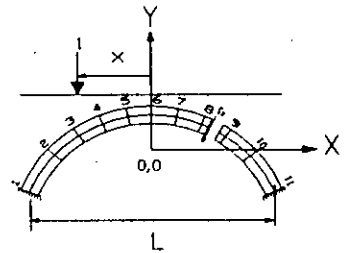
THRUSTS AT THE DIFFERENT RADIAL PLANES (RISE-TO-SPAN RATIO 0.050)



		POSITION OF UNIT LOAD FROM THE CROWN										
X/L		-0.50	-0.40	-0.30	-0.20	-0.10	0.00	0.10	0.20	0.30	0.40	0.50
DIFFERENT SECTIONS	1	0.0000	0.7923	2.0669	3.4024	4.3635	4.6924	4.3050	3.2901	1.9102	0.6055	0.0000
	2	0.0000	0.5998	2.0453	3.3952	4.3689	4.7062	4.3221	3.3053	1.9199	0.6087	0.0000
	3	0.0000	0.6043	1.9017	3.3825	4.3672	4.7124	4.3321	3.3151	1.9265	0.6110	0.0000
	4	0.0000	0.6079	1.9134	3.2853	4.3586	4.7110	4.3352	3.3196	1.9299	0.6123	0.0000
	5	0.0000	0.6104	1.9221	3.3017	4.3035	4.7023	4.3314	3.3188	1.9304	0.6126	0.0000
	6	0.0000	0.6120	1.9277	3.3129	4.3208	4.6862	4.3208	3.3129	1.9277	0.6120	0.0000
	7	0.0000	0.6126	1.9304	3.3188	4.3314	4.7023	4.3035	3.3017	1.9221	0.6104	0.0000
	8	0.0000	0.6123	1.9299	3.3196	4.3352	4.7110	4.3586	3.2853	1.9134	0.6079	0.0000
	9	0.0000	0.6110	1.9265	3.3151	4.3321	4.7124	4.3672	3.3825	1.9017	0.6043	0.0000
	10	0.0000	0.6087	1.9199	3.3053	4.3221	4.7062	4.3689	3.3952	2.0453	0.5998	0.0000
	11	0.0000	0.6055	1.9102	3.2901	4.3050	4.6924	4.3635	3.4024	2.0669	0.7923	0.0000

TABLE A.10

SHEAR FORCES ALONG THE DIFFERENT RADIAL PLANES (RISE-TO-SPAN RATIO 0.050)



		POSITION OF UNIT LOAD FROM THE CROWN										
X/L		-0.50	-0.40	-0.30	-0.20	-0.10	0.00	0.10	0.20	0.30	0.40	0.50
DIFFERENT SECTIONS	1	0.0000	0.8314	0.4962	0.1120	-0.2207	-0.4379	-0.5103	-0.4439	-0.2794	-0.0936	0.0000
	2	0.0000	-0.1248	0.5789	0.2489	-0.0449	-0.2487	-0.3367	-0.3111	-0.2023	-0.0692	0.0000
	3	0.0000	-0.1007	-0.3327	0.3844	0.1298	-0.0603	-0.1636	-0.1787	-0.1254	-0.0448	0.0000
	4	0.0000	-0.0765	-0.2567	-0.4781	0.3034	0.1272	0.0089	-0.0467	-0.0487	-0.0204	0.0000
	5	0.0000	-0.0524	-0.1806	-0.3475	-0.5231	0.3140	0.1809	0.0851	0.0279	0.0039	0.0000
	6	0.0000	0.0282	0.1044	0.2164	0.3523	-0.5000	-0.3523	-0.2164	-0.1044	-0.0282	0.0000
	7	0.0000	0.0039	0.0279	0.0851	0.1809	0.3140	-0.5231	-0.3475	-0.1806	-0.0524	0.0000
	8	0.0000	-0.0204	-0.0487	-0.0467	0.0089	0.1272	0.3034	-0.4781	-0.2567	-0.0765	0.0000
	9	0.0000	-0.0448	-0.1254	-0.1787	-0.1636	-0.0603	0.1298	0.3844	-0.3327	-0.1007	0.0000
	10	0.0000	-0.0692	-0.2023	-0.3111	-0.3367	-0.2487	-0.0449	0.2489	0.5789	-0.1248	0.0000
	11	0.0000	-0.0936	-0.2794	-0.4439	-0.5103	-0.4379	-0.2207	0.1120	0.4962	0.8314	0.0000

TABLE A.11

BENDING MOMENTS AT DIFFERENT SECTIONS (RISE-TO-SPAN RATIO 0.100)
=INFLUENCE VALUE*(L)

		POSITION OF UNIT LOAD FROM THE CROWN										
X/L		-0.50	-0.40	-0.30	-0.20	-0.10	0.00	0.10	0.20	0.30	0.40	0.50
DIFFER- -ENT SECTIONS	1	0.0000	-0.0597	-0.0617	-0.0343	0.0018	0.0323	0.0487	0.0480	0.0328	0.0117	0.0000
	2	0.0000	0.0259	-0.0083	-0.0176	-0.0133	-0.0041	0.0042	0.0083	0.0073	0.0030	0.0000
	3	0.0000	0.0143	0.0539	0.0141	-0.0091	-0.0196	-0.0210	-0.0165	-0.0094	-0.0029	0.0000
	4	0.0000	0.0053	0.0242	0.0597	0.0132	-0.0156	-0.0281	-0.0274	-0.0180	-0.0061	0.0000
	5	0.0000	-0.0012	0.0023	0.0186	0.0527	0.0072	-0.0179	-0.0250	-0.0188	-0.0069	0.0000
	6	0.0000	-0.0053	-0.0120	-0.0096	0.0091	0.0482	0.0091	-0.0096	-0.0120	-0.0053	0.0000
	7	0.0000	-0.0069	-0.0188	-0.0250	-0.0179	0.0072	0.0527	0.0186	0.0023	-0.0012	0.0000
	8	0.0000	-0.0061	-0.0180	-0.0274	-0.0281	-0.0156	0.0132	0.0597	0.0242	0.0053	0.0000
	9	0.0000	-0.0029	-0.0094	-0.0165	-0.0210	-0.0196	-0.0091	0.0141	0.0539	0.0143	0.0000
	10	0.0000	0.0030	0.0073	0.0083	0.0042	-0.0041	-0.0133	-0.0176	-0.0083	0.0259	0.0000
	11	0.0000	0.0117	0.0328	0.0480	0.0487	0.0323	0.0018	-0.0343	-0.0617	-0.0597	0.0000

TABLE A.12

VERTICAL SHEAR FORCES AT DIFFERENT SECTIONS (RISE-TO-SPAN RATIO 0.100)

		POSITION OF UNIT LOAD FROM THE CROWN										
X/L		-0.50	-0.40	-0.30	-0.20	-0.10	0.00	0.10	0.20	0.30	0.40	0.50
DIFFER- -ENT SECTIONS	1	0.0000	0.9714	0.8945	0.7823	0.6469	0.5000	0.3531	0.2177	0.1055	0.0286	0.0000
	2	0.0000	-0.0286	0.8945	0.7823	0.6469	0.5000	0.3531	0.2177	0.1055	0.0286	0.0000
	3	0.0000	-0.0286	-0.1055	0.7823	0.6469	0.5000	0.3531	0.2177	0.1055	0.0286	0.0000
	4	0.0000	-0.0286	-0.1055	-0.2177	0.6469	0.5000	0.3531	0.2177	0.1055	0.0286	0.0000
	5	0.0000	-0.0286	-0.1055	-0.2177	-0.3531	0.5000	0.3531	0.2177	0.1055	0.0286	0.0000
	6	0.0000	-0.0286	-0.1055	-0.2177	-0.3531	0.5000	0.3531	0.2177	0.1055	0.0286	0.0000
	7	0.0000	-0.0286	-0.1055	-0.2177	-0.3531	-0.5000	0.3531	0.2177	0.1055	0.0286	0.0000
	8	0.0000	-0.0286	-0.1055	-0.2177	-0.3531	-0.5000	-0.6469	0.2177	0.1055	0.0286	0.0000
	9	0.0000	-0.0286	-0.1055	-0.2177	-0.3531	-0.5000	-0.6469	-0.7823	0.1055	0.0286	0.0000
	10	0.0000	-0.0286	-0.1055	-0.2177	-0.3531	-0.5000	-0.6469	-0.7823	-0.8945	0.0286	0.0000
	11	0.0000	-0.0286	-0.1055	-0.2177	-0.3531	-0.5000	-0.6469	-0.7823	-0.8945	-0.9714	0.0000

TABLE A.13

HORIZONTAL THRUSTS AT DIFFERENT SECTIONS (RISE-TO-SPAN RATIO 0.100)

		POSITION OF UNIT LOAD FROM THE CROWN										
X/L		-0.50	-0.40	-0.30	-0.20	-0.10	0.00	0.10	0.20	0.30	0.40	0.50
DIFFER- -ENT SECTIONS	1	0.0000	0.3128	0.9754	1.6643	2.1616	2.3411	2.1616	1.6643	0.9754	0.3128	0.0000
	2	0.0000	0.3128	0.9754	1.6643	2.1616	2.3411	2.1616	1.6643	0.9754	0.3128	0.0000
	3	0.0000	0.3128	0.9754	1.6643	2.1616	2.3411	2.1616	1.6643	0.9754	0.3128	0.0000
	4	0.0000	0.3128	0.9754	1.6643	2.1616	2.3411	2.1616	1.6643	0.9754	0.3128	0.0000
	5	0.0000	0.3128	0.9754	1.6643	2.1616	2.3411	2.1616	1.6643	0.9754	0.3128	0.0000
	6	0.0000	0.3128	0.9754	1.6643	2.1616	2.3411	2.1616	1.6643	0.9754	0.3128	0.0000
	7	0.0000	0.3128	0.9754	1.6643	2.1616	2.3411	2.1616	1.6643	0.9754	0.3128	0.0000
	8	0.0000	0.3128	0.9754	1.6643	2.1616	2.3411	2.1616	1.6643	0.9754	0.3128	0.0000
	9	0.0000	0.3128	0.9754	1.6643	2.1616	2.3411	2.1616	1.6643	0.9754	0.3128	0.0000
	10	0.0000	0.3128	0.9754	1.6643	2.1616	2.3411	2.1616	1.6643	0.9754	0.3128	0.0000
	11	0.0000	0.3128	0.9754	1.6643	2.1616	2.3411	2.1616	1.6643	0.9754	0.3128	0.0000

TABLE A.14

THRUSTS AT THE DIFFERENT RADIAL PLANES (RISE-TO-SPAN RATIO 0.100)

		POSITION OF UNIT LOAD FROM THE CROWN										
X/L		-0.50	-0.40	-0.30	-0.20	-0.10	0.00	0.10	0.20	0.30	0.40	0.50
DIFFER- -ENT SECTIONS	1	0.0000	0.6624	1.2444	1.8372	2.2441	2.3533	2.1311	1.6200	0.9409	0.2998	0.0000
	2	0.0000	0.2889	1.2033	1.8243	2.2558	2.3814	2.1654	1.6505	0.9605	0.3065	0.0000
	3	0.0000	0.2978	0.9247	1.7999	2.2525	2.3933	2.1847	1.6696	0.9734	0.3110	0.0000
	4	0.0000	0.3047	0.9475	1.6110	2.2354	2.3902	2.1902	1.6780	0.9800	0.3135	0.0000
	5	0.0000	0.3097	0.9644	1.6426	2.1280	2.3726	2.1824	1.6761	0.9806	0.3141	0.0000
	6	0.0000	0.3128	0.9754	1.6643	2.1616	2.3411	2.1616	1.6643	0.9754	0.3128	0.0000
	7	0.0000	0.3141	0.9806	1.6761	2.1824	2.3726	2.1280	1.6426	0.9644	0.3097	0.0000
	8	0.0000	0.3135	0.9800	1.6780	2.1902	2.3902	2.2354	1.6110	0.9475	0.3047	0.0000
	9	0.0000	0.3110	0.9734	1.6696	2.1847	2.3933	2.2525	1.7999	0.9247	0.2978	0.0000
	10	0.0000	0.3065	0.9605	1.6505	2.1654	2.3814	2.2558	1.8243	1.2033	0.2889	0.0000
	11	0.0000	0.2998	0.9409	1.6200	2.1311	2.3533	2.2441	1.8372	1.2444	0.6624	0.0000

TABLE A.15

SHEAR FORCES ALONG THE DIFFERENT RADIAL PLANES (RISE-TO-SPAN RATIO 0.100)

		POSITION OF UNIT LOAD FROM THE CROWN										
X/L		-0.50	-0.40	-0.30	-0.20	-0.10	0.00	0.10	0.20	0.30	0.40	0.50
DIFFER- -ENT SECTIONS	1	0.0000	0.7763	0.4506	0.0820	-0.2342	-0.4389	-0.5054	-0.4392	-0.2778	-0.0939	0.0000
	2	0.0000	-0.1235	0.5510	0.2323	-0.0496	-0.2446	-0.3291	-0.3050	-0.1997	-0.0690	0.0000
	3	0.0000	-0.1001	-0.3277	0.3771	0.1306	-0.0538	-0.1553	-0.1723	-0.1224	-0.0443	0.0000
	4	0.0000	-0.0764	-0.2543	-0.4711	0.3067	0.1339	0.0163	-0.0410	-0.0458	-0.0198	0.0000
	5	0.0000	-0.0526	-0.1802	-0.3451	-0.5183	0.3184	0.1858	0.0890	0.0301	0.0045	0.0000
	6	0.0000	0.0286	0.1055	0.2177	0.3531	-0.5000	-0.3531	-0.2177	-0.1055	-0.0286	0.0000
	7	0.0000	0.0045	0.0301	0.0890	0.1858	0.3184	-0.5183	-0.3451	-0.1802	-0.0526	0.0000
	8	0.0000	-0.0198	-0.0458	-0.0410	0.0163	0.1339	0.3067	-0.4711	-0.2543	-0.0764	0.0000
	9	0.0000	-0.0443	-0.1224	-0.1723	-0.1553	-0.0538	0.1306	0.3771	-0.3277	-0.1001	0.0000
	10	0.0000	-0.0690	-0.1997	-0.3050	-0.3291	-0.2446	-0.0496	0.2323	0.5510	-0.1235	0.0000
	11	0.0000	-0.0939	-0.2778	-0.4392	-0.5054	-0.4389	-0.2342	0.0820	0.4506	0.7763	0.0000

TABLE A.16

BENDING MOMENTS AT DIFFERENT SECTIONS (RISE-TO-SPAN RATIO 0.150)
=INFLUENCE VALUE*(L)

		POSITION OF UNIT LOAD FROM THE CROWN										
X/L		-0.50	-0.40	-0.30	-0.20	-0.10	0.00	0.10	0.20	0.30	0.40	0.50
DIFFER- -ENT SECTIONS	1	0.0000	-0.0582	-0.0589	-0.0313	0.0040	0.0336	0.0496	0.0489	0.0338	0.0123	0.0000
	2	0.0000	0.0264	-0.0075	-0.0172	-0.0139	-0.0055	0.0025	0.0069	0.0066	0.0029	0.0000
	3	0.0000	0.0144	0.0540	0.0140	-0.0097	-0.0207	-0.0224	-0.0179	-0.0104	-0.0032	0.0000
	4	0.0000	0.0053	0.0243	0.0600	0.0135	-0.0154	-0.0283	-0.0279	-0.0187	-0.0065	0.0000
	5	0.0000	-0.0013	0.0024	0.0192	0.0539	0.0084	-0.0170	-0.0247	-0.0190	-0.0072	0.0000
	6	0.0000	-0.0054	-0.0120	-0.0089	0.0105	0.0498	0.0105	-0.0089	-0.0120	-0.0054	0.0000
	7	0.0000	-0.0072	-0.0190	-0.0247	-0.0170	0.0084	0.0539	0.0192	0.0024	-0.0013	0.0000
	8	0.0000	-0.0065	-0.0187	-0.0279	-0.0283	-0.0154	0.0135	0.0600	0.0243	0.0053	0.0000
	9	0.0000	-0.0032	-0.0104	-0.0179	-0.0224	-0.0207	-0.0097	0.0140	0.0540	0.0144	0.0000
	10	0.0000	0.0029	0.0066	0.0069	0.0025	-0.0055	-0.0139	-0.0172	-0.0075	0.0264	0.0000
	11	0.0000	0.0123	0.0338	0.0489	0.0496	0.0336	0.0040	-0.0313	-0.0589	-0.0582	0.0000

TABLE A.17

VERTICAL SHEAR FORCES AT DIFFERENT SECTIONS (RISE-TO-SPAN RATIO 0.150)

		POSITION OF UNIT LOAD FROM THE CROWN										
X/L		-0.50	-0.40	-0.30	-0.20	-0.10	0.00	0.10	0.20	0.30	0.40	0.50
DIFFER- -ENT SECTIONS	1	0.0000	0.9705	0.8926	0.7802	0.6456	0.5000	0.3544	0.2198	0.1074	0.0295	0.0000
	2	0.0000	-0.0295	0.8926	0.7802	0.6456	0.5000	0.3544	0.2198	0.1074	0.0295	0.0000
	3	0.0000	-0.0295	-0.1074	0.7802	0.6456	0.5000	0.3544	0.2198	0.1074	0.0295	0.0000
	4	0.0000	-0.0295	-0.1074	-0.2198	0.6456	0.5000	0.3544	0.2198	0.1074	0.0295	0.0000
	5	0.0000	-0.0295	-0.1074	-0.2198	-0.3544	0.5000	0.3544	0.2198	0.1074	0.0295	0.0000
	6	0.0000	-0.0295	-0.1074	-0.2198	-0.3544	0.5000	0.3544	0.2198	0.1074	0.0295	0.0000
	7	0.0000	-0.0295	-0.1074	-0.2198	-0.3544	-0.5000	0.3544	0.2198	0.1074	0.0295	0.0000
	8	0.0000	-0.0295	-0.1074	-0.2198	-0.3544	-0.5000	-0.6456	0.2198	0.1074	0.0295	0.0000
	9	0.0000	-0.0295	-0.1074	-0.2198	-0.3544	-0.5000	-0.6456	-0.7802	0.1074	0.0295	0.0000
	10	0.0000	-0.0295	-0.1074	-0.2198	-0.3544	-0.5000	-0.6456	-0.7802	-0.8926	0.0295	0.0000
	11	0.0000	-0.0295	-0.1074	-0.2198	-0.3544	-0.5000	-0.6456	-0.7802	-0.8926	-0.9705	0.0000

TABLE A.18

HORIZONTAL THRUSTS AT DIFFERENT SECTIONS (RISE-TO-SPAN RATIO 0.150)

		POSITION OF UNIT LOAD FROM THE CROWN										
X/L		-0.50	-0.40	-0.30	-0.20	-0.10	0.00	0.10	0.20	0.30	0.40	0.50
DIFFER- -ENT SECTIONS	1	0.0000	0.2164	0.6628	1.1179	1.4422	1.5586	1.4422	1.1179	0.6628	0.2164	0.0000
	2	0.0000	0.2164	0.6628	1.1179	1.4422	1.5586	1.4422	1.1179	0.6628	0.2164	0.0000
	3	0.0000	0.2164	0.6628	1.1179	1.4422	1.5586	1.4422	1.1179	0.6628	0.2164	0.0000
	4	0.0000	0.2164	0.6628	1.1179	1.4422	1.5586	1.4422	1.1179	0.6628	0.2164	0.0000
	5	0.0000	0.2164	0.6628	1.1179	1.4422	1.5586	1.4422	1.1179	0.6628	0.2164	0.0000
	6	0.0000	0.2164	0.6628	1.1179	1.4422	1.5586	1.4422	1.1179	0.6628	0.2164	0.0000
	7	0.0000	0.2164	0.6628	1.1179	1.4422	1.5586	1.4422	1.1179	0.6628	0.2164	0.0000
	8	0.0000	0.2164	0.6628	1.1179	1.4422	1.5586	1.4422	1.1179	0.6628	0.2164	0.0000
	9	0.0000	0.2164	0.6628	1.1179	1.4422	1.5586	1.4422	1.1179	0.6628	0.2164	0.0000
	10	0.0000	0.2164	0.6628	1.1179	1.4422	1.5586	1.4422	1.1179	0.6628	0.2164	0.0000
	11	0.0000	0.2164	0.6628	1.1179	1.4422	1.5586	1.4422	1.1179	0.6628	0.2164	0.0000

TABLE A.19

THRUSTS AT THE DIFFERENT RADIAL PLANES (RISE-TO-SPAN RATIO 0.150)

		POSITION OF UNIT LOAD FROM THE CROWN										
X/L		-0.50	-0.40	-0.30	-0.20	-0.10	0.00	0.10	0.20	0.30	0.40	0.50
DIFFER- -ENT SECTIONS	1	0.0000	0.7149	1.0447	1.3628	1.5594	1.5765	1.3992	1.0543	0.6125	0.1968	0.0000
	2	0.0000	0.1813	0.9882	1.3472	1.5792	1.6195	1.4510	1.1004	0.6424	0.2072	0.0000
	3	0.0000	0.1945	0.5902	1.3128	1.5745	1.6363	1.4784	1.1277	0.6611	0.2139	0.0000
	4	0.0000	0.2046	0.6229	1.0421	1.5490	1.6305	1.4849	1.1388	0.6702	0.2175	0.0000
	5	0.0000	0.2118	0.6470	1.0869	1.3945	1.6042	1.4725	1.1353	0.6706	0.2183	0.0000
	6	0.0000	0.2164	0.6628	1.1179	1.4422	1.5586	1.4422	1.1179	0.6628	0.2164	0.0000
	7	0.0000	0.2183	0.6706	1.1353	1.4725	1.6042	1.3945	1.0869	0.6470	0.2118	0.0000
	8	0.0000	0.2175	0.6702	1.1388	1.4849	1.6305	1.5490	1.0421	0.6229	0.2046	0.0000
	9	0.0000	0.2139	0.6611	1.1277	1.4784	1.6363	1.5745	1.3128	0.5902	0.1945	0.0000
	10	0.0000	0.2072	0.6424	1.1004	1.4510	1.6195	1.5792	1.3472	0.9882	0.1813	0.0000
	11	0.0000	0.1968	0.6125	1.0543	1.3992	1.5765	1.5594	1.3628	1.0447	0.7149	0.0000

TABLE A.20

SHEAR FORCES ALONG THE DIFFERENT RADIAL PLANES (RISE-TO-SPAN RATIO 0.150)

		POSITION OF UNIT LOAD FROM THE CROWN										
X/L		-0.50	-0.40	-0.30	-0.20	-0.10	0.00	0.10	0.20	0.30	0.40	0.50
DIFFER- -ENT SECTIONS	1	0.0000	0.6912	0.3804	0.0360	-0.2549	-0.4405	-0.4980	-0.4319	-0.2752	-0.0945	0.0000
	2	0.0000	-0.1217	0.5095	0.2082	-0.0555	-0.2375	-0.3169	-0.2950	-0.1955	-0.0688	0.0000
	3	0.0000	-0.0993	-0.3202	0.3672	0.1330	-0.0428	-0.1418	-0.1618	-0.1176	-0.0436	0.0000
	4	0.0000	-0.0764	-0.2507	-0.4605	0.3122	0.1445	0.0282	-0.0318	-0.0412	-0.0189	0.0000
	5	0.0000	-0.0531	-0.1797	-0.3415	-0.5111	0.3254	0.1935	0.0954	0.0337	0.0055	0.0000
	6	0.0000	0.0295	0.1074	0.2198	0.3544	-0.5000	-0.3544	-0.2198	-0.1074	-0.0295	0.0000
	7	0.0000	0.0055	0.0337	0.0954	0.1935	0.3254	-0.5111	-0.3415	-0.1797	-0.0531	0.0000
	8	0.0000	-0.0189	-0.0412	-0.0318	0.0282	0.1445	0.3122	-0.4605	-0.2507	-0.0764	0.0000
	9	0.0000	-0.0436	-0.1176	-0.1618	-0.1418	-0.0428	0.1330	0.3672	-0.3202	-0.0993	0.0000
	10	0.0000	-0.0688	-0.1955	-0.2950	-0.3169	-0.2375	-0.0555	0.2082	0.5095	-0.1217	0.0000
	11	0.0000	-0.0945	-0.2752	-0.4319	-0.4980	-0.4405	-0.2549	0.0360	0.3804	0.6912	0.0000

TABLE A.21
 BENDING MOMENTS AT DIFFERENT SECTIONS (RISE-TO-SPAN RATIO 0.200)
 =INFLUENCE VALUE*(L)

		POSITION OF UNIT LOAD FROM THE CROWN										
X/L		-0.50	-0.40	-0.30	-0.20	-0.10	0.00	0.10	0.20	0.30	0.40	0.50
DIFFER- ENT SECTIONS	1	0.0000	-0.0562	-0.0549	-0.0273	0.0070	0.0355	0.0508	0.0501	0.0351	0.0131	0.0000
	2	0.0000	0.0272	-0.0065	-0.0170	-0.0149	-0.0075	0.0001	0.0049	0.0055	0.0026	0.0000
	3	0.0000	0.0146	0.0543	0.0139	-0.0104	-0.0221	-0.0242	-0.0197	-0.0117	-0.0038	0.0000
	4	0.0000	0.0053	0.0245	0.0604	0.0140	-0.0151	-0.0284	-0.0286	-0.0195	-0.0070	0.0000
	5	0.0000	-0.0014	0.0027	0.0202	0.0555	0.0102	-0.0158	-0.0243	-0.0193	-0.0076	0.0000
	6	0.0000	-0.0057	-0.0119	-0.0079	0.0123	0.0521	0.0123	-0.0079	-0.0119	-0.0057	0.0000
	7	0.0000	-0.0076	-0.0193	-0.0243	-0.0158	0.0102	0.0555	0.0202	0.0027	-0.0014	0.0000
	8	0.0000	-0.0070	-0.0195	-0.0286	-0.0284	-0.0151	0.0140	0.0604	0.0245	0.0053	0.0000
	9	0.0000	-0.0038	-0.0117	-0.0197	-0.0242	-0.0221	-0.0104	0.0139	0.0543	0.0146	0.0000
	10	0.0000	0.0026	0.0055	0.0049	0.0001	-0.0075	-0.0149	-0.0170	-0.0065	0.0272	0.0000
	11	0.0000	0.0131	0.0351	0.0501	0.0508	0.0355	0.0070	-0.0273	-0.0549	-0.0562	0.0000

TABLE A.22
 VERTICAL SHEAR FORCES AT DIFFERENT SECTIONS (RISE-TO-SPAN RATIO 0.200)

		POSITION OF UNIT LOAD FROM THE CROWN										
X/L		-0.50	-0.40	-0.30	-0.20	-0.10	0.00	0.10	0.20	0.30	0.40	0.50
DIFFER- ENT SECTIONS	1	0.0000	0.9693	0.8900	0.7774	0.6438	0.5000	0.3562	0.2226	0.1100	0.0307	0.0000
	2	0.0000	-0.0307	0.8900	0.7774	0.6438	0.5000	0.3562	0.2226	0.1100	0.0307	0.0000
	3	0.0000	-0.0307	-0.1100	0.7774	0.6438	0.5000	0.3562	0.2226	0.1100	0.0307	0.0000
	4	0.0000	-0.0307	-0.1100	-0.2226	0.6438	0.5000	0.3562	0.2226	0.1100	0.0307	0.0000
	5	0.0000	-0.0307	-0.1100	-0.2226	-0.3562	0.5000	0.3562	0.2226	0.1100	0.0307	0.0000
	6	0.0000	-0.0307	-0.1100	-0.2226	-0.3562	0.5000	0.3562	0.2226	0.1100	0.0307	0.0000
	7	0.0000	-0.0307	-0.1100	-0.2226	-0.3562	-0.5000	0.3562	0.2226	0.1100	0.0307	0.0000
	8	0.0000	-0.0307	-0.1100	-0.2226	-0.3562	-0.5000	-0.6438	0.2226	0.1100	0.0307	0.0000
	9	0.0000	-0.0307	-0.1100	-0.2226	-0.3562	-0.5000	-0.6438	-0.7774	0.1100	0.0307	0.0000
	10	0.0000	-0.0307	-0.1100	-0.2226	-0.3562	-0.5000	-0.6438	-0.7774	-0.8900	0.0307	0.0000
	11	0.0000	-0.0307	-0.1100	-0.2226	-0.3562	-0.5000	-0.6438	-0.7774	-0.8900	-0.9693	0.0000

TABLE A.23
HORIZONTAL THRUSTS AT DIFFERENT SECTIONS (RISE-TO-SPAN RATIO 0.200)

		POSITION OF UNIT LOAD FROM THE CROWN										
X/L		-0.50	-0.40	-0.30	-0.20	-0.10	0.00	0.10	0.20	0.30	0.40	0.50
DIFFER- -ENT SECTIONS	1	0.0000	0.1707	0.5099	0.8466	1.0827	1.1669	1.0827	0.8466	0.5099	0.1707	0.0000
	2	0.0000	0.1707	0.5099	0.8466	1.0827	1.1669	1.0827	0.8466	0.5099	0.1707	0.0000
	3	0.0000	0.1707	0.5099	0.8466	1.0827	1.1669	1.0827	0.8466	0.5099	0.1707	0.0000
	4	0.0000	0.1707	0.5099	0.8466	1.0827	1.1669	1.0827	0.8466	0.5099	0.1707	0.0000
	5	0.0000	0.1707	0.5099	0.8466	1.0827	1.1669	1.0827	0.8466	0.5099	0.1707	0.0000
	6	0.0000	0.1707	0.5099	0.8466	1.0827	1.1669	1.0827	0.8466	0.5099	0.1707	0.0000
	7	0.0000	0.1707	0.5099	0.8466	1.0827	1.1669	1.0827	0.8466	0.5099	0.1707	0.0000
	8	0.0000	0.1707	0.5099	0.8466	1.0827	1.1669	1.0827	0.8466	0.5099	0.1707	0.0000
	9	0.0000	0.1707	0.5099	0.8466	1.0827	1.1669	1.0827	0.8466	0.5099	0.1707	0.0000
	10	0.0000	0.1707	0.5099	0.8466	1.0827	1.1669	1.0827	0.8466	0.5099	0.1707	0.0000
	11	0.0000	0.1707	0.5099	0.8466	1.0827	1.1669	1.0827	0.8466	0.5099	0.1707	0.0000

TABLE A.24
THRUSTS AT THE DIFFERENT RADIAL PLANES (RISE-TO-SPAN RATIO 0.200)

		POSITION OF UNIT LOAD FROM THE CROWN										
X/L		-0.50	-0.40	-0.30	-0.20	-0.10	0.00	0.10	0.20	0.30	0.40	0.50
DIFFER- -ENT SECTIONS	1	0.0000	0.7921	0.9830	1.1492	1.2280	1.1898	1.0297	0.7666	0.4452	0.1448	0.0000
	2	0.0000	0.1254	0.9163	1.1350	1.2582	1.2491	1.0996	0.8289	0.4860	0.1593	0.0000
	3	0.0000	0.1427	0.4187	1.0924	1.2521	1.2692	1.1331	0.8628	0.5098	0.1681	0.0000
	4	0.0000	0.1556	0.4598	0.7523	1.2183	1.2595	1.1390	0.8752	0.5205	0.1726	0.0000
	5	0.0000	0.1649	0.4899	0.8078	1.0233	1.2247	1.1215	0.8692	0.5202	0.1733	0.0000
	6	0.0000	0.1707	0.5099	0.8466	1.0827	1.1669	1.0827	0.8466	0.5099	0.1707	0.0000
	7	0.0000	0.1733	0.5202	0.8692	1.1215	1.2247	1.0233	0.8078	0.4899	0.1649	0.0000
	8	0.0000	0.1726	0.5205	0.8752	1.1390	1.2595	1.2183	0.7523	0.4598	0.1556	0.0000
	9	0.0000	0.1681	0.5098	0.8628	1.1331	1.2692	1.2521	1.0924	0.4187	0.1427	0.0000
	10	0.0000	0.1593	0.4860	0.8289	1.0996	1.2491	1.2582	1.1350	0.9163	0.1254	0.0000
	11	0.0000	0.1448	0.4452	0.7666	1.0297	1.1898	1.2280	1.1492	0.9830	0.7921	0.0000

TABLE A.25
SHEAR FORCES ALONG THE DIFFERENT RADIAL PLANES (RISE-TO-SPAN RATIO 0.200)

		POSITION OF UNIT LOAD FROM THE CROWN										
X/L		-0.50	-0.40	-0.30	-0.20	-0.10	0.00	0.10	0.20	0.30	0.40	0.50
DIFFER- -ENT SECTIONS	1	0.0000	0.5841	0.2928	-0.0209	-0.2805	-0.4427	-0.4888	-0.4226	-0.2720	-0.0955	0.0000
	2	0.0000	-0.1198	0.4609	0.1813	-0.0605	-0.2268	-0.3003	-0.2814	-0.1896	-0.0686	0.0000
	3	0.0000	-0.0986	-0.3112	0.3574	0.1380	-0.0277	-0.1237	-0.1476	-0.1108	-0.0427	0.0000
	4	0.0000	-0.0766	-0.2464	-0.4475	0.3201	0.1587	0.0437	-0.0195	-0.0349	-0.0176	0.0000
	5	0.0000	-0.0540	-0.1793	-0.3373	-0.5022	0.3343	0.2035	0.1037	0.0386	0.0069	0.0000
	6	0.0000	0.0307	0.1100	0.2226	0.3562	-0.5000	-0.3562	-0.2226	-0.1100	-0.0307	0.0000
	7	0.0000	0.0069	0.0386	0.1037	0.2035	0.3343	-0.5022	-0.3373	-0.1793	-0.0540	0.0000
	8	0.0000	-0.0176	-0.0349	-0.0195	0.0437	0.1587	0.3201	-0.4475	-0.2464	-0.0766	0.0000
	9	0.0000	-0.0427	-0.1108	-0.1476	-0.1237	-0.0277	0.1380	0.3574	-0.3112	-0.0986	0.0000
	10	0.0000	-0.0686	-0.1896	-0.2814	-0.3003	-0.2268	-0.0605	0.1813	0.4609	-0.1198	0.0000
	11	0.0000	-0.0955	-0.2720	-0.4226	-0.4888	-0.4427	-0.2805	-0.0209	0.2928	0.5841	0.0000

TABLE A.26
BENDING MOMENTS AT DIFFERENT SECTIONS (RISE-TO-SPAN RATIO 0.250)
=TABLE COEFF.*(L)

		POSITION OF UNIT LOAD FROM THE CROWN										
X/L		-0.50	-0.40	-0.30	-0.20	-0.10	0.00	0.10	0.20	0.30	0.40	0.50
DIFFER- -ENT SECTIONS	1	0.0000	-0.0533	-0.0497	-0.0222	0.0107	0.0377	0.0523	0.0516	0.0367	0.0142	0.0000
	2	0.0000	0.0281	-0.0054	-0.0169	-0.0164	-0.0103	-0.0031	0.0021	0.0038	0.0021	0.0000
	3	0.0000	0.0149	0.0547	0.0139	-0.0112	-0.0237	-0.0263	-0.0219	-0.0135	-0.0045	0.0000
	4	0.0000	0.0053	0.0249	0.0612	0.0149	-0.0145	-0.0285	-0.0293	-0.0205	-0.0077	0.0000
	5	0.0000	-0.0015	0.0031	0.0216	0.0576	0.0124	-0.0141	-0.0237	-0.0196	-0.0080	0.0000
	6	0.0000	-0.0060	-0.0117	-0.0066	0.0147	0.0549	0.0147	-0.0066	-0.0117	-0.0060	0.0000
	7	0.0000	-0.0080	-0.0196	-0.0237	-0.0141	0.0124	0.0576	0.0216	0.0031	-0.0015	0.0000
	8	0.0000	-0.0077	-0.0205	-0.0293	-0.0285	-0.0145	0.0149	0.0612	0.0249	0.0053	0.0000
	9	0.0000	-0.0045	-0.0135	-0.0219	-0.0263	-0.0237	-0.0112	0.0139	0.0547	0.0149	0.0000
	10	0.0000	0.0021	0.0038	0.0021	-0.0031	-0.0103	-0.0164	-0.0169	-0.0054	0.0281	0.0000
	11	0.0000	0.0142	0.0367	0.0516	0.0523	0.0377	0.0107	-0.0222	-0.0497	-0.0533	0.0000

TABLE A.27
VERTICAL SHEAR FORCES AT DIFFERENT SECTIONS (RISE-TO-SPAN RATIO 0.250)

		POSITION OF UNIT LOAD FROM THE CROWN										
X/L		-0.50	-0.40	-0.30	-0.20	-0.10	0.00	0.10	0.20	0.30	0.40	0.50
DIFFER- ENT SECTIONS	1	0.0000	0.9675	0.8865	0.7738	0.6416	0.5000	0.3584	0.2262	0.1135	0.0325	0.0000
	2	0.0000	-0.0325	0.8865	0.7738	0.6416	0.5000	0.3584	0.2262	0.1135	0.0325	0.0000
	3	0.0000	-0.0325	-0.1135	0.7738	0.6416	0.5000	0.3584	0.2262	0.1135	0.0325	0.0000
	4	0.0000	-0.0325	-0.1135	-0.2262	0.6416	0.5000	0.3584	0.2262	0.1135	0.0325	0.0000
	5	0.0000	-0.0325	-0.1135	-0.2262	-0.3584	0.5000	0.3584	0.2262	0.1135	0.0325	0.0000
	6	0.0000	-0.0325	-0.1135	-0.2262	-0.3584	0.5000	0.3584	0.2262	0.1135	0.0325	0.0000
	7	0.0000	-0.0325	-0.1135	-0.2262	-0.3584	-0.5000	0.3584	0.2262	0.1135	0.0325	0.0000
	8	0.0000	-0.0325	-0.1135	-0.2262	-0.3584	-0.5000	-0.6416	0.2262	0.1135	0.0325	0.0000
	9	0.0000	-0.0325	-0.1135	-0.2262	-0.3584	-0.5000	-0.6416	-0.7738	0.1135	0.0325	0.0000
	10	0.0000	-0.0325	-0.1135	-0.2262	-0.3584	-0.5000	-0.6416	-0.7738	-0.8865	0.0325	0.0000
	11	0.0000	-0.0325	-0.1135	-0.2262	-0.3584	-0.5000	-0.6416	-0.7738	-0.8865	-0.9675	0.0000

TABLE A.28
HORIZONTAL THRUSTS AT DIFFERENT SECTIONS (RISE-TO-SPAN RATIO 0.250)

		POSITION OF UNIT LOAD FROM THE CROWN										
X/L		-0.50	-0.40	-0.30	-0.20	-0.10	0.00	0.10	0.20	0.30	0.40	0.50
DIFFER- ENT SECTIONS	1	0.0000	0.1457	0.4207	0.6850	0.8671	0.9314	0.8671	0.6850	0.4207	0.1457	0.0000
	2	0.0000	0.1457	0.4207	0.6850	0.8671	0.9314	0.8671	0.6850	0.4207	0.1457	0.0000
	3	0.0000	0.1457	0.4207	0.6850	0.8671	0.9314	0.8671	0.6850	0.4207	0.1457	0.0000
	4	0.0000	0.1457	0.4207	0.6850	0.8671	0.9314	0.8671	0.6850	0.4207	0.1457	0.0000
	5	0.0000	0.1457	0.4207	0.6850	0.8671	0.9314	0.8671	0.6850	0.4207	0.1457	0.0000
	6	0.0000	0.1457	0.4207	0.6850	0.8671	0.9314	0.8671	0.6850	0.4207	0.1457	0.0000
	7	0.0000	0.1457	0.4207	0.6850	0.8671	0.9314	0.8671	0.6850	0.4207	0.1457	0.0000
	8	0.0000	0.1457	0.4207	0.6850	0.8671	0.9314	0.8671	0.6850	0.4207	0.1457	0.0000
	9	0.0000	0.1457	0.4207	0.6850	0.8671	0.9314	0.8671	0.6850	0.4207	0.1457	0.0000
	10	0.0000	0.1457	0.4207	0.6850	0.8671	0.9314	0.8671	0.6850	0.4207	0.1457	0.0000
	11	0.0000	0.1457	0.4207	0.6850	0.8671	0.9314	0.8671	0.6850	0.4207	0.1457	0.0000

TABLE A.29
THRUSTS AT THE DIFFERENT RADIAL PLANES (RISE-TO-SPAN RATIO 0.250)

		POSITION OF UNIT LOAD FROM THE CROWN										
X/L		-0.50	-0.40	-0.30	-0.20	-0.10	0.00	0.10	0.20	0.30	0.40	0.50
DIFFERENT SECTIONS	1	0.0000	0.8614	0.9616	1.0300	1.0335	0.9589	0.8070	0.5920	0.3432	0.1134	0.0000
	2	0.0000	0.0912	0.8906	1.0215	1.0768	1.0357	0.8957	0.6711	0.3959	0.1327	0.0000
	3	0.0000	0.1122	0.3145	0.9723	1.0686	1.0571	0.9327	0.7095	0.4235	0.1434	0.0000
	4	0.0000	0.1276	0.3622	0.5765	1.0268	1.0425	0.9362	0.7213	0.4349	0.1484	0.0000
	5	0.0000	0.1386	0.3971	0.6399	0.7986	0.9994	0.9133	0.7123	0.4334	0.1490	0.0000
	6	0.0000	0.1457	0.4207	0.6850	0.8671	0.9314	0.8671	0.6850	0.4207	0.1457	0.0000
	7	0.0000	0.1490	0.4334	0.7123	0.9133	0.9994	0.7986	0.6399	0.3971	0.1386	0.0000
	8	0.0000	0.1484	0.4349	0.7213	0.9362	1.0425	1.0268	0.5765	0.3622	0.1276	0.0000
	9	0.0000	0.1434	0.4235	0.7095	0.9327	1.0571	1.0686	0.9723	0.3145	0.1122	0.0000
	10	0.0000	0.1327	0.3959	0.6711	0.8957	1.0357	1.0768	1.0215	0.8906	0.0912	0.0000
	11	0.0000	0.1134	0.3432	0.5920	0.8070	0.9589	1.0335	1.0300	0.9616	0.8614	0.0000

TABLE A.30
SHEAR FORCES ALONG THE DIFFERENT RADIAL PLANES (RISE-TO-SPAN RATIO 0.250)

		POSITION OF UNIT LOAD FROM THE CROWN										
X/L		-0.50	-0.40	-0.30	-0.20	-0.10	0.00	0.10	0.20	0.30	0.40	0.50
DIFFERENT SECTIONS	1	0.0000	0.4640	0.1954	-0.0837	-0.3087	-0.4451	-0.4786	-0.4122	-0.2684	-0.0971	0.0000
	2	0.0000	-0.1182	0.4119	0.1562	-0.0620	-0.2119	-0.2795	-0.2645	-0.1820	-0.0683	0.0000
	3	0.0000	-0.0984	-0.3015	0.3500	0.1466	-0.0085	-0.1017	-0.1303	-0.1023	-0.0414	0.0000
	4	0.0000	-0.0774	-0.2422	-0.4335	0.3303	0.1756	0.0621	-0.0048	-0.0271	-0.0159	0.0000
	5	0.0000	-0.0553	-0.1794	-0.3329	-0.4926	0.3445	0.2151	0.1137	0.0447	0.0087	0.0000
	6	0.0000	0.0325	0.1135	0.2262	0.3584	-0.5000	-0.3584	-0.2262	-0.1135	-0.0325	0.0000
	7	0.0000	0.0087	0.0447	0.1137	0.2151	0.3445	-0.4926	-0.3329	-0.1794	-0.0553	0.0000
	8	0.0000	-0.0159	-0.0271	-0.0048	0.0621	0.1756	0.3303	-0.4335	-0.2422	-0.0774	0.0000
	9	0.0000	-0.0414	-0.1023	-0.1303	-0.1017	-0.0085	0.1466	0.3500	-0.3015	-0.0984	0.0000
	10	0.0000	-0.0683	-0.1820	-0.2645	-0.2795	-0.2119	-0.0620	0.1562	0.4119	-0.1182	0.0000
	11	0.0000	-0.0971	-0.2684	-0.4122	-0.4786	-0.4451	-0.3087	-0.0837	0.1954	0.4640	0.0000

TABLE A.31
 BENDING MOMENTS AT DIFFERENT SECTIONS (RISE-TO-SPAN RATIO 0.300)
 =INFLUENCE VALUE*(L)

		POSITION OF UNIT LOAD FROM THE CROWN										
X/L		-0.50	-0.40	-0.30	-0.20	-0.10	0.00	0.10	0.20	0.30	0.40	0.50
DIFFER- ENT SECTIONS	1	0.0000	-0.0496	-0.0435	-0.0162	0.0151	0.0405	0.0541	0.0532	0.0386	0.0156	0.0000
	2	0.0000	0.0293	-0.0042	-0.0171	-0.0184	-0.0138	-0.0073	-0.0015	0.0015	0.0014	0.0000
	3	0.0000	0.0154	0.0552	0.0140	-0.0119	-0.0253	-0.0286	-0.0243	-0.0155	-0.0055	0.0000
	4	0.0000	0.0054	0.0255	0.0623	0.0162	-0.0136	-0.0282	-0.0299	-0.0216	-0.0085	0.0000
	5	0.0000	-0.0017	0.0037	0.0233	0.0601	0.0151	-0.0121	-0.0228	-0.0199	-0.0086	0.0000
	6	0.0000	-0.0063	-0.0113	-0.0048	0.0176	0.0582	0.0176	-0.0048	-0.0113	-0.0063	0.0000
	7	0.0000	-0.0086	-0.0199	-0.0228	-0.0121	0.0151	0.0601	0.0233	0.0037	-0.0017	0.0000
	8	0.0000	-0.0085	-0.0216	-0.0299	-0.0282	-0.0136	0.0162	0.0623	0.0255	0.0054	0.0000
	9	0.0000	-0.0055	-0.0155	-0.0243	-0.0286	-0.0253	-0.0119	0.0140	0.0552	0.0154	0.0000
	10	0.0000	0.0014	0.0015	-0.0015	-0.0073	-0.0138	-0.0184	-0.0171	-0.0042	0.0293	0.0000
	11	0.0000	0.0156	0.0386	0.0532	0.0541	0.0405	0.0151	-0.0162	-0.0435	-0.0496	0.0000

TABLE A.32
 VERTICAL SHEAR FORCES AT DIFFERENT SECTIONS (RISE-TO-SPAN RATIO 0.300)

		POSITION OF UNIT LOAD FROM THE CROWN										
X/L		-0.50	-0.40	-0.30	-0.20	-0.10	0.00	0.10	0.20	0.30	0.40	0.50
DIFFER- ENT SECTIONS	1	0.0000	0.9652	0.8822	0.7695	0.6390	0.5000	0.3610	0.2305	0.1178	0.0348	0.0000
	2	0.0000	-0.0348	0.8822	0.7695	0.6390	0.5000	0.3610	0.2305	0.1178	0.0348	0.0000
	3	0.0000	-0.0348	-0.1178	0.7695	0.6390	0.5000	0.3610	0.2305	0.1178	0.0348	0.0000
	4	0.0000	-0.0348	-0.1178	-0.2305	0.6390	0.5000	0.3610	0.2305	0.1178	0.0348	0.0000
	5	0.0000	-0.0348	-0.1178	-0.2305	-0.3610	0.5000	0.3610	0.2305	0.1178	0.0348	0.0000
	6	0.0000	-0.0348	-0.1178	-0.2305	-0.3610	0.5000	0.3610	0.2305	0.1178	0.0348	0.0000
	7	0.0000	-0.0348	-0.1178	-0.2305	-0.3610	-0.5000	0.3610	0.2305	0.1178	0.0348	0.0000
	8	0.0000	-0.0348	-0.1178	-0.2305	-0.3610	-0.5000	-0.6390	0.2305	0.1178	0.0348	0.0000
	9	0.0000	-0.0348	-0.1178	-0.2305	-0.3610	-0.5000	-0.6390	-0.7695	0.1178	0.0348	0.0000
	10	0.0000	-0.0348	-0.1178	-0.2305	-0.3610	-0.5000	-0.6390	-0.7695	-0.8822	0.0348	0.0000
	11	0.0000	-0.0348	-0.1178	-0.2305	-0.3610	-0.5000	-0.6390	-0.7695	-0.8822	-0.9652	0.0000

TABLE A.33
HORIZONTAL THRUSTS AT DIFFERENT SECTIONS (RISE-TO-SPAN RATIO 0.300)

		POSITION OF UNIT LOAD FROM THE CROWN										
X/L		-0.50	-0.40	-0.30	-0.20	-0.10	0.00	0.10	0.20	0.30	0.40	0.50
DIFFER- ENT SECTIONS	1	0.0000	0.1311	0.3628	0.5778	0.7233	0.7743	0.7233	0.5778	0.3628	0.1311	0.0000
	2	0.0000	0.1311	0.3628	0.5778	0.7233	0.7743	0.7233	0.5778	0.3628	0.1311	0.0000
	3	0.0000	0.1311	0.3628	0.5778	0.7233	0.7743	0.7233	0.5778	0.3628	0.1311	0.0000
	4	0.0000	0.1311	0.3628	0.5778	0.7233	0.7743	0.7233	0.5778	0.3628	0.1311	0.0000
	5	0.0000	0.1311	0.3628	0.5778	0.7233	0.7743	0.7233	0.5778	0.3628	0.1311	0.0000
	6	0.0000	0.1311	0.3628	0.5778	0.7233	0.7743	0.7233	0.5778	0.3628	0.1311	0.0000
	7	0.0000	0.1311	0.3628	0.5778	0.7233	0.7743	0.7233	0.5778	0.3628	0.1311	0.0000
	8	0.0000	0.1311	0.3628	0.5778	0.7233	0.7743	0.7233	0.5778	0.3628	0.1311	0.0000
	9	0.0000	0.1311	0.3628	0.5778	0.7233	0.7743	0.7233	0.5778	0.3628	0.1311	0.0000
	10	0.0000	0.1311	0.3628	0.5778	0.7233	0.7743	0.7233	0.5778	0.3628	0.1311	0.0000
	11	0.0000	0.1311	0.3628	0.5778	0.7233	0.7743	0.7233	0.5778	0.3628	0.1311	0.0000

TABLE A.34
THRUSTS AT THE DIFFERENT RADIAL PLANES (RISE-TO-SPAN RATIO 0.300)

		POSITION OF UNIT LOAD FROM THE CROWN										
X/L		-0.50	-0.40	-0.30	-0.20	-0.10	0.00	0.10	0.20	0.30	*****	0.90
DIFFER- ENT SECTIONS	1	0.0000	0.9133	0.9491	0.9509	0.9042	0.8055	0.6589	0.4753	0.2747	0.0924	0.0000
	2	0.0000	0.0683	0.8797	0.9525	0.9634	0.9014	0.7672	0.5720	0.3402	0.1174	0.0000
	3	0.0000	0.0928	0.2454	0.8976	0.9519	0.9216	0.8047	0.6122	0.3702	0.1296	0.0000
	4	0.0000	0.1104	0.2979	0.4593	0.9022	0.9009	0.8041	0.6220	0.3811	0.1349	0.0000
	5	0.0000	0.1229	0.3363	0.5281	0.6482	0.8503	0.7756	0.6094	0.3779	0.1352	0.0000
	6	0.0000	0.1311	0.3628	0.5778	0.7233	0.7743	0.7233	0.5778	0.3628	0.1311	0.0000
	7	0.0000	0.1352	0.3779	0.6094	0.7756	0.8503	0.6482	0.5281	0.3363	0.1229	0.0000
	8	0.0000	0.1349	0.3811	0.6220	0.8041	0.9009	0.9022	0.4593	0.2979	0.1104	0.0000
	9	0.0000	0.1296	0.3702	0.6122	0.8047	0.9216	0.9519	0.8976	0.2454	0.0928	0.0000
	10	0.0000	0.1174	0.3402	0.5720	0.7672	0.9014	0.9634	0.9525	0.8797	0.0683	0.0000
	11	0.0000	0.0924	0.2747	0.4753	0.6589	0.8055	0.9042	0.9509	0.9491	0.9133	0.0000

TABLE A.35
SHEAR FORCES ALONG THE DIFFERENT RADIAL PLANES (RISE-TO-SPAN RATIO 0.300)

		POSITION OF UNIT LOAD FROM THE CROWN										
X/L		-0.50	-0.40	-0.30	-0.20	-0.10	0.00	0.10	0.20	0.30	0.40	0.50
DIFFER- ENT SECTIONS	1	0.0000	0.3386	0.0950	-0.1477	-0.3375	-0.4479	-0.4683	-0.4014	-0.2647	-0.0993	0.0000
	2	0.0000	-0.1172	0.3688	0.1372	-0.0579	-0.1924	-0.2548	-0.2446	-0.1727	-0.0679	0.0000
	3	0.0000	-0.0989	-0.2920	0.3469	0.1592	0.0143	-0.0766	-0.1103	-0.0921	-0.0399	0.0000
	4	0.0000	-0.0788	-0.2383	-0.4196	0.3426	0.1946	0.0825	0.0117	-0.0178	-0.0137	0.0000
	5	0.0000	-0.0574	-0.1800	-0.3289	-0.4830	0.3555	0.2277	0.1249	0.0519	0.0111	0.0000
	6	0.0000	0.0348	0.1178	0.2305	0.3610	-0.5000	-0.3610	-0.2305	-0.1178	-0.0348	0.0000
	7	0.0000	0.0111	0.0519	0.1249	0.2277	0.3555	-0.4830	-0.3289	-0.1800	-0.0574	0.0000
	8	0.0000	-0.0137	-0.0178	0.0117	0.0825	0.1946	0.3426	-0.4196	-0.2383	-0.0788	0.0000
	9	0.0000	-0.0399	-0.0921	-0.1103	-0.0766	0.0143	0.1592	0.3469	-0.2920	-0.0989	0.0000
	10	0.0000	-0.0679	-0.1727	-0.2446	-0.2548	-0.1924	-0.0579	0.1372	0.3688	-0.1172	0.0000
	11	0.0000	-0.0993	-0.2647	-0.4014	-0.4683	-0.4479	-0.3375	-0.1477	0.0950	0.3386	0.0000

TABLE A.36
BENDING MOMENTS AT DIFFERENT SECTIONS (RISE-TO-SPAN RATIO 0.350)
=INFLUENCE VALUE*(L)

		POSITION OF UNIT LOAD FROM THE CROWN										
X/L		-0.50	-0.40	-0.30	-0.20	-0.10	0.00	0.10	0.20	0.30	0.40	0.50
DIFFER- ENT SECTIONS	1	0.0000	-0.0449	-0.0363	-0.0095	0.0200	0.0436	0.0562	0.0551	0.0408	0.0173	0.0000
	2	0.0000	0.0307	-0.0031	-0.0177	-0.0211	-0.0181	-0.0122	-0.0060	-0.0014	0.0004	0.0000
	3	0.0000	0.0160	0.0560	0.0143	-0.0124	-0.0267	-0.0308	-0.0269	-0.0177	-0.0067	0.0000
	4	0.0000	0.0057	0.0265	0.0639	0.0179	-0.0122	-0.0276	-0.0302	-0.0227	-0.0094	0.0000
	5	0.0000	-0.0017	0.0046	0.0256	0.0632	0.0183	-0.0096	-0.0215	-0.0199	-0.0093	0.0000
	6	0.0000	-0.0067	-0.0107	-0.0027	0.0209	0.0620	0.0209	-0.0027	-0.0107	-0.0067	0.0000
	7	0.0000	-0.0093	-0.0199	-0.0215	-0.0096	0.0183	0.0632	0.0256	0.0046	-0.0017	0.0000
	8	0.0000	-0.0094	-0.0227	-0.0302	-0.0276	-0.0122	0.0179	0.0639	0.0265	0.0057	0.0000
	9	0.0000	-0.0067	-0.0177	-0.0269	-0.0308	-0.0267	-0.0124	0.0143	0.0560	0.0160	0.0000
	10	0.0000	0.0004	-0.0014	-0.0060	-0.0122	-0.0181	-0.0211	-0.0177	-0.0031	0.0307	0.0000
	11	0.0000	0.0173	0.0408	0.0551	0.0562	0.0436	0.0200	-0.0095	-0.0363	-0.0449	0.0000

TABLE A.37
VERTICAL SHEAR FORCES AT DIFFERENT SECTIONS (RISE-TO-SPAN RATIO 0.350)

		POSITION OF UNIT LOAD FROM THE CROWN										
X/L		-0.50	-0.40	-0.30	-0.20	-0.10	0.00	0.10	0.20	0.30	0.40	0.50
DIFFER- -ENT SECTIONS	1	0.0000	0.9622	0.8771	0.7647	0.6361	0.5000	0.3639	0.2353	0.1229	0.0378	0.0000
	2	0.0000	-0.0378	0.8771	0.7647	0.6361	0.5000	0.3639	0.2353	0.1229	0.0378	0.0000
	3	0.0000	-0.0378	-0.1229	0.7647	0.6361	0.5000	0.3639	0.2353	0.1229	0.0378	0.0000
	4	0.0000	-0.0378	-0.1229	-0.2353	0.6361	0.5000	0.3639	0.2353	0.1229	0.0378	0.0000
	5	0.0000	-0.0378	-0.1229	-0.2353	-0.3639	0.5000	0.3639	0.2353	0.1229	0.0378	0.0000
	6	0.0000	-0.0378	-0.1229	-0.2353	-0.3639	0.5000	0.3639	0.2353	0.1229	0.0378	0.0000
	7	0.0000	-0.0378	-0.1229	-0.2353	-0.3639	-0.5000	0.3639	0.2353	0.1229	0.0378	0.0000
	8	0.0000	-0.0378	-0.1229	-0.2353	-0.3639	-0.5000	-0.6361	0.2353	0.1229	0.0378	0.0000
	9	0.0000	-0.0378	-0.1229	-0.2353	-0.3639	-0.5000	-0.6361	-0.7647	0.1229	0.0378	0.0000
	10	0.0000	-0.0378	-0.1229	-0.2353	-0.3639	-0.5000	-0.6361	-0.7647	-0.8771	0.0378	0.0000
	11	0.0000	-0.0378	-0.1229	-0.2353	-0.3639	-0.5000	-0.6361	-0.7647	-0.8771	-0.9622	0.0000

TABLE A.38
HORIZONTAL THRUSTS AT DIFFERENT SECTIONS (RISE-TO-SPAN RATIO 0.350)

		POSITION OF UNIT LOAD FROM THE CROWN										
X/L		-0.50	-0.40	-0.30	-0.20	-0.10	0.00	0.10	0.20	0.30	0.40	0.50
DIFFER- -ENT SECTIONS	1	0.0000	0.1226	0.3226	0.5015	0.6205	0.6618	0.6205	0.5015	0.3226	0.1226	0.0000
	2	0.0000	0.1226	0.3226	0.5015	0.6205	0.6618	0.6205	0.5015	0.3226	0.1226	0.0000
	3	0.0000	0.1226	0.3226	0.5015	0.6205	0.6618	0.6205	0.5015	0.3226	0.1226	0.0000
	4	0.0000	0.1226	0.3226	0.5015	0.6205	0.6618	0.6205	0.5015	0.3226	0.1226	0.0000
	5	0.0000	0.1226	0.3226	0.5015	0.6205	0.6618	0.6205	0.5015	0.3226	0.1226	0.0000
	6	0.0000	0.1226	0.3226	0.5015	0.6205	0.6618	0.6205	0.5015	0.3226	0.1226	0.0000
	7	0.0000	0.1226	0.3226	0.5015	0.6205	0.6618	0.6205	0.5015	0.3226	0.1226	0.0000
	8	0.0000	0.1226	0.3226	0.5015	0.6205	0.6618	0.6205	0.5015	0.3226	0.1226	0.0000
	9	0.0000	0.1226	0.3226	0.5015	0.6205	0.6618	0.6205	0.5015	0.3226	0.1226	0.0000
	10	0.0000	0.1226	0.3226	0.5015	0.6205	0.6618	0.6205	0.5015	0.3226	0.1226	0.0000
	11	0.0000	0.1226	0.3226	0.5015	0.6205	0.6618	0.6205	0.5015	0.3226	0.1226	0.0000

TABLE A.39
THRUSTS AT THE DIFFERENT RADIAL PLANES (RISE-TO-SPAN RATIO 0.350)

		POSITION OF UNIT LOAD FROM THE CROWN										
X/L		-0.50	-0.40	-0.30	-0.20	-0.10	0.00	0.10	0.20	0.30	0.40	0.50
DIFFERENT SECTIONS	1	0.0000	0.9460	0.9345	0.8901	0.8101	0.6963	0.5543	0.3928	0.2259	0.0775	0.0000
	2	0.0000	0.0524	0.8721	0.9055	0.8874	0.8123	0.6827	0.5077	0.3052	0.1093	0.0000
	3	0.0000	0.0799	0.1972	0.8453	0.8711	0.8285	0.7176	0.5469	0.3358	0.1226	0.0000
	4	0.0000	0.0994	0.2528	0.3763	0.8140	0.8012	0.7117	0.5532	0.3452	0.1278	0.0000
	5	0.0000	0.1133	0.2938	0.4484	0.5410	0.7440	0.6778	0.5368	0.3400	0.1275	0.0000
	6	0.0000	0.1226	0.3226	0.5015	0.6205	0.6618	0.6205	0.5015	0.3226	0.1226	0.0000
	7	0.0000	0.1275	0.3400	0.5368	0.6778	0.7440	0.5410	0.4484	0.2938	0.1133	0.0000
	8	0.0000	0.1278	0.3452	0.5532	0.7117	0.8012	0.8140	0.3763	0.2528	0.0994	0.0000
	9	0.0000	0.1226	0.3358	0.5469	0.7176	0.8285	0.8711	0.8453	0.1972	0.0799	0.0000
	10	0.0000	0.1093	0.3052	0.5077	0.6827	0.8123	0.8874	0.9055	0.8721	0.0524	0.0000
	11	0.0000	0.0775	0.2259	0.3928	0.5543	0.6963	0.8101	0.8901	0.9345	0.9460	0.0000

TABLE A.40
SHEAR FORCES ALONG THE DIFFERENT RADIAL PLANES (RISE-TO-SPAN RATIO 0.350)

		POSITION OF UNIT LOAD FROM THE CROWN										
X/L		-0.50	-0.40	-0.30	-0.20	-0.10	0.00	0.10	0.20	0.30	0.40	0.50
DIFFERENT SECTIONS	1	0.0000	0.2142	-0.0029	-0.2095	-0.3652	-0.4507	-0.4584	-0.3907	-0.2611	-0.1022	0.0000
	2	0.0000	-0.1171	0.3359	0.1273	-0.0468	-0.1677	-0.2264	-0.2218	-0.1615	-0.0672	0.0000
	3	0.0000	-0.1003	-0.2834	0.3488	0.1756	0.0399	-0.0492	-0.0884	-0.0804	-0.0379	0.0000
	4	0.0000	-0.0811	-0.2352	-0.4066	0.3563	0.2146	0.1040	0.0296	-0.0074	-0.0110	0.0000
	5	0.0000	-0.0602	-0.1814	-0.3254	-0.4740	0.3667	0.2408	0.1369	0.0601	0.0141	0.0000
	6	0.0000	0.0378	0.1229	0.2353	0.3639	-0.5000	-0.3639	-0.2353	-0.1229	-0.0378	0.0000
	7	0.0000	0.0141	0.0601	0.1369	0.2408	0.3667	-0.4740	-0.3254	-0.1814	-0.0602	0.0000
	8	0.0000	-0.0110	-0.0074	0.0296	0.1040	0.2146	0.3563	-0.4066	-0.2352	-0.0811	0.0000
	9	0.0000	-0.0379	-0.0804	-0.0884	-0.0492	0.0399	0.1756	0.3488	-0.2834	-0.1003	0.0000
	10	0.0000	-0.0672	-0.1615	-0.2218	-0.2264	-0.1677	-0.0468	0.1273	0.3359	-0.1171	0.0000
	11	0.0000	-0.1022	-0.2611	-0.3907	-0.4584	-0.4507	-0.3652	-0.2095	-0.0029	0.2142	0.0000

TABLE A.41
BENDING MOMENTS AT DIFFERENT SECTIONS (RISE-TO-SPAN RATIO 0.400)
=INFLUENCE VALUE*(L)

		POSITION OF UNIT LOAD FROM THE CROWN										
X/L		-0.50	-0.40	-0.30	-0.20	-0.10	0.00	0.10	0.20	0.30	0.40	0.50
DIFFER- -ENT SECTIONS	1	0.0000	-0.0390	-0.0282	-0.0022	0.0255	0.0472	0.0585	0.0572	0.0430	0.0193	0.0000
	2	0.0000	0.0323	-0.0020	-0.0186	-0.0242	-0.0229	-0.0177	-0.0111	-0.0050	-0.0010	0.0000
	3	0.0000	0.0169	0.0572	0.0151	-0.0125	-0.0278	-0.0327	-0.0293	-0.0200	-0.0081	0.0000
	4	0.0000	0.0061	0.0278	0.0660	0.0202	-0.0103	-0.0266	-0.0303	-0.0237	-0.0105	0.0000
	5	0.0000	-0.0017	0.0059	0.0282	0.0667	0.0219	-0.0066	-0.0199	-0.0198	-0.0100	0.0000
	6	0.0000	-0.0070	-0.0098	-0.0002	0.0247	0.0662	0.0247	-0.0002	-0.0098	-0.0070	0.0000
	7	0.0000	-0.0100	-0.0198	-0.0199	-0.0066	0.0219	0.0667	0.0282	0.0059	-0.0017	0.0000
	8	0.0000	-0.0105	-0.0237	-0.0303	-0.0266	-0.0103	0.0202	0.0660	0.0278	0.0061	0.0000
	9	0.0000	-0.0081	-0.0200	-0.0293	-0.0327	-0.0278	-0.0125	0.0151	0.0572	0.0169	0.0000
	10	0.0000	-0.0010	-0.0050	-0.0111	-0.0177	-0.0229	-0.0242	-0.0186	-0.0020	0.0323	0.0000
	11	0.0000	0.0193	0.0430	0.0572	0.0585	0.0472	0.0255	-0.0022	-0.0282	-0.0390	0.0000

TABLE A.42
VERTICAL SHEAR FORCES AT DIFFERENT SECTIONS (RISE-TO-SPAN RATIO 0.400)

		POSITION OF UNIT LOAD FROM THE CROWN										
X/L		-0.50	-0.40	-0.30	-0.20	-0.10	0.00	0.10	0.20	0.30	0.40	0.50
DIFFER- -ENT SECTIONS	1	0.0000	0.9583	0.8712	0.7593	0.6330	0.5000	0.3670	0.2407	0.1288	0.0417	0.0000
	2	0.0000	-0.0417	0.8712	0.7593	0.6330	0.5000	0.3670	0.2407	0.1288	0.0417	0.0000
	3	0.0000	-0.0417	-0.1288	0.7593	0.6330	0.5000	0.3670	0.2407	0.1288	0.0417	0.0000
	4	0.0000	-0.0417	-0.1288	-0.2407	0.6330	0.5000	0.3670	0.2407	0.1288	0.0417	0.0000
	5	0.0000	-0.0417	-0.1288	-0.2407	-0.3670	0.5000	0.3670	0.2407	0.1288	0.0417	0.0000
	6	0.0000	-0.0417	-0.1288	-0.2407	-0.3670	0.5000	0.3670	0.2407	0.1288	0.0417	0.0000
	7	0.0000	-0.0417	-0.1288	-0.2407	-0.3670	-0.5000	0.3670	0.2407	0.1288	0.0417	0.0000
	8	0.0000	-0.0417	-0.1288	-0.2407	-0.3670	-0.5000	-0.6330	0.2407	0.1288	0.0417	0.0000
	9	0.0000	-0.0417	-0.1288	-0.2407	-0.3670	-0.5000	-0.6330	-0.7593	0.1288	0.0417	0.0000
	10	0.0000	-0.0417	-0.1288	-0.2407	-0.3670	-0.5000	-0.6330	-0.7593	-0.8712	0.0417	0.0000
	11	0.0000	-0.0417	-0.1288	-0.2407	-0.3670	-0.5000	-0.6330	-0.7593	-0.8712	-0.9583	0.0000

TABLE A.43
HORIZONTAL THRUSTS AT DIFFERENT SECTIONS (RISE-TO-SPAN RATIO 0.400)

		POSITION OF UNIT LOAD FROM THE CROWN										
X/L		-0.50	-0.40	-0.30	-0.20	-0.10	0.00	0.10	0.20	0.30	0.40	0.50
DIFFERENT SECTIONS	1	0.0000	0.1179	0.2931	0.4443	0.5432	0.5774	0.5432	0.4443	0.2931	0.1179	0.0000
	2	0.0000	0.1179	0.2931	0.4443	0.5432	0.5774	0.5432	0.4443	0.2931	0.1179	0.0000
	3	0.0000	0.1179	0.2931	0.4443	0.5432	0.5774	0.5432	0.4443	0.2931	0.1179	0.0000
	4	0.0000	0.1179	0.2931	0.4443	0.5432	0.5774	0.5432	0.4443	0.2931	0.1179	0.0000
	5	0.0000	0.1179	0.2931	0.4443	0.5432	0.5774	0.5432	0.4443	0.2931	0.1179	0.0000
	6	0.0000	0.1179	0.2931	0.4443	0.5432	0.5774	0.5432	0.4443	0.2931	0.1179	0.0000
	7	0.0000	0.1179	0.2931	0.4443	0.5432	0.5774	0.5432	0.4443	0.2931	0.1179	0.0000
	8	0.0000	0.1179	0.2931	0.4443	0.5432	0.5774	0.5432	0.4443	0.2931	0.1179	0.0000
	9	0.0000	0.1179	0.2931	0.4443	0.5432	0.5774	0.5432	0.4443	0.2931	0.1179	0.0000
	10	0.0000	0.1179	0.2931	0.4443	0.5432	0.5774	0.5432	0.4443	0.2931	0.1179	0.0000
	11	0.0000	0.1179	0.2931	0.4443	0.5432	0.5774	0.5432	0.4443	0.2931	0.1179	0.0000

TABLE A.44
THRUSTS AT THE DIFFERENT RADIAL PLANES (RISE-TO-SPAN RATIO 0.400)

		POSITION OF UNIT LOAD FROM THE CROWN										
X/L		-0.50	-0.40	-0.30	-0.20	-0.10	0.00	0.10	0.20	0.30	0.40	0.50
DIFFERENT SECTIONS	1	0.0000	0.9609	0.9143	0.8384	0.7368	0.6146	0.4773	0.3323	0.1900	0.0665	0.0000
	2	0.0000	0.0412	0.8632	0.8704	0.8337	0.7512	0.6260	0.4656	0.2838	0.1062	0.0000
	3	0.0000	0.0712	0.1623	0.8047	0.8110	0.7608	0.6552	0.5011	0.3130	0.1200	0.0000
	4	0.0000	0.0923	0.2196	0.3152	0.7472	0.7268	0.6434	0.5030	0.3201	0.1248	0.0000
	5	0.0000	0.1075	0.2624	0.3888	0.4612	0.6639	0.6044	0.4828	0.3126	0.1238	0.0000
	6	0.0000	0.1179	0.2931	0.4443	0.5432	0.5774	0.5432	0.4443	0.2931	0.1179	0.0000
	7	0.0000	0.1238	0.3126	0.4828	0.6044	0.6639	0.4612	0.3888	0.2624	0.1075	0.0000
	8	0.0000	0.1248	0.3201	0.5030	0.6434	0.7268	0.7472	0.3152	0.2196	0.0923	0.0000
	9	0.0000	0.1200	0.3130	0.5011	0.6552	0.7608	0.8110	0.8047	0.1623	0.0712	0.0000
	10	0.0000	0.1062	0.2838	0.4656	0.6260	0.7512	0.8337	0.8704	0.8632	0.0412	0.0000
	11	0.0000	0.0665	0.1900	0.3323	0.4773	0.6146	0.7368	0.8384	0.9143	0.9609	0.0000

TABLE A.45
SHEAR FORCES ALONG THE DIFFERENT RADIAL PLANES (RISE-TO-SPAN RATIO 0.400)

		POSITION OF UNIT LOAD FROM THE CROWN										
X/L		-0.50	-0.40	-0.30	-0.20	-0.10	0.00	0.10	0.20	0.30	0.40	0.50
DIFFER- -ENT SECTIONS	1	0.0000	0.0953	-0.0947	-0.2668	-0.3910	-0.4536	-0.4494	-0.3807	-0.2577	-0.1059	0.0000
	2	0.0000	-0.1181	0.3159	0.1279	-0.0282	-0.1381	-0.1946	-0.1963	-0.1483	-0.0660	0.0000
	3	0.0000	-0.1028	-0.2760	0.3556	0.1953	0.0674	-0.0205	-0.0650	-0.0672	-0.0353	0.0000
	4	0.0000	-0.0844	-0.2330	-0.3950	0.3709	0.2350	0.1259	0.0482	0.0042	-0.0077	0.0000
	5	0.0000	-0.0639	-0.1835	-0.3227	-0.4659	0.3777	0.2539	0.1493	0.0691	0.0178	0.0000
	6	0.0000	0.0417	0.1288	0.2407	0.3670	-0.5000	-0.3670	-0.2407	-0.1288	-0.0417	0.0000
	7	0.0000	0.0178	0.0691	0.1493	0.2539	0.3777	-0.4659	-0.3227	-0.1835	-0.0639	0.0000
	8	0.0000	-0.0077	0.0042	0.0482	0.1259	0.2350	0.3709	-0.3950	-0.2330	-0.0844	0.0000
	9	0.0000	-0.0353	-0.0672	-0.0650	-0.0205	0.0674	0.1953	0.3556	-0.2760	-0.1028	0.0000
	10	0.0000	-0.0660	-0.1483	-0.1963	-0.1946	-0.1381	-0.0282	0.1279	0.3159	-0.1181	0.0000
	11	0.0000	-0.1059	-0.2577	-0.3807	-0.4494	-0.4536	-0.3910	-0.2668	-0.0947	0.0953	0.0000

TABLE A.46
BENDING MOMENTS AT DIFFERENT SECTIONS (RISE-TO-SPAN RATIO 0.450)
=INFLUENCE VALUE*(L)

		POSITION OF UNIT LOAD FROM THE CROWN										
X/L		-0.50	-0.40	-0.30	-0.20	-0.10	0.00	0.10	0.20	0.30	0.40	0.50
DIFFER- -ENT SECTIONS	1	0.0000	-0.0320	-0.0193	0.0057	0.0313	0.0511	0.0611	0.0594	0.0454	0.0216	0.0000
	2	0.0000	0.0342	-0.0009	-0.0196	-0.0273	-0.0278	-0.0235	-0.0167	-0.0092	-0.0029	0.0000
	3	0.0000	0.0182	0.0588	0.0163	-0.0121	-0.0284	-0.0342	-0.0315	-0.0224	-0.0097	0.0000
	4	0.0000	0.0068	0.0296	0.0685	0.0229	-0.0080	-0.0252	-0.0300	-0.0245	-0.0117	0.0000
	5	0.0000	-0.0015	0.0076	0.0313	0.0707	0.0259	-0.0033	-0.0180	-0.0195	-0.0107	0.0000
	6	0.0000	-0.0073	-0.0086	0.0027	0.0288	0.0708	0.0288	0.0027	-0.0086	-0.0073	0.0000
	7	0.0000	-0.0107	-0.0195	-0.0180	-0.0033	0.0259	0.0707	0.0313	0.0076	-0.0015	0.0000
	8	0.0000	-0.0117	-0.0245	-0.0300	-0.0252	-0.0080	0.0229	0.0685	0.0296	0.0068	0.0000
	9	0.0000	-0.0097	-0.0224	-0.0315	-0.0342	-0.0284	-0.0121	0.0163	0.0588	0.0182	0.0000
	10	0.0000	-0.0029	-0.0092	-0.0167	-0.0235	-0.0278	-0.0273	-0.0196	-0.0009	0.0342	0.0000
	11	0.0000	0.0216	0.0454	0.0594	0.0611	0.0511	0.0313	0.0057	-0.0193	-0.0320	0.0000

TABLE A.47
VERTICAL SHEAR FORCES AT DIFFERENT SECTIONS (RISE-TO-SPAN RATIO 0.450)

		POSITION OF UNIT LOAD FROM THE CROWN										
X/L		-0.50	-0.40	-0.30	-0.20	-0.10	0.00	0.10	0.20	0.30	0.40	0.50
DIFFER- -ENT SECTIONS	1	0.0000	0.9536	0.8647	0.7536	0.6298	0.5000	0.3702	0.2464	0.1353	0.0464	0.0000
	2	0.0000	-0.0464	0.8647	0.7536	0.6298	0.5000	0.3702	0.2464	0.1353	0.0464	0.0000
	3	0.0000	-0.0464	-0.1353	0.7536	0.6298	0.5000	0.3702	0.2464	0.1353	0.0464	0.0000
	4	0.0000	-0.0464	-0.1353	-0.2464	0.6298	0.5000	0.3702	0.2464	0.1353	0.0464	0.0000
	5	0.0000	-0.0464	-0.1353	-0.2464	-0.3702	0.5000	0.3702	0.2464	0.1353	0.0464	0.0000
	6	0.0000	-0.0464	-0.1353	-0.2464	-0.3702	0.5000	0.3702	0.2464	0.1353	0.0464	0.0000
	7	0.0000	-0.0464	-0.1353	-0.2464	-0.3702	-0.5000	0.3702	0.2464	0.1353	0.0464	0.0000
	8	0.0000	-0.0464	-0.1353	-0.2464	-0.3702	-0.5000	-0.6298	0.2464	0.1353	0.0464	0.0000
	9	0.0000	-0.0464	-0.1353	-0.2464	-0.3702	-0.5000	-0.6298	-0.7536	0.1353	0.0464	0.0000
	10	0.0000	-0.0464	-0.1353	-0.2464	-0.3702	-0.5000	-0.6298	-0.7536	-0.8647	0.0464	0.0000
	11	0.0000	-0.0464	-0.1353	-0.2464	-0.3702	-0.5000	-0.6298	-0.7536	-0.8647	-0.9536	0.0000

TABLE A.48
HORIZONTAL THRUSTS AT DIFFERENT SECTIONS (RISE-TO-SPAN RATIO 0.450)

		POSITION OF UNIT LOAD FROM THE CROWN										
X/L		-0.50	-0.40	-0.30	-0.20	-0.10	0.00	0.10	0.20	0.30	0.40	0.50
DIFFER- -ENT SECTIONS	1	0.0000	0.1157	0.2705	0.3997	0.4831	0.5117	0.4831	0.3997	0.2705	0.1157	0.0000
	2	0.0000	0.1157	0.2705	0.3997	0.4831	0.5117	0.4831	0.3997	0.2705	0.1157	0.0000
	3	0.0000	0.1157	0.2705	0.3997	0.4831	0.5117	0.4831	0.3997	0.2705	0.1157	0.0000
	4	0.0000	0.1157	0.2705	0.3997	0.4831	0.5117	0.4831	0.3997	0.2705	0.1157	0.0000
	5	0.0000	0.1157	0.2705	0.3997	0.4831	0.5117	0.4831	0.3997	0.2705	0.1157	0.0000
	6	0.0000	0.1157	0.2705	0.3997	0.4831	0.5117	0.4831	0.3997	0.2705	0.1157	0.0000
	7	0.0000	0.1157	0.2705	0.3997	0.4831	0.5117	0.4831	0.3997	0.2705	0.1157	0.0000
	8	0.0000	0.1157	0.2705	0.3997	0.4831	0.5117	0.4831	0.3997	0.2705	0.1157	0.0000
	9	0.0000	0.1157	0.2705	0.3997	0.4831	0.5117	0.4831	0.3997	0.2705	0.1157	0.0000
	10	0.0000	0.1157	0.2705	0.3997	0.4831	0.5117	0.4831	0.3997	0.2705	0.1157	0.0000
	11	0.0000	0.1157	0.2705	0.3997	0.4831	0.5117	0.4831	0.3997	0.2705	0.1157	0.0000

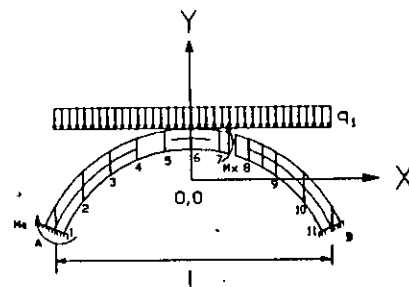
TABLE A.49
THRUSTS AT THE DIFFERENT RADIAL SECTIONS (RISE-TO-SPAN RATIO 0.450)

		POSITION OF UNIT LOAD FROM THE CROWN										
X/L		-0.50	-0.40	-0.30	-0.20	-0.10	0.00	0.10	0.20	0.30	0.40	0.50
DIFFER- -ENT SECTIONS	1	0.0000	0.9605	0.8883	0.7914	0.6770	0.5510	0.4189	0.2869	0.1629	0.0583	0.0000
	2	0.0000	0.0332	0.8518	0.8418	0.7937	0.7078	0.5872	0.4382	0.2715	0.1070	0.0000
	3	0.0000	0.0652	0.1363	0.7705	0.7635	0.7090	0.6086	0.4678	0.2978	0.1206	0.0000
	4	0.0000	0.0877	0.1943	0.2687	0.6937	0.6684	0.5905	0.4647	0.3020	0.1246	0.0000
	5	0.0000	0.1042	0.2382	0.3427	0.3998	0.6009	0.5471	0.4407	0.2920	0.1227	0.0000
	6	0.0000	0.1157	0.2705	0.3997	0.4831	0.5117	0.4831	0.3997	0.2705	0.1157	0.0000
	7	0.0000	0.1227	0.2920	0.4407	0.5471	0.6009	0.3998	0.3427	0.2382	0.1042	0.0000
	8	0.0000	0.1246	0.3020	0.4647	0.5905	0.6684	0.6937	0.2687	0.1943	0.0877	0.0000
	9	0.0000	0.1206	0.2978	0.4678	0.6086	0.7090	0.7635	0.7705	0.1363	0.0652	0.0000
	10	0.0000	0.1070	0.2715	0.4382	0.5872	0.7078	0.7937	0.8418	0.8518	0.0332	0.0000
	11	0.0000	0.0583	0.1629	0.2869	0.4189	0.5510	0.6770	0.7914	0.8883	0.9605	0.0000

TABLE A.50
SHEAR FORCES ALONG THE DIFFERENT RADIAL PLANES (RISE-TO-SPAN RATIO 0.450)

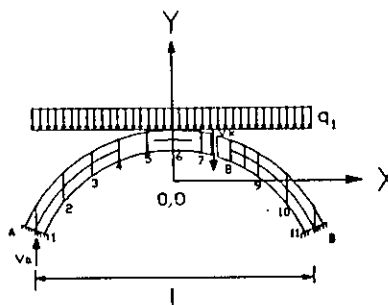
		POSITION OF UNIT LOAD FROM THE CROWN										
X/L		-0.50	-0.40	-0.30	-0.20	-0.10	0.00	0.10	0.20	0.30	0.40	0.50
DIFFER- -ENT SECTIONS	1	0.0000	-0.0150	-0.1782	-0.3184	-0.4143	-0.4564	-0.4416	-0.3717	-0.2548	-0.1102	0.0000
	2	0.0000	-0.1202	0.3087	0.1386	-0.0028	-0.1042	-0.1600	-0.1688	-0.1332	-0.0640	0.0000
	3	0.0000	-0.1063	-0.2700	0.3663	0.2172	0.0959	0.0088	-0.0408	-0.0528	-0.0318	0.0000
	4	0.0000	-0.0886	-0.2317	-0.3850	0.3857	0.2552	0.1475	0.0670	0.0165	-0.0035	0.0000
	5	0.0000	-0.0685	-0.1864	-0.3209	-0.4589	0.3882	0.2667	0.1619	0.0788	0.0224	0.0000
	6	0.0000	0.0464	0.1353	0.2464	0.3702	-0.5000	-0.3702	-0.2464	-0.1353	-0.0464	0.0000
	7	0.0000	0.0224	0.0788	0.1619	0.2667	0.3882	-0.4589	-0.3209	-0.1864	-0.0685	0.0000
	8	0.0000	-0.0035	0.0165	0.0670	0.1475	0.2552	0.3857	-0.3850	-0.2317	-0.0886	0.0000
	9	0.0000	-0.0318	-0.0528	-0.0408	0.0088	0.0959	0.2172	0.3663	-0.2700	-0.1063	0.0000
	10	0.0000	-0.0640	-0.1332	-0.1688	-0.1600	-0.1042	-0.0028	0.1386	0.3087	-0.1202	0.0000
	11	0.0000	-0.1102	-0.2548	-0.3717	-0.4416	-0.4564	-0.4143	-0.3184	-0.1782	-0.0150	0.0000

TABLE A.51
BENDING MOMENTS AT DIFFERENT SECTIONS FOR FILL LOAD ABOVE THE CROWN
=TABLE COEFF.*(Q*L*L)



		SECTION NUMBER										
(N)		1	2	3	4	5	6	7	8	9	10	11
RISE- -TO- SPAN RATIO	0.050	0.00029	-0.00007	-0.00012	-0.00003	0.00007	0.00011	0.00007	-0.00003	-0.00012	-0.00007	0.00029
	0.100	0.00114	-0.00029	-0.00046	-0.00011	0.00027	0.00043	0.00027	-0.00011	-0.00046	-0.00029	0.00114
	0.150	0.00255	-0.00070	-0.00101	-0.00021	0.00063	0.00097	0.00063	-0.00021	-0.00101	-0.00070	0.00255
	0.200	0.00451	-0.00139	-0.00174	-0.00028	0.00117	0.00175	0.00117	-0.00028	-0.00174	-0.00139	0.00451
	0.250	0.00699	-0.00241	-0.00259	-0.00026	0.00192	0.00275	0.00192	-0.00026	-0.00259	-0.00241	0.00699
	0.300	0.00998	-0.00384	-0.00348	-0.00007	0.00289	0.00400	0.00289	-0.00007	-0.00348	-0.00384	0.00998
	0.350	0.01346	-0.00567	-0.00431	0.00033	0.00411	0.00551	0.00411	0.00033	-0.00431	-0.00567	0.01346
	0.400	0.01741	-0.00783	-0.00496	0.00100	0.00560	0.00727	0.00560	0.00100	-0.00496	-0.00783	0.01741
	0.450	0.02181	-0.01014	-0.00535	0.00199	0.00738	0.00931	0.00738	0.00199	-0.00535	-0.01014	0.02181

TABLE A.52
VERTICAL SHEAR FORCES AT DIFFERENT SECTIONS FOR FILL LOAD ABOVE THE CROWN
=TABLE COEFF.*(Q*L)



		SECTION NUMBER										
(N)		1	2	3	4	5	6	7	8	9	10	11
RISE- -TO- SPAN RATIO	0.050	0.50000	0.40000	0.30000	0.20000	0.10000	0.00000	-0.10000	-0.20000	-0.30000	-0.40000	-0.50000
	0.100	0.50000	0.40000	0.30000	0.20000	0.10000	0.00000	-0.10000	-0.20000	-0.30000	-0.40000	-0.50000
	0.150	0.50000	0.40000	0.30000	0.20000	0.10000	0.00000	-0.10000	-0.20000	-0.30000	-0.40000	-0.50000
	0.200	0.50000	0.40000	0.30000	0.20000	0.10000	0.00000	-0.10000	-0.20000	-0.30000	-0.40000	-0.50000
	0.250	0.50000	0.40000	0.30000	0.20000	0.10000	0.00000	-0.10000	-0.20000	-0.30000	-0.40000	-0.50000
	0.300	0.50000	0.40000	0.30000	0.20000	0.10000	0.00000	-0.10000	-0.20000	-0.30000	-0.40000	-0.50000
	0.350	0.50000	0.40000	0.30000	0.20000	0.10000	0.00000	-0.10000	-0.20000	-0.30000	-0.40000	-0.50000
	0.400	0.50000	0.40000	0.30000	0.20000	0.10000	0.00000	-0.10000	-0.20000	-0.30000	-0.40000	-0.50000
	0.450	0.50000	0.40000	0.30000	0.20000	0.10000	0.00000	-0.10000	-0.20000	-0.30000	-0.40000	-0.50000

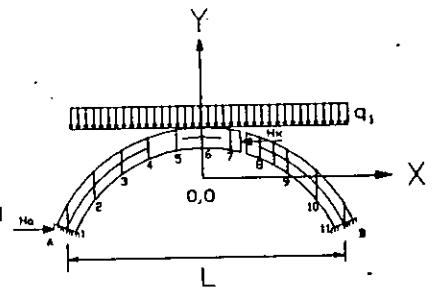


TABLE A.53

HORIZONTAL FORCES AT DIFFERENT SECTIONS FOR FILL LOAD ABOVE THE CROWN
=TABLE COEFF.*(Q*L)

		SECTION NUMBER										
(N)		1	2	3	4	5	6	7	8	9	10	11
RISE- -TO- SPAN RATIO	0.050	2.50368	2.50368	2.50368	2.50368	2.50368	2.50368	2.50368	2.50368	2.50368	2.50368	2.50368
	0.100	1.25709	1.25709	1.25709	1.25709	1.25709	1.25709	1.25709	1.25709	1.25709	1.25709	1.25709
	0.150	0.84384	0.84384	0.84384	0.84384	0.84384	0.84384	0.84384	0.84384	0.84384	0.84384	0.84384
	0.200	0.63880	0.63880	0.63880	0.63880	0.63880	0.63880	0.63880	0.63880	0.63880	0.63880	0.63880
	0.250	0.51695	0.51695	0.51695	0.51695	0.51695	0.51695	0.51695	0.51695	0.51695	0.51695	0.51695
	0.300	0.43659	0.43659	0.43659	0.43659	0.43659	0.43659	0.43659	0.43659	0.43659	0.43659	0.43659
	0.350	0.37986	0.37986	0.37986	0.37986	0.37986	0.37986	0.37986	0.37986	0.37986	0.37986	0.37986
	0.400	0.33784	0.33784	0.33784	0.33784	0.33784	0.33784	0.33784	0.33784	0.33784	0.33784	0.33784
	0.450	0.30556	0.30556	0.30556	0.30556	0.30556	0.30556	0.30556	0.30556	0.30556	0.30556	0.30556

TABLE A.54

THRUSTS AT THE DIFFERENT RADIAL SECTIONS FOR FILL LOAD ABOVE THE CROWN
=TABLE.COEFF.*(Q*L)

		SECTION NUMBER										
(N)		1	2	3	4	5	6	7	8	9	10	11
RISE- -TO- SPAN RATIO	0.050	2.5531	2.5354	2.5216	2.5117	2.5057	2.5037	2.5057	2.5117	2.5216	2.5354	2.5531
	0.100	1.3527	1.3192	1.2924	1.2729	1.2611	1.2571	1.2611	1.2729	1.2924	1.3192	1.3527
	0.150	0.9797	0.9338	0.8956	0.8672	0.8497	0.8438	0.8497	0.8672	0.8956	0.9338	0.9797
	0.200	0.8074	0.7535	0.7057	0.6692	0.6465	0.6388	0.6465	0.6692	0.7057	0.7535	0.8074
	0.250	0.7102	0.6532	0.5975	0.5538	0.5263	0.5169	0.5263	0.5538	0.5975	0.6532	0.7102
	0.300	0.6466	0.5916	0.5292	0.4791	0.4474	0.4366	0.4474	0.4791	0.5292	0.5916	0.6466
	0.350	0.5998	0.5512	0.4829	0.4272	0.3919	0.3799	0.3919	0.4272	0.4829	0.5512	0.5998
	0.400	0.5620	0.5234	0.4495	0.3891	0.3509	0.3378	0.3509	0.3891	0.4495	0.5234	0.5620
	0.450	0.5293	0.5034	0.4242	0.3599	0.3193	0.3056	0.3193	0.3599	0.4242	0.5034	0.5293

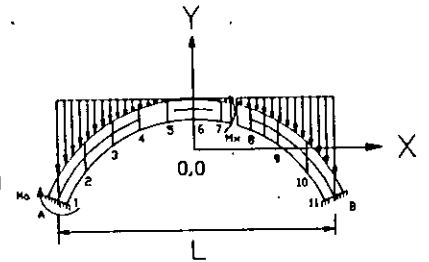
TABLE A.55

SHEAR FORCES ALONG THE DIFFERENT RADIAL PLANES FOR FILL LOAD ABOVE THE CROWN
 =TABLE.COEFF.*(Q*L)

		SECTION NUMBER											
		(N)	1	2	3	4	5	6	7	8	9	10	11
RISE- -TO- SPAN RATIO	0.050	0.0057	0.0017	-0.0004	-0.0011	-0.0008	0.0000	-0.0008	-0.0011	-0.0004	0.0017	0.0057	
	0.100	0.0220	0.0062	-0.0018	-0.0042	-0.0030	0.0000	-0.0030	-0.0042	-0.0018	0.0062	0.0220	
	0.150	0.0471	0.0125	-0.0045	-0.0093	-0.0065	0.0000	-0.0065	-0.0093	-0.0045	0.0125	0.0471	
	0.200	0.0785	0.0188	-0.0088	-0.0160	-0.0109	0.0000	-0.0109	-0.0160	-0.0088	0.0188	0.0785	
	0.250	0.1136	0.0235	-0.0150	-0.0241	-0.0160	0.0000	-0.0160	-0.0241	-0.0150	0.0235	0.1136	
	0.300	0.1499	0.0248	-0.0234	-0.0330	-0.0214	0.0000	-0.0214	-0.0330	-0.0234	0.0248	0.1499	
	0.350	0.1858	0.0217	-0.0336	-0.0426	-0.0268	0.0000	-0.0268	-0.0426	-0.0336	0.0217	0.1858	
	0.400	0.2198	0.0136	-0.0455	-0.0523	-0.0322	0.0000	-0.0322	-0.0523	-0.0455	0.0136	0.2198	
	0.450	0.2514	0.0008	-0.0584	-0.0619	-0.0372	0.0000	-0.0372	-0.0619	-0.0584	0.0008	0.2514	

TABLE A.56

BENDING MOMENTS AT DIFFERENT SECTIONS FOR FILL LOAD BELOW THE CROWN
 =TABLE COEFF.*(L*L*L)*(UNIT WT. OF FILL)



		SECTION NUMBER											
		(N)	1	2	3	4	5	6	7	8	9	10	11
RISE- -TO- SPAN RATIO	0.050	-0.00191	-0.00071	0.00003	0.00046	0.00068	0.00074	0.00068	0.00046	0.00003	-0.00071	-0.00191	
	0.100	-0.00050	0.00008	0.00018	0.00006	-0.00008	-0.00015	-0.00008	0.00006	0.00018	0.00008	-0.00050	
	0.150	-0.00061	0.00016	0.00026	0.00006	-0.00016	-0.00025	-0.00016	0.00006	0.00026	0.00016	-0.00061	
	0.200	-0.00070	0.00021	0.00031	0.00007	-0.00021	-0.00032	-0.00021	0.00007	0.00031	0.00021	-0.00070	
	0.250	-0.00071	0.00025	0.00035	0.00006	-0.00025	-0.00037	-0.00025	0.00006	0.00035	0.00025	-0.00071	
	0.300	-0.00063	0.00027	0.00036	0.00006	-0.00028	-0.00041	-0.00028	0.00006	0.00036	0.00027	-0.00063	
	0.350	-0.00045	0.00026	0.00036	0.00005	-0.00029	-0.00043	-0.00029	0.00005	0.00036	0.00026	-0.00045	
	0.400	-0.00017	0.00023	0.00035	0.00005	-0.00029	-0.00043	-0.00029	0.00005	0.00035	0.00023	-0.00017	
	0.450	0.00019	0.00019	0.00034	0.00006	-0.00027	-0.00041	-0.00027	0.00006	0.00034	0.00019	0.00019	

TABLE A.59

THRUSTS AT THE DIFFERENT RADIAL PLANES FOR FILL LOAD BELOW THE CROWN
 =TABLE.COEFF.*(L*L)

SECTION NUMBER

	(N)	1	2	3	4	5	6	7	8	9	10	11
RISE-	0.050	0.0333	0.0325	0.0323	0.0322	0.0322	0.0323	0.0322	0.0322	0.0323	0.0325	0.0333
	0.100	0.0218	0.0185	0.0171	0.0167	0.0167	0.0168	0.0167	0.0167	0.0171	0.0185	0.0218
-TO-	0.150	0.0277	0.0209	0.0180	0.0172	0.0172	0.0173	0.0172	0.0172	0.0180	0.0209	0.0277
	0.200	0.0339	0.0227	0.0181	0.0169	0.0169	0.0170	0.0169	0.0169	0.0181	0.0227	0.0339
SPAN	0.250	0.0401	0.0245	0.0182	0.0165	0.0165	0.0166	0.0165	0.0165	0.0182	0.0245	0.0401
	0.300	0.0457	0.0260	0.0181	0.0160	0.0160	0.0162	0.0160	0.0160	0.0181	0.0260	0.0457
RATIO	0.350	0.0501	0.0270	0.0179	0.0155	0.0154	0.0156	0.0154	0.0155	0.0179	0.0270	0.0501
	0.400	0.0530	0.0276	0.0177	0.0149	0.0149	0.0151	0.0149	0.0149	0.0177	0.0276	0.0530
	0.450	0.0542	0.0278	0.0173	0.0144	0.0143	0.0145	0.0143	0.0144	0.0173	0.0278	0.0542

TABLE A.60

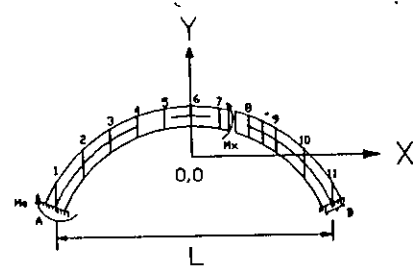
SHEAR FORCES ALONG THE DIFFERENT RADIAL PLANES FILL LOAD BELOW THE CROWN
 =TABLE.COEFF.*(L*L)

SECTION NUMBER

	(N)	1	2	3	4	5	6	7	8	9	10	11
RISE-	0.050	-0.0017	0.0009	0.0021	0.0020	0.0012	0.0000	0.0012	0.0020	0.0021	0.0009	-0.0017
	0.100	-0.0087	-0.0028	0.0005	0.0016	0.0012	0.0000	0.0012	0.0016	0.0005	-0.0028	-0.0087
-TO-	0.150	-0.0106	-0.0033	0.0010	0.0024	0.0017	0.0000	0.0017	0.0024	0.0010	-0.0033	-0.0106
	0.200	-0.0109	-0.0035	0.0012	0.0029	0.0021	0.0000	0.0021	0.0029	0.0012	-0.0035	-0.0109
SPAN	0.250	-0.0093	-0.0034	0.0014	0.0033	0.0024	0.0000	0.0024	0.0033	0.0014	-0.0034	-0.0093
	0.300	-0.0060	-0.0032	0.0015	0.0035	0.0026	0.0000	0.0026	0.0035	0.0015	-0.0032	-0.0060
RATIO	0.350	-0.0016	-0.0029	0.0015	0.0035	0.0026	0.0000	0.0026	0.0035	0.0015	-0.0029	-0.0016
	0.400	0.0036	-0.0028	0.0013	0.0034	0.0026	0.0000	0.0026	0.0034	0.0013	-0.0028	0.0036
	0.450	0.0089	-0.0029	0.0011	0.0033	0.0026	0.0000	0.0026	0.0033	0.0011	-0.0029	0.0089

TABLE A.61

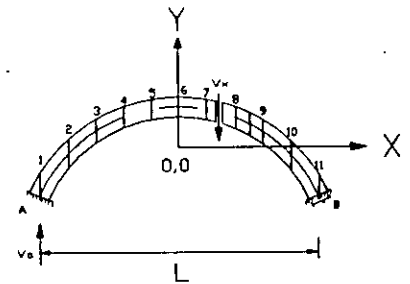
BENDING MOMENTS AT DIFFERENT SECTIONS FOR SELF LOAD OF THE ARCH
 =TABLE COEFF.*(T*L)*(UNIT WT.OF ARCH MATERIAL)*WIDTH



		SECTION NUMBER										
(N)		1	2	3	4	5	6	7	8	9	10	11
RISE- -TO- SPAN RATIO RATIO	0.050	0.00019	-0.00005	-0.00008	-0.00002	0.00004	0.00007	0.00004	-0.00002	-0.00008	-0.00005	0.00019
	0.100	0.00078	-0.00020	-0.00031	-0.00008	0.00019	0.00029	0.00019	-0.00008	-0.00031	-0.00020	0.00078
	0.150	0.00180	-0.00050	-0.00070	-0.00014	0.00044	0.00067	0.00044	-0.00014	-0.00070	-0.00050	0.00180
	0.200	0.00331	-0.00102	-0.00124	-0.00019	0.00084	0.00124	0.00084	-0.00019	-0.00124	-0.00102	0.00331
	0.250	0.00539	-0.00185	-0.00191	-0.00016	0.00142	0.00202	0.00142	-0.00016	-0.00191	-0.00185	0.00539
	0.300	0.00812	-0.00307	-0.00263	0.00000	0.00222	0.00304	0.00222	0.00000	-0.00263	-0.00307	0.00812
	0.350	0.01160	-0.00473	-0.00335	0.00037	0.00328	0.00434	0.00328	0.00037	-0.00335	-0.00473	0.01160
0.400	0.01590	-0.00676	-0.00394	0.00100	0.00464	0.00595	0.00464	0.00100	-0.00394	-0.00676	0.01590	
0.450	0.02114	-0.00903	-0.00431	0.00195	0.00635	0.00790	0.00635	0.00195	-0.00431	-0.00903	0.02114	

TABLE A.62

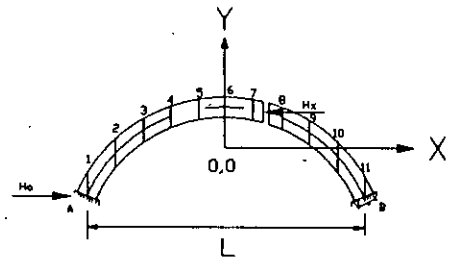
VERTICAL SHEAR FORCES AT DIFFERENT SECTIONS FOR SELF LOAD OF THE ARCH
 =TABLE COEFF.*(T*L)*(UNIT WT. OF ARCH MATERIAL)*WIDTH



		SECTION NUMBER										
(N)		1	2	3	4	5	6	7	8	9	10	11
RISE- -TO- SPAN RATIO RATIO	0.050	0.50333	0.40169	0.30071	0.20021	0.10003	0.00000	-0.10003	-0.20021	-0.30071	-0.40169	-0.50333
	0.100	0.51323	0.40660	0.30273	0.20080	0.10010	0.00000	-0.10010	-0.20080	-0.30273	-0.40660	-0.51323
	0.150	0.52948	0.41421	0.30574	0.20165	0.10020	0.00000	-0.10020	-0.20165	-0.30574	-0.41421	-0.52948
	0.200	0.55173	0.42371	0.30930	0.20263	0.10032	0.00000	-0.10032	-0.20263	-0.30930	-0.42371	-0.55173
	0.250	0.57956	0.43406	0.31291	0.20358	0.10043	0.00000	-0.10043	-0.20358	-0.31291	-0.43406	-0.57956
	0.300	0.61248	0.44408	0.31615	0.20440	0.10053	0.00000	-0.10053	-0.20440	-0.31615	-0.44408	-0.61248
	0.350	0.64999	0.45264	0.31872	0.20504	0.10060	0.00000	-0.10060	-0.20504	-0.31872	-0.45264	-0.64999
0.400	0.69161	0.45892	0.32048	0.20546	0.10065	0.00000	-0.10065	-0.20546	-0.32048	-0.45892	-0.69161	
0.450	0.73689	0.46254	0.32146	0.20569	0.10067	0.00000	-0.10067	-0.20569	-0.32146	-0.46254	-0.73689	

TABLE A.63

HORIZONTAL FORCES AT DIFFERENT SECTIONS FOR SELF LOAD OF THE ARCH
 =TABLE COEFF.*(TXL)*(UNIT WT. OF ARCH MATERIAL)*WIDTH



SECTION NUMBER

	(N)	1	2	3	4	5	6	7	8	9	10	11
	0.050	2.51066	2.51066	2.51066	2.51066	2.51066	2.51066	2.51066	2.51066	2.51066	2.51066	2.51066
RISE-	0.100	1.27101	1.27101	1.27101	1.27101	1.27101	1.27101	1.27101	1.27101	1.27101	1.27101	1.27101
-TO-	0.150	0.86410	0.86410	0.86410	0.86410	0.86410	0.86410	0.86410	0.86410	0.86410	0.86410	0.86410
SPAN	0.200	0.66469	0.66469	0.66469	0.66469	0.66469	0.66469	0.66469	0.66469	0.66469	0.66469	0.66469
RATIO	0.250	0.54760	0.54760	0.54760	0.54760	0.54760	0.54760	0.54760	0.54760	0.54760	0.54760	0.54760
	0.300	0.47106	0.47106	0.47106	0.47106	0.47106	0.47106	0.47106	0.47106	0.47106	0.47106	0.47106
	0.350	0.41714	0.41714	0.41714	0.41714	0.41714	0.41714	0.41714	0.41714	0.41714	0.41714	0.41714
	0.400	0.37691	0.37691	0.37691	0.37691	0.37691	0.37691	0.37691	0.37691	0.37691	0.37691	0.37691
	0.450	0.34542	0.34542	0.34542	0.34542	0.34542	0.34542	0.34542	0.34542	0.34542	0.34542	0.34542

TABLE A.64

THRUSTS AT THE DIFFERENT RADIAL PLANES FOR SELF LOAD OF THE ARCH
 =TABLE.COEFF.*(TXL)*(UNIT WT. OF ARCH MATERIAL)*WIDTH

SECTION NUMBER

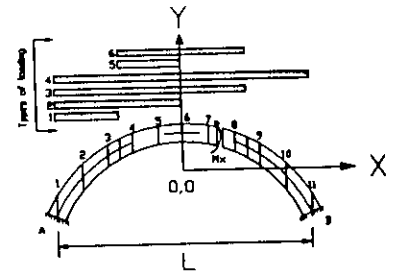
	(N)	1	2	3	4	5	6	7	8	9	10	11
	0.050	2.5606	2.5426	2.5286	2.5186	2.5127	2.5107	2.5127	2.5186	2.5286	2.5426	2.5606
RISE-	0.100	1.3706	1.3345	1.3066	1.2868	1.2749	1.2710	1.2749	1.2868	1.3066	1.3345	1.3706
-TO-	0.150	1.0129	0.9582	0.9166	0.8873	0.8699	0.8641	0.8699	0.8873	0.9166	0.9582	1.0129
SPAN	0.200	0.8618	0.7881	0.7331	0.6948	0.6722	0.6647	0.6722	0.6948	0.7331	0.7881	0.8618
RATIO	0.250	0.7922	0.6986	0.6306	0.5840	0.5566	0.5476	0.5566	0.5840	0.6306	0.6986	0.7922
	0.300	0.7621	0.6471	0.5670	0.5129	0.4814	0.4711	0.4814	0.5129	0.5670	0.6471	0.7621
	0.350	0.7535	0.6154	0.5242	0.4636	0.4286	0.4171	0.4286	0.4636	0.5242	0.6154	0.7535
	0.400	0.7575	0.5938	0.4932	0.4272	0.3893	0.3769	0.3893	0.4272	0.4932	0.5938	0.7575
	0.450	0.7691	0.5773	0.4690	0.3987	0.3585	0.3454	0.3585	0.3987	0.4690	0.5773	0.7691

TABLE A.65

SHEAR FORCES ALONG THE DIFFERENT RADIAL PLANES FOR SELF LOAD OF THE ARCH
 =TABLE. COEFF.*(T*L)*(UNIT WT. OF ARCH MATERIAL)*WIDTH

		SECTION NUMBER										
(N)		1	2	3	4	5	6	7	8	9	10	11
RISE- -TO- SPAN RATIO	0.050	0.0038	0.0011	-0.0003	-0.0007	-0.0005	0.0000	-0.0005	-0.0007	-0.0003	0.0011	0.0038
	0.100	0.0151	0.0042	-0.0012	-0.0029	-0.0020	0.0000	-0.0020	-0.0029	-0.0012	0.0042	0.0151
	0.150	0.0336	0.0086	-0.0032	-0.0064	-0.0045	0.0000	-0.0045	-0.0064	-0.0032	0.0086	0.0336
	0.200	0.0589	0.0133	-0.0065	-0.0114	-0.0077	0.0000	-0.0077	-0.0114	-0.0065	0.0133	0.0589
	0.250	0.0903	0.0169	-0.0117	-0.0176	-0.0115	0.0000	-0.0115	-0.0176	-0.0117	0.0169	0.0903
	0.300	0.1274	0.0180	-0.0188	-0.0250	-0.0158	0.0000	-0.0158	-0.0250	-0.0188	0.0180	0.1274
	0.350	0.1695	0.0150	-0.0281	-0.0332	-0.0204	0.0000	-0.0204	-0.0332	-0.0281	0.0150	0.1695
	0.400	0.2159	0.0073	-0.0392	-0.0421	-0.0252	0.0000	-0.0252	-0.0421	-0.0392	0.0073	0.2159
	0.450	0.2662	-0.0054	-0.0519	-0.0513	-0.0300	0.0000	-0.0300	-0.0513	-0.0519	-0.0054	0.2662

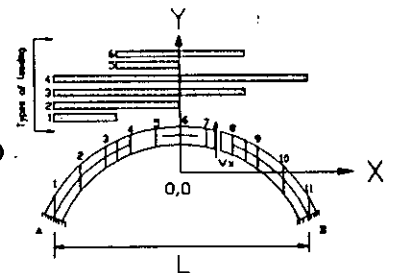
TABLE A.66
BENDING MOMENTS AT THE DIFFERENT SECTIONS (RISE-TO-SPAN RATIO = 0.050)
=TABLE COEFF.*(Q*L*L)



SECTION NUMBER

	N	1	2	3	4	5	6	7	8	9	10	11
TYPES OF LOAD- ING	1	-0.01310	0.00082	0.00581	0.00310	0.00018	-0.00171	-0.00257	-0.00239	-0.00118	0.00109	0.00443
	2	-0.01542	-0.00248	0.00560	0.00876	0.00692	0.00005	-0.00685	-0.00879	-0.00572	0.00242	0.01571
	3	-0.00413	-0.00115	0.00106	0.00236	0.00263	0.00182	-0.00011	-0.00313	-0.00592	-0.00088	0.01339
	4	0.00030	-0.00006	-0.00012	-0.00004	0.00006	0.00010	0.00006	-0.00004	-0.00012	-0.00006	0.00030
	5	-0.00232	-0.00330	-0.00020	0.00566	0.00675	0.00177	-0.00428	-0.00640	-0.00454	0.00133	0.01128
	6	0.00896	-0.00197	-0.00474	-0.00073	0.00246	0.00353	0.00246	-0.00073	-0.00474	-0.00197	0.00896

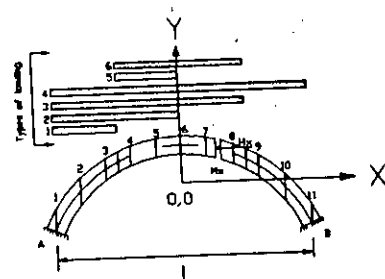
TABLE A.67
VERTICAL SHEAR FORCES AT THE DIFFERENT SECTIONS (RISE-TO-SPAN RATIO 0.050)
=TABLE COEFF.*(Q*L)



SECTION NUMBER

	N	1	2	3	4	5	6	7	8	9	10	11
TYPES OF LOAD- ING	1	0.23628	0.13628	0.03628	-0.01372	-0.01372	-0.01372	-0.01372	-0.01372	-0.01372	-0.01372	-0.01372
	2	0.40612	0.30612	0.20612	0.10612	0.00612	-0.09388	-0.09388	-0.09388	-0.09388	-0.09388	-0.09388
	3	0.48628	0.38628	0.28628	0.18628	0.08628	-0.01372	-0.11372	-0.21372	-0.26372	-0.26372	-0.26372
	4	0.50000	0.40000	0.30000	0.20000	0.10000	0.00000	-0.10000	-0.20000	-0.30000	-0.40000	-0.50000
	5	0.16985	0.16985	0.16985	0.11985	0.01985	-0.08015	-0.08015	-0.08015	-0.08015	-0.08015	-0.08015
	6	0.25000	0.25000	0.25000	0.20000	0.10000	0.00000	-0.10000	-0.20000	-0.25000	-0.25000	-0.25000

TABLE A.68
HORIZONTAL FORCES AT THE DIFFERENT SECTIONS (RISE-TO-SPAN RATIO 0.050)
=TABLE COEFF.*(Q*L)



SECTION NUMBER

	N	1	2	3	4	5	6	7	8	9	10	11
TYPES OF LOAD- ING	1	0.26001	0.26001	0.26001	0.26001	0.26001	0.26001	0.26001	0.26001	0.26001	0.26001	0.26001
	2	1.25184	1.25184	1.25184	1.25184	1.25184	1.25184	1.25184	1.25184	1.25184	1.25184	1.25184
	3	2.24375	2.24375	2.24375	2.24375	2.24375	2.24375	2.24375	2.24375	2.24375	2.24375	2.24375
	4	2.50401	2.50401	2.50401	2.50401	2.50401	2.50401	2.50401	2.50401	2.50401	2.50401	2.50401
	5	0.99178	0.99178	0.99178	0.99178	0.99178	0.99178	0.99178	0.99178	0.99178	0.99178	0.99178
	6	1.98361	1.98361	1.98361	1.98361	1.98361	1.98361	1.98361	1.98361	1.98361	1.98361	1.98361

TABLE A.69
BENDING MOMENTS AT THE DIFFERENT SECTIONS (RISE-TO-SPAN RATIO 0.100)
=TABLE COEFF.*(Q*L*L)

SECTION NUMBER

	N	1	2	3	4	5	6	7	8	9	10	11
TYPES OF LOAD- ING	1	-0.01284	0.00090	0.00582	0.00310	0.00018	-0.00172	-0.00260	-0.00246	-0.00126	0.00104	0.00452
	2	-0.01481	-0.00244	0.00555	0.00879	0.00706	0.00022	-0.00679	-0.00891	-0.00600	0.00216	0.01594
	3	-0.00338	-0.00133	0.00080	0.00234	0.00287	0.00215	0.00010	-0.00321	-0.00628	-0.00118	0.01398
	4	0.00114	-0.00029	-0.00046	-0.00011	0.00027	0.00043	0.00027	-0.00011	-0.00046	-0.00029	0.00114
	5	-0.00196	-0.00334	-0.00028	0.00570	0.00689	0.00194	-0.00419	-0.00645	-0.00474	0.00112	0.01142
	6	0.00946	-0.00223	-0.00502	-0.00075	0.00270	0.00387	0.00270	-0.00075	-0.00502	-0.00223	0.00946

TABLE A.70
 VERTICAL SHEAR FORCES AT THE DIFFERENT SECTIONS (RISE-TO-SPAN RATIO = 0.100)
 =TABLE COEFF.*(Q*L)

		SECTION NUMBER											
		N	1	2	3	4	5	6	7	8	9	10	11
TYPES OF LOAD- ING	1	0.23611	0.13611	0.03611	-0.01389	-0.01389	-0.01389	-0.01389	-0.01389	-0.01389	-0.01389	-0.01389	-0.01389
	2	0.40575	0.30575	0.20575	0.10575	0.00575	-0.09425	-0.09425	-0.09425	-0.09425	-0.09425	-0.09425	-0.09425
	3	0.48611	0.38611	0.28611	0.18611	0.08611	-0.01389	-0.11389	-0.21389	-0.26389	-0.26389	-0.26389	-0.26389
	4	0.50000	0.40000	0.30000	0.20000	0.10000	0.00000	-0.10000	-0.20000	-0.30000	-0.40000	-0.50000	-0.50000
	5	0.16963	0.16963	0.16963	0.11963	0.01963	-0.08037	-0.08037	-0.08037	-0.08037	-0.08037	-0.08037	-0.08037
	6	0.25000	0.25000	0.25000	0.20000	0.10000	0.00000	-0.10000	-0.20000	-0.25000	-0.25000	-0.25000	-0.25000

TABLE A.71
 HORIZONTAL FORCES AT THE DIFFERENT SECTIONS (RISE-TO-SPAN RATIO 0.100)
 =TABLE COEFF.*(Q*L)

		SECTION NUMBER											
		N	1	2	3	4	5	6	7	8	9	10	11
TYPES OF LOAD- ING	1	0.13183	0.13183	0.13183	0.13183	0.13183	0.13183	0.13183	0.13183	0.13183	0.13183	0.13183	0.13183
	2	0.62855	0.62855	0.62855	0.62855	0.62855	0.62855	0.62855	0.62855	0.62855	0.62855	0.62855	0.62855
	3	1.12527	1.12527	1.12527	1.12527	1.12527	1.12527	1.12527	1.12527	1.12527	1.12527	1.12527	1.12527
	4	1.25714	1.25714	1.25714	1.25714	1.25714	1.25714	1.25714	1.25714	1.25714	1.25714	1.25714	1.25714
	5	0.49671	0.49671	0.49671	0.49671	0.49671	0.49671	0.49671	0.49671	0.49671	0.49671	0.49671	0.49671
	6	0.99343	0.99343	0.99343	0.99343	0.99343	0.99343	0.99343	0.99343	0.99343	0.99343	0.99343	0.99343

TABLE A.72
 BENDING MOMENTS AT THE DIFFERENT SECTIONS (RISE-TO-SPAN RATIO = 0.150)
 =TABLE COEFF.*(Q*L*L)

		SECTION NUMBER											
		N	1	2	3	4	5	6	7	8	9	10	11
TYPES OF LOAD- ING	1	-0.01242	0.00103	0.00585	0.00310	0.00018	-0.00173	-0.00265	-0.00256	-0.00140	0.00095	0.00468	0.00468
	2	-0.01379	-0.00240	0.00546	0.00887	0.00730	0.00049	-0.00667	-0.00908	-0.00647	0.00170	0.01634	0.01634
	3	-0.00212	-0.00165	0.00038	0.00234	0.00328	0.00271	0.00045	-0.00332	-0.00686	-0.00173	0.01497	0.01497
	4	0.00255	-0.00070	-0.00101	-0.00021	0.00063	0.00097	0.00063	-0.00021	-0.00101	-0.00070	0.00255	0.00255
	5	-0.00137	-0.00343	-0.00039	0.00576	0.00712	0.00222	-0.00402	-0.00652	-0.00507	0.00075	0.01166	0.01166
	6	0.01029	-0.00268	-0.00547	-0.00076	0.00310	0.00444	0.00310	-0.00076	-0.00547	-0.00268	0.01029	0.01029

TABLE A.73
 VERTICAL SHEAR FORCES AT THE DIFFERENT SECTIONS (RISE-TO-SPAN RATIO = 0.150)
 =TABLE COEFF.*(Q*L)

		SECTION NUMBER											
		N	1	2	3	4	5	6	7	8	9	10	11
TYPES OF LOAD- ING	1	0.23584	0.13584	0.03584	-0.01416	-0.01416	-0.01416	-0.01416	-0.01416	-0.01416	-0.01416	-0.01416	-0.01416
	2	0.40512	0.30512	0.20512	0.10512	0.00512	-0.09488	-0.09488	-0.09488	-0.09488	-0.09488	-0.09488	-0.09488
	3	0.48584	0.38584	0.28584	0.18584	0.08584	-0.01416	-0.11416	-0.21416	-0.26416	-0.26416	-0.26416	-0.26416
	4	0.50000	0.40000	0.30000	0.20000	0.10000	0.00000	-0.10000	-0.20000	-0.30000	-0.40000	-0.50000	-0.50000
	5	0.16928	0.16928	0.16928	0.11928	0.01928	-0.08072	-0.08072	-0.08072	-0.08072	-0.08072	-0.08072	-0.08072
	6	0.25000	0.25000	0.25000	0.20000	0.10000	0.00000	-0.10000	-0.20000	-0.25000	-0.25000	-0.25000	-0.25000

TABLE A.74
 HORIZONTAL FORCES AT THE DIFFERENT SECTIONS (RISE-TO-SPAN RATIO = 0.150)
 =TABLE COEFF.*(Q*L)

		SECTION NUMBER											
		N	1	2	3	4	5	6	7	8	9	10	11
TYPES OF LOAD- ING	1	0.08991	0.08991	0.08991	0.08991	0.08991	0.08991	0.08991	0.08991	0.08991	0.08991	0.08991	0.08991
	2	0.42192	0.42192	0.42192	0.42192	0.42192	0.42192	0.42192	0.42192	0.42192	0.42192	0.42192	0.42192
	3	0.75393	0.75393	0.75393	0.75393	0.75393	0.75393	0.75393	0.75393	0.75393	0.75393	0.75393	0.75393
	4	0.84385	0.84385	0.84385	0.84385	0.84385	0.84385	0.84385	0.84385	0.84385	0.84385	0.84385	0.84385
	5	0.33201	0.33201	0.33201	0.33201	0.33201	0.33201	0.33201	0.33201	0.33201	0.33201	0.33201	0.33201
	6	0.66402	0.66402	0.66402	0.66402	0.66402	0.66402	0.66402	0.66402	0.66402	0.66402	0.66402	0.66402

TABLE A.75
 BENDING MOMENTS AT THE DIFFERENT SECTIONS (RISE-TO-SPAN RATIO = 0.200)
 =TABLE COEFF.*(Q*L*L)

		SECTION NUMBER											
		N	1	2	3	4	5	6	7	8	9	10	11
TYPES OF LOAD- ING	1	-0.01181	0.00120	0.00589	0.00312	0.00019	-0.00174	-0.00272	-0.00270	-0.00159	0.00081	0.00489	0.00489
	2	-0.01237	-0.00239	0.00535	0.00901	0.00766	0.00087	-0.00649	-0.00929	-0.00710	0.00101	0.01688	0.01688
	3	-0.00039	-0.00219	-0.00016	0.00241	0.00389	0.00349	0.00098	-0.00341	-0.00764	-0.00258	0.01631	0.01631
	4	0.00451	-0.00139	-0.00174	-0.00028	0.00117	0.00175	0.00117	-0.00028	-0.00174	-0.00139	0.00451	0.00451
	5	-0.00056	-0.00359	-0.00054	0.00588	0.00747	0.00262	-0.00377	-0.00660	-0.00551	0.00020	0.01198	0.01198
	6	0.01142	-0.00339	-0.00605	-0.00071	0.00369	0.00523	0.00369	-0.00071	-0.00605	-0.00339	0.01142	0.01142

TABLE A.76
 VERTICAL SHEAR FORCES AT THE DIFFERENT SECTIONS (RISE-TO-SPAN RATIO = 0.200)
 =TABLE COEFF.*(Q*L)

		SECTION NUMBER											
		N	1	2	3	4	5	6	7	8	9	10	11
TYPES OF LOAD- ING	1	0.23545	0.13545	0.03545	-0.01455	-0.01455	-0.01455	-0.01455	-0.01455	-0.01455	-0.01455	-0.01455	-0.01455
	2	0.40425	0.30425	0.20425	0.10425	0.00425	-0.09575	-0.09575	-0.09575	-0.09575	-0.09575	-0.09575	-0.09575
	3	0.48545	0.38545	0.28545	0.18545	0.08545	-0.01455	-0.11455	-0.21455	-0.26455	-0.26455	-0.26455	-0.26455
	4	0.50000	0.40000	0.30000	0.20000	0.10000	0.00000	-0.10000	-0.20000	-0.30000	-0.40000	-0.50000	-0.50000
	5	0.16880	0.16880	0.16880	0.11880	0.01880	-0.08120	-0.08120	-0.08120	-0.08120	-0.08120	-0.08120	-0.08120
	6	0.25000	0.25000	0.25000	0.20000	0.10000	0.00000	-0.10000	-0.20000	-0.25000	-0.25000	-0.25000	-0.25000

TABLE A.77
 HORIZONTAL FORCES AT THE DIFFERENT SECTIONS (RISE-TO-SPAN RATIO = 0.200)
 =TABLE COEFF.*(Q*L)

		SECTION NUMBER											
		N	1	2	3	4	5	6	7	8	9	10	11
TYPES OF LOAD- ING	1	0.06955	0.06955	0.06955	0.06955	0.06955	0.06955	0.06955	0.06955	0.06955	0.06955	0.06955	0.06955
	2	0.31940	0.31940	0.31940	0.31940	0.31940	0.31940	0.31940	0.31940	0.31940	0.31940	0.31940	0.31940
	3	0.56925	0.56925	0.56925	0.56925	0.56925	0.56925	0.56925	0.56925	0.56925	0.56925	0.56925	0.56925
	4	0.63881	0.63881	0.63881	0.63881	0.63881	0.63881	0.63881	0.63881	0.63881	0.63881	0.63881	0.63881
	5	0.24985	0.24985	0.24985	0.24985	0.24985	0.24985	0.24985	0.24985	0.24985	0.24985	0.24985	0.24985
	6	0.49969	0.49969	0.49969	0.49969	0.49969	0.49969	0.49969	0.49969	0.49969	0.49969	0.49969	0.49969

TABLE A.78
 BENDING MOMENTS AT THE DIFFERENT SECTIONS (RISE-TO-SPAN RATIO 0.250)
 =TABLE COEFF.*(Q*L*L)

		SECTION NUMBER											
		N	1	2	3	4	5	6	7	8	9	10	11
TYPES OF LOAD- ING	1	-0.01101	0.00140	0.00596	0.00317	0.00023	-0.00175	-0.00279	-0.00286	-0.00184	0.00059	0.00517	0.00517
	2	-0.01057	-0.00245	0.00527	0.00925	0.00815	0.00138	-0.00623	-0.00950	-0.00786	0.00004	0.01756	0.01756
	3	0.00182	-0.00300	-0.00076	0.00261	0.00471	0.00450	0.00169	-0.00343	-0.00855	-0.00381	0.01800	0.01800
	4	0.00699	-0.00241	-0.00259	-0.00026	0.00192	0.00275	0.00192	-0.00026	-0.00259	-0.00241	0.00699	0.00699
	5	0.00044	-0.00386	-0.00069	0.00608	0.00792	0.00312	-0.00344	-0.00664	-0.00602	-0.00055	0.01239	0.01239
	6	0.01283	-0.00440	-0.00672	-0.00056	0.00448	0.00625	0.00448	-0.00056	-0.00672	-0.00440	0.01283	0.01283

TABLE A.79
 VERTICAL SHEAR FORCES AT THE DIFFERENT SECTIONS (RISE-TO-SPAN RATIO = 0.250)
 =TABLE COEFF.*(Q*L)

		SECTION NUMBER										
N		1	2	3	4	5	6	7	8	9	10	11
TYPES OF LOAD- ING	1	0.23492	0.13492	0.03492	-0.01508	-0.01508	-0.01508	-0.01508	-0.01508	-0.01508	-0.01508	-0.01508
	2	0.40312	0.30312	0.20312	0.10312	0.00312	-0.09688	-0.09688	-0.09688	-0.09688	-0.09688	-0.09688
	3	0.48492	0.38492	0.28492	0.18492	0.08492	-0.01508	-0.11508	-0.21508	-0.26508	-0.26508	-0.26508
	4	0.50000	0.40000	0.30000	0.20000	0.10000	0.00000	-0.10000	-0.20000	-0.30000	-0.40000	-0.50000
	5	0.16820	0.16820	0.16820	0.11820	0.01820	-0.08180	-0.08180	-0.08180	-0.08180	-0.08180	-0.08180
	6	0.25000	0.25000	0.25000	0.20000	0.10000	0.00000	-0.10000	-0.20000	-0.25000	-0.25000	-0.25000

TABLE A.80
 HORIZONTAL FORCES AT THE DIFFERENT SECTIONS (RISE-TO-SPAN RATIO 0.250)
 =TABLE COEFF.*(Q*L)

		SECTION NUMBER										
N		1	2	3	4	5	6	7	8	9	10	11
TYPES OF LOAD- ING	1	0.05782	0.05782	0.05782	0.05782	0.05782	0.05782	0.05782	0.05782	0.05782	0.05782	0.05782
	2	0.25847	0.25847	0.25847	0.25847	0.25847	0.25847	0.25847	0.25847	0.25847	0.25847	0.25847
	3	0.45913	0.45913	0.45913	0.45913	0.45913	0.45913	0.45913	0.45913	0.45913	0.45913	0.45913
	4	0.51695	0.51695	0.51695	0.51695	0.51695	0.51695	0.51695	0.51695	0.51695	0.51695	0.51695
	5	0.20065	0.20065	0.20065	0.20065	0.20065	0.20065	0.20065	0.20065	0.20065	0.20065	0.20065
	6	0.40131	0.40131	0.40131	0.40131	0.40131	0.40131	0.40131	0.40131	0.40131	0.40131	0.40131

TABLE A.81
 BENDING MOMENTS AT THE DIFFERENT SECTIONS (RISE-TO-SPAN RATIO = 0.300)
 =TABLE COEFF.*(Q*L*L)

		SECTION NUMBER										
N		1	2	3	4	5	6	7	8	9	10	11
TYPES OF LOAD- ING	1	-0.01001	0.00163	0.00606	0.00324	0.00028	-0.00174	-0.00287	-0.00305	-0.00214	0.00029	0.00550
	2	-0.00838	-0.00262	0.00524	0.00961	0.00877	0.00200	-0.00588	-0.00969	-0.00872	-0.00122	0.01836
	3	0.00448	-0.00412	-0.00134	0.00298	0.00576	0.00575	0.00261	-0.00332	-0.00954	-0.00547	0.01999
	4	0.00998	-0.00384	-0.00348	-0.00007	0.00289	0.00400	0.00289	-0.00007	-0.00348	-0.00384	0.00998
	5	0.00162	-0.00425	-0.00082	0.00637	0.00849	0.00374	-0.00301	-0.00663	-0.00658	-0.00151	0.01286
	6	0.01449	-0.00576	-0.00740	-0.00026	0.00548	0.00749	0.00548	-0.00026	-0.00740	-0.00576	0.01449

TABLE A.82
 VERTICAL SHEAR FORCES AT THE DIFFERENT SECTIONS (RISE-TO-SPAN RATIO 0.300)
 =TABLE COEFF.*(Q*L)

		SECTION NUMBER										
N		1	2	3	4	5	6	7	8	9	10	11
TYPES OF LOAD- ING	1	0.23426	0.13426	0.03426	-0.01574	-0.01574	-0.01574	-0.01574	-0.01574	-0.01574	-0.01574	-0.01574
	2	0.40175	0.30175	0.20175	0.10175	0.00175	-0.09825	-0.09825	-0.09825	-0.09825	-0.09825	-0.09825
	3	0.48426	0.38426	0.28426	0.18426	0.08426	-0.01574	-0.11574	-0.21574	-0.26574	-0.26574	-0.26574
	4	0.50000	0.40000	0.30000	0.20000	0.10000	0.00000	-0.10000	-0.20000	-0.30000	-0.40000	-0.50000
	5	0.16749	0.16749	0.16749	0.11749	0.01749	-0.08251	-0.08251	-0.08251	-0.08251	-0.08251	-0.08251
	6	0.25000	0.25000	0.25000	0.20000	0.10000	0.00000	-0.10000	-0.20000	-0.25000	-0.25000	-0.25000

TABLE A.83
 HORIZONTAL FORCES AT THE DIFFERENT SECTIONS (RISE-TO-SPAN RATIO 0.300)
 =TABLE COEFF.*(Q*L)

		SECTION NUMBER										
N		1	2	3	4	5	6	7	8	9	10	11
TYPES OF LOAD- ING	1	0.05038	0.05038	0.05038	0.05038	0.05038	0.05038	0.05038	0.05038	0.05038	0.05038	0.05038
	2	0.21829	0.21829	0.21829	0.21829	0.21829	0.21829	0.21829	0.21829	0.21829	0.21829	0.21829
	3	0.38620	0.38620	0.38620	0.38620	0.38620	0.38620	0.38620	0.38620	0.38620	0.38620	0.38620
	4	0.43659	0.43659	0.43659	0.43659	0.43659	0.43659	0.43659	0.43659	0.43659	0.43659	0.43659
	5	0.16791	0.16791	0.16791	0.16791	0.16791	0.16791	0.16791	0.16791	0.16791	0.16791	0.16791
	6	0.33582	0.33582	0.33582	0.33582	0.33582	0.33582	0.33582	0.33582	0.33582	0.33582	0.33582

TABLE A.84
 BENDING MOMENTS AT THE DIFFERENT SECTIONS (RISE-TO-SPAN RATIO 0.350)
 =TABLE COEFF.*(Q*L*L)

		SECTION NUMBER										
N		1	2	3	4	5	6	7	8	9	10	11
TYPESM OF LOAD- ING	1	-0.00880	0.00188	0.00621	0.00337	0.00037	-0.00172	-0.00294	-0.00326	-0.00248	-0.00012	0.00589
	2	-0.00584	-0.00289	0.00531	0.01014	0.00954	0.00275	-0.00543	-0.00981	-0.00961	-0.00278	0.01930
	3	0.00757	-0.00555	-0.00182	0.00359	0.00705	0.00723	0.00374	-0.00304	-0.01051	-0.00755	0.02226
	4	0.01346	-0.00567	-0.00431	0.00033	0.00411	0.00551	0.00411	0.00033	-0.00431	-0.00567	0.01346
	5	0.00296	-0.00477	-0.00090	0.00677	0.00917	0.00447	-0.00249	-0.00655	-0.00713	-0.00266	0.01341
	6	0.01637	-0.00743	-0.00803	0.00022	0.00668	0.00894	0.00668	0.00022	-0.00803	-0.00743	0.01637

TABLE A.85
 VERTICAL SHEAR FORCES AT THE DIFFERENT SECTIONS (RISE-TO-SPAN RATIO 0.350)
 =TABLE COEFF.*(Q*L)

		SECTION NUMBER										
N		1	2	3	4	5	6	7	8	9	10	11
TYPES OF LOAD- ING	1	0.23344	0.13344	0.03344	-0.01656	-0.01656	-0.01656	-0.01656	-0.01656	-0.01656	-0.01656	-0.01656
	2	0.40013	0.30013	0.20013	0.10013	0.00013	-0.09987	-0.09987	-0.09987	-0.09987	-0.09987	-0.09987
	3	0.48344	0.38344	0.28344	0.18344	0.08344	-0.01656	-0.11656	-0.21656	-0.26656	-0.26656	-0.26656
	4	0.50000	0.40000	0.30000	0.20000	0.10000	0.00000	-0.10000	-0.20000	-0.30000	-0.40000	-0.50000
	5	0.16669	0.16669	0.16669	0.11669	0.01669	-0.08331	-0.08331	-0.08331	-0.08331	-0.08331	-0.08331
	6	0.25000	0.25000	0.25000	0.20000	0.10000	0.00000	-0.10000	-0.20000	-0.25000	-0.25000	-0.25000

TABLE A.86
 HORIZONTAL FORCES AT THE DIFFERENT SECTIONS (RISE-TO-SPAN RATIO 0.350)
 =TABLE COEFF.*(Q*L)

		SECTION NUMBER										
N		1	2	3	4	5	6	7	8	9	10	11
TYPES OF LOAD- ING	1	0.04540	0.04540	0.04540	0.04540	0.04540	0.04540	0.04540	0.04540	0.04540	0.04540	0.04540
	2	0.18993	0.18993	0.18993	0.18993	0.18993	0.18993	0.18993	0.18993	0.18993	0.18993	0.18993
	3	0.33446	0.33446	0.33446	0.33446	0.33446	0.33446	0.33446	0.33446	0.33446	0.33446	0.33446
	4	0.37986	0.37986	0.37986	0.37986	0.37986	0.37986	0.37986	0.37986	0.37986	0.37986	0.37986
	5	0.14453	0.14453	0.14453	0.14453	0.14453	0.14453	0.14453	0.14453	0.14453	0.14453	0.14453
	6	0.28907	0.28907	0.28907	0.28907	0.28907	0.28907	0.28907	0.28907	0.28907	0.28907	0.28907

TABLE A.87
 BENDING MOMENTS AT THE DIFFERENT SECTIONS (RISE-TO-SPAN RATIO 0.400)
 =TABLE COEFF.*(Q*L*L)

		SECTION NUMBER										
N		1	2	3	4	5	6	7	8	9	10	11
TYPES OF LOAD- ING	1	-0.00737	0.00216	0.00642	0.00355	0.00050	-0.00166	-0.00301	-0.00347	-0.00286	-0.00063	0.00633
	2	-0.00293	-0.00322	0.00554	0.01085	0.01047	0.00364	-0.00487	-0.00984	-0.01050	-0.00460	0.02034
	3	0.01108	-0.00720	-0.00210	0.00447	0.00861	0.00894	0.00510	-0.00255	-0.01138	-0.00999	0.02478
	4	0.01741	-0.00783	-0.00496	0.00100	0.00560	0.00727	0.00560	0.00100	-0.00496	-0.00783	0.01741
	5	0.00443	-0.00538	-0.00088	0.00730	0.00997	0.00530	-0.00186	-0.00637	-0.00764	-0.00397	0.01401
	6	0.01845	-0.00936	-0.00852	0.00092	0.00810	0.01060	0.00810	0.00092	-0.00852	-0.00936	0.01845

TABLE A.88
 VERTICAL SHEAR FORCES AT THE DIFFERENT SECTIONS (RISE-TO-SPAN RATIO 0.400)
 =TABLE COEFF.*(Q*L)

		SECTION NUMBER												
		N	1	2	3	4	5	6	7	8	9	10	11	
TYPES OF LOAD- ING		1	0.23245	0.13245	0.03245	-0.01755	-0.01755	-0.01755	-0.01755	-0.01755	-0.01755	-0.01755	-0.01755	-0.01755
		2	0.39828	0.29828	0.19828	0.09828	-0.00172	-0.10172	-0.10172	-0.10172	-0.10172	-0.10172	-0.10172	-0.10172
		3	0.48245	0.38245	0.28245	0.18245	0.08245	-0.01755	-0.11755	-0.21755	-0.26755	-0.26755	-0.26755	-0.26755
		4	0.50000	0.40000	0.30000	0.20000	0.10000	0.00000	-0.10000	-0.20000	-0.30000	-0.40000	-0.50000	-0.50000
		5	0.16583	0.16583	0.16583	0.11583	0.01583	-0.08417	-0.08417	-0.08417	-0.08417	-0.08417	-0.08417	-0.08417
		6	0.25000	0.25000	0.25000	0.20000	0.10000	0.00000	-0.10000	-0.20000	-0.25000	-0.25000	-0.25000	-0.25000

TABLE A.89
 HORIZONTAL FORCES AT THE DIFFERENT SECTIONS (RISE-TO-SPAN RATIO = 0.400)
 =TABLE COEFF.*(Q*L)

		SECTION NUMBER											
		N	1	2	3	4	5	6	7	8	9	10	11
TYPES OF LOAD- ING		1	0.04193	0.04193	0.04193	0.04193	0.04193	0.04193	0.04193	0.04193	0.04193	0.04193	0.04193
		2	0.16892	0.16892	0.16892	0.16892	0.16892	0.16892	0.16892	0.16892	0.16892	0.16892	0.16892
		3	0.29591	0.29591	0.29591	0.29591	0.29591	0.29591	0.29591	0.29591	0.29591	0.29591	0.29591
		4	0.33784	0.33784	0.33784	0.33784	0.33784	0.33784	0.33784	0.33784	0.33784	0.33784	0.33784
		5	0.12699	0.12699	0.12699	0.12699	0.12699	0.12699	0.12699	0.12699	0.12699	0.12699	0.12699
		6	0.25398	0.25398	0.25398	0.25398	0.25398	0.25398	0.25398	0.25398	0.25398	0.25398	0.25398

TABLE A.90
 BENDING MOMENTS AT THE DIFFERENT SECTIONS (RISE-TO-SPAN RATIO = 0.450)
 =TABLE COEFF.*(Q*L*L)

		SECTION NUMBER											
		N	1	2	3	4	5	6	7	8	9	10	11
TYPES OF LOAD- ING		1	-0.00572	0.00248	0.00671	0.00380	0.00069	-0.00157	-0.00305	-0.00368	-0.00327	-0.00124	0.00683
		2	0.00031	-0.00355	0.00597	0.01175	0.01157	0.00465	-0.00419	-0.00977	-0.01131	-0.00659	0.02150
		3	0.01498	-0.00890	-0.00208	0.00566	0.01043	0.01088	0.00669	-0.00182	-0.01205	-0.01262	0.02753
		4	0.02181	-0.01014	-0.00535	0.00199	0.00738	0.00931	0.00738	0.00199	-0.00535	-0.01014	0.02181
		5	0.00602	-0.00602	-0.00074	0.00795	0.01088	0.00623	-0.00114	-0.00609	-0.00805	-0.00535	0.01467
		6	0.02070	-0.01138	-0.00878	0.00186	0.00973	0.01246	0.00973	0.00186	-0.00878	-0.01138	0.02070

TABLE A.104
 AXIAL THRUSTS AT THE DIFFERENT SECTIONS FOR UNIT OUTWARD HORIZONTAL DISPLACEMENT AT THE LEFT SUPPORT
 =TABLE COEFF.*(E*I/L/L/L)

RISE-TO-SPAN RATIO	SECTION NUMBER										
	(1)	(2)	(3)	(4)	(5)	(6)	(7)	(8)	(9)	(10)	(11)
.050	-4377.589	-4409.631	-4434.392	-4451.994	-4462.522	-4466.025	-4462.522	-4451.994	-4434.392	-4409.631	-4377.589
.100	-1007.930	-1038.951	-1062.452	-1078.925	-1088.689	-1091.925	-1088.689	-1078.925	-1062.452	-1038.951	-1007.930
.150	-390.981	-420.464	-442.038	-456.825	-465.472	-468.318	-465.472	-456.825	-442.038	-420.464	-390.981
.200	-181.995	-209.613	-228.801	-241.575	-248.924	-251.327	-248.924	-241.575	-228.801	-209.613	-181.995
.250	-91.237	-116.840	-133.398	-144.065	-150.102	-152.061	-150.102	-144.065	-133.398	-116.840	-91.237
.300	-46.657	-70.228	-84.112	-92.765	-97.589	-99.145	-97.589	-92.765	-84.112	-70.228	-46.657
.350	-23.298	-44.892	-56.218	-63.076	-66.853	-68.066	-66.853	-63.076	-56.218	-44.892	-23.298
.400	-10.658	-30.354	-39.365	-44.703	-47.620	-48.553	-47.620	-44.703	-39.365	-30.354	-10.658
.450	-3.746	-21.623	-28.640	-32.745	-34.977	-35.690	-34.977	-32.745	-28.640	-21.623	-3.746

TABLE A.105
 SHEAR FORCES ALONG THE DIFFERENT RADIAL SECTIONS FOR UNIT OUTWARD HORIZONTAL DISPLACEMENT AT THE LEFT SUPPORT
 =TABLE COEFF.*(E*I/L/L/L)

RISE-TO-SPAN RATIO	SECTION NUMBER										
	(1)	(2)	(3)	(4)	(5)	(6)	(7)	(8)	(9)	(10)	(11)
.050	884.361	707.489	530.617	353.745	176.872	.000	176.872	353.745	530.617	707.489	884.361
.100	419.971	335.977	251.983	167.988	83.994	.000	83.994	167.988	251.983	335.977	419.971
.150	257.790	206.232	154.674	103.116	51.558	.000	51.558	103.116	154.674	206.232	257.790
.200	173.329	138.663	103.997	69.332	34.666	.000	34.666	69.332	103.997	138.663	173.329
.250	121.649	97.319	72.989	48.660	24.330	.000	24.330	48.660	72.989	97.319	121.649
.300	87.481	69.985	52.489	34.993	17.496	.000	17.496	34.993	52.489	69.985	87.481
.350	63.955	51.164	38.373	25.582	12.791	.000	12.791	25.582	38.373	51.164	63.955
.400	47.369	37.895	28.421	18.948	9.474	.000	9.474	18.948	28.421	37.895	47.369
.450	35.493	28.394	21.296	14.197	7.099	.000	7.099	14.197	21.296	28.394	35.493

**A.2 Detail analysis for particular live load and permissible
load capacity**

A.2.1 Analysis due to clockwise rotation

A.2.2 Analysis due to counter clockwise rotation

A.2.1 Analysis due to clockwise rotation

SPAN(L)=15.000 FT
 RISE-TO-SPAN RATIO(H/L)= .250
 RADIAL THICKNESS(T)= .833 FT
 FILL DEPTH ABOVE THE CROWN=1.000 FT
 DENSITY OF FILL OVER THE ARCH= 110.00 #/FT/FT/FT
 DENSITY OF THE MASONRY UNITS= 110.00 #/FT/FT/FT
 MODULOUS OF ELASTICITY=432000000.00 PSF

 CALCULATION FOR DEAD LOAD

BENDING MOMENT AT THE LEFT SUPPORT 20.475 #-FT
 VERTICAL REACTION AT THE LEFT SUPPORT 2553.107 #
 HORIZONTAL THRUST AT THE LEFT SUPPORT 2017.498 #
 AXIAL THRUST AT THE LEFT SUPPORT 3252.985 #
 RADIAL SHEAR FORCE AT THE LEFT SUPPORT 82.1343 #

INTERNAL FORCES

	SECTION NUMBER										
	(1)	(2)	(3)	(4)	(5)	(6)	(7)	(8)	(9)	(10)	(11)
BENDING MOMENTS (#-FT)	20.48	-5.54	25.91	14.22	-15.21	-29.34	-15.21	14.22	25.91	-5.54	20.48
VERTICAL SHEAR FORCES (#)	2553.11	1709.74	1110.01	663.45	309.66	.00	-309.66	-663.45	-1110.01	-1709.74	-2553.11
HORIZONTAL THRUSTS (#)	2017.50	2017.50	2017.50	2017.50	2017.50	2017.50	2017.50	2017.50	2017.50	2017.50	2017.50
AXIAL THRUSTS (#)	3252.99	2644.43	2302.69	2123.72	2041.05	2017.50	2041.05	2123.72	2302.69	2644.43	3252.99
RADIAL SHEAR FORCES (#)	82.13	-22.52	-5.38	17.03	17.13	.00	-17.13	-17.03	5.38	22.52	-82.13

STRESSES AT THE DIFFERENT RADIAL PLANES

	SECTION NUMBER										
	(1)	(2)	(3)	(4)	(5)	(6)	(7)	(8)	(9)	(10)	(11)
MAXIMUM STRESSES (+VE COMP.) (PSI)	28.349	22.378	20.753	18.559	17.929	18.581	17.929	18.559	20.753	22.378	28.349
MINIMUM STRESSES (+VE COMP.) (PSI)	25.890	21.713	17.641	16.851	16.103	15.058	16.103	16.851	17.641	21.713	25.890
SHEARING STRESSES (PSI)	.6847	.1878	.0448	.1420	.1428	.0000	.1428	.1420	.0448	.1878	.6847

4 CALCULATION FOR SUPPORT DISPLACEMENTS

ROTATION (CLOCK-WISE) AT THE LEFT SUPPORT .00000500 RADIAN
VERTICAL DIPLACEMENT(DOWNWARD) AT THE LEFT SUPPORT .00000000 FT
HORIZONTAL DIPLACEMENT(OUTWARD) AT THE LEFT SUPPORT .00000000 FT

BENDING MOMENT AT THE LEFT SUPPORT 50.3006 (#-FT)
VERTICAL REACTION AT THE LEFT SUPPORT -2.117 (#)
HORIZONTAL THRUSTS AT THE LEFT SUPPORT 11.546 (#)

INTERNAL FORCES

	SECTION NUMBER										
	(1)	(2)	(3)	(4)	(5)	(6)	(7)	(8)	(9)	(10)	(11)
BENDING MOMENTS (#-FT)	50.301	28.900	13.937	3.168	-4.305	-8.875	-10.656	-9.535	-5.118	3.493	18.543
VERTICAL SHEAR FORCES (#)	-2.12	-2.12	-2.12	-2.12	-2.12	-2.12	-2.12	-2.12	-2.12	-2.12	-2.12
HORIZONTAL THRUSTS (#)	11.55	11.55	11.55	11.55	11.55	11.55	11.55	11.55	11.55	11.55	11.55
AXIAL THRUSTS (#)	5.23	7.52	9.11	10.26	11.06	11.55	11.74	11.62	11.14	10.23	8.62
RADIAL SHEAR FORCES (#)	-10.51	-9.02	-7.40	-5.70	-3.94	-2.12	.24	-1.69	-3.68	-5.76	-7.97

STRESSES AT THE DIFFERENT RADIAL PLANES

	SECTION NUMBER										
	(1)	(2)	(3)	(4)	(5)	(6)	(7)	(8)	(9)	(10)	(11)
MAXIMUM STRESSES (+VE COMP.) (PSI)	3.064	1.798	.913	.276	.351	.629	.738	.669	.400	.295	1.185
MINIMUM STRESSES (+VE COMP.) (PSI)	-2.977	-1.673	-.761	-.105	-.166	-.437	-.542	-.476	-.214	-.125	-1.042
SHEARING STRESSES (PSI)	.0876	.0752	.0617	.0475	.0328	.0177	.0020	.0141	.0307	.0480	.0664

CALCULATION FOR LIVE LOAD

CONCENTRATED LIVE LOAD 500.00 #

BENDING MOMENTS AT THE DIFFERENT SECTIONS
(#-FT)

POSITION OF LOAD	SECTION NUMBER										
	(1)	(2)	(3)	(4)	(5)	(6)	(7)	(8)	(9)	(10)	(11)
1	-22.135	1.133	12.547	10.068	1.770	-3.892	-7.021	-7.513	-5.012	1.298	13.457
2	-48.314	2.210	27.402	22.710	4.159	-8.532	-15.569	-16.720	-11.189	2.845	29.933
3	-95.406	-2.327	59.402	62.626	17.245	-18.619	-39.169	-43.782	-30.297	6.216	78.080
4	-69.364	-48.630	53.117	128.086	79.143	-12.822	-69.695	-90.045	-68.923	4.968	159.870
5	43.459	-67.871	-43.040	70.483	174.165	70.498	-53.731	-116.574	-109.713	-14.161	217.554
6	175.651	-48.694	-109.483	-63.736	65.738	189.405	65.738	-63.736	-109.483	-48.694	175.651

VERTICAL SHEAR FORCES AT THE DIFFERENT SECTIONS
(#)

POSITION OF LOAD	SECTION NUMBER										
	(1)	(2)	(3)	(4)	(5)	(6)	(7)	(8)	(9)	(10)	(11)
1	32.449	20.647	8.846	-2.930	-2.930	-2.930	-2.930	-2.930	-2.930	-2.930	-2.930
2	71.113	45.522	19.931	-5.660	-6.576	-6.576	-6.576	-6.576	-6.576	-6.576	-6.576
3	133.048	111.476	57.122	2.767	-18.805	-18.805	-18.805	-18.805	-18.805	-18.805	-18.805
4	166.704	166.704	166.704	58.546	-49.613	-49.613	-49.613	-49.613	-49.613	-49.613	-49.613
5	182.737	182.737	182.737	182.737	40.128	-102.480	-102.480	-102.480	-102.480	-102.480	-102.480
6	159.091	159.091	159.091	159.091	159.091	.000	-159.091	-159.091	-159.091	-159.091	-159.091

HORIZONTAL THRUSTS AT THE DIFFERENT SECTIONS
(#)

POSITION OF LOAD	SECTION NUMBER										
	(1)	(2)	(3)	(4)	(5)	(6)	(7)	(8)	(9)	(10)	(11)
1	10.487	10.487	10.487	10.487	10.487	10.487	10.487	10.487	10.487	10.487	10.487
2	23.409	23.409	23.409	23.409	23.409	23.409	23.409	23.409	23.409	23.409	23.409
3	63.396	63.396	63.396	63.396	63.396	63.396	63.396	63.396	63.396	63.396	63.396
4	145.277	145.277	145.277	145.277	145.277	145.277	145.277	145.277	145.277	145.277	145.277
5	244.176	244.176	244.176	244.176	244.176	244.176	244.176	244.176	244.176	244.176	244.176
6	293.302	293.302	293.302	293.302	293.302	293.302	293.302	293.302	293.302	293.302	293.302

SHEAR FORCES ALONG THE DIFFERENT RADIAL PLANES
(#)

POSITION OF LOAD	SECTION NUMBER										
	(1)	(2)	(3)	(4)	(5)	(6)	(7)	(8)	(9)	(10)	(11)
1	32.251	21.272	13.446	8.998	9.883	10.487	10.821	10.873	10.606	9.933	8.636
2	70.936	47.121	30.103	20.367	22.055	23.409	24.160	24.282	23.692	22.196	19.306
3	144.476	120.057	83.034	60.948	59.571	63.396	65.588	66.080	64.642	60.747	53.082
4	220.529	218.318	207.465	156.373	135.467	145.277	151.343	153.514	151.261	143.379	126.856
5	292.695	304.570	301.921	289.812	247.451	244.176	257.427	264.130	263.398	253.206	228.490
6	303.254	327.184	333.668	328.789	314.978	293.302	314.978	328.789	333.668	327.184	303.254

SHEAR FORCES ALONG THE DIFFERENT RADIAL PLANES
(#)

POSITION OF LOAD	SECTION NUMBER										
	(1)	(2)	(3)	(4)	(5)	(6)	(7)	(8)	(9)	(10)	(11)
1	3290.470	2673.219	2325.250	2142.978	2061.994	2039.531	2063.610	2146.208	2324.443	2664.590	3270.243
2	3329.154	2699.068	2341.908	2154.347	2074.167	2052.453	2076.949	2159.617	2337.530	2676.852	3280.912
3	3402.695	2772.003	2394.839	2194.928	2111.682	2092.440	2118.377	2201.415	2378.479	2715.404	3314.688
4	3478.748	2870.264	2519.270	2290.352	2187.579	2174.321	2204.133	2288.849	2465.098	2798.036	3388.463
5	3550.914	2956.517	2613.726	2423.792	2299.562	2273.220	2310.216	2399.465	2577.235	2907.863	3490.096
6	3561.473	2979.131	2645.473	2462.769	2367.090	2322.346	2367.767	2464.124	2647.506	2981.841	3564.860

AXIAL THRUSTS AT THE DIFFERENT SECTIONS
(#)

POSITION OF LOAD	SECTION NUMBER										
	(1)	(2)	(3)	(4)	(5)	(6)	(7)	(8)	(9)	(10)	(11)
1	-81.562	22.661	.704	-28.864	-25.633	-5.047	-15.668	-19.300	-.771	12.301	-96.732
2	-68.701	33.504	4.226	-35.585	-31.299	-8.693	-14.137	-19.981	-3.776	6.832	-104.882
3	-63.529	58.590	17.658	-40.397	-49.769	-20.922	-8.463	-21.191	-12.241	-9.363	-129.535
4	-108.840	48.622	74.489	-13.753	-93.280	-51.730	8.847	-18.205	-24.517	-38.095	-176.555
5	-178.340	-2.355	41.082	72.260	-20.520	-104.598	45.209	.235	-25.609	-60.768	-223.953
6	-231.828	-51.964	-3.242	34.137	89.050	-2.117	93.230	38.149	.472	-48.711	-229.288

MAXIMUM STRESSES(+VE. COMPRESSION)
(PSI)

	(N)	SECTION NUMBER											
		1	2	3	4	5	6	7	8	9	10	12	
POSITION OF LOAD	1	30.3523	23.7565	22.5310	19.5143	18.2554	19.5312	19.1782	18.0618	20.3257	22.2587	30.4139	
	2	29.1028	24.0367	23.5619	20.3682	18.2135	19.9176	19.8027	18.7264	20.0639	22.3641	31.4922	
	3	29.8462	24.3723	25.9247	23.1034	17.7404	20.8566	21.5652	20.6998	20.3993	22.8878	34.6649	
	4	29.0859	25.4458	26.5846	27.8297	21.8179	21.1912	24.1131	24.2068	23.4408	23.5018	40.1913	
	5	36.4623	27.3203	21.9815	25.4831	28.4574	20.8897	24.0389	26.7220	26.8250	25.2150	44.5024	
	6	44.4883	26.3572	26.2359	23.3141	22.5095	28.4394	22.1338	24.0882	27.3970	27.9054	42.6095	

MINIMUM STRESSES(+VE. COMPRESSION)
(PSI)

	(N)	SECTION NUMBER											
		1	2	3	4	5	6	7	8	9	10	12	
POSITION OF LOAD	1	24.5108	20.8149	16.2386	16.2163	16.1249	14.4745	15.2291	17.7227	18.4305	22.1689	24.1119	
	2	26.4053	20.9658	15.4855	15.5519	16.3698	14.3036	14.8270	17.2816	18.9105	22.2680	23.2115	
	3	26.8881	21.8462	14.0052	13.4934	17.4684	14.0313	13.7552	16.0051	19.2579	22.3870	20.6019	
	4	28.9164	22.4111	15.4200	10.3582	14.6563	15.0620	12.6371	13.9560	17.6606	23.1508	16.3056	
	5	22.7432	21.9747	21.5981	14.9295	9.8840	17.0124	14.4801	13.2851	16.1461	23.2687	13.6892	
	6	14.8934	23.3148	17.8730	17.7485	16.9577	10.2819	17.3448	16.9970	16.7457	21.8118	16.8286	

SHARING STRESSES ALONG THE DIFFERENT RADIAL PLANES
(PSI)

(N)	SECTION NUMBER											
	1	2	3	4	5	6	7	8	9	10	12	
1	-.6800	.1889	.0059	-.2406	-.2137	-.0421	-.1306	-.1609	-.0064	.1026	-.8064	
2	-.5727	.2793	.0352	-.2967	-.2609	-.0725	-.1179	-.1666	-.0315	.0570	-.8744	
3	-.5296	.4884	.1472	-.3368	-.4149	-.1744	-.0706	-.1767	-.1021	-.0781	-1.0799	
4	-.9074	.4053	.6210	-.1147	-.7776	-.4313	.0738	-.1518	-.2044	-.3176	-1.4719	
5	-1.4868	-.0196	.3425	.6024	-.1711	-.8720	.3769	.0020	-.2135	-.5066	-1.8670	
6	-1.9327	-.4332	-.0270	.2846	.7424	-.0177	.7772	.3180	.0039	-.4061	-1.9115	

CONCENTRATE LIVE LOADS 20000.000 #

	POSITION OF LOAD	SECTION NUMBER
MAXIMUM COMPRESSIVE STRESS 628.27473 PSI	5	11
MINIMUM STRESS -421.50535 PSI (+VE COMP.)	5	11
MAXIMUM SHEAR STRESS -47.18661 PSI	6	1

CONCENTRATE LIVE LOADS 10000.000 #

	POSITION OF LOAD	SECTION NUMBER
MAXIMUM COMPRESSIVE STRESS 328.90430 PSI	5	11
MINIMUM STRESS -198.32868 PSI (+VE COMP.)	5	11
MAXIMUM SHEAR STRESS -23.97947 PSI	6	1

CONCENTRATE LIVE LOADS 5000.000 #

	POSITION OF LOAD	SECTION NUMBER
MAXIMUM COMPRESSIVE STRESS 179.21908 PSI	5	11
MINIMUM STRESS -86.74034 PSI (+VE COMP.)	5	11
MAXIMUM SHEAR STRESS -12.37589 PSI	6	1

CONCENTRATE LIVE LOADS 2500.000 #

	POSITION OF LOAD	SECTION NUMBER
MAXIMUM COMPRESSIVE STRESS 104.37647 PSI	5	11
MINIMUM STRESS -30.94618 PSI (+VE COMP.)	5	11
MAXIMUM SHEAR STRESS -6.57411 PSI	6	1

CONCENTRATE LIVE LOADS 1250.000 #

	POSITION OF LOAD	SECTION NUMBER
MAXIMUM COMPRESSIVE STRESS 66.95517 PSI	5	11
MINIMUM STRESS -3.11044 PSI (+VE COMP.)	6	6
MAXIMUM SHEAR STRESS -3.67321 PSI	6	1

CONCENTRATE LIVE LOADS 625.000 #

	POSITION OF LOAD	SECTION NUMBER
MAXIMUM COMPRESSIVE STRESS 48.24452 PSI	5	11
MINIMUM STRESS 7.78516 PSI (+VE COMP.)	5	5
MAXIMUM SHEAR STRESS -2.22277 PSI	6	1

CONCENTRATE LIVE LOADS 937.500 #

	POSITION OF LOAD	SECTION NUMBER
MAXIMUM COMPRESSIVE STRESS 57.59984 PSI	5	11
MINIMUM STRESS 2.46970 PSI (+VE COMP.)	6	6
MAXIMUM SHEAR STRESS -2.94799 PSI	6	1

CONCENTRATE LIVE LOADS 1093.750 #

	POSITION OF LOAD	SECTION NUMBER
MAXIMUM COMPRESSIVE STRESS 62.27751 PSI	5	11
MINIMUM STRESS -.32037 PSI (+VE COMP.)	6	6
MAXIMUM SHEAR STRESS -3.31060 PSI	6	1

CONCENTRATE LIVE LOADS 1015.625 #

	POSITION OF LOAD	SECTION NUMBER
MAXIMUM COMPRESSIVE STRESS 59.93868 PSI	5	11
MINIMUM STRESS 1.07466 PSI (+VE COMP.)	6	6
MAXIMUM SHEAR STRESS -3.12930 PSI	6	1

CONCENTRATE LIVE LOADS 1054.688 #

	POSITION OF LOAD	SECTION NUMBER
MAXIMUM COMPRESSIVE STRESS 61.10809 PSI	5	11
MINIMUM STRESS .37715 PSI (+VE COMP.)	6	6
MAXIMUM SHEAR STRESS -3.21995 PSI	6	1

CONCENTRATE LIVE LOADS 1074.219 #

	POSITION OF LOAD	SECTION NUMBER
MAXIMUM COMPRESSIVE STRESS 61.69280 PSI	5	11
MINIMUM STRESS .02839 PSI (+VE COMP.)	6	6
MAXIMUM SHEAR STRESS -3.26527 PSI	6	1

CONCENTRATE LIVE LOADS 1083.984 #

	POSITION OF LOAD	SECTION NUMBER
MAXIMUM COMPRESSIVE STRESS 61.98515 PSI	5	11
MINIMUM STRESS -.14599 PSI (+VE COMP.)	6	6
MAXIMUM SHEAR STRESS -3.28794 PSI	6	1

CONCENTRATE LIVE LOADS 1079.102 #

	POSITION OF LOAD	SECTION NUMBER
MAXIMUM COMPRESSIVE STRESS 61.83898 PSI	5	11
MINIMUM STRESS -.05880 PSI (+VE COMP.)	6	6
MAXIMUM SHEAR STRESS -3.27661 PSI	6	1

CONCENTRATE LIVE LOADS 1076.660 #

	POSITION OF LOAD	SECTION NUMBER
MAXIMUM COMPRESSIVE STRESS 61.76589 PSI	5	11
MINIMUM STRESS -.01521 PSI (+VE COMP.)	6	6
MAXIMUM SHEAR STRESS -3.27094 PSI	6	1

CONCENTRATE LIVE LOADS 1075.439 #

	POSITION OF LOAD	SECTION NUMBER
MAXIMUM COMPRESSIVE STRESS 61.72934 PSI	5	11
MINIMUM STRESS .00659 PSI (+VE COMP.)	6	6
MAXIMUM SHEAR STRESS -3.26811 PSI	6	1

CONCENTRATE LIVE LOADS 1076.050 #

	POSITION OF LOAD	SECTION NUMBER
MAXIMUM COMPRESSIVE STRESS 61.74762 PSI	5	11
MINIMUM STRESS -.00431 PSI (+VE COMP.)	6	6
MAXIMUM SHEAR STRESS -3.26952 PSI	6	1

CONCENTRATE LIVE LOADS 1075.745 #

		POSITION OF LOAD	SECTION NUMBER
MAXIMUM COMPRESSIVE STRESS	61.73848 PSI	5	11
MINIMUM STRESS (+VE COMP.)	.00114 PSI	6	6
MAXIMUM SHEAR STRESS	-3.26882 PSI	6	1

CONCENTRATE LIVE LOADS 1075.897 #

		POSITION OF LOAD	SECTION NUMBER
MAXIMUM COMPRESSIVE STRESS	61.74305 PSI	5	11
MINIMUM STRESS (+VE COMP.)	-.00158 PSI	6	6
MAXIMUM SHEAR STRESS	-3.26917 PSI	6	1

CONCENTRATE LIVE LOADS 1075.821 #

		POSITION OF LOAD	SECTION NUMBER
MAXIMUM COMPRESSIVE STRESS	61.74076 PSI	5	11
MINIMUM STRESS (+VE COMP.)	-.00022 PSI	6	6
MAXIMUM SHEAR STRESS	-3.26899 PSI	6	1

CONCENTRATE LIVE LOADS 1075.783 #

		POSITION OF LOAD	SECTION NUMBER
MAXIMUM COMPRESSIVE STRESS	61.73962 PSI	5	11
MINIMUM STRESS (+VE COMP.)	.00046 PSI	6	6
MAXIMUM SHEAR STRESS	-3.26890 PSI	6	1

CONCENTRATE LIVE LOADS = 1075.783 #

POSITION OF LOAD	(1)	(2)	(3)	(4)	(5)	(6)
LOADING INTENSITY	16.928	36.707	77.965	158.209	275.043	342.295
ACTUAL LOAD ON THE ARCH	76.120	167.152	326.722	465.420	613.663	684.589

BENDING MOMENTS AT THE DIFFERENT SECTIONS
(#-FT)

POSITION OF LOAD	(1)	(2)	(3)	(4)	(5)	(6)	(7)	(8)	(9)	(10)	(11)
1	23.15	25.80	66.84	39.06	-15.70	-46.59	-40.97	-11.48	10.01	.75	67.97
2	-33.18	28.12	98.80	66.26	-10.56	-56.57	-59.36	-31.28	-3.28	4.08	103.42
3	-134.50	18.35	167.65	152.14	17.59	-78.27	-110.14	-89.51	-44.39	11.33	207.01
4	-78.47	-81.27	154.13	292.98	150.77	-65.80	-175.82	-189.05	-127.50	8.64	382.99
5	164.28	-122.67	-52.76	169.04	355.22	113.47	-141.47	-246.13	-215.26	-32.51	507.10
6	448.70	-81.41	-195.71	-119.74	121.93	369.30	115.58	-132.44	-214.77	-106.81	416.94

VERTICAL SHEAR FORCES AT THE DIFFERENT SECTIONS
(#)

POSITION OF LOAD	SECTION NUMBER										
	(1)	(2)	(3)	(4)	(5)	(6)	(7)	(8)	(9)	(10)	(11)
1	2620.81	1752.05	1126.92	655.03	301.24	-8.42	-318.09	-671.88	-1118.43	-1718.16	-2561.53
2	2703.99	1805.57	1150.77	649.16	293.40	-16.27	-325.93	-679.72	-1126.27	-1726.01	-2569.37
3	2837.25	1947.47	1230.79	667.29	267.09	-42.58	-352.24	-706.03	-1152.59	-1752.32	-2595.68
4	2909.67	2066.30	1466.57	787.30	200.80	-108.86	-418.53	-772.32	-1218.87	-1818.60	-2661.97
5	2944.16	2100.79	1501.06	1054.51	393.88	-222.61	-532.27	-886.06	-1332.62	-1932.35	-2775.72
6	2893.28	2049.92	1450.19	1003.63	649.84	-2.12	-654.08	-1007.87	-1454.42	-2054.15	-2897.52

HORIZONTAL THRUSTS AT THE DIFFERENT SECTIONS
(#)

POSITION OF LOAD	SECTION NUMBER										
	(1)	(2)	(3)	(4)	(5)	(6)	(7)	(8)	(9)	(10)	(11)
1	2051.61	2051.61	2051.61	2051.61	2051.61	2051.61	2051.61	2051.61	2051.61	2051.61	2051.61
2	2079.41	2079.41	2079.41	2079.41	2079.41	2079.41	2079.41	2079.41	2079.41	2079.41	2079.41
3	2165.45	2165.45	2165.45	2165.45	2165.45	2165.45	2165.45	2165.45	2165.45	2165.45	2165.45
4	2341.62	2341.62	2341.62	2341.62	2341.62	2341.62	2341.62	2341.62	2341.62	2341.62	2341.62
5	2554.40	2554.40	2554.40	2554.40	2554.40	2554.40	2554.40	2554.40	2554.40	2554.40	2554.40
6	2660.10	2660.10	2660.10	2660.10	2660.10	2660.10	2660.10	2660.10	2660.10	2660.10	2660.10

AXIAL THRUSTS AT THE DIFFERENT SECTIONS
(#)

POSITION OF LOAD	SECTION NUMBER										
	(1)	(2)	(3)	(4)	(5)	(6)	(7)	(8)	(9)	(10)	(11)
1	3327.61	2697.71	2340.73	2153.34	2073.38	2051.61	2076.07	2158.73	2336.66	2676.03	3280.19
2	3410.84	2753.33	2376.57	2177.80	2099.57	2079.41	2104.77	2187.58	2364.81	2702.41	3303.14
3	3569.07	2910.26	2490.46	2265.11	2180.28	2165.45	2193.91	2277.51	2452.92	2785.36	3375.81
4	3732.70	3121.67	2758.18	2470.43	2343.58	2341.62	2378.41	2465.63	2639.29	2963.15	3534.55
5	3887.97	3307.25	2961.41	2757.53	2584.52	2554.40	2606.66	2703.63	2880.56	3199.45	3753.22
6	3910.69	3355.90	3029.71	2841.39	2729.81	2660.10	2730.49	2842.75	3031.75	3358.61	3914.08

SHEAR FORCES ALONG THE DIFFERENT RADIAL PLANES
(#)

POSITION OF LOAD	SECTION NUMBER										
	(1)	(2)	(3)	(4)	(5)	(6)	(7)	(8)	(9)	(10)	(11)
1	-68.80	33.20	3.84	-35.93	-30.90	-8.42	-14.27	-19.97	-3.61	7.17	-104.37
2	-41.13	56.53	11.42	-50.39	-43.09	-16.27	-10.98	-21.43	-10.07	-4.60	-121.90
3	-30.00	110.50	40.32	-60.74	-82.83	-42.58	1.23	-24.04	-28.29	-39.45	-174.95
4	-127.49	89.06	162.60	-3.41	-176.44	-108.86	38.48	-17.61	-54.70	-101.26	-276.11
5	-277.03	-20.62	90.72	181.65	-19.89	-222.61	116.71	22.06	-57.05	-150.05	-378.09
6	-392.11	-127.36	-4.65	99.62	215.85	-2.12	220.03	103.64	-.93	-124.11	-389.57

MAXIMUM STRESSES(+VE COMPRESSION)
(PSI)

		SECTION NUMBER											
(N)		1	2	3	4	5	6	7	8	9	10	12	
POSITION OF LOAD	1	29.1313	24.0391	23.5277	20.2969	18.2279	19.9011	19.7675	18.6857	20.0810	22.3541	31.4273	
	2	30.4272	24.6419	25.7457	22.1341	18.1376	20.7323	21.1112	20.1157	19.9116	22.7739	33.7474	
	3	37.8305	25.3640	30.8294	28.0191	19.2328	22.7527	24.9034	24.3617	23.1148	23.9008	40.5737	
	4	35.8300	30.9044	32.2493	38.1879	28.5911	23.4725	30.3855	31.9071	29.6590	25.2217	52.4641	
	5	42.2774	34.9375	27.8562	33.1393	42.8763	28.1088	30.2258	37.3187	36.9403	28.6250	61.7396	
	6	59.5457	32.8654	37.0099	30.8779	30.0791	44.3523	29.7034	31.6520	38.1710	34.4136	57.6670	

MINIMUM STRESSES(+VE COMPRESSION)
(PSI)

		SECTION NUMBER											
(N)		1	2	3	4	5	6	7	8	9	10	12	
POSITION OF LOAD	1	26.3510	20.9408	15.5001	15.6065	16.3421	14.3061	14.8475	17.3075	18.8789	22.2642	23.2643	
	2	26.4429	21.2653	13.8797	14.1771	16.8691	13.9384	13.9824	16.3586	19.5177	22.2843	21.3270	
	3	21.6778	23.1597	10.6948	9.7479	17.1198	13.3525	11.6764	13.6120	17.7835	22.5404	15.7124	
	4	26.4066	21.1443	13.7387	3.0023	10.4841	15.5700	9.2706	9.2032	14.3467	24.1838	6.4686	
	5	22.5480	20.2054	21.5204	12.8379	.2162	14.4817	13.2360	7.7598	11.0882	24.7204	.8390	
	6	5.6585	23.0887	13.5056	16.4976	15.4359	.0005	15.8229	15.7461	12.3783	21.5857	7.5937	

SHARING STRESSES ALONG THE DIFFERENT RADIAL PLANES
(PSI)

		SECTION NUMBER											
(N)		1	2	3	4	5	6	7	8	9	10	12	
POSITION OF LOAD	1	-.5736	.2768	.0320	-.2995	-.2576	-.0702	-.1190	-.1665	-.0301	.0597	-.8701	
	2	-.3429	.4713	.0952	-.4201	-.3592	-.1356	-.0915	-.1787	-.0840	-.0384	-1.0163	
	3	-.2501	.9212	.3362	-.5064	-.6905	-.3550	.0103	-.2004	-.2358	-.3289	-1.4585	
	4	-1.0629	.7424	1.3555	-.0285	-1.4710	-.9075	.3208	-.1468	-.4560	-.8442	-2.3019	
	5	-2.3095	-.1719	.7563	1.5143	-.1659	-1.8558	.9730	.1839	-.4756	-1.2509	-3.1520	
	6	-3.2689	-1.0618	-.0387	.8305	1.7995	-.0177	1.8343	.8640	-.0078	-1.0346	-3.2477	

	POSITION OF LOAD	SECTION NUMBER
MAXIMUM COMPRESSIVE STRESS 61.73962 PSI	5	11
MINIMUM STRESS .00046 PSI (+VE COMP.)	6	6
MAXIMUM SHEAR STRESS -3.26890 PSI	6	1

PERMISSIBLE LOADS 1075.78 #

A.2.2 Analysis due to counter clockwise rotation

SPAN(L)=15.000 FT
 RISE-TO-SPAN RATIO(H/L)= .250
 RADIAL THICKNESS(T)= .833 FT
 FILL DEPTH ABOVE THE CROWN=1.000 FT
 DENSITY OF FILL OVER THE ARCH= 110.00 #/FT/FT/FT
 DENSITY OF THE MASONRY UNITS= 110.00 #/FT/FT/FT
 MODULOUS OF ELASTICITY=432000000.00 PSF

CALCULATION FOR DEAD LOAD

BENDING MOMENT AT THE LEFT SUPPORT 20.475 #-FT
 VERTICAL REACTION AT THE LEFT SUPPORT 2553.107 #
 HORIZONTAL THRUST AT THE LEFT SUPPORT 2017.498 #
 AXIAL THRUST AT THE LEFT SUPPORT 3252.985 #
 RADIAL SHEAR FORCE AT THE LEFT SUPPORT 82.1343 #

INTERNAL FORCES

	SECTION NUMBER										
	(1)	(2)	(3)	(4)	(5)	(6)	(7)	(8)	(9)	(10)	(11)
BENDING MOMENTS (#-FT)	20.48	-5.54	25.91	14.22	-15.21	-29.34	-15.21	14.22	25.91	-5.54	20.48
VERTICAL SHEAR FORCES (#)	2553.11	1709.74	1110.01	663.45	309.66	.00	-309.66	-663.45	-1110.01	-1709.74	-2553.11
HORIZONTAL THRUSTS (#)	2017.50	2017.50	2017.50	2017.50	2017.50	2017.50	2017.50	2017.50	2017.50	2017.50	2017.50
AXIAL THRUSTS (#)	3252.99	2644.43	2302.69	2123.72	2041.05	2017.50	2041.05	2123.72	2302.69	2644.43	3252.99
RADIAL SHEAR FORCES (#)	82.13	-22.52	-5.38	17.03	17.13	.00	-17.13	-17.03	5.38	22.52	-82.13

STRESSES AT THE DIFFERENT RADIAL PLANES

	SECTION NUMBER										
	(1)	(2)	(3)	(4)	(5)	(6)	(7)	(8)	(9)	(10)	(11)
MAXIMUM STRESSES (+VE COMP.) (PSI)	28.349	22.378	20.753	18.559	17.929	18.581	17.929	18.559	20.753	22.378	28.349
MINIMUM STRESSES (+VE COMP.) (PSI)	25.890	21.713	17.641	16.851	16.103	15.058	16.103	16.851	17.641	21.713	25.890
SHEARING STRESSES (PSI)	.6847	.1878	.0448	.1420	.1428	.0000	.1428	.1420	.0448	.1878	.6847

CALCULATION FOR SUPPORT DISPLACEMENTS

ROTATION (CLOCK-WISE) AT THE LEFT SUPPORT -.00000500 RADIAN
 VERTICAL DIPLACEMENT(DOWNWARD) AT THE LEFT SUPPORT .00000000 FT
 HORIZONTAL DISPLACEMENT(OUTWARD) AT THE LEFT SUPPORT .00000000 FT

BENDING MOMENT AT THE LEFT SUPPORT -50.3006 (#-FT)
 VERTICAL REACTION AT THE LEFT SUPPORT 2.117 (#)
 HORIZONTAL THRUSTS AT THE LEFT SUPPORT -11.546 (#)

INTERNAL FORCES

	SECTION NUMBER										
	(1)	(2)	(3)	(4)	(5)	(6)	(7)	(8)	(9)	(10)	(11)
BENDING MOMENTS (#- FT)	-50.301	-28.900	-13.937	-3.168	4.305	8.875	10.656	9.535	5.118	-3.493	-18.543
VERTICAL SHEAR FORCES (#)	2.12	2.12	2.12	2.12	2.12	2.12	2.12	2.12	2.12	2.12	2.12
HORIZONTAL THRUSTS (#)	-11.55	-11.55	-11.55	-11.55	-11.55	-11.55	-11.55	-11.55	-11.55	-11.55	-11.55
AXIAL THRUSTS (#)	-5.23	-7.52	-9.11	-10.26	-11.06	-11.55	-11.74	-11.62	-11.14	-10.23	-8.62
RADIAL SHEAR FORCES (#)	10.51	9.02	7.40	5.70	3.94	2.12	-.24	1.69	3.68	5.76	7.97

STRESSES AT THE DIFFERENT RADIAL PLANES

	SECTION NUMBER										
	(1)	(2)	(3)	(4)	(5)	(6)	(7)	(8)	(9)	(10)	(11)
MAXIMUM STRESSES (+VE COMP.) (PSI)	2.977	1.673	.761	.105	.166	.437	.542	.476	.214	.125	1.042
MINIMUM STRESSES (+VE COMP.) (PSI)	-3.064	-1.798	-.913	-.276	-.351	-.629	-.738	-.669	-.400	-.295	-1.185
SHEARING STRESSES (PSI)	.0876	.0752	.0617	.0475	.0328	.0177	.0020	.0141	.0307	.0480	.0664

CALCULATION FOR LIVE LOAD

CONCENTRATED LIVE LOAD 500.00 #

BENDING MOMENTS AT THE DIFFERENT SECTIONS
(#-FT)

POSITION OF LOAD	SECTION NUMBER										
	(1)	(2)	(3)	(4)	(5)	(6)	(7)	(8)	(9)	(10)	(11)
1	-22.135	1.133	12.547	10.068	1.770	-3.892	-7.021	-7.513	-5.012	1.298	13.457
2	-48.314	2.210	27.402	22.710	4.159	-8.532	-15.569	-16.720	-11.189	2.845	29.933
3	-95.406	-2.327	59.402	62.626	17.245	-18.619	-39.169	-43.782	-30.297	6.216	78.080
4	-69.364	-48.630	53.117	128.086	79.143	-12.822	-69.695	-90.045	-68.923	4.968	159.870
5	43.459	-67.871	-43.040	70.483	174.165	70.498	-53.731	-116.574	-109.713	-14.161	217.554
6	175.651	-48.694	-109.483	-63.736	65.738	189.405	65.738	-63.736	-109.483	-48.694	175.651

VERTICAL SHEAR FORCES AT THE DIFFERENT SECTIONS
(#)

POSITION OF LOAD	SECTION NUMBER										
	(1)	(2)	(3)	(4)	(5)	(6)	(7)	(8)	(9)	(10)	(11)
1	32.449	20.647	8.846	-2.930	-2.930	-2.930	-2.930	-2.930	-2.930	-2.930	-2.930
2	71.113	45.522	19.931	-5.660	-6.576	-6.576	-6.576	-6.576	-6.576	-6.576	-6.576
3	133.048	111.476	57.122	2.767	-18.805	-18.805	-18.805	-18.805	-18.805	-18.805	-18.805
4	166.704	166.704	166.704	58.546	-49.613	-49.613	-49.613	-49.613	-49.613	-49.613	-49.613
5	182.737	182.737	182.737	182.737	40.128	-102.480	-102.480	-102.480	-102.480	-102.480	-102.480
6	159.091	159.091	159.091	159.091	159.091	.000	-159.091	-159.091	-159.091	-159.091	-159.091

HORIZONTAL THRUSTS AT THE DIFFERENT SECTIONS
(#)

POSITION OF LOAD	SECTION NUMBER										
	(1)	(2)	(3)	(4)	(5)	(6)	(7)	(8)	(9)	(10)	(11)
1	10.487	10.487	10.487	10.487	10.487	10.487	10.487	10.487	10.487	10.487	10.487
2	23.409	23.409	23.409	23.409	23.409	23.409	23.409	23.409	23.409	23.409	23.409
3	63.396	63.396	63.396	63.396	63.396	63.396	63.396	63.396	63.396	63.396	63.396
4	145.277	145.277	145.277	145.277	145.277	145.277	145.277	145.277	145.277	145.277	145.277
5	244.176	244.176	244.176	244.176	244.176	244.176	244.176	244.176	244.176	244.176	244.176
6	293.302	293.302	293.302	293.302	293.302	293.302	293.302	293.302	293.302	293.302	293.302

SHEAR FORCES ALONG THE DIFFERENT RADIAL PLANES
(#)

POSITION OF LOAD	SECTION NUMBER										
	(1)	(2)	(3)	(4)	(5)	(6)	(7)	(8)	(9)	(10)	(11)
1	32.251	21.272	13.446	8.998	9.883	10.487	10.821	10.873	10.606	9.933	8.636
2	70.936	47.121	30.103	20.367	22.055	23.409	24.160	24.282	23.692	22.196	19.306
3	144.476	120.057	83.034	60.948	59.571	63.396	65.588	66.080	64.642	60.747	53.082
4	220.529	218.318	207.465	156.373	135.467	145.277	151.343	153.514	151.261	143.379	126.856
5	292.695	304.570	301.921	289.812	247.451	244.176	257.427	264.130	263.398	253.206	228.490
6	303.254	327.184	333.668	328.789	314.978	293.302	314.978	328.789	333.668	327.184	303.254

SHEAR FORCES ALONG THE DIFFERENT RADIAL PLANES
(#)

POSITION OF LOAD	SECTION NUMBER										
	(1)	(2)	(3)	(4)	(5)	(6)	(7)	(8)	(9)	(10)	(11)
1	3280.002	2658.186	2307.025	2122.455	2039.878	2016.440	2040.138	2122.976	2302.153	2644.137	3253.000
2	3318.687	2684.035	2323.683	2133.825	2052.050	2029.362	2053.477	2136.385	2315.240	2656.399	3263.670
3	3392.228	2756.970	2376.614	2174.406	2089.566	2069.349	2094.906	2178.183	2356.189	2694.951	3297.445
4	3468.281	2855.231	2501.045	2269.830	2165.462	2151.230	2180.661	2265.617	2442.808	2777.583	3371.220
5	3540.446	2941.484	2595.501	2403.270	2277.446	2250.128	2286.744	2376.233	2554.945	2887.410	3472.854
6	3551.005	2964.098	2627.248	2442.246	2344.973	2299.255	2344.296	2440.891	2625.216	2961.388	3547.618

AXIAL THRUSTS AT THE DIFFERENT SECTIONS
(#)

POSITION OF LOAD	SECTION NUMBER										
	(1)	(2)	(3)	(4)	(5)	(6)	(7)	(8)	(9)	(10)	(11)
1	-60.548	40.693	15.502	-17.463	-17.758	-8.813	-16.153	-15.922	6.598	23.826	-80.799
2	-47.687	51.536	19.024	-24.184	-23.425	-4.459	-14.622	-16.604	3.594	18.357	-88.950
3	-42.515	76.622	32.457	-28.996	-41.894	-16.688	-8.949	-17.813	-4.872	2.162	-113.602
4	-87.826	66.654	89.287	-2.352	-85.406	-47.496	8.361	-14.827	-17.148	-26.570	-160.622
5	-157.326	15.678	55.881	83.661	-12.645	-100.363	44.724	3.613	-18.240	-49.243	-208.020
6	-210.815	-33.932	11.556	45.538	96.925	2.117	92.745	41.526	7.842	-37.186	-213.355

MAXIMUM STRESSES(+VE COMPRESSION)
(PSI)

	(N)	SECTION NUMBER											
		1	2	3	4	5	6	7	8	9	10	12	
POSITION OF LOAD	1	30.4644	24.1603	20.7053	18.9627	17.5541	18.2729	17.7027	18.6741	20.7545	22.5077	28.0433	
	2	32.3589	24.3112	21.7362	19.8166	17.5121	18.6592	18.3272	18.2331	20.4927	22.5170	29.1216	
	3	35.7998	25.1916	24.0990	22.5518	17.8010	19.5983	20.0897	19.3611	19.6867	22.6360	32.2943	
	4	34.8700	28.7912	24.7589	27.2781	22.1505	19.9328	22.6377	22.8680	22.6404	23.3999	37.8206	
	5	30.3342	30.6657	23.5033	24.9316	28.7900	21.7631	22.5635	25.3832	26.0246	25.4640	42.1317	
	6	38.3601	29.7026	27.7577	23.5235	22.8421	29.3127	23.2179	22.7494	26.5966	28.1544	40.2389	

MINIMUM STRESSES(+VE COMPRESSION)
(PSI)

	(N)	SECTION NUMBER											
		1	2	3	4	5	6	7	8	9	10	12	
POSITION OF LOAD	1	24.2242	20.1605	17.7605	16.4257	16.4575	15.3479	16.3132	16.7230	17.6301	21.5789	26.1951	
	2	22.9746	20.4406	17.0074	15.7613	16.7024	15.1770	15.9111	17.3876	18.1101	21.7740	25.2947	
	3	20.7599	20.7763	15.5271	13.7028	17.0390	14.9047	14.8393	16.9565	19.5988	22.2978	22.6851	
	4	22.9578	18.8151	16.9418	10.5676	13.9549	15.9353	13.7212	14.9074	18.0894	22.9117	18.3888	
	5	28.6969	18.3787	19.7724	15.1389	9.1826	15.7541	15.5642	14.2366	16.5749	22.6787	15.7723	
	6	20.8470	19.7188	16.0472	17.1969	16.2564	9.0235	15.8693	17.9484	17.1745	21.2218	18.9118	

SHARING STRESSES ALONG THE DIFFERENT RADIAL PLANES
(PSI)

		SECTION NUMBER										
(N)		1	2	3	4	5	6	7	8	9	10	12
POSITION OF LOAD	1	-.5048	.3392	.1292	-.1456	-.1480	-.0068	-.1347	-.1327	.0550	.1986	-.6736
	2	-.3976	.4296	.1586	-.2016	-.1953	-.0372	-.1219	-.1384	.0300	.1530	-.7415
	3	-.3544	.6388	.2706	-.2417	-.3493	-.1391	-.0746	-.1485	-.0406	.0180	-.9471
	4	-.7322	.5557	.7444	-.0196	-.7120	-.3960	.0697	-.1236	-.1430	-.2215	-1.3391
	5	-1.3116	.1307	.4659	.6975	-.1054	-.8367	.3729	.0301	-.1521	-.4105	-1.7342
	6	-1.7575	-.2829	.0963	.3796	.8080	.0177	.7732	.3462	.0654	-.3100	-1.7787

CONCENTRATE LIVE LOADS 20000.000 #

	POSITION OF LOAD	SECTION NUMBER
MAXIMUM COMPRESSIVE STRESS 625.90408 PSI	5	11
MINIMUM STRESS -419.42219 PSI (+VE COMP.)	5	11
MAXIMUM SHEAR STRESS -47.03261 PSI	6	11

CONCENTRATE LIVE LOADS 10000.000 #

	POSITION OF LOAD	SECTION NUMBER
MAXIMUM COMPRESSIVE STRESS 326.53365 PSI	5	11
MINIMUM STRESS -196.24552 PSI (+VE COMP.)	5	11
MAXIMUM SHEAR STRESS -23.82546 PSI	6	11

CONCENTRATE LIVE LOADS 5000.000 #

	POSITION OF LOAD	SECTION NUMBER
MAXIMUM COMPRESSIVE STRESS 176.84843 PSI	5	11
MINIMUM STRESS -84.65718 PSI (+VE COMP.)	5	11
MAXIMUM SHEAR STRESS -12.22189 PSI	6	11

CONCENTRATE LIVE LOADS 2500.000 #

	POSITION OF LOAD	SECTION NUMBER
MAXIMUM COMPRESSIVE STRESS 102.00582 PSI	5	11
MINIMUM STRESS -28.86301 PSI (+VE COMP.)	5	11
MAXIMUM SHEAR STRESS -6.42010 PSI	6	11

CONCENTRATE LIVE LOADS 1250.000 #

	POSITION OF LOAD	SECTION NUMBER
MAXIMUM COMPRESSIVE STRESS 64.58452 PSI	5	11
MINIMUM STRESS -4.36880 PSI (+VE COMP.)	6	6
MAXIMUM SHEAR STRESS -3.51921 PSI	6	11

CONCENTRATE LIVE LOADS 625.000 #

	POSITION OF LOAD	SECTION NUMBER
MAXIMUM COMPRESSIVE STRESS 45.87387 PSI	5	11
MINIMUM STRESS 6.79147 PSI (+VE COMP.)	6	6
MAXIMUM SHEAR STRESS -2.06876 PSI	6	11

CONCENTRATE LIVE LOADS 937.500 #

	POSITION OF LOAD	SECTION NUMBER
MAXIMUM COMPRESSIVE STRESS 55.22919 PSI	5	11
MINIMUM STRESS 1.21134 PSI (+VE COMP.)	6	6
MAXIMUM SHEAR STRESS -2.79398 PSI	6	11

CONCENTRATE LIVE LOADS 1093.750 #

	POSITION OF LOAD	SECTION NUMBER
MAXIMUM COMPRESSIVE STRESS 59.90686 PSI	5	11
MINIMUM STRESS -1.57873 PSI (+VE COMP.)	6	6
MAXIMUM SHEAR STRESS -3.15660 PSI	6	11

CONCENTRATE LIVE LOADS 1015.625 #

	POSITION OF LOAD	SECTION NUMBER
MAXIMUM COMPRESSIVE STRESS 57.56803 PSI	5	11
MINIMUM STRESS -.18370 PSI (+VE COMP.)	6	6
MAXIMUM SHEAR STRESS -2.97529 PSI	6	11

CONCENTRATE LIVE LOADS 976.563 #

	POSITION OF LOAD	SECTION NUMBER
MAXIMUM COMPRESSIVE STRESS 56.39861 PSI	5	11
MINIMUM STRESS .51382 PSI (+VE COMP.)	6	6
MAXIMUM SHEAR STRESS -2.88464 PSI	6	11

CONCENTRATE LIVE LOADS 996.094 #

	POSITION OF LOAD	SECTION NUMBER
MAXIMUM COMPRESSIVE STRESS 56.98332 PSI	5	11
MINIMUM STRESS .16506 PSI (+VE COMP.)	6	6
MAXIMUM SHEAR STRESS -2.92996 PSI	6	11

CONCENTRATE LIVE LOADS 1005.859 #

	POSITION OF LOAD	SECTION NUMBER
MAXIMUM COMPRESSIVE STRESS 57.27567 PSI	5	11
MINIMUM STRESS -.00932 PSI (+VE COMP.)	6	6
MAXIMUM SHEAR STRESS -2.95263 PSI	6	11

CONCENTRATE LIVE LOADS 1000.977 #

	POSITION OF LOAD	SECTION NUMBER
MAXIMUM COMPRESSIVE STRESS 57.12949 PSI	5	11
MINIMUM STRESS .07787 PSI (+VE COMP.)	6	6
MAXIMUM SHEAR STRESS -2.94129 PSI	6	11

CONCENTRATE LIVE LOADS 1003.418 #

	POSITION OF LOAD	SECTION NUMBER
MAXIMUM COMPRESSIVE STRESS 57.20258 PSI	5	11
MINIMUM STRESS .03428 PSI (+VE COMP.)	6	6
MAXIMUM SHEAR STRESS -2.94696 PSI	6	11

CONCENTRATE LIVE LOADS 1004.639 #

	POSITION OF LOAD	SECTION NUMBER
MAXIMUM COMPRESSIVE STRESS 57.23913 PSI	5	11
MINIMUM STRESS .01248 PSI (+VE COMP.)	6	6
MAXIMUM SHEAR STRESS -2.94979 PSI	6	11

CONCENTRATE LIVE LOADS 1005.249 #

	POSITION OF LOAD	SECTION NUMBER
MAXIMUM COMPRESSIVE STRESS 57.25740 PSI	5	11
MINIMUM STRESS .00158 PSI (+VE COMP.)	6	6
MAXIMUM SHEAR STRESS -2.95121 PSI	6	11

CONCENTRATE LIVE LOADS 1005.554 #

	POSITION OF LOAD	SECTION NUMBER
MAXIMUM COMPRESSIVE STRESS 57.26654 PSI	5	11
MINIMUM STRESS -.00387 PSI (+VE COMP.)	6	6
MAXIMUM SHEAR STRESS -2.95192 PSI	6	11

CONCENTRATE LIVE LOADS 1005.402 #

	POSITION OF LOAD	SECTION NUMBER
MAXIMUM COMPRESSIVE STRESS 57.26197 PSI	5	11
MINIMUM STRESS -.00114 PSI (+VE COMP.)	6	6
MAXIMUM SHEAR STRESS -2.95156 PSI	6	11

CONCENTRATE LIVE LOADS 1005.325 #

	POSITION OF LOAD	SECTION NUMBER
MAXIMUM COMPRESSIVE STRESS 57.25968 PSI	5	11
MINIMUM STRESS .00022 PSI (+VE COMP.)	6	6
MAXIMUM SHEAR STRESS -2.95139 PSI	6	11

CONCENTRATE LIVE LOADS = 1005.325 #

	(1)	(2)	(3)	(4)	(5)	(6)
LOADING INTENSITY	15.819	34.303	72.858	147.847	257.029	319.876
ACTUAL LOAD ON THE ARCH	71.134	156.204	305.324	434.938	573.472	639.752

BENDING MOMENTS AT THE DIFFERENT SECTIONS
(#-FT)

POSITION OF LOAD	SECTION NUMBER										
	(1)	(2)	(3)	(4)	(5)	(6)	(7)	(8)	(9)	(10)	(11)
1	-74.33	-32.16	37.20	31.30	-7.34	-28.29	-18.67	8.65	20.95	-6.42	28.99
2	-126.97	-30.00	67.07	56.72	-2.54	-37.62	-35.85	-9.86	8.53	-3.31	62.12
3	-221.65	-39.12	131.41	136.98	23.77	-57.90	-83.30	-64.27	-29.89	3.47	158.92
4	-169.29	-132.22	118.77	268.59	148.23	-46.24	-144.68	-157.29	-107.55	.96	323.38
5	57.55	-170.90	-74.56	152.77	339.28	121.28	-112.58	-210.63	-189.57	-37.50	439.36
6	323.35	-132.35	-208.16	-117.09	121.28	360.36	127.63	-104.39	-189.10	-106.94	355.11

VERTICAL SHEAR FORCES AT THE DIFFERENT SECTIONS
(#)

POSITION OF LOAD	SECTION NUMBER										
	(1)	(2)	(3)	(4)	(5)	(6)	(7)	(8)	(9)	(10)	(11)
1	2620.47	1753.37	1129.91	659.68	305.89	-3.77	-313.44	-667.23	-1113.78	-1713.52	-2556.88
2	2698.21	1803.39	1152.20	654.19	298.56	-11.10	-320.77	-674.56	-1121.11	-1720.85	-2564.21
3	2822.74	1936.00	1226.98	671.14	273.97	-35.69	-345.36	-699.15	-1145.70	-1745.43	-2588.80
4	2890.41	2047.04	1447.31	783.29	212.03	-97.64	-407.30	-761.09	-1207.65	-1807.38	-2650.74
5	2922.64	2079.28	1479.55	1032.99	392.46	-203.94	-513.60	-867.39	-1313.94	-1913.68	-2757.04
6	2875.10	2031.74	1432.00	985.45	631.66	2.12	-627.42	-981.21	-1427.77	-2027.50	-2870.87

HORIZONTAL THRUSTS AT THE DIFFERENT SECTIONS
(#)

POSITION OF LOAD	SECTION NUMBER										
	(1)	(2)	(3)	(4)	(5)	(6)	(7)	(8)	(9)	(10)	(11)
1	2027.04	2027.04	2027.04	2027.04	2027.04	2027.04	2027.04	2027.04	2027.04	2027.04	2027.04
2	2053.02	2053.02	2053.02	2053.02	2053.02	2053.02	2053.02	2053.02	2053.02	2053.02	2053.02
3	2133.42	2133.42	2133.42	2133.42	2133.42	2133.42	2133.42	2133.42	2133.42	2133.42	2133.42
4	2298.05	2298.05	2298.05	2298.05	2298.05	2298.05	2298.05	2298.05	2298.05	2298.05	2298.05
5	2496.90	2496.90	2496.90	2496.90	2496.90	2496.90	2496.90	2496.90	2496.90	2496.90	2496.90
6	2595.68	2595.68	2595.68	2595.68	2595.68	2595.68	2595.68	2595.68	2595.68	2595.68	2595.68

AXIAL THRUSTS AT THE DIFFERENT SECTIONS
(#)

POSITION OF LOAD	SECTION NUMBER										
	(1)	(2)	(3)	(4)	(5)	(6)	(7)	(8)	(9)	(10)	(11)
1	3312.60	2679.68	2320.61	2131.55	2049.87	2027.04	2051.07	2133.96	2312.87	2654.18	3261.73
2	3390.38	2731.66	2354.11	2154.41	2074.34	2053.02	2077.89	2160.93	2339.18	2678.83	3283.18
3	3538.24	2878.31	2460.53	2236.00	2149.77	2133.42	2161.19	2244.97	2421.52	2756.34	3351.09
4	3691.16	3075.87	2710.72	2427.87	2302.37	2298.05	2333.62	2420.77	2595.68	2922.49	3499.43
5	3836.26	3249.30	2900.64	2696.17	2527.53	2496.90	2546.91	2643.18	2821.15	3143.31	3703.78
6	3857.49	3294.77	2964.47	2774.54	2663.31	2595.68	2662.63	2773.18	2962.44	3292.06	3854.10

SHEAR FORCES ALONG THE DIFFERENT RADIAL PLANES
(#)

POSITION OF LOAD	SECTION NUMBER										
	(1)	(2)	(3)	(4)	(5)	(6)	(7)	(8)	(9)	(10)	(11)
1	-49.35	49.94	18.26	-23.66	-22.38	-3.77	-14.93	-16.51	4.11	19.32	-87.50
2	-23.49	71.74	25.34	-37.17	-33.77	-11.10	-11.85	-17.88	-1.93	8.32	-103.89
3	-13.09	122.18	52.35	-46.85	-70.91	-35.69	-.44	-20.31	-18.95	-24.24	-153.46
4	-104.20	102.14	166.61	6.72	-158.39	-97.64	34.36	-14.31	-43.64	-82.01	-248.00
5	-243.94	-.35	99.44	179.66	-12.10	-203.94	107.48	22.77	-45.83	-127.60	-343.30
6	-351.48	-100.10	10.32	103.01	208.21	2.12	204.03	99.00	6.61	-103.35	-354.02

MAXIMUM STRESSES(+VE COMPRESSION)
(PSI)

	(N)	SECTION NUMBER										
		1	2	3	4	5	6	7	8	9	10	12
POSITION OF LOAD	1	32.0795	24.2708	21.5801	19.6495	17.5299	18.5974	18.2200	18.3098	20.5397	22.5126	28.9327
	2	35.8887	24.5741	23.6527	21.3665	17.4456	19.3743	19.4756	18.6069	20.0133	22.5314	31.1008
	3	42.8071	26.3444	28.4035	26.8660	19.3495	21.2623	23.0194	22.5748	21.9821	23.1868	37.4800
	4	40.9376	33.5818	29.7304	36.3688	28.0949	21.9350	28.1425	29.6260	28.0976	24.4212	48.5916
	5	35.4377	37.3508	28.6591	31.6508	41.4445	28.0988	27.9932	34.6832	34.9021	28.4568	57.2597
	6	51.5750	35.4144	37.2133	30.1617	29.4855	43.2784	29.8612	29.3876	36.0522	33.8662	53.4538

MINIMUM STRESSES(+VE COMPRESSION)
(PSI)

		SECTION NUMBER											
(N)		1	2	3	4	5	6	7	8	9	10	12	
POSITION OF LOAD	1	23.1526	20.4085	17.1123	15.8905	16.6482	15.2000	15.9783	17.2705	18.0236	21.7414	25.4512	
	2	20.6402	20.9718	15.5981	14.5547	17.1406	14.8564	15.1698	17.4230	18.9887	22.1337	23.6407	
	3	16.1872	21.6466	12.6217	10.4156	16.4944	14.3089	13.0148	14.8563	18.3927	22.7706	18.3938	
	4	20.6063	17.7033	15.4663	4.1118	10.2933	16.3812	10.7667	10.7362	15.1810	24.3064	9.7555	
	5	28.5256	16.8259	19.7042	13.3033	.6979	13.5330	14.4723	9.3874	12.1359	23.9527	4.4946	
	6	12.7422	19.5203	12.2143	16.0991	14.9207	.0002	14.5337	16.8506	13.3415	21.0233	10.8070	

SHARING STRESSES ALONG THE DIFFERENT RADIAL PLANES
(PSI)

		SECTION NUMBER											
(N)		1	2	3	4	5	6	7	8	9	10	12	
POSITION OF LOAD	1	-.4114	.4164	.1522	-.1972	-.1866	-.0315	-.1244	-.1376	.0343	.1611	-.7295	
	2	-.1958	.5981	.2112	-.3099	-.2815	-.0926	-.0988	-.1490	-.0161	.0694	-.8661	
	3	-.1092	1.0186	.4364	-.3906	-.5911	-.2976	-.0037	-.1693	-.1580	-.2021	-1.2793	
	4	-.8687	.8515	1.3890	.0560	-1.3205	-.8140	.2865	-.1193	-.3638	-.6837	-2.0675	
	5	-2.0336	-.0029	.8290	1.4978	-.1008	-1.7001	.8960	.1898	-.3821	-1.0637	-2.8620	
	6	-2.9302	-.8345	.0861	.8588	1.7358	.0177	1.7009	.8253	.0551	-.8616	-2.9514	

MAXIMUM COMPRESSIVE STRESS 57.25968 PSI POSITION OF LOAD 5 SECTION NUMBER 11
 MINIMUM STRESS .00022 PSI 6 6
 (+VE COMP.)
 MAXIMUM SHEAR STRESS -2.95139 PSI 6 11

PERMISSIBLE LOADS 1005.33 #

A.3 The permissible live load capacity for different arches

SUPPORT CONDITIONS

ROTATION .000000 RADIAN
 VERTICAL DISPLACEMENT .000000 FT
 HORIZONTAL DISPLACEMENT .000000 FT

MATERIAL PROPERTIES

DENSITY OF MASONRY UNITS 110.00 #/FT/FT/FT
 DENSITY OF FILL OVER THE ARCH 110.00 #/FT/FT/FT
 DENSITY OF WEARING COAT MATERIAL 110.00 #/FT/FT/FT
 MODULOUS OF ELASTICITY 432000000.00 PSF

STRESS CONDITIONS

ALLOWABLE LIMIT OF MAXIMUM COMPRESSIVE STRESS 1000 - 1125 PSI
 ALLOWABLE LIMIT OF MINIMUM COMPRESSIVE STRESS 0.0 -0.0005 PSI
 ALLOWABLE LIMIT OF SHEAR STRESS 50 - 55 PSI

SPAN(L) (FT)	(H/L)	(T) (FT)	FILL- DEPTH (FT)	MAX.COMP. STRESS PSI	POSITION OF LOAD	SECTION NUMBER	MAX.SHEAR STRESS PSI	POSITION OF LOAD	SECTION NUMBER	MIN.COMP. STRESS PSI	POSITION OF LOAD	SECTION NUMBER	P.LOADS (#)
10.000	.20	.416	1.000	65.782	5	11	-2.328	5	11	.00030	5	11	522.894
10.000	.20	.416	1.500	81.803	5	11	-3.243	5	11	.00034	5	11	874.269
10.000	.20	.416	2.000	98.335	5	11	-4.213	5	11	.00007	5	11	1361.418
10.000	.20	.833	1.000	48.269	5	11	-3.430	5	11	.00045	5	11	1399.422
10.000	.20	.833	1.500	58.749	5	11	-4.381	5	11	.00025	5	11	2561.426
10.000	.20	.833	2.000	70.438	5	11	-5.489	5	11	.00043	5	11	4352.283
10.000	.20	1.250	1.000	47.844	5	11	-5.047	5	11	.00028	5	11	3077.698
10.000	.20	1.250	1.500	56.694	5	11	-6.125	5	11	.00010	4	11	5606.270
10.000	.20	1.250	2.000	66.476	5	11	-7.356	5	11	.00003	4	11	9382.629
10.000	.30	.416	1.000	53.584	5	11	-3.132	6	11	.00049	5	11	111.556
10.000	.30	.416	1.500	64.050	5	11	-4.000	6	11	.00043	5	11	1.740
10.000	.30	.416	2.000										
													PERMISSIBLE LOAD CAPACITY ---- IMPOSSIBLE
10.000	.30	.833	1.000	35.750	5	11	-3.187	6	11	.00033	5	11	606.441
10.000	.30	.833	1.500	41.776	5	11	-3.830	6	11	.00014	5	11	919.819
10.000	.30	.833	2.000	47.919	5	11	-4.513	5	11	.00003	5	11	1296.711

SPAN(L) (FT)	(H/L)	(T) (FT)	FILL- DEPTH (FT)	MAX.COMP. STRESS PSI	POSITION OF LOAD	SECTION NUMBER	MAX.SHEAR STRESS PSI	POSITION OF LOAD	SECTION NUMBER	MIN.COMP. STRESS PSI	POSITION OF LOAD	SECTION NUMBER	P.LOADS (#)
10.000	.30	1.250	1.000	31.255	5	11	-3.718	6	11	.00012	5	11	1436.043
10.000	.30	1.250	1.500	36.042	5	11	-4.339	6	11	.00028	5	11	2417.183
10.000	.30	1.250	2.000	41.190	5	11	-5.058	5	11	.00028	5	11	3791.046
10.000	.40	.416	1.000										PERMISSIBLE LOAD CAPACITY ---- IMPOSSIBLE
10.000	.40	.416	1.500										PERMISSIBLE LOAD CAPACITY ---- IMPOSSIBLE
10.000	.40	.416	2.000										PERMISSIBLE LOAD CAPACITY ---- IMPOSSIBLE
10.000	.40	.833	1.000										PERMISSIBLE LOAD CAPACITY ---- IMPOSSIBLE
10.000	.40	.833	1.500										PERMISSIBLE LOAD CAPACITY ---- IMPOSSIBLE
10.000	.40	.833	2.000										PERMISSIBLE LOAD CAPACITY ---- IMPOSSIBLE
10.000	.40	1.250	1.000	25.788	5	11	-3.652	6	11	.00019	5	11	282.240
10.000	.40	1.250	1.500	28.893	5	11	-4.142	6	11	.00020	5	11	257.587
10.000	.40	1.250	2.000	31.961	5	11	-4.634	6	11	.00004	5	11	110.817
20.000	.20	.416	1.000										PERMISSIBLE LOAD CAPACITY ---- IMPOSSIBLE
20.000	.20	.416	1.500	168.349	3	1	3.233	3	1	.00025	3	1	437.057
20.000	.20	.416	2.000	204.902	3	1	2.785	3	1	.00014	3	1	1611.483
20.000	.20	.833	1.000	85.949	3	1	2.638	3	1	.00037	5	5	1466.036
20.000	.20	.833	1.500	109.034	5	11	-3.379	5	11	.00023	5	5	2786.398
20.000	.20	.833	2.000	131.468	5	11	-4.659	5	11	.00022	5	11	4189.062
20.000	.20	1.250	1.000	72.997	5	11	-3.291	6	1	.00013	5	5	2641.153
20.000	.20	1.250	1.500	94.553	5	11	-4.837	5	11	.00014	5	11	4999.161
20.000	.20	1.250	2.000	106.230	5	11	-5.680	5	11	.00002	5	11	7122.135
20.000	.30	.416	1.000	128.390	5	11	-4.689	6	11	.00027	4	4	353.342
20.000	.30	.416	1.500	163.393	5	11	-6.442	6	11	.00031	5	11	214.344
20.000	.30	.416	2.000										PERMISSIBLE LOAD CAPACITY ---- IMPOSSIBLE
20.000	.30	.833	1.000	82.058	5	11	-4.407	6	11	.00020	6	6	816.536
20.000	.30	.833	1.500	96.542	5	11	-5.420	6	1	.00023	5	11	1005.054
20.000	.30	.833	2.000	107.078	5	11	-6.262	6	11	.00047	5	11	895.929
20.000	.30	1.250	1.000	62.315	5	11	-4.350	6	11	.00035	6	6	1302.958

SPAN(L) (FT)	(H/L)	(T) (FT)	FILL- DEPTH (FT)	MAX.COMP. STRESS PSI	POSITION OF LOAD	SECTION NUMBER	MAX.SHEAR STRESS PSI	POSITION OF LOAD	SECTION NUMBER	MIN.COMP. STRESS PSI	POSITION OF LOAD	SECTION NUMBER	P.LOADS (#)
20.000	.30	1.250	1.500	75.288	5	11	-5.448	6	11	.00017	5	11	2151.108
20.000	.30	1.250	2.000	82.733	5	11	-6.120	6	11	.00046	5	11	2592.468
20.000	.40	.416	1.000										PERMISSIBLE LOAD CAPACITY ---- IMPOSSIBLE
20.000	.40	.416	1.500										PERMISSIBLE LOAD CAPACITY ---- IMPOSSIBLE
20.000	.40	.416	2.000										PERMISSIBLE LOAD CAPACITY ---- IMPOSSIBLE
20.000	.40	.833	1.000										PERMISSIBLE LOAD CAPACITY ---- IMPOSSIBLE
20.000	.40	.833	1.500										PERMISSIBLE LOAD CAPACITY ---- IMPOSSIBLE
20.000	.40	.833	2.000										PERMISSIBLE LOAD CAPACITY ---- IMPOSSIBLE
20.000	.40	1.250	1.000										PERMISSIBLE LOAD CAPACITY ---- IMPOSSIBLE
20.000	.40	1.250	1.500										PERMISSIBLE LOAD CAPACITY ---- IMPOSSIBLE
20.000	.40	1.250	2.000										PERMISSIBLE LOAD CAPACITY ---- IMPOSSIBLE
30.000	.20	.416	1.000										PERMISSIBLE LOAD CAPACITY ---- IMPOSSIBLE
30.000	.20	.416	1.500										PERMISSIBLE LOAD CAPACITY ---- IMPOSSIBLE
30.000	.20	.416	2.000										PERMISSIBLE LOAD CAPACITY ---- IMPOSSIBLE
30.000	.20	.833	1.000										PERMISSIBLE LOAD CAPACITY ---- IMPOSSIBLE
30.000	.20	.833	1.500	164.730	3	1	4.766	3	1	.00001	3	1	865.746
30.000	.20	.833	2.000	192.210	3	1	4.458	3	1	.00016	3	1	2982.616
30.000	.20	1.250	1.000	112.779	3	1	4.131	3	1	.00024	3	1	2664.995
30.000	.20	1.250	1.500	128.872	3	1	3.955	3	1	.00034	5	5	4950.428
30.000	.20	1.250	2.000	147.863	5	11	-4.419	5	6	.00033	4	4	7706.261
30.000	.30	.416	1.000										PERMISSIBLE LOAD CAPACITY ---- IMPOSSIBLE
30.000	.30	.416	1.500										PERMISSIBLE LOAD CAPACITY ---- IMPOSSIBLE
30.000	.30	.416	2.000	331.758	5	11	-10.766	6	11	.00031	5	11	553.536
30.000	.30	.833	1.000	93.957	3	1	-3.478	6	1	.00006	3	6	596.619

SPAN(L) (FT)	(H/L)	(T) (FT)	FILL- DEPTH (FT)	MAX.COMP. STRESS PSI	POSITION OF LOAD	SECTION NUMBER	MAX.SHEAR STRESS PSI	POSITION OF LOAD	SECTION NUMBER	MIN.COMP. STRESS PSI	POSITION OF LOAD	SECTION NUMBER	P.LOADS (#)
30.000	.30	.833	1.500	170.672	5	11	-7.204	6	11	.00032	4	4	1958.275
30.000	.30	.833	2.000	186.839	5	11	-8.235	6	11	.00020	5	11	1746.893
30.000	.30	1.250	1.000	98.848	5	11	-5.099	6	1	.00015	6	6	1742.053
30.000	.30	1.250	1.500	123.049	5	11	-6.611	6	11	.00030	6	6	2756.882
30.000	.30	1.250	2.000	139.499	5	11	-7.727	6	11	.00005	5	11	3369.951
30.000	.40	.416	1.000										PERMISSIBLE LOAD CAPACITY ---- IMPOSSIBLE
30.000	.40	.416	1.500										PERMISSIBLE LOAD CAPACITY ---- IMPOSSIBLE
30.000	.40	.416	2.000										PERMISSIBLE LOAD CAPACITY ---- IMPOSSIBLE
30.000	.40	.833	1.000										PERMISSIBLE LOAD CAPACITY ---- IMPOSSIBLE
30.000	.40	.833	1.500										PERMISSIBLE LOAD CAPACITY ---- IMPOSSIBLE
30.000	.40	.833	2.000										PERMISSIBLE LOAD CAPACITY ---- IMPOSSIBLE
30.000	.40	1.250	1.000										PERMISSIBLE LOAD CAPACITY ---- IMPOSSIBLE
30.000	.40	1.250	1.250										PERMISSIBLE LOAD CAPACITY ---- IMPOSSIBLE
30.000	.40	1.250	2.000										PERMISSIBLE LOAD CAPACITY ---- IMPOSSIBLE

